République Algérienne Démocratique et Populaire

Ministère de l'Enseignement Supérieur et de la Recherche Scientifique

UNIVERSITE DJILLALI LIABES DE SIDI-BEL-ABBES

Faculté de Génie Electrique

Département d'Electrotechnique

Thèse présentée par :

DJEHAF Mohammed Abd El Djalil

Pour l'obtention du diplôme de :

Doctorat 3ème Cycle : Electrotechnique

Option : Réseaux Électriques

Intitulé de la thèse :

Contribution à l'analyse d'une liaison HVDC-VSC à base de convertisseurs multiniveaux

Présentée devant le jury composé de :

Pr. HADJERI Samir	Professeur (U.D.L. Sidi Bel-Abbès)	Président
Pr. ZIDI Sid Ahmed	Professeur (U.D.L. Sidi Bel-Abbès)	Directeur de thèse
Pr. Damien Ernst	Professeur (U.L.G. Liége)	Co- directeur de thèse
Dr. KHATIR Mohamed	MC A (U.D.L. Sidi Bel-Abbès)	Examinateur
Pr. SAYAH Houari	Professeur (U.D.L. Sidi Bel-Abbès)	Examinateur
Dr. LAKDJA Fatiha	MC A (Université de Saida)	Examinateur

Soutenue le : 18/01/2017

Laboratoire de Recherche ICEPS (Intelligent Control & Electrical Power Systems)

To my lovely parents

To my dear brother and sisters

To my fiancee

As well as my fellows

M.A DJEHAF

"The greatest enemy of knowledge is not ignorance, it is the illusion of knowledge".

__ Stephen Hawking__

ACKNOWLEDGEMENT

As my thesis came to its end I can't hold my feeling of gratitude to Allah and all those who have been part of it. First, I would like to express my sincere appreciation to my PhD advisor Pr Zidi Sid Ahmed for all his support through the past few years, for his guidance and encouragement over my studies, He was a true mentor, he pushed me to improve myself and guide me toward success.

I would like to extend my deepest gratitude to Pr Damien Ernst Who has been a great supervisor, I appreciate him for accepting me to the university of liege، providing me with valuable knowledge, time, and expertise. It was a great honour to work with him.

I want to address my highest appreciation for the Professor HADJERI Samir for accepting to chair the jury of the thesis defense.

I want to thank also the jury's members: the Professor SAYAH Houari, Dr KHATIR Mohamed and Dr LAKDJA Fatiha, for their time, interest, helpful comments and insightful questions.

I would like to express my gratitude also to ICEPS laboratory members and Smart Grid unit members who have served me with their knowledge and helped me in my studies, for giving me the opportunity to learn and work in a lovely and an appropriate atmosphere. It has been a long journey and I am thankful to all those who walked me by; first my parents and my family members for their support, compassion and patience without, I wouldn't be standing here and achieving my dream. To all my friends and colleagues who helped me and stood by me especially Mr Djilani Kobibi Youcef.

Finally my work is done but my seeking of knowledge isn't; the road to excellence and success is always under construction.

RESUME

Le développement atteint dans le domaine de l'électronique de puissance, précisément la progression de la technologie des semi-conducteurs commandés à l'ouverture et à la fermeture (les thyristors GTO et les transistors IGBT), a permis de réaliser des liaisons HVDC équipées de convertisseurs source de tension VSC qui peuvent aussi interrompe le courant, et non seulement le commuter, comme dans le cas des convertisseurs à commutation de phase (à base des thyristors). La nouvelle technologie VSC-HVDC offre des nouvelles possibilités de transport tel que la connexion avec les réseaux faibles et morts et bien d'autres avantages, on peut citer en autre la rentabilité, la compacité, et le respect de l'environnement, et la facilité d'application. Il est prévu que cette technologie deviendra rapidement la solution privilégiée pour le transport de l'énergie, dans le cas de nombreuses applications où le transport en CA et les liaisons HVDC conventionnelles présentent des limitations. Dans ce contexte, l'intérêt d'utiliser des convertisseurs à niveaux multiples réside dans leur capacité à générer des formes d'ondes de très bonne qualité, et de définition temporelle augmentée. Ces propriétés sont liées à de nombreux avantages, à commencer par la réduction des harmoniques de courant produits dans le circuit interfacé, en plus on peut attendre des niveaux de tension très élevés.

MOTS CLES

HVDC; VSC-HVDC; Convertisseurs Multiniveaux; PWM.

ABSTRACT

The development achieved in power electronics field, precisely, the progress of semiconductor opening/closing controlled devices (GTO thyristors and IGBT transistors) allow the installation of HVDC transmission systems equipped with voltage source converters which can not only switch the current, as in the case of the Line-Commutated Converters (thyristors based), but also, interrupt it.The new VSC-HVDC technology offers new transportation options such as the connection with the weak and dead networks and many other advantages including the profitability, compactness, environmental sustainability and ease of application. It is envisaged that this technology will quickly become the preferred solution for energy transport for many applications where public AC and conventional HVDC links have many limitations. In this context, the advantage of using multilevel converters lies in their ability to generate high quality waves. These properties are related to many advantages, starting with the reduction of current harmonics in the circuit interfaced, and more can be expected voltage levels

KEYWORDS

HVDC; VSC-HVDC; Multilevel Converter; PWM.

ملخص

أدى التطور الحاصل في مجال الإلكترونيات الصناعية والمحرز تحديدا في تكنولوجيا أنصاف النواقل، ترنزستر ثنائي القطبية ذو بوابة معزولة والثايرستور ذو بوابة الإطفاء الى تطوير نظام تيار الجهد العالي المستمر مزود بمحولات منبع التوترقادرة على قطع التيار الكهربائي وليس فقط تحويله كما هو الحال بالنسبة لمحولات منبع التيار القائمة على الثايرستورات. هذا وتفتح التكنولوجيا الجديدة-تيارمستمر.محول منبع الثوثر سبلا جديدة للنقل على غرار الاتصال مع الشبكات الضعيفة والميتة والعديد من المزايا الأخرى المتعلقة بالربحية و العائدات اضافة الى احترام البيئة و سهولة التطبيق ومن المتوقع أن تصبح سريعا هذه التكنولوجيا الخيار الامثل لنقل الطاقة، في حالة العديد من التطبيقات التي يتعرض فيها النقل بواسطة التيارالمتناوب و التيارالمستمر بالطرق التقليدية الى العيد من العوائق في هذا السياق، تكمن اهمية استخدام المحولات متعددة المستويات في قدرتها على توليد موجات عالية الجودة تترتب عنها العديد من المزايا بدءا بالحد من التوافقيات الواقعة في في الشبكات المغلقة ، وصولا الى تحقيق مستويات عالية جدا من الجهد.

الكلمات المفتاحية

نظام تيار الجهد العالي المستمر (HVDC)، محول منبع الثوثر(VSC-HVDC)، PWM.

CONTENTS

LIST OF FIGURES

LIST OF TABLES

NOMENCLATURE

List of Acronyms

° C	Degree Celsius
AAC	Alternate Arm Converter
AC, ac	Alternating Current
ABB	ASEA Brown Boveri
APOD	Alternative Phase Opposite Disposition
AVM	Average Value Models
BJT	Bipolar Junction Transistor
BCA	Balancing Control Algorithm
BTB	Back-to-back
CCSC	Circulating Current Suppressing Controller
CDSM	Clamp Double Sub-module
C-EPRI	China Electric Power Research Institute
CSC	Current Source Converter
CSSM	Clamped single- Sub-module
DC,dc	Direct Current
DCPFCs	Dc Power Flow Control Devices
DFIG	Double Fed Induction Generators
DM	Detailed Model
DSPs	Digital Signal Processors
EM	Equivalent Model
EMT	Electromagnetic Transient
EMTP-RV	Electromagnetic Transients Program – Restructured Version
ENTSO-E	European Network of Transmission System Operators for Electricity
FBSM	Full Bridge Sub-module
FRT	Fault Ride Through
GTO	Gate Turn-off Thyristor
HBSM	Half-Bridge Sub-module
HVAC	High Voltage Alternating Current
HVDC	High Voltage Direct Current
IGBT	Insulated Gate Bipolar Transistor
KVL	Kirchhoff's Voltage Law
LCC	Line Commutated Converter
MMC	Modular Multi-level Converter

MOSFET	Metal-Oxide-Semiconductor Field-Effect Transistor
MTDC	Multi-terminal Direct Current
NLC	Nearest Level Control
NPC	Neutral Point Clamped Converter
O&M	Operation and Maintenance
OWF	Offshore Wind Farm
PCC	Point of Common Coupling
PLL	Phase-Locked Loop
PLUS	Power Link Universal System
POD	Phase Opposite Disposition
PS	phase-shifted
p.u	Per Unit
PWM	Pulse Width Modulation
RAM	Random Access Memory
RTE	Réseau de transport d'électricité
SCR	Short Circuit Ratio
SFM	Switching Functions Model
SHE	Selective Harmonic Eliminated
SMs	Sub-modules
SiC	Silicon Carbide
SPWM	Sinusoidal Pulse Width Modulation
STATCOM	Static Synchronous Compensator
SVS	Series Voltage Sources
TSOs	Transmission System Operators
UFMCB	Ultra-Fast Mechatronic Circuit Breaker
UHV	Ultra-High Voltage
VSC	Voltage-Source Converter
VSR	Variable Series Resistors
XLPE	eXtruded cross-bound PolyEthylene

List of Main Symbols

a,b,c	Phases a, b, c
C	Submodule capacitance
d,q	Components of the synchronous dq reference frame
k	Phase number
K_{droop}	Droop gain
L	Inductance
m	Carrier index
N,n	Number of sub-modules
P	Active output power
Q	Reactive output power
R	Resistance
T, t	Time
Udc	DC Voltage
X	Reactance
α	Firing angle
μ	Commutation angle
δ	Phase angle of reference voltage
Y	Star Transformer Connection
Δ	Delta Transformer Connection
ω	System frequency
θ	Voltage-reference phase shift
φ	Phase angle
*, ref	Reference

RÉSUMÉ DE LA THÉSE EN LANGUE FRANÇAISE

INTRODUCTION

L'électricité est traditionnellement produite, transportée et distribuée sous forme de courant alternatif et utilisée sous cette même forme, à l'exception de quelques systèmes de traction et processus industriels sous forme de courant continu. Ce choix technique fut effectué durant la fin XIXème siècle lors de la « la guerre des courants » pour les raisons majeures que l'on citera, à savoir sa simplicité de production (les alternateurs sont plus simples et plus fiables que les génératrices à courant continu), sa facilité à changer de niveau de tension à l'aide de transformateurs, ainsi que sa facilité à interrompre le courant du fait que celui-ci s'annule naturellement de façon périodique. Ainsi, les réseaux électriques se sont donc développés, en courant alternatif, avec le déploiement de gros moyens de production centralisés raccordés à des réseaux de transport maillés interconnectés auxquels sont connectés les réseaux de distribution. En parallèle, les besoins en consommation électrique sont en croissance soutenue, et devraient doubler au niveau mondial d'ici 2040. Les marchés de l'électricité se sont ouverts à la concurrence (libéralisation du marché de l'électricité), et les énergies renouvelables se développent pour la production d'énergie électrique dans le cadre des engagements pris par l'Union Européenne, ce qui implique une nécessité de renforcer et d'interconnecter les réseaux électriques. Ainsi, il est parfois nécessaire de construire de très longues lignes aériennes, des lignes souterraines enterrées ou sous-marines, ou de relier des réseaux frontaliers (parfois asynchrones). Or, dans ce domaine, le transport HVAC « High Voltage Alternating Current » montre ses faiblesses et limites, voire ses incapacités (interconnexion de réseaux asynchrones), et laisse la place au courant continu, le HVDC « High Voltage Direct Current » pour lever ces problématiques.

Grâce à l'évolution de l'électronique de puissance, l'utilisation du courant continu à haute tension est devenue possible, donnant naissance à l'appellation HVDC, ou encore CCHT pour l'appellation française « Courant Continu à Haute Tension », à partir de 1954. C'est une technologie permettant de transporter de très fortes puissances (7200MW en 2013). Le principe est de convertir, grâce à l'électronique de puissance, un courant alternatif en courant continu (redresseur), transporter cette puissance sur de grandes distances, puis reconvertir la puissance en sens inverse (onduleur).

La conception des convertisseurs a alors tiré parti de ces technologies. Nous les rencontrons à présent sous la forme de convertisseurs fonctionnant en source de tension (VSC : Voltage Source Converter). Ces convertisseurs sont du type quatre quadrants. De plus, ils opèrent à n'importe quel facteur de puissance et des commandes conçues à partir de Modulation de Largeur d'Impulsion (MLI ; en anglo-saxon PWM, Pulse Width Modulation) peuvent leur être associées. Ces commandes permettent l'approximation de la tension de référence de sortie par la réalisation d'une tension moyenne de même valeur sur une période de commutation. Pour cela, elles utilisent une modulation temporelle des niveaux possibles les plus proches. Leur profil de tension de sortie AC est meilleur du point de vue harmonique. Ces convertisseurs représentent l'avenir pour la conception des systèmes HVDC et ils peuvent être les candidats idéaux pour les domaines d'application suivants :

- La connexion de sources d'énergie renouvelables telles que les éoliennes.
- L'acheminement d'électricité vers des îles.
- L'apport d'énergie à des grandes villes qui sont soumises à des contraintes environnementales et de sécurité.

CONTEXTE GENERAL DE LA THESE

Actuellement, l'une des préoccupations des intervenants dans le secteur de l'énergie est la limitation de la capacité d'échange entre les différentes régions et l'approche qui s'ensuit des limites de stabilité du réseau électrique. Cette capacité d'échange entre zones, est limitée à cause de l'insuffisance d'interconnexions physiques et de la capacité réduite des lignes et câbles. De plus, plusieurs facteurs ont un impact sur la surexploitation de lignes :

- L'intégration massive de sources d'électricité d'origine renouvelable, notamment des fermes éoliennes offshores et des grands parcs solaires.
- L'augmentation de la consommation électrique.
- La libéralisation du marché électrique, qui impose des échanges commerciaux qui ne sont pas toujours compatibles avec les réalités physiques.

Ces facteurs viennent accroître le besoin de renforcer les réseaux et la capacité de transport des lignes, et à réfléchir sur un nouveau paradigme de réseau électrique du futur. Les avantages des liaisons HVDC peuvent représenter une solution attractive pour résoudre les problèmes d'interconnexion entre les grands centres de production d'électricité d'origine renouvelable (éolien offshore, PV, etc.) et les centres de consommation. En Algérie, les liaisons HVDC auront certainement une place dans l'intégration des énergies renouvelables dans le sud algérien ainsi que l'interconnexion dans le bassin méditerranéen, où ils seront utilisés pour relier les ressources éoliennes, hydrauliques et solaires avec les pays voisins en constituant un réseau DC robuste densément maillé.

Dans le cas des interconnexions transméditerranéennes l'installation des HVDC est largement motivée pour la nature sous-marine et les longues distances d'interconnexion, sauf exceptions comme le détroit de Gibraltar (30 km) ou la connexion Sicile-Calabre (38 km). On peut imaginer que ces liaisons, assez espacées pour l'instant, deviennent progressivement les éléments constitutifs d'un grand réseau hétérogène où il y aura place pour différentes technologies. On trouvera ainsi des lignes HVAC pour les interconnexions courtes, des liaisons HVDC point-à-point pour des longues distances sous-marines ou terrestres, et des réseaux DC multi-terminaux, notamment pour interconnecter les groupements de fermes éoliennes et solaires entre eux et avec les points d'évacuation.

En termes de technologies, une grande diversité est probable. Les liaisons HVDC en source de courant seront utilisées pour les interconnexions de plus hautes puissances pour relier des réseaux forts. Les liaisons HVDC en source de tension seront probablement davantage utilisées que les liaisons de type CSC pour interconnecter des sources intermittentes et des réseaux faibles, comme les réseaux insulaires ou ceux des sources d'électricité d'origine renouvelable.

La compagnie nationale algérienne Sonelgaz envisage d'exporter de l'électricité en Espagne en installant :

- entre l'Algérie et l'Espagne (REE/Sonelgaz) : deux câbles de 1000 – 2000 MW, 400/500 kV relie Terga (Algérie) avec le Littorale de Almeria (Espagne) par un câble de 280 km. Un investissement de cette nature serait très utile pour éviter de congestionner les réseaux à 400kV tant de l'ONE que de la REE. Le coût de ce projet serait de l'ordre de 800 M€. Ce projet pose des problèmes de financement et de statut juridique (ligne régulée, ou ligne privée ?) qui ne sont pas encore tranchés. La Sonelgaz (Société algérienne de l'électricité et du gaz) a d'ailleurs négocié un droit de transit auprès de l'ONE pour pouvoir accéder aux câbles du détroit de Gibraltar ;

- entre l'Algérie et l'Italie (TERNA/Sonelgaz): deux câbles de 500 –-1000 MW, 400/500 kV entre El Hadjar (Algerie) et Sardaigne (Italie) par un câble de 350 km. Ces câbles arriveraient en Sardaigne et se connecteraient aux liaisons Italie-Corse et Italie-Sardaigne (de deux fois 500 MW, 500 MW ont déjà été mis en service depuis 2008), ce qui conduirait à renforcer le réseau de transport de la Sardaigne. En outre, on notera que, techniquement, les profondeurs rencontrées (2 000 m) correspondent aux limites des possibilités actuelles de la technologie de pose des câbles. Le coût de ce projet serait de l'ordre de 700 M€ ;

TECHNOLOGIE DES LIAISONS A CONVERTISSEURS SOURCE DE TENSION (VSC-HVDC)

L'expérience industrielle des liaisons VSC-HVDC est très récente en comparaison de celle des liaisons CSC-HVDC. Le premier système VSC-HVDC comportant des IGBT et une commande de type MLI (Modulation de largeur d'impulsion) a été installé à Hellsjön (Suède) en 1997. L'interconnexion faisait 10 km et pouvait transporter 3 MW sous ± 10 kV. Depuis 1997, l'évolution de cette technologie a été très rapide, les IGBT sont désormais les semi-conducteurs de puissance standard pour ce type d'applications. Malgré leur niveau de puissance plus modeste par rapport aux CSC-HVDC les liaisons VSC-HVDC présentent plusieurs facteurs intéressants [1] [2] [3] [4] [5] [6] [7]:

• elles ne souffrent pas de raté de commutation causées par les perturbations du réseau,

• les puissances active et réactive peuvent être commandées librement dans les quatre quadrants,

• il est possible de connecter un VSC-HVDC à un système électrique qualifié de « faible » (à puissance de court-circuit réduite) ou même sans source de génération propre,

• les transformateurs ne sont pas nécessaires pour assister à la commutation des semi-conducteurs totalement commandés,

• elles offrent une dynamique plus élevée et, à la faveur des commandes de type MLI, les filtres sont plus réduits.

L'inconvénient principal des liaisons VSC-HVDC se trouve dans les niveaux de tension et puissance qui peuvent être atteints. Ces niveaux de puissance et tension sont beaucoup plus faibles que dans les liaisons CSC-HVDC. Cependant cette différence est en train d'être réduite.

La technologie du VSC à deux niveaux, est très proche d'atteindre un degré de maturité, quand il s'agit d'applications en basse et moyenne puissance. Plusieurs applications ont été mises en œuvre, notamment dans les entraînements en moyenne puissance. Néanmoins, afin de pouvoir évoluer de la même façon dans les applications de fortes puissances, il est nécessaire de progresser sur les points suivants : • composants, • topologie, • commande.

La course incessante se poursuit pour développer des semi-conducteurs de puissance à haute tension et à haute intensité capable d'entraîner des systèmes de forte puissance. Actuellement, une forte concurrence subsiste entre l'utilisation de topologies de convertisseurs classiques avec des semi-conducteurs de haute tension, et l'utilisation de nouvelles topologies de convertisseurs utilisant des composants de moyenne tension.

Finalement, la topologie multi-niveaux la plus récente, et qui s'avère être la plus prometteuse, est: le Modular Multilevel Converter. Il a été proposé en 2002 par R. Marquardt, A. Lesnicar, and J. Hildinger. Le principe de fonctionnement de la topologie multi-niveaux réside dans l'insertion de sous-modules, composés par deux interrupteurs, ayant comme finalité d'engendrer une forme d'onde multi-niveaux. Un tel convertisseur produit de faibles pertes de commutation, parce qu'il fonctionne à une fréquence de commutation relativement faible et, en conséquence, possède un contenu harmonique réduit quand on le compare aux convertisseurs classiques à deux niveaux.

Cet aspect permet d'atteindre de bonnes performances avec des filtres notablement plus réduits, voire inexistants. La topologie MMC admet en option de fonctionner sans transformateur, car la tension est distribuée également entre chaque condensateur. Sa modularité assure un fonctionnement plus fiable et facilite sa maintenance. Il présente un seul lien en continu auquel il est possible de raccorder un ou plusieurs convertisseurs, adapté aux applications multi-terminaux sans avoir besoin d'un condensateur entre les deux terminaux. La plupart des efforts de recherche en cours actuellement sont axés sur la conception des systèmes de régulation adaptés à ce type de convertisseurs.

Le premier convertisseur modulaire multi-niveaux assurant une liaison à tension continue (HVDC) est opérationnel depuis 2010. Il montre à la fois la viabilité industrielle et la jeunesse de ces systèmes. En effet, le Trans-Bay-Cable Project assure un transfert de puissance de 400 MW de Pittsburg à San

Francisco (Californie, USA) via un câble sous-marin de 88 km. Cette réalisation a clairement permis de valider les avantages théoriques de ce type de structure. Le volume d'occupation est très faible en raison de l'absence de filtres. Certains dispositifs à l'étude pourraient atteindre des capacités de transmission allant jusqu'à 1000 MW. Ces systèmes permettront de relever les défis futurs imposés aux réseaux de transport, comme l'intégration de grandes quantités de sources d'énergies renouvelables ou en augmentant la capacité de transmission de puissance des réseaux existants.

Cette topologie est constituée de plusieurs sous-modules (SMs) connectés en séries. Chaque sous-module contient deux IGBTs avec leurs diodes antiparallèles et un condensateur qui sert comme accumulateur d'énergie. Dépendamment de l'application et de la capacité de puissance requise, les niveaux du MMC peut varier de quelques dizaines à des centaines de sous-modules par demi-bras. Pour les systèmes HVDC et FACTS, un MMC peut comprendre des milliers de commutateurs de puissance. Le projet Trans Bay Cable, par exemple, comprend plus de 200 SMs par demi-bras et le projet INELFE utilise plus de 400 SMs par demi-bras.

Récemment, des projets de VSC-HVDC associés à des niveaux de tension et de puissance plus importants ont été réalisés :

• plusieurs interconnexions entre l'Allemagne et des fermes éoliennes offshores ont été réalisé durant les années 2012, 2013 et 2014 : les interconnexions BorWin2, Dolwin1, Helwin1 et SylWin1. Ces interconnexions ont une capacité de transport d'entre 546 et 864 MW et une tension d'entre 250 et 320 kV. Les distances d'interconnexion varient entre 130 et 205 km.

• l'interconnexion NordBalt, entre la Suède et la Lituanie, avec une puissance nominale de 700 MW et une tension de 300 kV pendant une distance de 450 km.

• le projet de Tres Amigas, aux Etats-Unis, permettra d'interconnecter les trois principaux réseaux électriques américains (le réseau est, le réseau ouest et le réseau de Texas). Cette interconnexion sera la première plate-forme de ce type dans le monde et représente, également, le plus grand projet de « smart grid » aux Etats-Unis. Les stations pourront fournir 750 MW à 345 kV. L'exploitation commerciale de cette interconnexion a commencé en 2015.

MODELISATION ET CONTROLE DES MMC

Compte tenu du nombre très élevé de composants semi-conducteurs dans les nouveaux convertisseurs de type MMC, il est très difficile de modéliser et simuler l'ensemble de ces composants dans les programmes d'Électromagnétique Transitoire (EMT). Les modèles MMC détaillés sont composés de milliers d'IGBT/diode et doivent utiliser de petits pas de temps d'intégration numérique pour représenter avec précision les événements de commutations rapides et simultanées. Les simulations et les calculs informatiques introduits par les modèles détaillés compliquent l'étude des événements en régime permanent et transitoire mettant en évidence la nécessité de développer des modèles plus efficaces qui assurent un comportement similaire de la réponse dynamique.. Une tendance actuelle est basée sur des modèles simplifiés à valeur moyenne (AVM) capable de fournir suffisamment de précision pour des simulations dynamiques. Les modèle MMC en AVM ont été présentés dans [8] et [9]. Ces modèles simplifiés sont capables de fournir suffisamment de précision pour les simulations de type EMT, cependant la validité de ces modèles doit être évaluée. Dans cette thèse, quatre différentes modélisations sont étudiées et présentées. Les limites de validité de chaque modèle sont discutées et détaillées [8].

L'objectif de cette thèse est de développer des modèles moyennés qui reproduit avec précision le comportement statique et dynamique, en plus les transitoires des systèmes VSC-HVDC dans des programmes de type EMT. Ces modèles simplifiés représentent la valeur moyenne des réponses des dispositifs de commutation, convertisseurs, et des contrôles à l'aide de techniques de valeur moyenne, de sources contrôlées et des fonctions de commutation. Cette thèse contribue également à l'élaboration de modèles détaillés utilisés pour valider les

modèles moyenne proposés. Comparaison des différentes topologies de convertisseur approprié pour VSC-HVDC transmission, y compris leurs avantages et leurs limitations, sont également discutés.

La particularité des liaisons HVDC est de faire appel à un système de contrôle dédié qui va en grande partie déterminer le comportement dynamique de la liaison tant pour des grosses perturbations (défauts sur le réseau) que pour des petites perturbations. Au vu du grand nombre de sous module (400 à 500) par demi-bras, il est difficile de réaliser le contrôle-commande du MMC complètement sans simplifications. Comme tout convertisseur le contrôle-commande peut être décomposé en deux parties :

Le contrôle éloigné Le contrôle éloigné se focalise sur le contrôle des grandeurs moyennes pendant la période de contrôle (calcul des 6 fonctions de conversion) pour engendrer les grandeurs souhaitées (Puissance AC de références ou puissance DC de référence, énergie stockée dans le convertisseur).

Le contrôle rapproché Le contrôle rapproché a pour rôle l'équilibrage des tensions des condensateurs des sous modules par demi-bras. Pour cela, il active le nombre de sous module nécessaire (fonction de connexion) en fonction de chacune des tensions des sous modules, du signe du courant, et du nombre de sous module actifs exigé par le contrôle éloigné.

INTEGRATION DES EOLIENNE DANS LES RESEAUX ELECTRIQUES

L'intégration des éoliennes à grande échelle devra se faire onshore, mais surtout offshore. La connexion de ces sites offshore représente alors des défis intéressants pour les gestionnaires de réseaux électriques nécessitant de nouvelles méthodes pour concevoir et exploiter le système. Cela passe notamment par la mise en place de réseaux à technologie continu qui seront ensuite raccordés aux réseaux alternatifs. Ce raccordement se fait par l'intermédiaire de convertisseurs utilisant la technologie VSC-HVDC. Cette technologie combine la fléxibilité, la capacité de transmission, la contrôlabilité et l'opérabilité nécessaire par les exigences techniques et commerciales. L'éolien offshore favorise la technologie " machine asynchrone double alimentation (MADA) " pour laquelle le parc est connecté au réseau principal à l'aide d'un système de transmission VSC, Il n'y a alors pas de lien direct entre les machines et le réseau principal AC. Il en résulte plusieurs avantages techniques et économiques pour les gestionnaires du système de transport (TSOs), les développeurs et les fabricants de parc éolien. Du point de vue des TSO, le convertisseur VSC cote réseau peut être directement relié à un centre de contrôle pour le pilotage des puissances active et réactive. En outre, le bus continu limite la propagation des perturbations du réseau vers l'éolienne (et vice-et-versa) [10] [11].

Par conséquent, il y a une réduction des contraintes mécaniques sur les éoliennes, ces contraintes étant reportées sur les convertisseurs de puissance. Les principales caractéristiques du système de transmission VSC-HVDC à grande échelle de l'énergie éolienne offshore sont :

• Le VSC-HVDC peut répondre aux recommandations du grid code ; • Les éoliennes n'ont plus besoin d'être conçu pour satisfaire le grid code, l'optimisation peut se concentrer sur le coût, l'éfficacité et la robustesse ;

• Le VSC-HVDC permet de découpler le parc éolien du réseau AC pour réduire la propagation des perturbations ;

• Le VSC-HVDC permet de contrôler la tension au point de raccordement et de éventuellement de participer au réglage de la fréquence. Ainsi, il peut être utilisé pour améliorer le niveau de la stabilité du réseau AC.

RESEAUX A COURANT CONTINU MULTI-TERMINAUX HAUTE TENSION

Un système multi-terminal HVDC (MTDC) est composé de plus de deux convertisseurs connectés par des câbles de courant continu et qui partagent le même bus DC. Les systèmes multi-terminaux HVDC ont des avantages sur les HVDC à deux terminaux sur plusieurs aspects [12] [13] [14]:

- les MTDC permettent l'interconnexion de plusieurs réseaux alternatifs sur des distances moyennes ou longues,

- ils ont des avantages économiques du fait que le coût total des convertisseurs installés dans un système MTDC est généralement inférieur à celui de plusieurs HVDC équivalents à deux terminaux,

- les systèmes MTDC peuvent offrir une plus grande flexibilité dans la distribution des flux de puissance dans des grands réseaux interconnectés, - ils peuvent aider à amortir les oscillations dynamiques non-désirées des réseaux.

En contrepartie, les systèmes multi-terminaux requièrent plus d'appareillage de connexion, pour s'adapter à configuration des interconnexions, ainsi que des systèmes complexes de coordination, de commande de télécommunications. La possibilité de mettre en œuvre des systèmes MTDC dépend fortement de la disponibilité de disjoncteurs à courant continu. Il existe des différences très significatives entre les exigences de disjoncteurs AC et de disjoncteurs DC, principalement à cause de l'absence d'un passage naturel par zéro du courant continu dans les systèmes DC. Les disjoncteurs DC doivent couper les courants de court-circuit très rapidement et ont besoin de dissiper l'énergie emmagasinée dans les inductances du système. Plusieurs stratégies couramment utilisées dans la commande de tension d'un réseau DC sont présentées et discutées. Les stratégies sont présentées dans le contexte de MMC, mais la philosophie s'étend facilement aux systèmes à convertisseurs VSC.

- Commande maître-esclave : un seul convertisseur, le maître régule la tension DC en un nœud, alors que le(s) autre(s) convertisseur(s) injecte(nt) une puissance fixe,
- Voltage margin control : quand la puissance du convertisseur régulant la tension DC dépasse sa limite, un autre convertisseur joue le rôle de régulateur de la tension,
- Voltage droop control : un convertisseur non chargé de réguler la tension DC varie sa puissance injectée/soutirée en fonction de la tension DC à ses bornes.

L'étude et l'analyse théorique ont été complétées par des simulations avec Matlab /Simulink, EMTP-rv et PSCAD.

ORGANISATION DU MANUSCRIT

Ce mémoire est structuré en six chapitres comme suit :

Après une courte introduction, le chapitre 1 est une introduction au transport de l'énergie en courant continu ; il explique pourquoi on s'intéresse au courant continu au lieu de rester en courant alternatif, les différences entre convertisseur source de tension (VSC) et convertisseur source de courant (LCC), et comment les liaisons à base de VSC sont actuellement contrôlées.

Le chapitre 2 présente la topologie du MMC et les équations dynamiques permettant de décrire mathématiquement son fonctionnement, De plus, quatre modèles de simulation du convertisseur, avec différents degrés de simplification, sont détaillés, étudiés, comparés et validés par rapport à un modèle de référence.

Dans les chapitres 3 et 4, Les différentes stratégies de contrôle et modulation du convertisseur modulaires multiniveaux est analysées, les modèles mathématiques de système VSC-HVDC à 401 niveaux reliant deux réseaux et leur validité en les simulant dans un environnement de simulation de type électromagnétique (EMT) EMTP-rv. Ensuite l'étude et la simulation d'un modèle VSC-HVDC à base de convertisseur modulaire multiniveaux pour l'interconnexion des parcs éoliens offshores pendant un fonctionnement normal et perturbé.

Dans les chapitres 5 et 6, les méthodes de contrôle des réseaux à courant continu multi-terminaux sont présentées. Tout d'abord, il s'agit d'une comparaison entre les systèmes alternatif et continu. Ensuite, les méthodes développées dans la littérature sont discutées et des considérations sur la dynamique de ces réseaux à courant continu sont mises en avant. Ensuite, l'étude et la simulation des modèles à 3 et 4 terminaux avec différentes stratégies de contrôle pendant un fonctionnement normal et perturbé. Enfin, une étude détaillé qui traite la faisabilité technique et économique des liaisons HVDC est présentée. Finalement, nous terminons par une conclusion générale qui synthétise notre travail et les suggestions pour l'avenir de recherche à suivre.

INTRODUCTION

BACKGROUND AND MOTIVATION

In an AC system, voltage conversion is simple. An AC transformer allows high power levels and high insulation levels within one unit, and has low losses. It is a relatively simple device, which requires little maintenance. Further, a three-phase synchronous generator is superior to a DC generator in every aspect. For these reasons, AC technology was introduced at a very early stage in the development of electrical power systems. It was soon accepted as the only feasible technology for generation, transmission and distribution of electrical energy.

However, high-voltage AC transmission links have disadvantages, which may compel a change to DC technology:

- Inductive and capacitive elements of overhead lines and cables put limits to the transmission capacity and the transmission distance of AC transmission links.
- This limitation is of particular significance for cables. Depending on the required transmission capacity, the system frequency and the loss evaluation, the achievable transmission distance for an AC cable will be in the range of 40 to 100 km. It will mainly be limited by the charging current.
- Direct connection between two AC systems with different frequencies is not possible.
- Direct connection between two AC systems with the same frequency or a new connection within a meshed grid may be impossible because of system instability, too high short-circuit levels or undesirable power flow scenarios.

Engineers were therefore engaged over generations in the development of technology for DC transmissions as a supplement to the AC transmissions.

HVDC will play an increasingly important role in the future grid because of its advantages in power flow control, efficiency, cost, and right-of-way. In applications such as off-shore wind, DC transmissions have distinct advantages. Most of today's DC transmissions are point-to-point, or two-terminal transmissions. To take full advantage of HVDC, multi-terminal HVDC need to be employed. Concepts such as the proposed European "Super-Grid" are based on multi-terminal HVDC, interfacing the off-shore DC grid with the on-shore AC grids at multiple points.

The use of Voltage Source Converter based High Voltage Direct Current (VSC HVDC) systems is considered to be a major step in facilitating long distance power transfer and integrating remotely located renewable energy sources to major consumption centres. First introduced in 1997, with the commissioning of a 3 MW technology demonstrator at Hellsjon, Sweden [15] [16], VSC technology has improved drastically over the years, in terms of power and voltage rating, harmonic performance and losses [17]. VSC-HVDC is a fairly recent technology, free of several constraints associated with the thyristor-based Line Commutated Converter (LCC) technology, with added degrees of freedom such as independent control of active and reactive power. The VSC eliminates the need for telecommunication links between stations (at least in a point-to-point configuration), which is otherwise a necessity in LCC-HVDC to perform the reversal of power flow. Additionally, VSC stations can be connected to weak ac grids and even perform black-start, in contrast to LCC stations that can only be connected to relatively strong ac grids. This also represents a limitation for the LCC-based technology when it comes to integration of large renewable power generation units (e.g. large scale wind farms), which usually comprise weak grids. These features render the VSC as an ideal candidate for implementation in Multi-terminal HVDC (MTDC) systems, with numerous stations connected in a variety of ways. VSC-

HVDC technology has become increasingly cost-effective and technically feasible in recent years. It is likely to play a vital role in integrating remotely-located renewable generation and reinforcing existing power systems.

The introduction of power electronics in power systems has offered a breakthrough in terms of controllability and stability. Different converter topologies have been proposed for VSC HVDC implementations. The multi-level converter family promises the advantages on modularity, high power density, and fault-tolerance. Simulation models are a vital tool in the research and development of VSC-HVDC systems. Highly accurate models are required in order to give a high degree of confidence in the simulation results and therefore ensure that the system operates in the expected way [18] [9].

The use of Multi-level converters in VSC-HVDC systems has presented a number of challenges. Applying traditional modelling techniques is computationally intensive and impractical in many cases. This has led to the development of new modelling techniques for Multi-level converters. The published literature validating these techniques are however, very limited in some areas, and non-existent in others. More research is therefore required in this area to give a higher degree of confidence to these models and also to assess which models are suitable for which studies. The potential development of HVDC grids has led to the need to produce highly accurate EMT grid models which are valid for a range of studies. The issue of accuracy vs. Computational efficiency is of greater concern for grids than radial systems due to the increased size of the model [19].

The concept of MTDC grids as a counterpart to the very well established High Voltage AC grids is an interesting approach when it comes to high power transmission over long distances. Relevant research in the field used to strictly consider LCC-HVDC stations [16], but recently there has been a shift of interest towards VSC technology.

DC voltage, which indicates the power balance and determines the power flow of DC systems, is of paramount importance in MTDC control. The stability of DC voltage ensures the stable operation of the overall DC system. Unlike frequency in AC systems, DC voltage varies at different terminals, which increases the difficulty in controlling the DC voltage and power flow [20]. This feature together with the fact that the frequency range of DC system dynamics is usually much faster than that of AC systems imply that the DC voltage regulation could be quite challenging. MTDC control has so far attracted a great deal of interest. Limited information however exists to provide a systematic description of the plant models and controller designs for MTDC studies. A variety of MTDC control strategies have been introduced in the previous literature, Different types of control strategies for VSC-MTDC grids have been suggested, e.g. the master/slave control, or droop-based control. Further development is required for control strategies that offer robust performance during steady-state and transient conditions, with improved power flow and direct-voltage handling capabilities.

AIMS AND OBJECTIVES

This thesis aims to address some of the issues raised in the previous section. In order to achieve these aims the following objectives have been identified:

- Design a complete modular multilevel converter based HVDC system using IGBTs in Half bridge submodules.
- Analyse the performance of MMC-HVDC system, power flow control and performance during normal operation and unbalance grid condition with different models (detailed model, equivalent model, switching function model and averaged value model).
- Analyse the performance of back to back MMC-HVDC system, power flow control and performance during normal operation and unbalance grid condition.
- Analyse the performance of offshore windfarms with HVDC system, power flow control and performance during normal operation and unbalance grid condition.
- Investigate and evaluate VSC-HVDC control strategies including both local converter control and MTDC control.
- Investigate the behaviours of MTDC system and perform detailed power flow analysis.

- Analyse the performance of MTDC-HVDC system, power flow control and performance during normal operation and unbalance grid condition with different control strategy.
- Investigate recent developments in HVDC supergrid technologies and the main obstacles and limitation.

OUTLINE OF THE THESIS

This thesis is divided into six chapters, the proceeding chapters are outlined below.

Chapter 1 is an introduction of DC transmission scheme; it explains why DC instead of AC, the differences between Voltage Source Converter (VSC) and Line Commutated Converter (LCC), and presents an overview of multilevel converter based VSC-HVDC.

Chapter 2 discusses the operating principle of the modular multilevel VSC. Concepts that have been identified for control of power transfer between the power converter and the DC circuit as well as the AC circuit will be presented. Also different modelling method for the MMC converter are also presented.

In chapter 3 a general overview of the basics of operation of the MMC along with its control challenges are discussed, followed by a review of latest contributions on MMC modulation techniques, design constraints, and various operational issues, such as capacitor voltage balancing and circulating current control.

Chapter 4 assesses the steady-state and transient performance of the MMC-HVDC link models developed in chapter 2 and the controller proposed in chapter 3 for the HVDC link with two cases, the interconnection of two asynchronous AC networks (50/60 Hz) and the connection of a typical windfarm.

Chapter 5 is dedicated to considerations on the DC grid; first of all, actual discussions on the definition of DC grid topologies are presented and then differences and similarities between AC and DC systems are outlined. The second part is a literature review on methodology to control DC grids. The third part emphasizes the general dynamics of the master/slave and droop controlled DC grid through simulations.

Chapter 6 start with different key drivers for building such installation. Different components of supergrid are analysed. Finally, a selection of several challenges not only technical but also political and economical standing up in the way to establish a supergrid and keeping out its realisation is described, in addition economic comparison between HVAC and HVDC is analysed.

Finally the conclusion concludes all the work presented in this thesis.

Chapter 1 STATE OF ART

High Voltage Direct Current (HVDC) seems going into another booming time since the first test line was developed by Dr. Uno Lamm about seventy years ago in Sweden. The boom of this time can be seen from not only fast increased project number but significant research interests around the whole world as well. The major motivation behind comes from new challenges to the conventional ac grid, e.g. increased proportion of renewable power generation, flexibility requirements from power market, and environment impact. The new HVDC technology based on the Voltage Source Converter (VSC) is a feasible and attractive solution that can fulfil almost all above challenges due to its distinct advantages in the areas of controllability and flexibility, e.g. independent control of active and reactive power, fast control response speed, etc. Therefore, much effort is devoted to further extend its advantages and eliminate its drawbacks, such as high losses compared to Current Source Converter (CSC) HVDC and ac system [21].

In this chapter, we try to follow and summarise the important researches and development of VSC HVDC technology, especially in the VSC and the MMC (Modular Multilevel Converter) topologies. All these researches will show profound and significant effects in the development of VSC-HVDC, and even on the future of electric power systems.

1.1 STATE OF ART

The most commonly used systems are based on current source converter (CSC) or line commutated converter (LCC) HVDC, using thyristor-type valves. Voltage source converter (VSC)-HVDC technology, which uses faster power electronic switches, is a recent development which is seen as a game changer and as the key enabling technology for future (DC) grids [22] [23]. This chapter discusses the overview of different HVDC technologies. The main emphasis is on VSC HVDC.

1.1.1 LCC-HVDC SYSTEMS

Line commutated converter (LCC) HVDC or classic HVDC is built using thyristors in a current source converter (CSC) topology. Thyristors can be switched on, but need the current to pass through zero in order to switch off. The angle at which the thyristors are switched in is called the firing angle, α. Figure 1.1 depicts the basic circuit of a HVDC connection: an AC transformer connected to a six-pulse thyristor bridge.

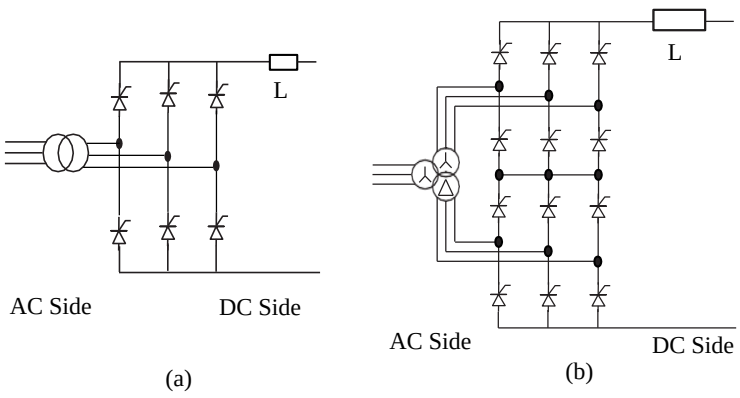

Figure 1.1 Converter topology for the line commutated converter. (a) Six-pulse LCC converter. (b) Twelve-pulse LCC converter.

The typical waveform of such a device is shown in Figure 1.2.

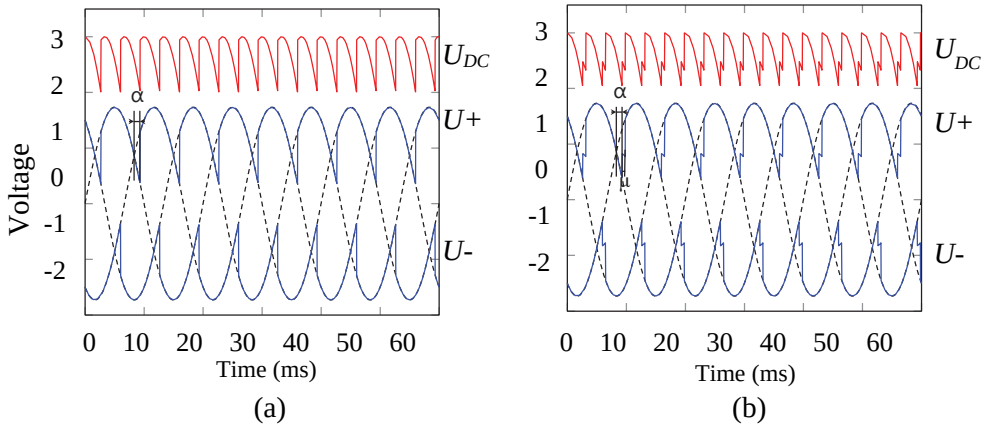

Figure 1.2 Basic waveforms for the six-pulse thyristor converter. (a) Six-pulse converter waveform, neglecting commutation ($\alpha = 27\circ$, $\mu = 0\circ$). (b) Six-pulse converter waveform, with commutation ($\alpha = 27\circ$, $\mu = 9\circ$).

Figure 1.2a shows the waveform for a system without commutation overlap, while in Figure 1.2b the effect of commutation is shown. The commutation process is caused by the system inductance and causes a short overlap period during the transfer of the current between two branches of the converter where both branches conduct. This commutation period is expressed as the commutation angle, μ. In order to reduce harmonics in the AC system, additional harmonic filters are needed. A reduction of the harmonics can also be obtained by utilizing converters with a higher order of pulses: 12-, 18-, or even 24-pulse converters. Most classic HVDC configurations use 12-pulse converters (Figure 1.1b), which cancels out the 5th, 7th, 17th, 19th…, ($6 \pm 1 + k \cdot 12$) harmonics.The transformer of a 12-pulse bridge has aY–Y–Δ three-winding configuration, or a combination of Y–Y and Y–Δ transformers. Both single-phase and three-phase units are used. The leakage reactance of the transformers is typically 10–18% in order to limit the current during a short-circuit fault of the bridge arm [24].

In order to reach the required high voltages, several thyristors are placed in series. A single thyristor can block up to 8.5 kV and can carry currents up to 5 kA. There is normal redundancy built in so that a single thyristor failure does not lead to a failure of the entire HVDC link. The current through the classic HVDC system is always in the same direction. Reversing the power flow is done by changing the polarity of the voltage. Hence, HVDC Classic transmission systems require, for proper converter operation, strong ac networks capable of providing the necessary reactive power. Usually, part of the reactive power is provided by

capacitor banks installed on the ac-side of the HVDC transmission system. Thus, HVDC Classic stations have large footprints and will be improbable on offshore wind farm installations. Nevertheless, HVDC Classic systems continue to be installed world wide for bulk power transmission. Figure 1.3 displays the evolution of HVDC Classic systems voltage with regard to commissioning year and transmission distance [25] [26] [4].

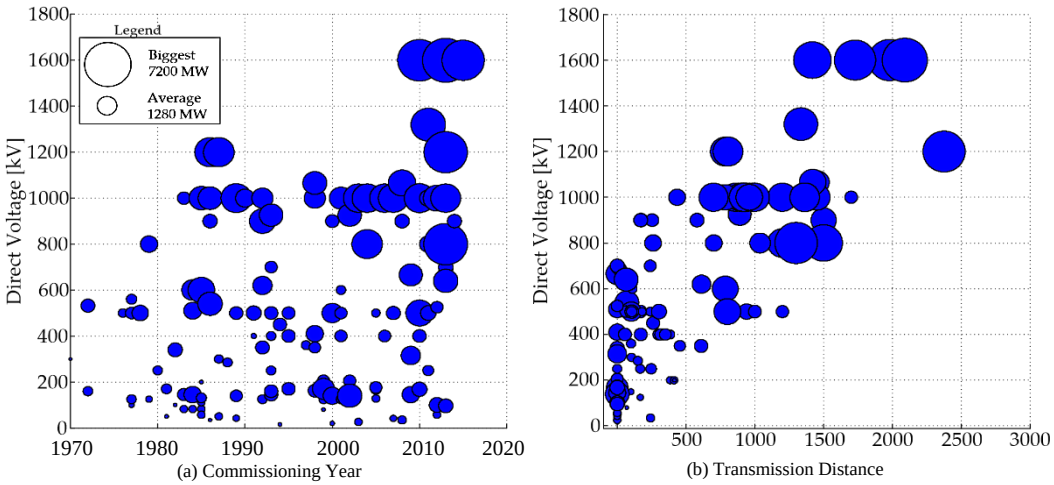

Figure 1.3 Evolution of CSC-HVDC transmission system voltage [27].

1.1.2 VSC-HVDC SYSTEMS

Recent developments of power electronic devices have led to the rise of selfcommutated voltage source converters (VSC) in power system applications. This is mainly attributed to the development of the insulated gate bipolar transistor (IGBT), a device which combines the controllability of the MOSFET with the reliability and power rating of the BJT. Together with the increased computational power of digital signal processors (DSPs), it was possible to use this technology in power transmission. The first VSC-HVDC application was built at the end of the 1990s [28] [29]. Voltage-source converters for HVDC transmission were first employed in 1999, when ABB commissioned the first commercial link, with a nominal power of 50 MW, between the Gotland Island and the mainland of Sweden [3]. Previously, HVDC applications utilised thyristor valves which can only be turned off by the line voltages.

On the other hand, voltage-source converters make use of self- commutating devices – such as the GTO and the IGBT – which can be commanded to turn both on and off. Therefore, a VSC provides a more controllable way to achieve sinusoidal voltages and currents at the output of the converter. However, the power ratings for a CSC-HVDC station are still much higher than those for a VSCHVDC, making the first the current choice for bulk power transmission. Another advantage of CSC-HVDC is that it has inherent lower percentage losses [3] . Table 1.1 shows a comparison between different characteristics of the CSC and VSC-HVDC technologies [3].

Table 1.1 Comparison between CSC and VSCHVDC technologies.

Characteristic	CSC-HVDC	VSC-HVDC
Converter	Line-commutated current-source.	Self-commutated voltage-source.
Switch	Thyristor: turn on capability only.	IGBT: turn-on and turn-off capabilities.
Age	Old: First commercial project in 1954.	New: First commercial project in 1999.
Projects World-wide	146	39
Power Rating	up to 8000 MW	up to 1000 MW
Voltage Rating	up to ± 800 kV	up to ± 320 kV
Footprint (400MW)	Very high. 27 000m² (100%)	Lower. 20 700m² (77%) if two-level 15 675m² (58%) if MMC
Control	Always consume reactive power (two-quadrant operation).	Independent control of active and reactive power (four-quadrant operation).
AC Network Requirements	Needs a reasonably strong ac system to operate (high minimum short-circuit ratio, e.g. SCR > 3)	Can operate with a weak ac network or be used to feed islands and passive ac networks providing frequency control.
AC Faults	Presents commutation failure during ac faults. In case of repeated commutation failures the converter is blocked.	Can maintain active power transfer even under ac faults, fault-ride through capable.
DC Faults	Is capable of extinguishing dc-side faults via control actions.	Has no way of limiting dc-fault currents (because of the free-wheeling diodes), therefore dc breakers are needed.
Losses [% of Rated Power]	0.75% per converter station	0.9% to 1.75% per converter station, depending on the technology used two-level converter, MCC,…
Communication	Special arrangements are needed to coordinate the operation of converter stations.	Communication between the rectifier station and the inverter station in theory is not necessary. The control of each converter station operates in an independent way.
Multi-terminal Operation	Difficult since there is need for coordination between the converters (current order synchronisation) and power-flow reversal involves polarity changes through mechanical switches.	Easier to accomplish since there is little need for coordination between the interconnected converters and power-flow reversal does not involve mechanical switches.
Filters	Harmonic orders are low (e.g. 11-th and 13-th), hence high filtering efforts are needed.	Filters are tuned to higher frequencies and are, therefore, smaller and cheaper.
Reactive power control	Naturally, the LCC HVDC consumes reactive power. This is compensated by shunt capacitor banks. The reactive power control is not easy.	VSC can continuously generate or absorb reactive power, within apparent power limitation.
Black start capability	Not possible	Possible

Voltage-source converters for HVDC transmission applications are now well established inside the power industry. According to ABB, on September 2009 there were ten VSC-HVDC systems in operation [49]. The

VSC technology is best suited for implementation of multi-terminal HVDC transmission networks for its control flexibility [46]. There are different topologies available for creating a VSC-HVDC station such as the one depicted in Figure 1.4. However, only three main converter categories have been implemented thus far: two-level converters, three-level converters and modular multilevel converters.

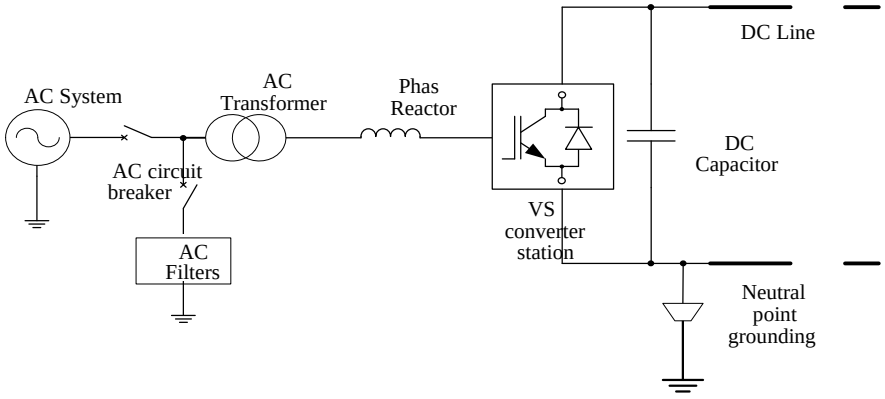

Figure 1.4 Typical layout of a VSC-HVDC station.

1.2 VSC HVDC CONVERTER TOPOLOGIES

The VSC-HVDC transmission system has been implemented using two-level VSCs and multilevel VSCs.

1.2.1 HVDC WITH TWO-LEVEL VOLTAGE SOURCE CONVERTER

Two-level Sinusoidal Pulse Width Modulation (SPWM) topology was used in the first generation of VSC HVDC in the period 1996–2006, and Table 1.2 shows some example HVDC installations. It is also currently commercially available in addition to MMC HVDC but mainly for lower power ratings.

Table 1.2 Examples of the VSC-HVDC transmission systems based on the two-level converter.

Project	Rating	PWM strategy	Applications	Distance (km)	Commissioning year
Terranora (Australia)	180 MW, Vdc = ±80 kV	SPWM	Controlled asynchronous connection for trading	59	2000
Tjareborg (Denmark)	8 MW, Vdc = ±9 kV	SPWM	Wind-power connection	4.3	2000
Gotland (Sweden)	50 MW, Vdc = ±80 kV	SPWM	Permission for under-ground cable	70	1999

Practically, the maximum switching frequency with two-level HVDC converters is around 1.5 to 1.9 kHz (27–33 frequency modulation ratio). Figure 1.5 shows a two-level VSC that uses self-commutated switching devices, mainly IGBTs. The capacitor C_{dc} of the VSC must be sized to maintain a constant DC voltage. The size (footprint) of the two-level VSC-HVDC terminal is around 50% size of the LCC HVDC station.

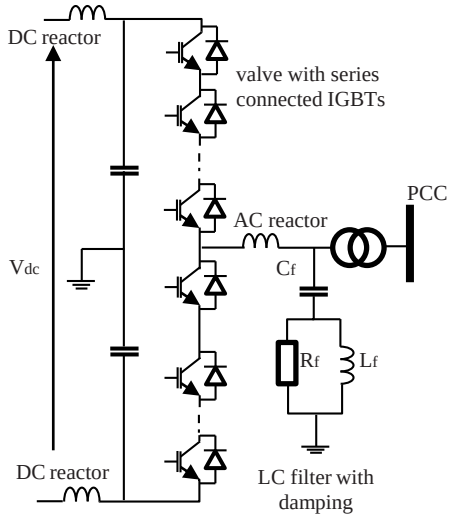

Figure 1.5 One phase of VSC HVDC station based on the two-level converter topology.

The main characteristics of this technology are:

- Simple converter construction that requires a simple control strategy to guarantee stable operation over the entire operating range.
- Lowest number of switches.
- High switching losses and relatively high filtering requirements (requires relatively large AC filters with damping, which adds losses). Note that filters are still much smaller than with LCC HVDC.
- High dv/dt because of large voltage difference at each switching, with a relatively high switching frequency and high common mode voltage. These impose high insulation requirements on the interfacing transformers, and also generate high electromagnetic interference.
- Poor DC fault ride through capability. This represents a major obstacle to the development of multiterminal HVDC, especially with the absence of reliable and proven DCCBs.

1.2.2 VSC HVDC WITH MULTILEVEL CONVERTER

The switching frequency of the multilevel converters compared to two-level converters is substantially lower therefore they may have remarkably lower losses [30]. The existing multilevel topologies are shown in Figure 1.6.

When increasing the number of levels, the voltage balancing will be difficult and the neutral point clamped converter will demand high numbers of clamping diodes making its structure rather complex. For flying capacitor multilevel converter topology a high number of level requires more capacitors more voluminous, pricey and hard loaded capacitors [31]. The application of cascaded H-Bridge converters is limited since separate DC sources are required [32]. The modular multilevel converters proposed first time by Prof. Rainer Marquardt from the University of Bundeswehr, in Munich, Germany [33] [34],are the last category of the multilevel converter used, it can be classified into shunts and series arrangement, all these categories are developed from a cascaded series connection of submodules [35]. The series categories are involved in HVDC application based on half bridge, full bridge, and wave shaping circuit which is the combination of the two-level converter (direct switch) and modular multilevel converter (half or full bridge) [30] [36].

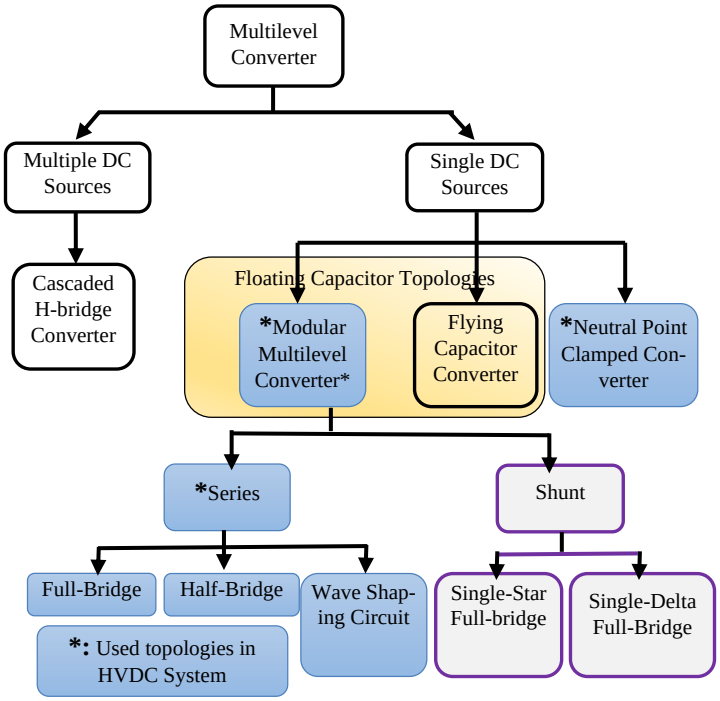

Figure 1.6 Multilevel Converter Family

1.2.3 HVDC WITH NEUTRAL POINT CLAMPED CONVERTER

As the second generation of VSC HVDC, the three-level diode clamped converter (also known as neutral point clamped (NPC) converter) was developed around 2000, with the following objectives:

- To reduce effective switching frequency per device (consequently, lowering switching losses).
- To lower *dv/dt* enabling the use of a transformer with reduced insulation requirements. It also enables low total harmonic distortion at the point of common coupling (PCC) (achieves a further reduction in filter size).

Figure 1.7 shows one-phase leg of the neutral-point clamped converter, which halves the voltage stress and the effective switching frequency per device compared to the two-level converter in Figure 1.5. As an additional benefit, the converter station loss is reduced significantly. However, with the NPC converter it is difficult to meet some grid code transient requirements, for example that the converter must remain in operation during AC grid faults in order to provide reactive power to support the grid. This is an issue because the NPC converter DC capacitor voltage balancing (at $\frac{1}{2}V_{dc}$) is challenging under asymmetrical AC faults, such as a single-phase open circuit fault, single-phase-to-ground and line-to-line faults. Consequently, HVDC manufacturers eventually abandoned the NPC converters in favour of improved two-level converters. Table 1.3 lists NPC VSC HVDC transmission installations.

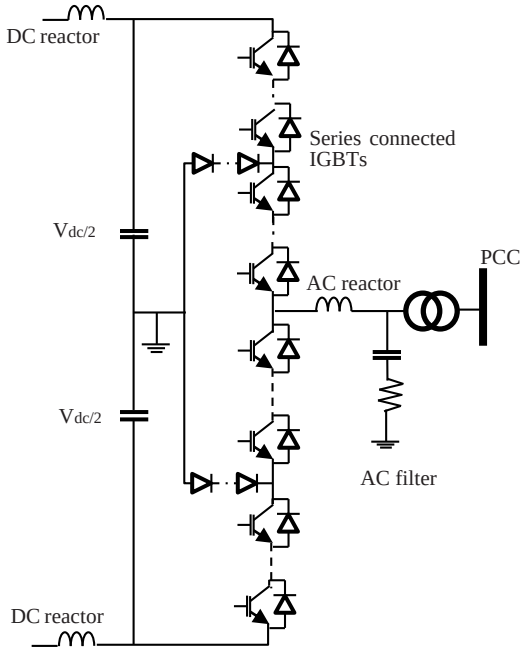

Figure 1.7 One phase of VSC HVDC station based on the neutral-point clamped (NPC) voltage source

Table 1.3 Examples of the VSC-HVDC transmission systems based on the NPC converter.

Project	Rating	PWM strategy	Applications	Distance	Commissioning year
Cross sound (USA) cable	330 MW, Vdc = ±150 kV, *fs* = 1.26 kHz	SPWM	Grid Re-enforcement	40 km	2002
Murray link (Australia)	220 MW, Vdc = ±150 kV, *fs* = 1.35 kHz	SPWM	Grid re-enforcement	180 km	2002
Eagle Pass (USA)	36 MVA, Vdc = ±16 kV, *fs* = 1.26 kHz	SPWM	Power trading and power quality	Back-to- back	2000

1.2.4 MODULAR MULTILEVEL CONVERTER VSC-HVDC TRANSMISSION SYSTEMS

This converter concept exploits the benefits of the multilevel structure and PWM. The filtering requirements are greatly reduced because of the generation of high-quality AC voltage (small AC filters might be required). One cell (module) per arm is switched at a time, which results in only 1–2 kV voltage increments at each switching instant, although some topologies use cells of higher voltages. The use of a large number of levels with small voltage steps results in low *dv/dt* at each switching and reduced voltage stress on the insulation of the interfacing transformers. This allows the use of standard transformers without the need to withstand the DC link voltage or harmonic currents. Furthermore, the effective switching frequency per device is low, resulting in lower switching losses and lower harmonics. On the downside, modular converters require larger number of switches, at least twice the number compared with two-level VSC.

Figure 1.8 shows three-phase of a 2n level modular converter, consisting of 2n-1 cells in each arm. This converter relies on the cell capacitors to create a multilevel voltage waveform at the converter terminal. Each cell has low voltage, which is of the order of a single switch rating or it is built up of a small number of series connected switches. Typically, hundreds of cells are required to build a single valve for DC transmission requirements. As the number of levels increases, the quality of AC voltage waveform becomes better and the harmonic content reduces. The DC link capacitors are not required as individual modules have capacitors. However, some small DC capacitors (around a few microfarads) might be installed in a typical symmetrical monopole configuration in order to create ground reference for the AC voltages. As this topology benefits from

the redundant combination of module connections for each required AC level, the balancing capability is better than with NPC converters.

The MMC performs better than the NPC converter during unbalanced operation and symmetrical/ asymmetrical AC faults which reduces the risk of device failure and system collapse. The ability of the modular converter to ride through different types of AC faults makes it suitable for applications subjected to stringent grid codes requirements. If there is an issue with one phase on the AC system, the remaining two phases of the converter will operate unaffected, potentially at full per-phase power, since there is no common DC capacitor to transfer ripple between phases. The absence of DC capacitors also reduces issues with DC faults, considering that MMC cell capacitors will not discharge into DC fault and this leads to faster post fault recovery. With 2/3 level VSC, post-DC fault recovery requires a period of DC capacitor charging.

The sizing of the cell capacitors requires careful considerations. They dominate the volume requirement for the modules but they are required to store sufficient energy to support the converter DC voltage during transient events. Otherwise the system may fail to meet transient requirements. It will be shown in the modelling section that the cell capacitors behave as series connected AC-side components.

The first commercial MMC based HVDC transmission system project is the 85 km, 400 MW, ±200 kV (±170 MVAr STATCOM functionality) Trans Bay cable project, commissioned in the United States in 2010, and some other example projects are listed in Table 1.4.

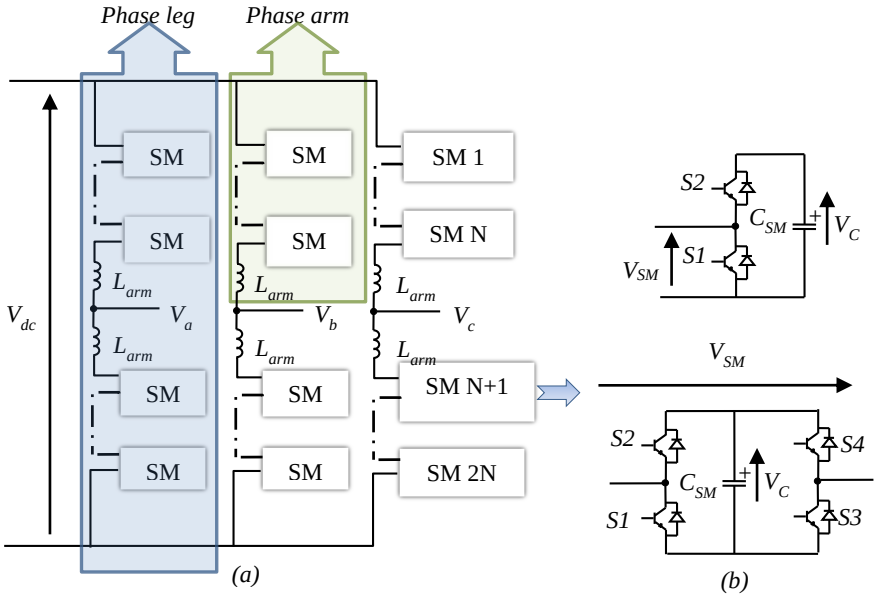

Figure 1.8 (a) Topology of three-phase MMC (b) Half- and full-Bridge sub-module.

Table 1.4 Examples of the VSC-HVDC transmission systems based on the MMC converter.

Project	Installed year	Manufac-turer	DC-link Volt-age(kV)	Power (MW)	Location
Trans bay Cable	2010	**Siemens**	±200	400	USA
Nanhui	2011	**C-EPRI**	±30	18	China
BorWin2	2013	**Siemens**	±300	800	Germany
HelWin1	2013	**Siemens**	±300	576	Germany
DolWin1	2013	**ABB**	±320	800	Germany
Nanao	2013	**C-EPRI**	±160	200/100/50	China
SylWin1	2014	**Siemens**	±320	864	Germany
South-West Link	2014	**Alstom**	±300	1440	Sweden
Mackinak	2014	**ABB**	±71	200	USA
Skagerrak 4	2014	**ABB**	±500	700	Norway-Den-mark
Zhoushan	2014	**C-EPRI**	±200	400/300/100/ 100/100	China
BorWin1	2015	**ABB**	±150	400	Germany
HelWin2	2015	**Siemens**	±320	690	Germany
DolWin2	2015	**ABB**	±320	900	Germany
INELFE	2015	**Siemens**	±320	2×1000	France-Spain
Aland	2015	**ABB**	±80	100	Finland
Troll A 3-4	2015	**ABB**	±60	2×50	Norway
Nordbalt	2015	**ABB**	±300	700	Sweden-Lithua-nia
Xiamen	2015	**C-EPRI**	±320	1000	China
Tres Amigas Super-station VSC	2016	**Alstom**	±345	750	USA
Luoping	2016	**C-EPRI**	±350	1000	China
DolWin3	2017	**Alstom**	±320	900	Germany
BorWin3	2019	**Siemens**	±320	900	Germany
Piedmont - Savoy Link	2019	**Alstom**	±320	2×600	France-Italy

MMC HVDC with full bridge converters is commercially available, however it has not been implemented at the time of writing. The full bridge MMC HVDC converter has similar overall structure as a half-bridge MMC, but each cell uses four switches in full H connection, as shown in Figure 1.8(b). The full bridge cell facilitates either positive or negative voltage at the cell terminals while the half bridge gives only positive voltage. Therefore, full bridge gives more control flexibility, although at the expense of twice the number of switches. Note that at least 3/4 of the (but not all) cells are required to assume full bridge topology in order to achieve system-level benefits. There are some important operational advantages of full bridge over half bridge MMC:

- Full bridge topology can actively control and interrupt DC fault current. It need not be tripped for DC faults. If it is tripped the full bridge converter becomes open circuit for DC faults.
- It can operate with reduced DC voltage. This implies that full bridge MMC can supply full reactive power to the AC system during DC fault conditions.
- The overrating of antiparallel diodes (which is required with half-bridge cells) may not be needed because a high fault current cannot occur.
- Direct current voltage polarity reversal is possible. This is very important to rapidly extinguish the DC fault current path. The post fault DC voltage ramp up can be controlled.
- It is possible to provide higher (typically by up to 20–30%) AC voltage for the same DC voltage using over modulation feasible only with full bridge topology. This implies that for a given IGBT current and DC voltage limitation, full bridge topology can transfer more power, at the expense of increased number of cells.

1.3 DIFFERENT SUBMODULE TOPOLOGIES

Figure 1.9 shows different Submodule topology of Modular multilevel converter [37] [38].

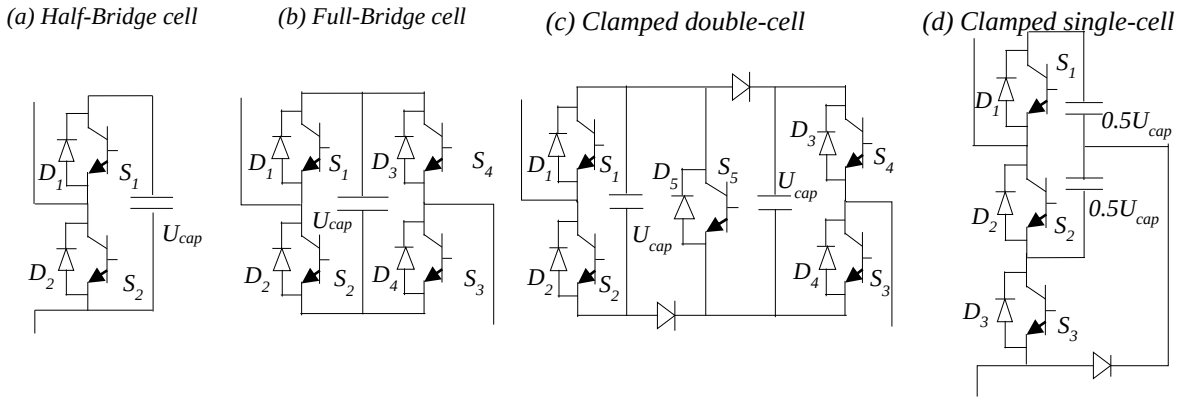

Figure 1.9 Different Submodule topology of Modular multilevel converter

- ***HBSM (Half Bridge- sub-module):*** It is mainly composed of two IGBT switches, two anti-parallel diodes and a dc storage as shown in Figure 1.9(a).
- ***FBSM (Full Bridge- sub-module):*** It consists of four IGBTs with anti-parallel diodes and a capacitor as shown in Figure 1.9 (b). Both the cost and total losses of an MMC-based on FBSMs are significantly higher than that of an MMC-based on HBSMs.When all of the IGBTs of the SMs are blocked, the capacitor voltages can generate reverse voltages to block the ac-side currents, which provide the dc-fault-handling capability [39].
- ***THE HYBRID MMC (FBSMs and HBSMs):*** uses a combination of full bridge and half bridge sub-modules in the arms as shown in Figure 1.10 (a) .The global structure is similar to MMC based on HBSMs, but the phase arms have strings with HBSMs and FBSMs. Both power losses and total number of semiconductors will be reduced compared to the MMC based on FBSMs.
- ***CDSM (Clamped Double-sub-module):*** CDSM represents two equivalent HBSMs shown in Figure 1.9(c). The half bridges are connected positive terminal to negative terminal, so the insert and bypass switch positions are interchanged. The output voltage of the cell is twice the voltage of half-bridge cell. Thus, the desired cell number for the same voltage rating is halved. Its additional devices offer the ability to block DC-side short circuit current by generating emf in the arms.For the clamped double-cell converter, the required number of cells for the same voltage rating is halved compared to the half-bridge MMC [38]. Only half the number of IGBTs and 1.5 times the number of diodes are additional compared to the MMC based on HBSMs. Both power losses and total number of semiconductors will be reduced compared to the MMC based on FBSMs.
- ***CSSM (Clamped single- sub-module):*** similar to the CDSM as shown in Figure 1.9(d), the CSSM is based on the half-bridge cell by adding one IGBT and two diodes. This topology can block dc short circuit with lower semiconductor cost than CDSM by additional devices, however the power losses are higher.
- ***AAC (Alternate-Arm Converter):*** this topology is similar to the standard two-level converter, its arms combine full bridge-cell and series switch strings as shown in Figure 1.10 (b), when the series switches turn on, the full bridge-cell functions as well as the FBSM based MMC. The full bridge-cells offers the converter the capability of controlling dc current during dc-side faults [39].

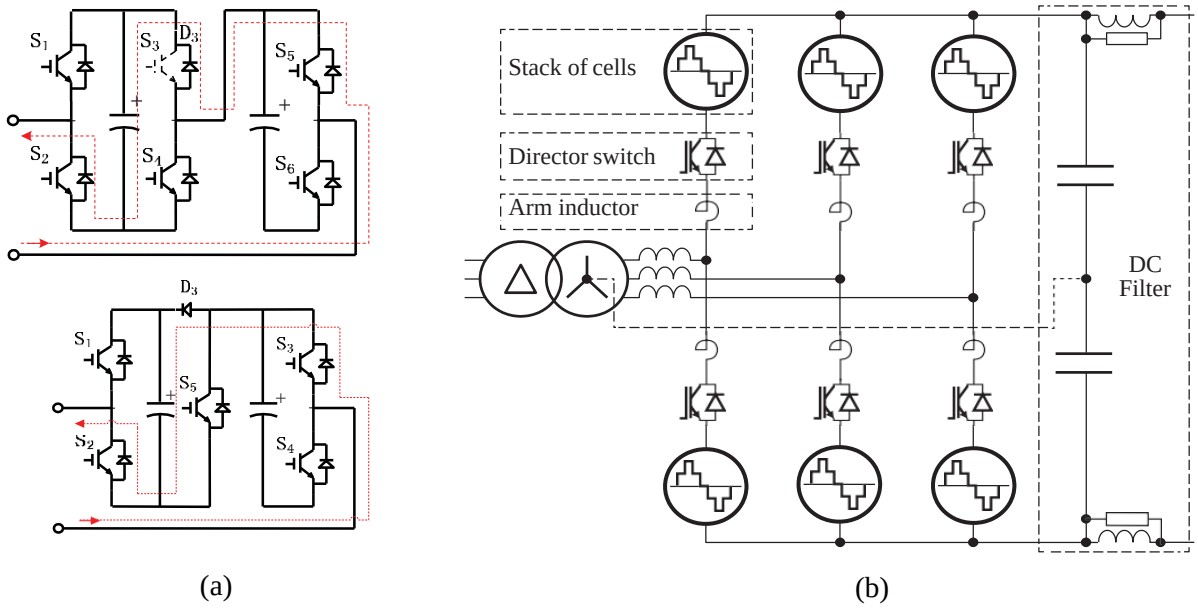

Figure 1.10 (a) hybrid MMC and (b) Schematic of the alternate arm converter

The losses in two level VSC stations with optimised pulse modulation are around 1.4% of the rated transmission capacity and around 80% of these are dissipated in the IGBT valves [15]. With MMC, the valve losses are expected to be much lower [40]. The choice of sub-module topology has a significant effect on valve losses and cost. Cost and Losses of Different Topologies of MMC converter shown in Figure 1.11 are mentioned in [41]; it's clearly that the HBSM implementation for MMCs would be preferred in future DC grid [35].

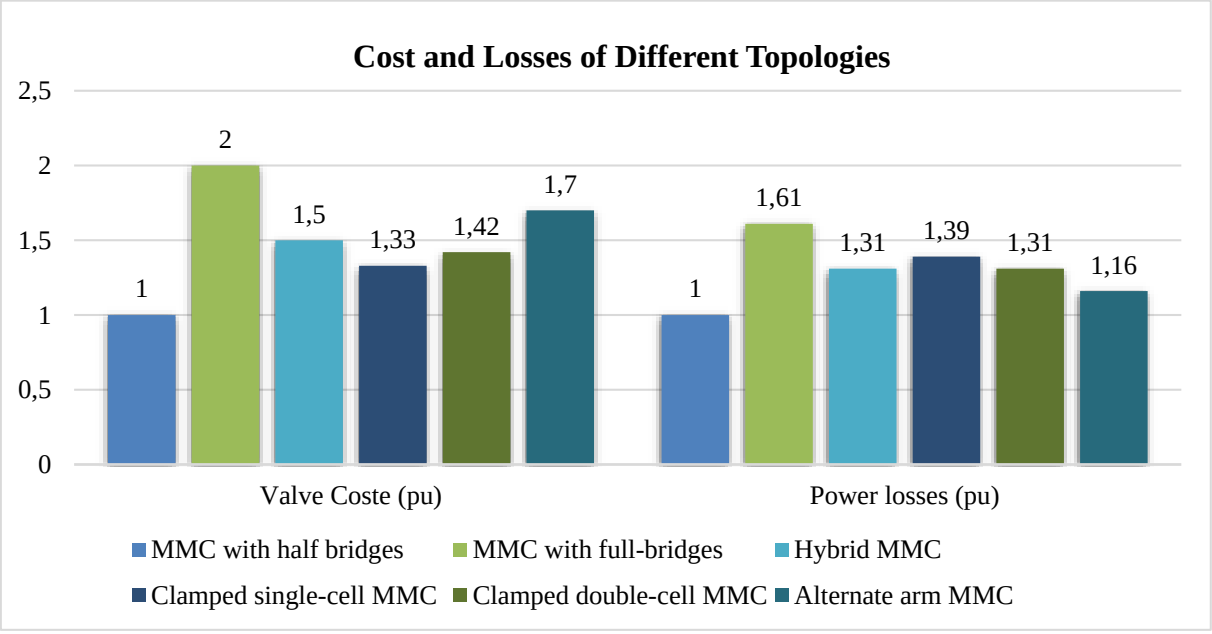

Figure 1.11 Cost and losses of different submodules topologies.

1.4 SUMMARY ON VSC TOPOLOGY

In Table 1.5 there is a summary of conclusions drawn by [42].

Table 1.5 Comparisons of VSC-HVDC topologies [42]

	Two-level	**NPC**	**MMC**
Reactive power capability	Limited by DC link voltage	Limited by DC link voltage and capacitor voltage balancing	Limited by DC link voltage and arm inductance voltage drop
Power flow	100% bidirectional	100% bidirectional (with some restrictions due to modulation index margin for capacitor balance)	100% bidirectional
Harmonic filters and interfacing reactors	Relatively large	Relatively large	Could be eliminated
Conversion losses	Very high	high	low
Switch stress	high	better	low
AC fault ride through capability	Yes	yes	yes
DC fault ride through capability	Poor	poor	excellent

Conclusions drawn on VSC topologies may change because of recent advances in semiconductor devices such as Silicon Carbide (SiC) which are not yet available for HVDC applications. Those devices are expected to improve significantly VSC substations because they can handle higher temperature (i.e 500°C instead of 150°C for silicon) [43].

In normal operation, from a macroscopic point of view, i.e. AC grid phase reactor current control, DC voltage control, active and reactive power control, the behaviors of any VSC topology are similar. Their behaviors differ in case of abnormal operations, for losses, and harmonics. Therefore, for studies focused on power management in normal operation such as dynamic stability phenomena, two-level converters are representative of any VSC topology. Indeed, for the sake of simplicity, computation time saving and development time saving, for those kinds of study, two-level converters can be simulated instead of MMC [44] [45].

1.5 COMMERCIAL VSC-HVDC PROJECT

The first VSC-HVDC-based technology, trademarked HVDC Light, was developed by ABB in 1997 [15]. A SPWM control philosophy is used to control the IGBTs gate switching frequency, producing a two-level AC waveform. Multilevel converter topologies are able to lower the harmonic distortion further and can lower the number of switching operations per switch. These higher-level converter topologies also promise lower switching losses. However, it becomes clear that the system complexity increases with the number of voltage levels. In practice, only two-and-three level converters are currently in use. The first three-level neutral point clamped have been used for the Eagle Pass (Texas and Mexico) in 2002 [7].Figure 1.12 shows the evolution

in converter technology used in a selection of commercial projects: from two-level and three-level NPC towards modular multilevel converters [15] [6] [31].

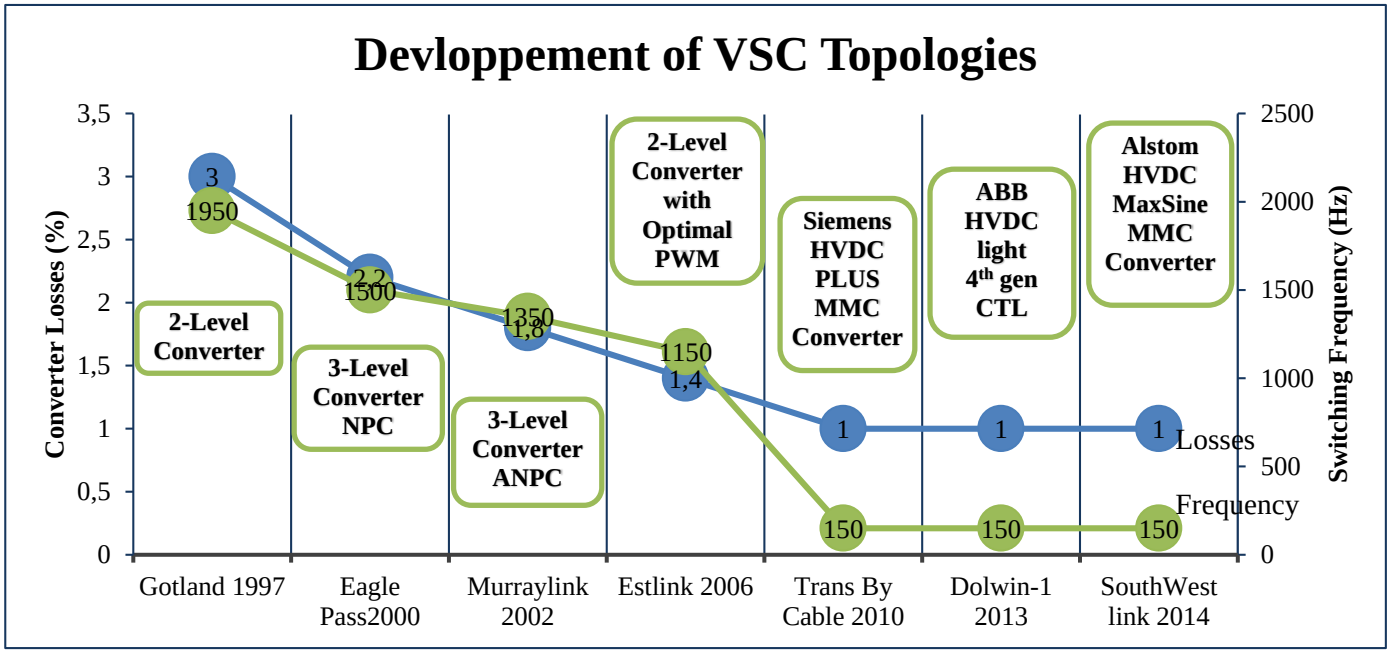

Figure 1.12 the Evolution of VSC-HVDC Technology

The two and three level VSC-HVDC converters have been commercialised exclusively by ABB.since ABB holds different patents when it comes to series-connected press-pack of IGBTs, which is needed for the manufacturing of two-and-three level converters to achieve high power high voltage applications [32]. These converters were developed and marketed over three generations under the brand of "HVDC Light" [2] [15]:

HVDC Light 1^{Gen}: was applied in Gotland (1997) based on two-level converter.

HVDC Light 2^{Gen}: was applied in Murray link (2002) based on three-level converter valves with active neutral point clamping (ANPC), which is an improvement of the neutral-point-clamped (NPC) converter.

HVDC Light 3^{Gen}: was applied in Estlink (2006) based on two-level converter with optimised pulse width modulation (third harmonic injection and selective harmonic elimination).

Due to technology progress, the major HVDC manufacturers have adopted multiple VSC solutions even though they may have different designs of the power electronic converters (HBSMs, FBSMs), the same concepts are followed (Marquardt structure) in order to bring the suitable technical solutions, the principles currently employed are as follows:

1.5.1 HVDC PLUS (POWER LINK UNIVERSAL SYSTEM)

Siemens was the first company to introduce the MMC technology for HVDC applications [46] [47], see Table 1.4. Their converter arm is formed by stacking a sufficient number of HBSMs equipped with a bypass thyristor and a bypass vacuum switch. For HVDC applications each arm has a number of SMs in the range of 200, therefore there is no need for AC filter due to the high number of SMs. They use a closed-loop control means in order to limit the circulating currents. To optimise the use of SM DC voltage, HVDC plus uses conventional Y/Δ transformer configuration to block the third harmonic component [48] [49].

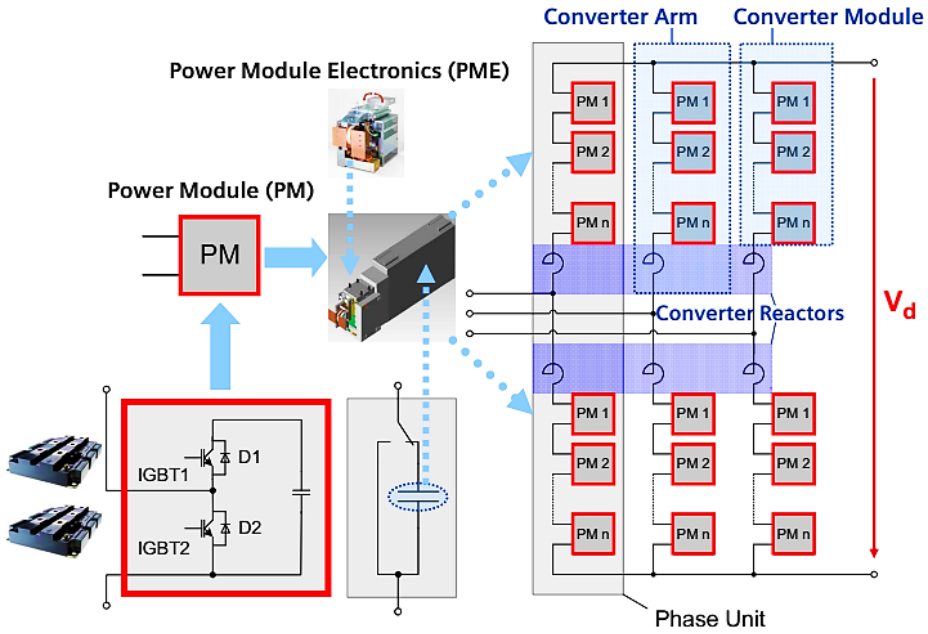

Figure 1.13 Principle schematic of an HVDC Plus converter [48]

1.5.2 HVDC LIGHT 4GEN

Cascaded Two Level Converters are the equivalent of MMC technology being offered by ABB for HVDC applications [2]. Their converter arm is similar to MMC with HBSMs, the main difference resides in the use of series-connected press-pack IGBT (around eight), having a short-circuit failure mode which allows the conventional two-level converter VSC technology to be extended to multi-level VSCs through a cascade connection. For HVDC applications each arm has a number of SMs in the range of 38, whereas a small filter is included in the HVDC Light. They use a parallel resonant filter located at the centre of the phase reactors and tuned at the 2nd harmonic in order to limit the circulating currents and eliminates the third harmonic, hence an Y/Y transformer is used [49].

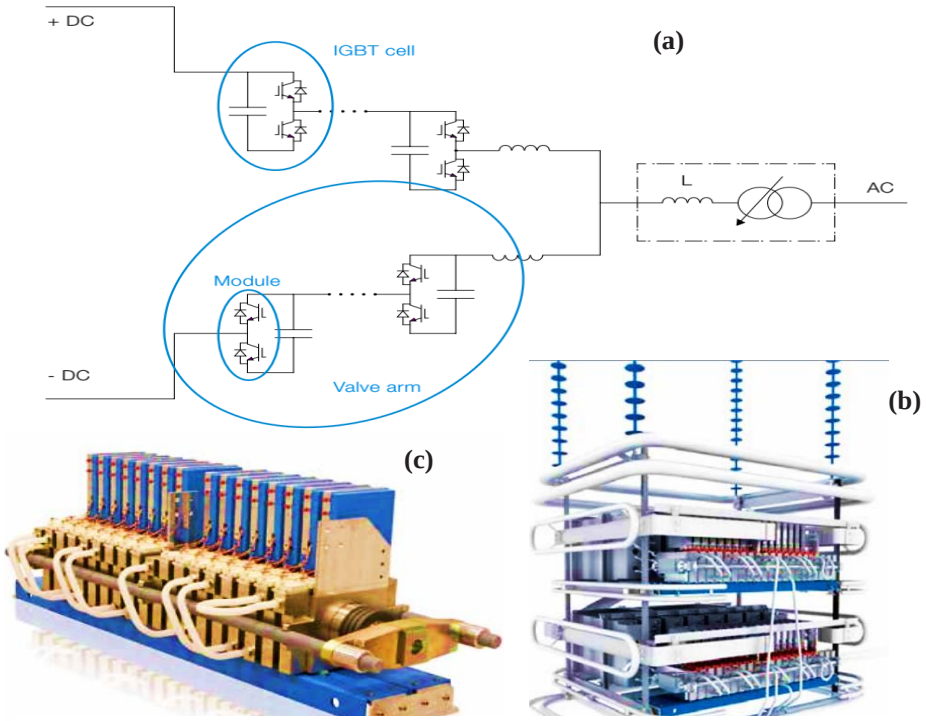

Figure 1.14 Principle schematic of an HVDC Light® converter: a: (one phase), b: One double cell, c: One IGBT module [92].

1.5.3 HVDC MAXSINE

The latest manufacturer to start offering VSC for HVDC applications, offered by Alstom under the brand of “HVDC Maxsine” [5]. Their converter arm is based on a hybrid design of both LCC and VSC technology whereby, multi-level converter elements comprising of FBSMs and HBSMs are used to synthesize the AC waveform, which is then directed to the network using semiconductor switches. Under this design, the semi-conductors are switched in the H-Bridge configuration at the frequency of the AC supply and near zero voltage, which enables the soft switching of the IGBTs, thus minimising switching losses. Another advantage is that we can save space when reducing the number of FBSMs(which are much more voluminous since it contains bulky capacitors) and replacing it with a stack of IGBTs in the director switch [30] [49].

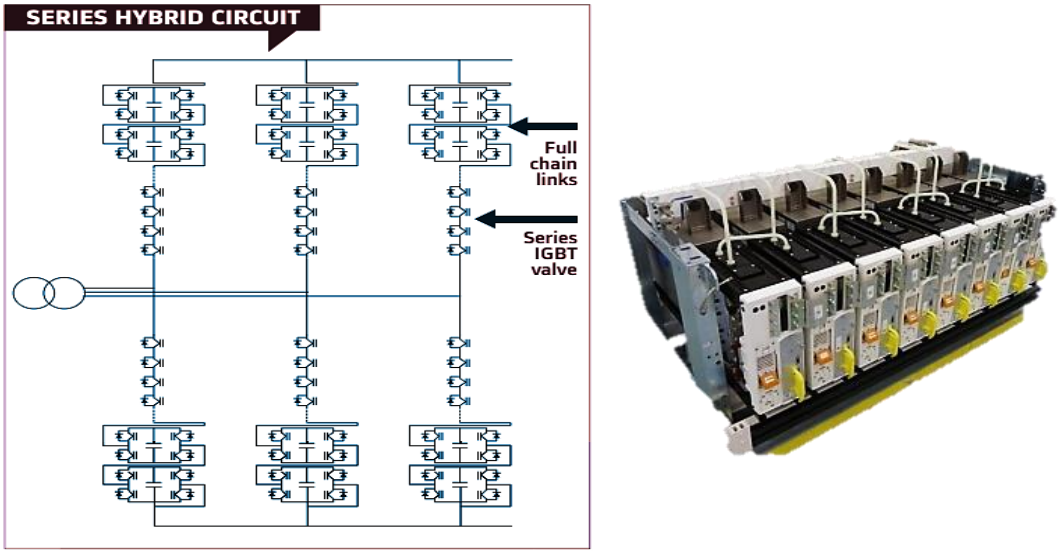

Figure 1.15 Principle schematic of an HVDC Maxsine converter [5].

1.5.4 HVDC FLEXIBLE

China Electric Power Research Institute “C-EPRI” has also developed a VSC converter based on MMC technology for HVDC applications under the name of HVDC Flexible system [50]. An HVDC Flexible converter consists of three phase units; each one includes two converter arms, both with an arm reactor. Depending on the power and voltage ratings, each converter arm could be formed by a number of vertically-stacked valve modules; each module contains six identical sub-modules connected in series. Each sub-module contains two IGBTs as the switching elements and a DC storage capacitor.

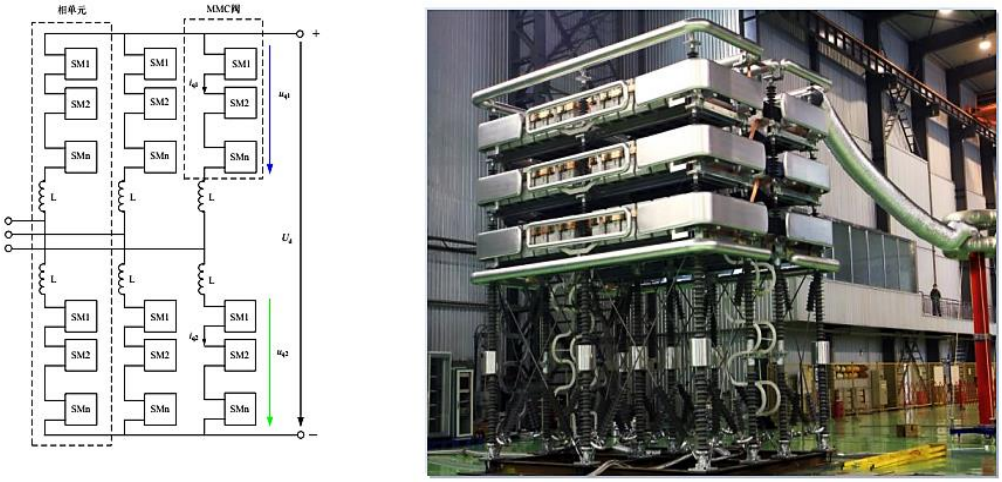

Figure 1.16 Principle schematic of an HVDC Flexible [50].

1.6 CONCLUSION

Voltage source converters have been identified to provide improved performance when used for the implementation of HVDC transmission. However, the standard two-level and three-level voltage source converter circuits are faced with limitations such as high harmonics on the AC waveform, limited number of voltage levels, and are not easily scalable. Modular voltage source converter circuits are a promising new breed of voltage source converters with solutions to most of the problems associated with VSC-HVDC systems using two-level and three-level converter circuits.

A number of the modular multilevel VSCs which have been considered for HVDC applications have been discussed in this chapter. The modular multilevel VSC which has already been implemented in industrial projects of VSC-HVDC was discussed in Section 2.4. Semiconductor loss performance and the cost of differents submodules of the modular multilevel VSC have been compared.

In the next Chapter, the operating principle of the modular multilevel VSC will be discussed. Concepts that have been identified for control of power transfer between the power converter and the DC circuit as well as the AC circuit will be presented. Also differents modelling method for the MMC converter are also presented.

Chapter 2 MMC OPERATION AND MODELLING

Modular multilevel converter (MMC) is an emerging multilevel converter topology introduced in 2001 and it is highly appealing for high voltage applications such as HVDC. MMC achieves high number of voltage levels by connecting several identical power electronic building blocks called sub-modules in series and it has the lowest semiconductor count comparing to other multilevel converters. Modular structure of MMC allows adding modules to the design, which provides redundancy and increases the reliability of the entire system. Several modulation techniques are used for MMC and for high voltage applications with large number of sub-modules switching frequency can be as low as fundamental frequency which greatly reduces the losses.

This chapter introduces the configuration of 3-phase MMC. Each phase of the MMC consists of half-bridge sub-module connected in series. Therefore, the operating states of the half-bridge sub-module are examined in detail. After describing the operation principle of MMC, its control and modulation methods are briefly discussed. The equivalent circuits of MMC on both the AC and the DC sides are derived according to basic circuit theory.

2.1 OPERATION PRINCIPLE OF MMC

2.1.1 CONFIGURATION OF MMC CONVERTER

Modular multi-level converter is introduced to avoid the drawbacks of conventional VSC in HVDC applications. The converter is made of series connection of identical submodules shown in Figure 2.1. Each phase of the converter consists of two arms and each arm includes several sub-modules that represent a controllable voltage source [51]. The three-phase MMC converter configuration used in HVDC applications is shown in Figure 2.1. The converter is composed of three-phase legs that each consists of several sub-modules in series with an arm inductor. The total DC voltage of each MMC arm equals the total DC link voltage and each sub-module in the arm will provide U_{dc}/N if there are N sub-modules in the arm.

Figure 2.1(a) illustrates the schematic diagram of 3-phase MMC. Each phase is composed of two arms, the upper arm and the lower arm. Inductor L_0 and its equivalent resistance R_0 are connected in series with each arm. Besides assisting in power control, the arm inductor L_0 suppresses the circulating current as well as limiting the short circuit fault current on either AC or DC side. Normally N identical sub-modules (SM) are connected in series in each arm [9].

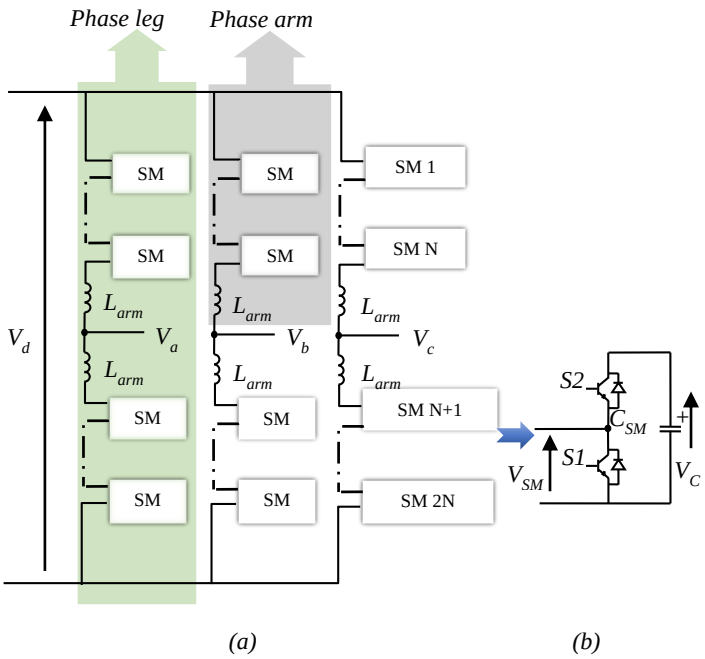

Figure 2.1 (a) Topology of three-phase MMC (b) Half-Bridge sub-module

Sub-modules are inserted or bypassed based on the switching state of two switching devices in each half bridge; two switches are complementary. Table 2.1depicts the sub-module output voltage in different switching states [20]. The switching state of each device depends on the direction of the arm current and reference modulation waveform. When upper switch or diode (S_1 or D_1) conduct the sub-module capacitor is inserted in the arm and conduction of the lower devices (S_2 or D_2) results in bypassing the sub-module capacitor. Once a sub-module is inserted in the arm, the sub-module capacitor can be charged or discharged based on the direction of current flowing into the capacitor. Figure 2.2 shows the switching states of a submodule in MMC [52].

Table 2.1 Sub-module operation states

State	Gate Signal of S_1	Gate Signal of S_2	S_1	S_2	D_1	D_2	Current	Capacitor *C* State	U_{SM}
Abnormal	0	0	Off Off	Off Off	On Off	Off On	Positive Negative	Charge Bypass	U_c 0
Insert/On	1	0	Off On	Off Off	On Off	Off Off	Positive Negative	Charge Discharge	U_c U_c
Bypass/Off	0	1	Off Off	On Off	Off Off	Off On	Positive Negative	Bypass Bypass	0 0

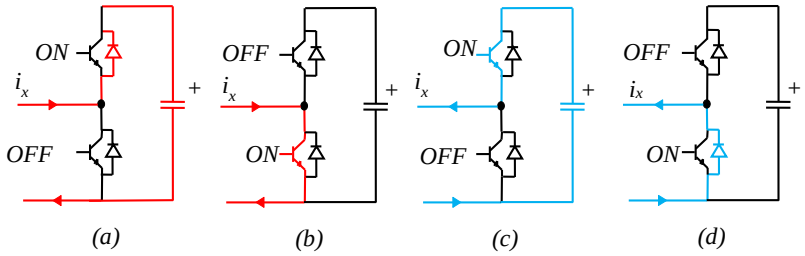

Figure 2.2 Positive and negative current flow in a sub-module with different switching states

According to the description discussed above, insert/on state and bypass/off state are the two required states for normal operation of MMC. The discussion is summarized in Table 2.1. In this table, '1' represents turn-on gate signal and '0' refers to turn-off gate signal. Table 2.1shows that when gate signal of S_1 is 1 and gate signal of S_2 is 0, the SM is inserted in the system. When gate signal of S_1 is 0 and S_2 is 1, the SM is bypassed. Thus, by controlling the gate signals to the two switches, each SM is inserted in or bypassed from any arm of Figure 2.1(a) to generate the voltage across the arm.

The currents in phase-k (k=a,b,c) consist of i_{k-up} and i_{k-low} which are the upper and lower arm current in each phase .Applying KVL to the arms of the converter yields to the following :

$$u_k - (u_0 + \frac{u_{dc}}{2} - u_{k-up}) = 2L\frac{di_{k-up}}{dt} \quad (2.1)$$

$$u_k - (u_0 + \frac{u_{dc}}{2} - u_{k-low}) = 2L\frac{di_{k-low}}{dt} \quad (2.2)$$

$$u_k - (u_0 + \frac{u_{k-low} - u_{k-up}}{2}) = L\frac{di_k}{dt} \quad (2.3)$$

$$i_{k1} + i_{k2} = i_k \quad (2.4)$$

$$i_{circ} = \frac{i_{upper} + i_{lower}}{2} \quad (2.5)$$

Where $u_k$is the phase k voltage,u_0 is the potential to ground DC side neutral point and the inductance of each arm equals 2L. The circulating current is the difference between the upper arm current (i_{k_up}) and the lower arm current(i_{k_low}).This current flows through the DC source to the phase leg for the single –phase configuration and it flows through different phase legs in three-phase configuration [51].

2.1.2 BASIC OPERATION PRINCIPLE

Whereas conventional VSCs operate by "chopping" a dc voltage into voltage pulses of constant magnitude but variable widths to represent amplitude varying waveform requested by the modulation signal, MMC creates its output voltage by connecting different numbers of 'on state' SMs in series.

To illustrate the "insertion of 'on states' " and "bypass" concepts, Figure 2.3reproduces Figure 2.1using four SMs to represent the upper arm and the lower arm of each phase. In Figure 2.3U_{dc} represents the total dc voltage and U_c denotes the balanced capacitor voltage per SM. The output voltages of the jth phase is u_j (j=a, b, c) with the arm voltages created by SM strings are written as u_{upperj} (j=a, b, c) for the upper arm and u_{lowerj} (j=a, b, c) for the lower arm. Figure 2.4 depicts the voltage u_{uppera} of the upper arm, u_{lowera} of the lower arm and the phase voltage output u_a corresponding to the four SM in the arms of phase-a of the MMC of Figure 2.3. In the full cycle of the "sine" wave voltage output u_a, the operation period is divided into eight sections (from I to VIII in Figure 2.4). Each section corresponds to the operation pattern of one arm formed by a string of SMs [51] [52].

For instance, section I of Figure 2.4 refers to the pattern that all SMs in the upper arm being in the ‘off state’ and all SMs in the lower arm being in the ‘on state’ (displayed in Figure 2.3 of phase-a). In this case, voltages generated in the upper arm and lower arm are zero and U_{dc} respectively. According to the circuit theory, at this time section, the output voltage of phase-a, which is measured at the mid-point between the upper and lower arm is $U_{dc}/2$. Detailed information about the arm SM string operation pattern in the eight sections is listed in Table 2.2.

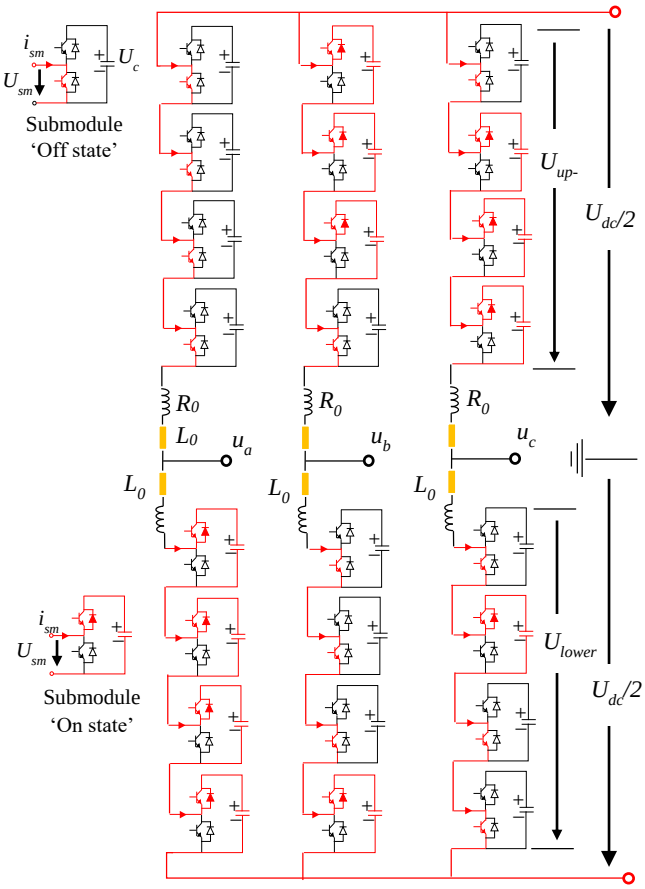

Figure 2.3 Illustration of MMC operation, each arm having four SMs. MMC operation is based on SM IGBTs bypassing the capacitors or connecting the apacitors in series to form a string

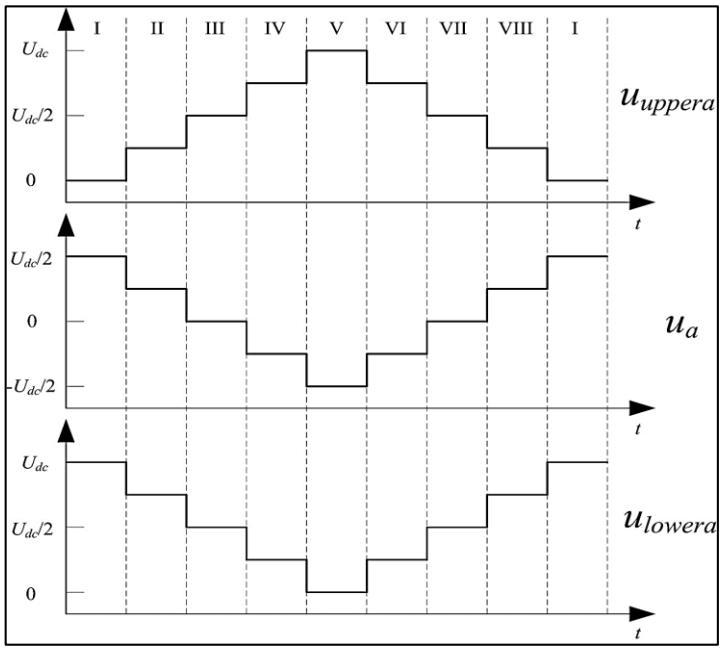

Figure 2.4 Illustration of a four SM MMC voltage waveforms of phase-a

As clearly shown in Figure 2.4 and Table 2.2, a four SM MMC produces five-level output voltage [52]. An MMC with *N* SMs in each arm in general generates *N*+1 level output voltage. The relationship between dc voltage and SM capacitor voltage is:

$$U_C = \frac{U_{dc}}{N} \tag{2-6}$$

Table 2.2 Phase-a voltage ua produced by Sub-Modules in Upper and Lower Arms

	Section							
	I	II	III	IV	V	VI	VII	VIII
Number of SM with 'on state' in the upper arm	0	1	2	3	4	3	2	1
Number of SM with 'on state' in the lower arm	4	3	2	1	0	1	2	3
Total number of SM with on state in one phase	4	4	4	4	4	4	4	4
Output voltage u_a	$U_{dc}/2$	$U_{dc}/4$	0	$-U_{dc}/4$	$-U_{dc}/2$	$-U_{dc}/4$	0	$U_{dc}/4$
DC voltage	U_{dc}	U_{dc}	U_{dc}	U_{dc}	U_{dc}	U_{dc}	U_{dc}	U_{dc}

The bigger *N* becomes, a better output waveform MMC is produced. In order to make the dc voltage to be constant, at any time of the operation, the total number of SMs in operation in one phase has to be equal to *N* which is the number of SMs in each arm. It follows that (2-7):

$$N_{up} + N_{low} = N \tag{2-7}$$

In equation (2-7), n_{up} represents the number of SMs with 'on state' in the upper arm. Similarly, n_{low} denotes the SM number with 'on state' in the lower arm of the same phase. From (2-7), it is noted that SMs in the upper and lower arm of the same phase are switched as a complementary pair, that could be used for modulation method which is about to be explained in the following section [53].

2.2 MATHEMATICAL MODELING METHODS FOR MMC- HVDC

Modular Multilevel Converter (MMC) concept exploits the benefits of the multilevel structure and the Pulse Width Modulation (PWM). The effective switching frequency per device is low, resulting in lower switching losses and lower harmonics (high-quality AC voltage), which reduces greatly the filtering requirements [6]. This converter relies on the cell capacitors to create a multilevel voltage waveform at the converter terminal. Typically, hundreds of cells are required to build a single valve for DC transmission requirements. As the number of levels increases, the quality of AC voltage waveform becomes better and the harmonic content reduces.

As this topology benefits from the redundant combination of module connections for each required AC level, the balancing capability is better than the one with NPC converters [54]. The MMC performs better than the NPC converter during unbalanced operation and symmetrical/asymmetrical AC faults, which reduces the risk of the device failure and system collapse [55]. This ability to bypass different types of AC faults makes the MMC suitable for applications subjected to stringent grid codes requirements (wind energy). If there is an issue with one phase on the AC system, the remaining two phases of the converter will operate unaffected, potentially at full per-phase power, since there is no common DC capacitor to transfer ripple between phases.

These key features, made of the MMC an attractive choice for VSC HVDC transmission system around the world [17], resulting in a rising interest to develop appropriate modeling technics to meet special purpose analysis (control, transient analysis…) and to reduce the simulation time.

The relatively high number of non-linear semi-conductors in the MMCs presents some challenges when triggered by relatively high-frequency signals requiring a significant computational effort for re-triangularisation of the electrical network subsystem's admittance matrix [56] [57], and making the simulation of the MMC in some occasions impractical when using a conventional modeling approach [58].

In order to overcome the above-mentioned challenges, the research community propose enhanced reduced order models that increase computational efficiency and maintain the targeted accuracy. A current trend is based on simplified and average value models (AVM) [59] [60] capable of delivering sufficient accuracy [61] in dynamic simulations. AVMs and other simplified modelling approaches for MMCs have been presented in [44] [45] [62].

This section tends to classify the modeling methods of the modular multilevel converter. Then, it makes a detailed descriptions and comparisons among the four models in terms of phenomena covering, accuracy, and application. Furthermore, it aims to help the reader to identify and choose the best-suited model for conducting his analysis.

2.2.1 FULL PHYSICS BASED MODEL

The modeling of MMCs could become extremely complex and its simulation could be highly time consuming, due to the large amount of cells. Different modeling levels can be achieved according to the type of study and the required accuracy. In this paper, models are introduced in decreasing complexity. It is expected that by decreasing model complexity, computational performance can be increased.

Each semiconductor device is represented by differential equations or by an equivalent circuit. Insulated gate bipolar transistor (IGBT) models may be classified as being either behavior models [63] or physical models. A behavior model is not based on physical principles but it is still able to accurately describe the device characteristics under particular conditions. However, analytical models [64] [65] [66] [67] [68] [69] [70] [71] are able to predict the IGBT behavior when the device parameters are changed (base width, channel length, gate oxide thickness …). These parameters strongly affect the device performance.

Since IGBT can be approximated as a combination of a MOS transistor and a BJT, an enhanced analytical model was proposed in [68] that use one-dimensional device simulation model for the BJT and an analytical model for the MOS to construct an IGBT equivalent circuit model as shown in Figure 2.5, which is compared to earlier physics based models presented in [64] [65] [72].

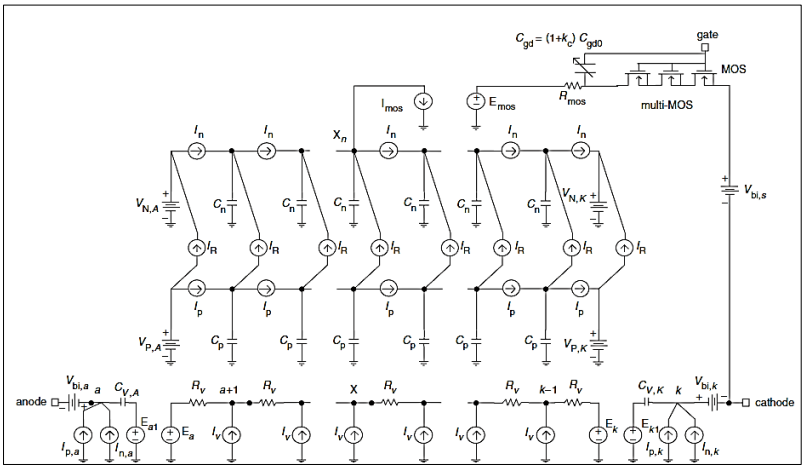

Figure 2.5 The equivalent circuit of the IGBT proposed in [73]

The full physics based models are useful for detailed analysis of the behavior of the semiconductor device in the design phase of the converter and they help determining the doping profile and the size of the IGBT. These models can accurately simulate switching losses at the expense of a very small integration time step (in the range of nanoseconds) in the EMTP and they are therefore not usually applied for power system studies. For that reason, this type will not be discussed in the following sections.

2.2.2 FULL DETAILED MODEL (NONLINEAR MODEL)

The anti-parallel IGBT/diode pair is represented by an ideal controlled switch, one series and one anti-parallel diodes and a snubber circuit [73], as shown Figure 2.6. The non-ideal voltage-current characteristic of the diode is represented using a non-linear resistance. The nonlinear characteristic can be adjusted according to the manufacturer's data.

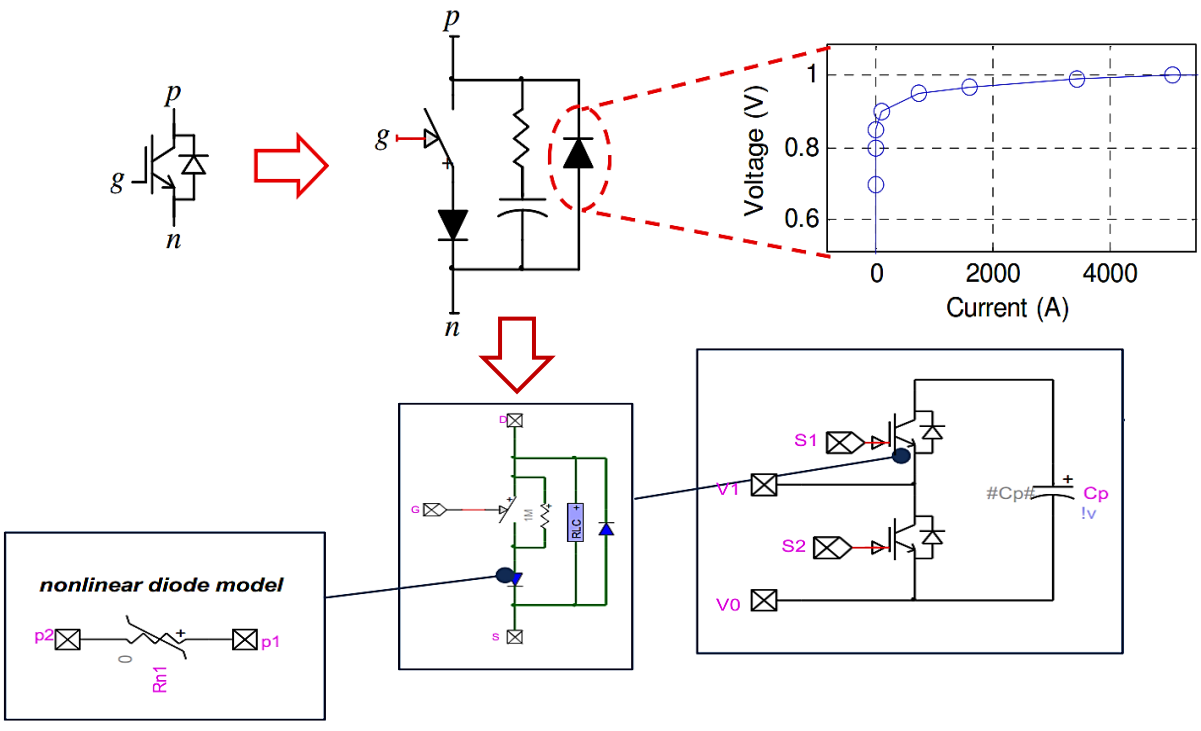

Figure 2.6 a) Representation of a nonlinear IGBT valve and Diode characteristic.

This model is the most accurate model for EMT-type programs and can account for every conduction mode of the MMC (see appendix A). The advantages lies in the increased accuracy in the modelling of the IGBT/diode pair, as the non-linear behavior during the commutation is included and the ability to achieve specific studies such as blocked states (g_1, g_2 OFF), submodules details, the converter start-up sequence and internal converter faults. Furthermore, these models are useful for benchmarking, tuning and validating of less detailed MMC models described in the following.

2.2.3 EQUIVALENT (OR SIMPLIFIED) DETAILED MODEL

A. IGBT/Diode representation

This model is based on the assumption that the IGBT device and its anti-parallel diode act as a bidirectional switch represented by a two-state resistance: R_{ON} (small conductive value) and R_{OFF} (large open-circuit value) shown in Figure 2.7. This approach [58] allows performing an arm circuit reduction for eliminating internal electrical nodes and allowing the creation of a Norton equivalent for each MMC arm. These two resistances are controlled and used for replacing the two IGTB/diode combinations. Their values depend on gating signals, current direction and capacitor voltage.

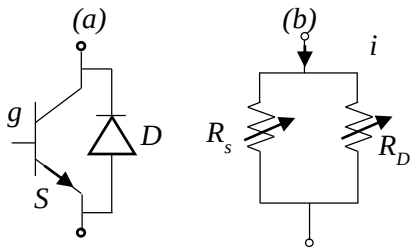

$$R_S = \begin{cases} R_{on} \text{ for } i>0A \\ R_{off} \text{ for } i<0A \end{cases}$$

$$R_D = \begin{cases} R_{on} \text{ for } i>0A \wedge g=1 \\ R_{off} \text{ for } i<0A \vee g=0 \end{cases}$$

Figure 2.7 a) Anti-parallel IGBT/diode. b) Simplified IGBT/diode model.

As either the diode or the IGBT is conducting at a given instance, the IGBT/diode pair can still be treated as a single two state resistance such illustrated in Figure 2.8.

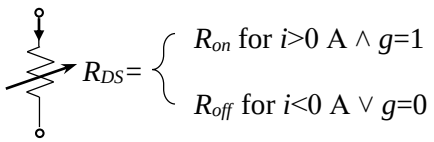

Figure 2.8 Single two state resistance model

B. Submodule capacitor representation

The capacitor C_{cap} can be represented by its Thevenin or Norton equivalents by applying the trapezoidal rule of integration according to Dommel's formulation [74]. The general Thevenin and Norton equivalents for the capacitor are derived respectively.

$$u_{cap}(t) = \frac{1}{c_{cap}} \int_{t_1-\Delta t}^{t_1} i_{cap}(t_1)\,dt + u_{cap}(t-\Delta t) \\ = R_{cap}.i_{cap}(t) + u_{Hist}(t-\Delta t) \tag{2.8}$$

Where $R_{cap} = \Delta t/2C_{cap}$, $u_{cap}(t)$ and $i_{cap}(t)$ are the voltage across and current through C_{cap}, respectively. Δt is the simulation step size.

$$i_{cap}(t) = \frac{2C_{cap}}{\Delta t}\left[u_{cap}(t) - u_{cap}(t-\Delta t)\right] - i_{cap}(t-\Delta t) \\ = \frac{u_{cap}(t)}{R_{cap}} + i_{Hist}(t-\Delta t) \tag{2.9}$$

From (2.9) it is evident that the capacitor can be represented by an equivalent resistance R_{cap} in parallel with a current source $i_{Hist}(t-\Delta t)$ given as:

$$i_{Hist}(t-\Delta t) = -\frac{u_{cap}(t-\Delta t)}{R_{cap}} - i_{cap}(t-\Delta t) \tag{2.10}$$

The Thevenin and the Norton equivalents in Figure 2.9b and c, are the dual of each-other and just algebraic manipulations of the actual circuit.

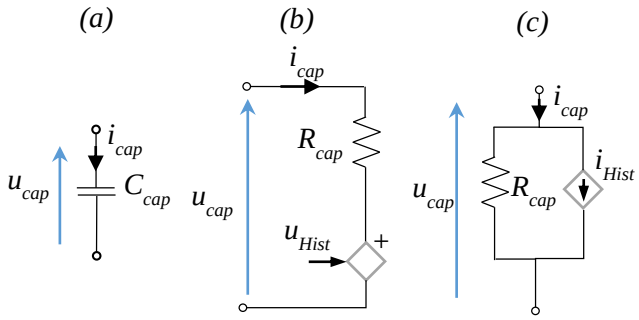

Figure 2.9 a) The capacitor and its b) Thévenin and c) Norton EMTP equivalents

Using the Thevenin equivalent in (1) for the SM capacitor, the *n*th SM half-bridge can be electrically represented as in Figure 2.10 [74].

The *n*th SM output voltage can be expressed as:

$$u_{smo,n} = \frac{i_{in}(t)}{1/R_{2,n}(t) + 1/\left[R_{1,n}(t) + R_{cap}\right]} + \frac{R_{2,n}(t).u_{Hist}(t-\Delta t)}{1/R_{2,n}(t) + 1/\left[R_{1,n}(t) + R_{cap}\right]} \\ = R_{EQ,n(t)}.i_{in}(t) + u_{EQ,n}(t) \tag{2.11}$$

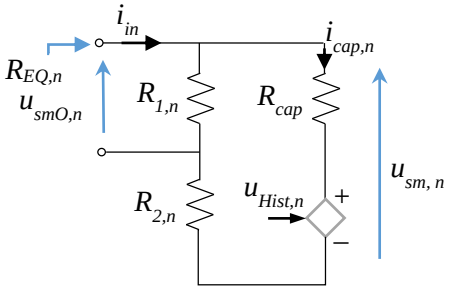

Figure 2.10 EMTP Equivalent model of the N[th] half bridge submodule

The capacitor current can be expressed as:

$$u_{smo,n} = \frac{i_{in}(t)}{1/R_{2,n}(t)+1/\left[R_{1,n}(t)+R_{cap}\right]} + \frac{u_{sm,n}(t-\Delta t)+R_c.i_{cap,n}(t-\Delta t)}{R_{2,n}(t)+R_{1,n}(t)+R_{cap}} \tag{2.12}$$

Similarly, the capacitor voltage is calculated as:

$$u_{sm,n}(t) = R_{cap}.\left[i_{cap,n}(t)+i_{cap,n}(t-\Delta t)\right]+u_{sm,n}(t-\Delta t) \tag{2.13}$$

The Thevenin parameters for the *n*th submodule ($R_{EQ,n}$ and $u_{EQ,n}$) are readily available in (2.11).

C. Phase Arm Equivalent

By series connecting the *N* SMs in the phase arm as Figure 2.11a, the arm equivalent shown in Figure 2.11b results, where the Thevenin parameters are:

$$u_{EQ,arm}(t) = \sum_{n=1}^{N} u_{EQ,n}(t) \tag{2.14}$$

$$R_{EQ,arm}(t) = \sum_{n=1}^{N} R_{EQ,n}(t) \tag{2.15}$$

Where $R_{EQ,n}$ and $u_{EQ,n}$ are given in (2.11).

Furthermore, from an implementation point of view, the model approach presented here will only require very little modification in order to model the full-bridge converter SM [58] [9].

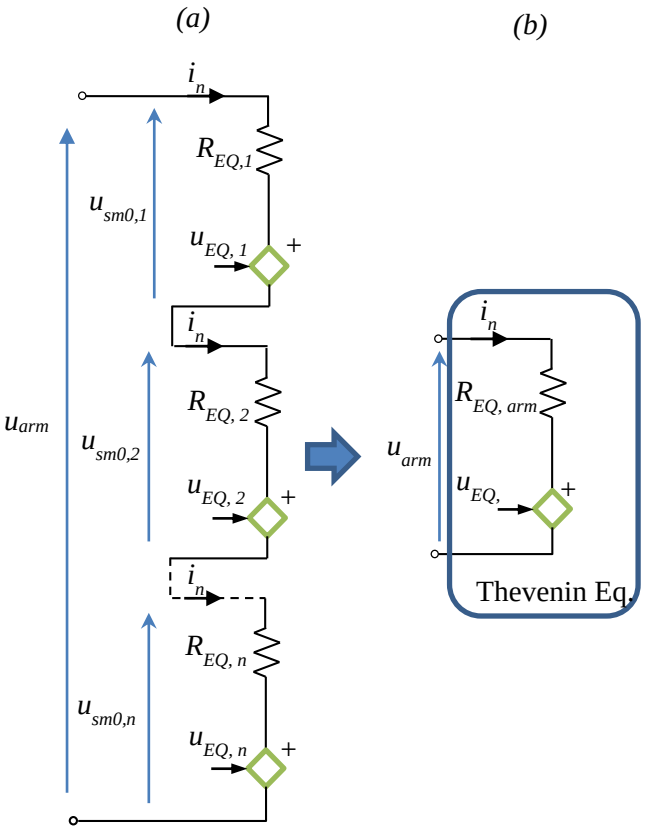

Figure 2.11 Thévenin equivalent of the MMC VSC-HVDC phase arm

Although less accurate compared to the full detailed models, the simplified detailed model is less computational heavy, which is of importance for power system studies [75]. The main advantage of this type is the

significant reduction in the number of electrical nodes in the main system of network equations. It still considers each SM separately and maintains a record for individual capacitor voltages and currents. It is applicable to any number of the SMs per arm (see appendix A) .

2.2.4 AVERAGED MODELS

Detailed models (DM) for the MMC that provide completely faithful representations of converter and system characteristics are very complex and computationally challenging for electromagnetic-transient (EMT) programs, given the large number of switching elements (IGBTs) [58] [76], which highlights the need to develop more efficient models, that provide similar dynamic response. These simplified models, known as average-value models (AVMs), replicate the average response of switching devices, converters and controls by using controlled sources and switching or averaged functions [77] [78] [79].

The averaged-value models (AVM) based on power frequency consider the fundamental frequency behavior on the ac side, and they find their application in system-level analysis [45]. An extension to the AVM (known as switching function model) uses the switching function of the half-bridge submodule, which make it able to correctly represent harmonics generated by the MMC. As a result, this type can be used instead of MMC EMT simulation model for full-scale simulations of HVDC grids. Hence, this type of model is significantly more efficient than models that consider the detailed MMC converter topology and has been proposed for studying the dynamic behavior of large systems, such as MTDC grids [80] [9] [73] [44].

The objective of Average-Value Modeling (AVM) is to replace the discontinuous switching cells with continuous blocks that represent the averaged behavior of the switching cell within a prototypical switching interval.

A. Averaged model based on the switching function

In this model, each MMC arm is averaged using the switching function S_n concept of a half-bridge converter. We assume that all internal variables in the MMC are perfectly controlled, all SM capacitor voltages are perfectly balanced and second harmonic circulating currents in each phase are suppressed (The accuracy of assumption increases when the number of SMs per arm is increased and/or when the fluctuation amplitudes of capacitor voltages are decreased). In this case, a single module as in Figure 2.12 can represent each arm (see appendix A).State-space modeling is a preferred approach to describe dynamic systems due to the inherent ease of manipulation that it offers as well as its frequency domain analysis capabilities. An explicit steady-state expression for the circulating current can be derived with this approach [81].

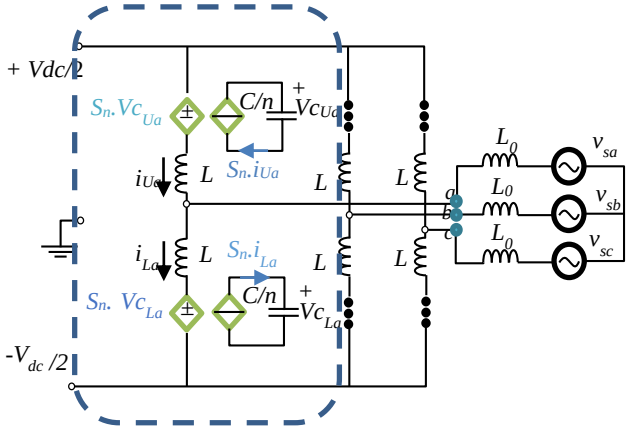

Figure 2.12 Averaged switching model of the MMC phase arm.

This model captures the information of individual capacitors provided that the switching frequency is high enough for the averaging method to be valid, and that all the module parameters and modulation commands

are balanced at the module level. However, circulating currents and the linear conduction losses can be represented. Moreover, the energy transferred from ac and dc sides into each arm of the MMC is taken into account, which is useful for control system strategies based on internal MMC energy balance [82] [83].

An obvious limitation of this approach is that the information of the individual modules cannot be differentiated within an arm, as all of them are assumed identical, and by reducing each arm to an equivalent switching function model, power switches are no longer represented.

Due to the simplifications presented before, this modeling approach requires significantly less computing time and can also use larger time steps than detailed modeling, it can be also used to study harmonics.

B. Average model based on Fundamental Frequency

This model uses the same mathematical formulation as the previous model except the switching functions are substituted by reference signals that replicates the overall dynamics of the MMC converter, consequently, the control blocks are suppressed. The MMC can be represented as a classical VSC (2- and 3-level topologies) [84], which was not the case in [73]. Thus, using an approach similar to [85], v_{ref} are the voltage references generated from the inner controller [86] (see appendix A). The ac-side representation of this model is shown in Figure 2.13(a).

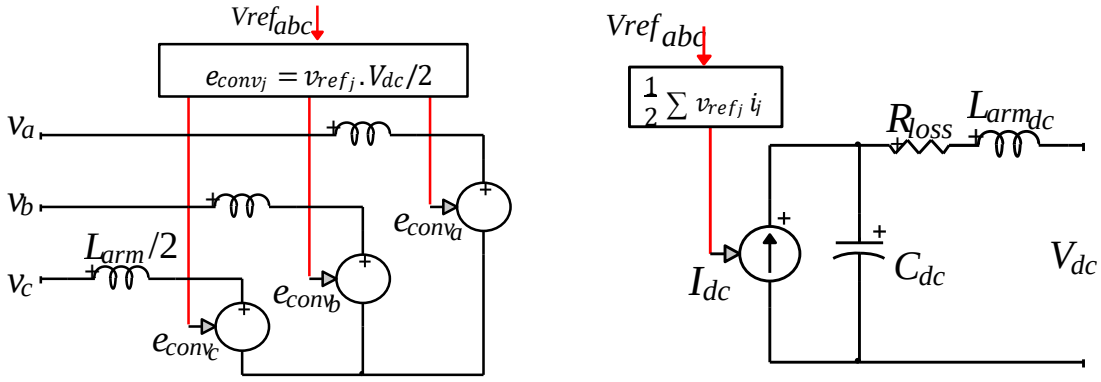

Figure 2.13 Averaged-value model of the MMC converter [8].

The dc-side model Figure 2.13(b) is derived using the principle of power balance; thus, it assumes that no energy is stored inside the MMC converter. Unlike the classical VSC model, an inductance is included in each arm of the MMC, thus an equivalent inductance should be also added on the dc side.

Finally, both average models used in this thesis present a satisfactory response during steady state and dynamic simulations. The switching function model is more accurate than the average model based on fundamental frequency, but it requires more computing time for the same Δt. System dynamics can be accurately modeled using both AVM and switched model for ac side faults, set point changes and loss of generation.

AVMs is only effective as long as the capacitors are large enough to maintain nearly constant voltage across each MMC submodule. The large-scale dynamic behavior is accurately modeled although the individual capacitor voltages are not calculated. Instead, a single dc-side voltage is calculated.

2.3 MODELS VALIDATION

This section provides a comparison between the four types of MMC models: Model DM, EM, SFM and AVM. The dynamic behavior comparison is conducted for normal operation and step-change of active power reference [10].

The studied system is presented in Figure 2.14. The control strategy considers an active/reactive power control on the sending end (VSC_1) and a dc voltage/reactive power control on the receiving end (VSC_2). The ac grids are represented as equivalent sources with a short circuit level of 10,000 MVA. The transmission capacity of the system is 1,000 MW from VSC1 to VSC2. The DC cable is modeled using a wideband line

model [27]. Each MMC station considers a 101-level MMC (100 SMs/arm). The Model 1 (with nonlinear IGBT/diode model) constitutes the reference model. Table I in appendix B provides parameters of the system of Figure 2.14 used for the simulation studies.

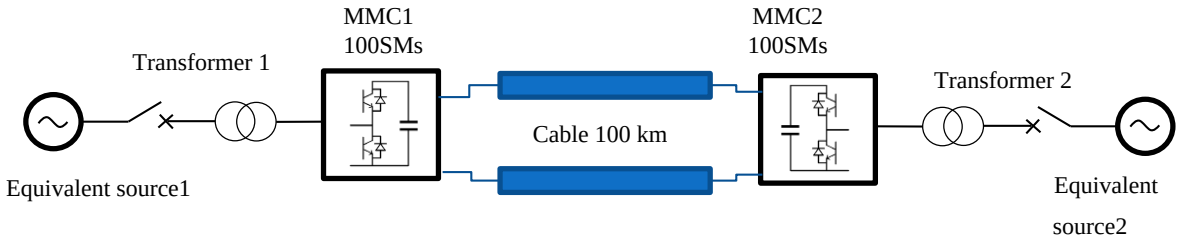

Figure 2.14 Point -to-point MMC -HVDC transmission test system

2.3.1 STEADY-STATE OPERATION

The steady-state waveforms produced by the models for 1GW MMC-HVDC system are shown in Figures below. The waveforms are virtually identical and this is confirmed by the very error shown in the zoomed waveform in figure below. The models were simulated for two converters operating as rectifier and inverter respectivly at 100MW. The results generally show that the accuracy is good for both active and reactive power in the the botch converters.

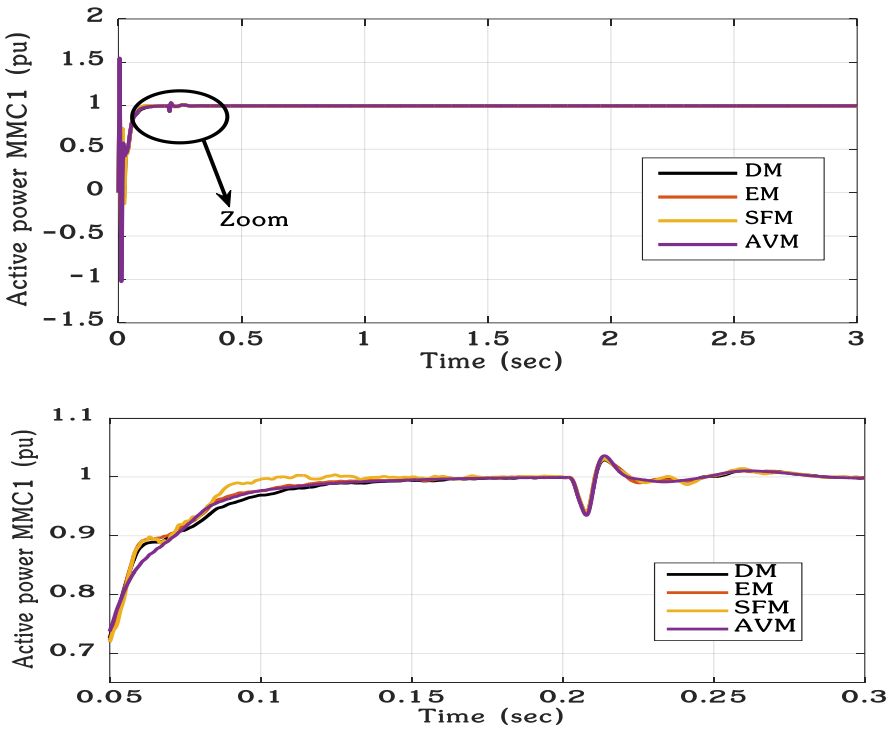

Figure 2.15 Steady-state simulation results for the four models. From top to bottom: (a Active power at MMC1, (b) Zoomed waveform of active power at MMC1.

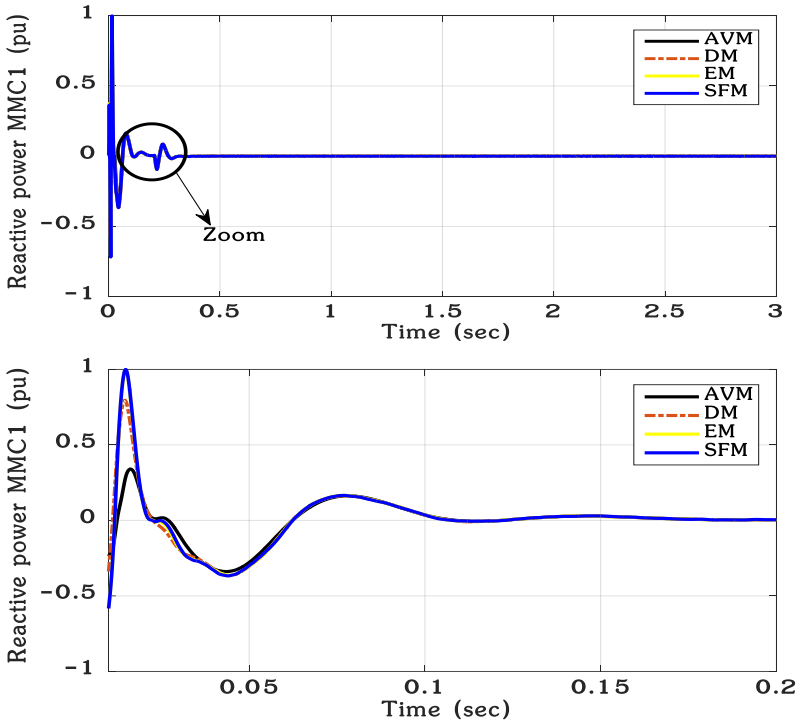

Figure 2.16 Steady-state simulation results for the four models. From top to bottom: (a Reactive power at MMC1, (b) Zoomed waveform of reactive power at MMC1.

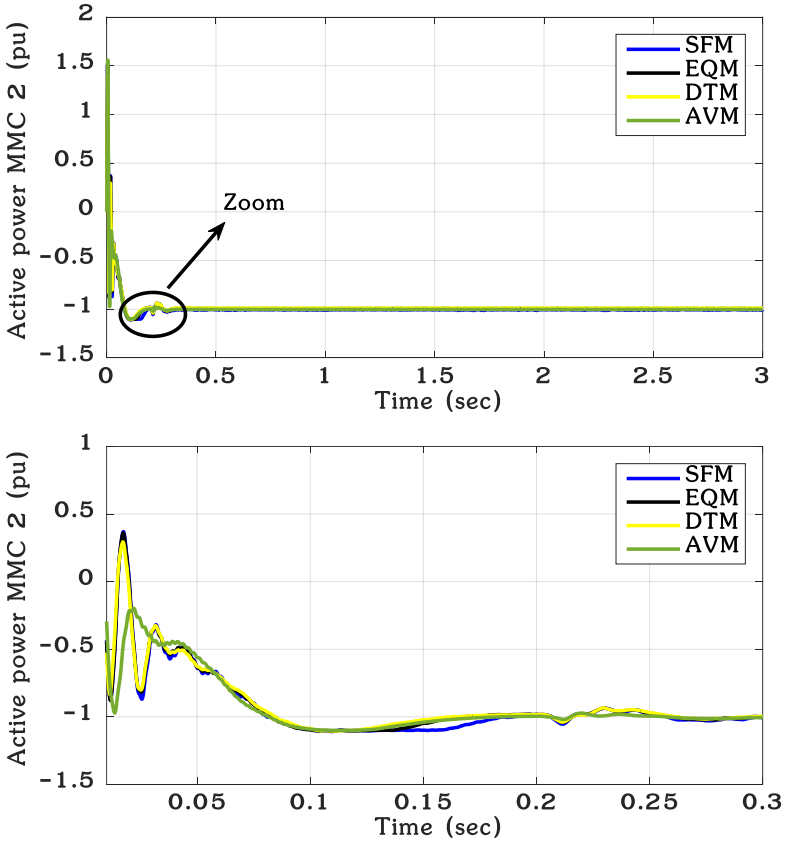

Figure 2.17 Steady-state simulation results for the four models. From top to bottom: (a) Active power at MMC2, (b) Zoomed waveform of active power at MMC2

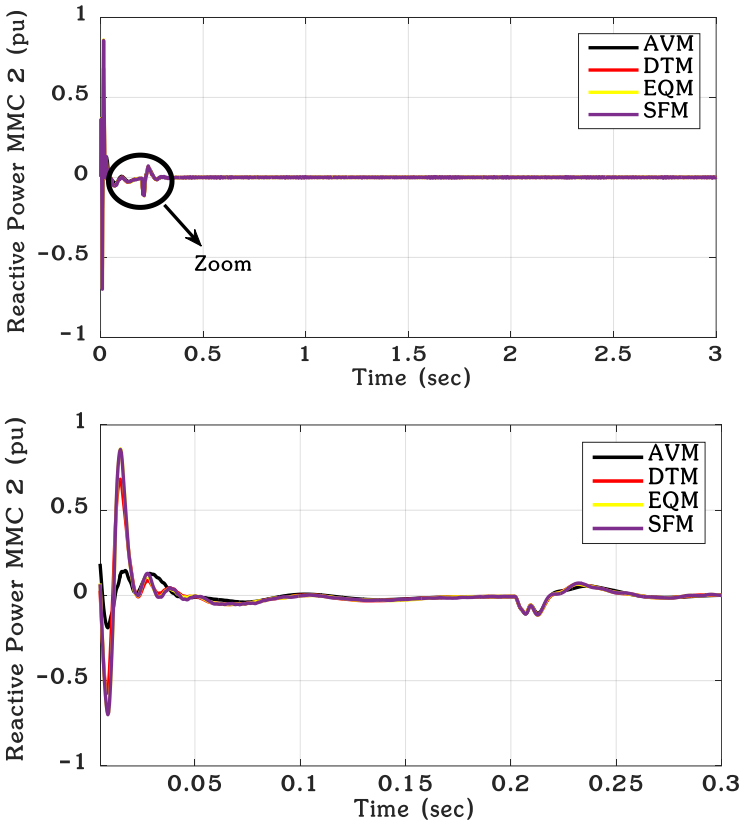

Figure 2.18 Steady-state simulation results for the four models. From top to bottom: (a Rective power at MMC2, (b) Zoomed waveform of reactive power at MMC2

A step change in the active power reference for VSC_1 is applied at 1 s of simulation. The active power reference is reduced from 0.5 to -0.5 pu (power flow reversal).in figure below all four models deliver identical results.

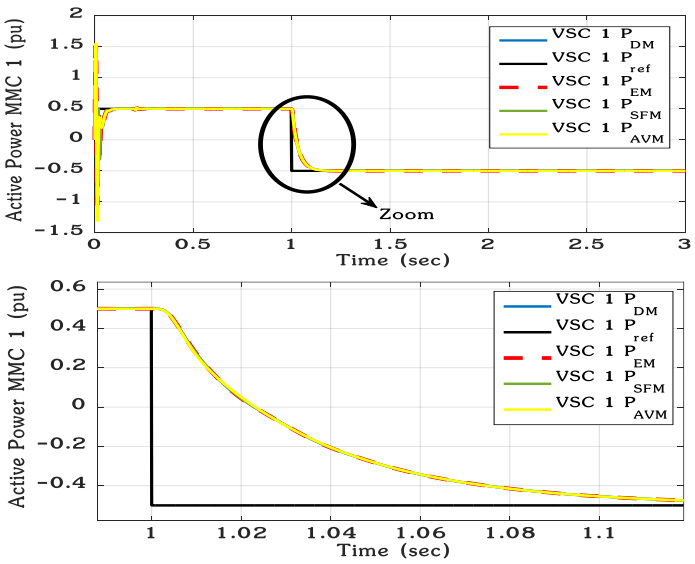

Figure 2.19 Step change simulation results for the four models. From top to bottom: (a Active power at MMC1, (b) Zoomed waveform of active power at MMC

Since in Figure 2.19 both Models EM, SFM and AVM are able to match the results from DM Model, it is concluded that these three simplified models can be used to study converter dynamics. The zoomed waveforms

of Figure 2.19 are used to highlight the accuracy in all models. It is observed that all models mimics the accuracy of DM into the step change on active power reference.

2.3.2 COMPUTING PERFORMANCE COMPARISON

This section presents a comparison of the computing performance for the different models developed and presented in this work and listed in Table 2.3 AM computing timings for a 3s simulation. The models are compared against their detailed versions. The computing performance tests were done on a computer with a 2.6 GHz Intel Core i5-3230M processor and 4 GB of RAM.

Table 2.3 AM computing timings for a 3s simulation

Model	Time-step (μs)	Time (s)
DM	10	9011.26985
EM	10	155.56419
SFM	10	31.29380
AVM	10	15.1477

The simulation performance results for the four models are presented in Table 2.3. The EM performs significantly better in terms of computer speed. A 3s simulation, using a timestep of 10μs, can be performed 56 times faster using the EM without compromising the accuracy of the system dynamic response. The Averaged models performs better in terms of computer speed. A simulation of 3s, using a time-step of 10μs, can be performed between 290 and 560 times faster using the SFM and AVM respectivly without compromising the accuracy of the system's dynamic response.

Both the SFM and AVM remains sufficiently precise when the time-step is increased up to 50μs. Since the switching valves are not modeled in the AVM, a slightly higher time-step can be used without compromising accuracy and therefore allowing further computational speed gains. The AVM approach is much faster than DMM and it can be used in very large systems. Table 2.4 presents a summary of advantages and limitations as well as suitability of each model for different systems studies [9] [19] [87].

Table 2.4 Summary Table and Comparison of Models

Features	DM	EM	SFM	AVM
Harmonics	Yes	Yes	Yes	No
Accuracy	Best	Very Good	Very good	Good
Simulation Time	Very Slow	Slow	Fast	Very Fast
AC Dynamics	Yes	Yes	Yes	Yes
AC Fast transients	Yes	Yes	Yes	Yes
DC Side transients	Yes	Yes	Yes/No	No
VSC Internal faults	Yes	No	No	No
Resonances	Yes	Yes	Yes	No
Controls interaction	Yes	Yes	Yes	Yes
Large systems	No	Yes	Yes	Yes
Converter Losses	Best	Good	Good	Good

2.4 CONCLUSION

The configuration of 3-phase MMC has been described in this chapter. Focusing on halfbridge sub-module, its three operation states are elaborated. Among them, two are expressed as the normal operation states which are ‘insert/on state’ and ‘bypass/off state’. Different levels of voltage can be generated via inserting and by-passing the SMs in each arm. By introducing the basic operation principle for each phase of MMC, it is noted that the number of SMs with ‘on state’ in one arm is complementary with the ‘on state’ number in the other arm of the same phase.

This chapter has presented the first independent comparison of two previously developed MMC modelling techniques (Detailed and Averaged Models). It has also presented the verification of all models, and verification of the Models in EMTP-rv. An MMC-HVDC test system was perofromed and the modelling techniques were compared against the DM model technique in terms of accuracy and simulation speed. The accuracy of the different models was evaluated graphically for steady-state and dynamic performance. These findings have shown that four modelling techniques offer a good level of accuracy but that the DM is generally the most accurate. The SFM and AVMM models have been shown to simulate significantly faster than the DM, and the EM is more computationally efficient than the DM. The DM model does however provide access to SM components (which is not possible with the EM) and so may be considered when this is an important factor.

Chapter 3 MMC HVDC CONTROL

The modular multilevel converter (MMC) has been a subject of increasing importance for medium/high power energy conversion systems especially in high voltage direct current transmission system. Over the past few years, significant research has been done to address the technical challenges associated with the operation and control of the MMC. In this chapter, a general overview of the basics of operation of the MMC along with its control challenges are discussed, followed by a review of latest contributions on MMC modulation techniques, design constraints, and various operational issues, such as capacitor voltage balancing and circulating current control.

This chapter also describes the numerous control functions which are required for a MMC-HVDC two terminal. The required control system functions are dependent upon whether the MMC is connected to an active AC network or a windfarm. The lower level MMC control system functions are, however, independent of the connected AC network.

3.1 PRINCIPLE OF OPERATION

In order to understand the principle of the VSC-MMC control system, let us first consider the two bus system (Figure 3.1), where Vs is the ac voltage source, is V_{conv} the ac voltage of the converter and X is the equivalent inductance between the ac source and converter (i.e. transformer leakage inductance, equivalent arm inductance, etc.). The losses are neglected for simplification purposes. The transferred active and reactive powers from the source to the converter are given by the following relationships [8] [88]:

$$P_R = \frac{V_s V_{conv}}{X} \sin(\delta) \tag{3.1}$$

$$Q_R = \frac{V_s V_{conv} \cos(\delta) - {V_{conv}}^2}{X} \tag{3.2}$$

Where δ is the angle between the two voltages.

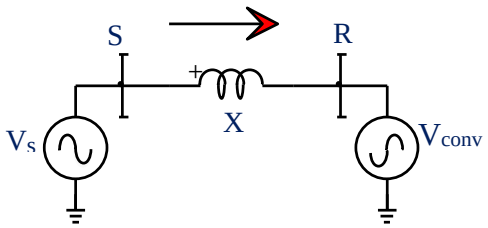

Figure 3.1 Two-bus system representing the functionality of the VSC-MMC control system

From (3.1) and (3.2), we can see that by controlling the voltage amplitude and phase angle of the converter, it is then possible to regulate the active and reactive powers at a desired set-point.

3.2 CONTROL HIERARCHY FOR THE MMC CONVERTER

New VSC technologies are based on multilevel configurations where 2L sub-modules (SMs) are connected in cascade to form a MMC. MMC topologies use a smaller switching frequency helping to reduce converter losses. In addition, filter requirements are eliminated by using a significant number of levels per phase. Scalability to higher voltages is easily achieved and reliability improved by increasing the number of SMs per multivalve arm [89].

Since the MMC topology is of VSC type [73], it uses an upper level control similar to the previous VSC technology. However, the MMC topology requires additional controllers in order to stabilize internal variables (Lower Level Control): The dc capacitors are now included in each SM and the series reactors, used to control the power flow and circulating currents, are embedded in the converter's phase arms. A Balancing Control Algorithm (BCA) is required to control arm currents and the dc voltage on each SM capacitor and modulation technique [83] [73]. A top level view of the control structure is presented in Figure 3.2.

Several control methods area available for Upper Level Control. Among them the power-angle and vectorcurrent controls are the mostly widely used. The principle of power-angle control is simple. The active power is controlled by the phase-angle shift between the VSC and the ac system, while the reactive power is controlled by varying the VSC voltage magnitude [88]. Power-angle control (or Voltage/Frequency control) is used when the VSC converter is connected to an ac system with passive load or for wind-turbine applications [6]. Vector-current control is a current-control-based technology. Thus, it can naturally limit the current flowing into the converter during disturbances. The basic principle of vector-current control is to regulate the instantaneous active and reactive powers independently through a fast inner current control loop. By using a dq decomposition technique with the grid voltage as phase reference, the inner current control loop decouples the current into d and q components, where outer loops can use the d component to control active power or dc voltage, and the q component to control reactive power or ac voltage. Due to its successful application in HVDC transmission system, vector-current control has become the dominant control method for gridconnected VSCs in almost all applications today [88].

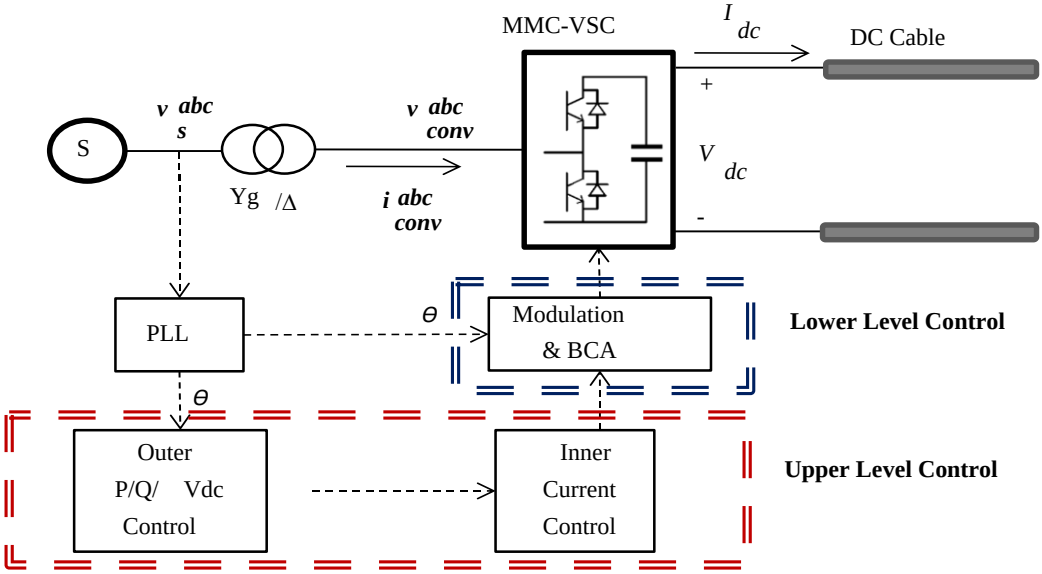

Figure 3.2 Control hierarchy for the MMC station

3.3 UPPER LEVEL CONTROL

The Upper Level Control block is presented in Figure 3.3. All variables are in pu except for the theta angle that is in radians.

The transformation matrix *T* in equation (3.5) transforms the three-phase variables (voltages and currents) to two quadrature axis (d and q reference frame) components rotating at synchronous speed $w = d\theta / dt$. The phase angle θ is derived, found by mans of an internal oscillator or found by the PLL allowing the synchronization of control parameters with the system voltage. In the matrix *T*, the direct axis d is aligned with the grid voltage.

$$T = \frac{2}{3}\begin{bmatrix} \cos(\omega t) & \cos(\omega t - \frac{2\pi}{3}) & \cos(\omega t + \frac{2\pi}{3t}) \\ -\sin(\omega t) & -\sin(\omega t - \frac{2\pi}{3}) & -\sin(\omega t + \frac{2\pi}{3}) \\ 1/2 & 1/2 & 1/2 \end{bmatrix} \tag{3.5}$$

Using the transformation matrix *T*, the dq voltage and current variables can be deduced:

$$i_{dq} = T_{i_{abc}} \tag{3.6}$$

$$v_{dq} = \mathrm{T} v_{abc-grid} \tag{3.7}$$

The active and reactive powers and the ac grid voltage (in p.u) are calculated from the dq reference as follows:

$$P = v_d i_d + v_q i_q \tag{3.8}$$

$$Q = -v_d i_q + v_q i_d \tag{3.9}$$

$$V_{grid} = \sqrt{{v_d}^2 + {v_q}^2} \tag{3.10}$$

The regulations of variables are performed through a PI control loop. The Synchronization block is required for synchronization with the ac grid. It includes PLL and the internal oscillator. The Linearization block is for linearization and converts from dq to abc reference [9].

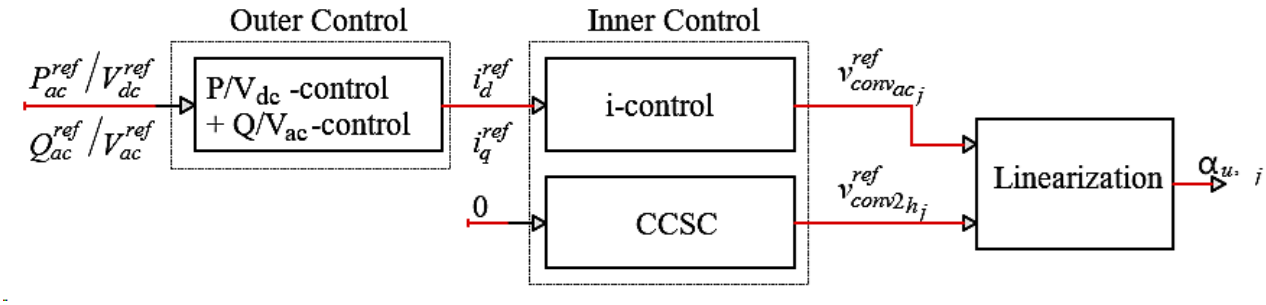

Figure 3.3 Upper Level Control block

3.3.1 VECTOR-CURRENT CONTROL (OUTER/INNER CONTROL)

Outer_control and Inner_control blocks represent the vector-current control. The basic principle of vectorcurrent control is to regulate the instantaneous active and reactive powers independently through a fast inner current control loop. By using a dq decomposition technique with the grid voltage as phase reference, the inner current control loop decouples the current into d and q components, where outer loops can use the d component to control active power (P control) or dc voltage (Vdc control), and the q component to control reactive power (Q control) or ac voltage (Vac control). One of the main advantages of this control system is his ability to limit

the current flowing into the converter during disturbances. Due to its successful application in HVDC transmission system, vector-current control has become the dominant control method for grid connected VSCs in almost all applications today [88].

Using the current sign convention from Figure 3.1 and Figure 3.3(current entering into the MMC) and neglecting the start point reactor, the following equations can be written for each phase *j = a,b,c*

$$\frac{V_{dc}}{2} = v_{u\,j} + L_{arm}\frac{di_{uj}}{dt} + R_{arm}\,i_{u\,j} - L_{transfo}\frac{di_j}{dt} - R_{transfo}\,i_j + v_{grid\,j} \quad (3.11)$$

$$\frac{V_{dc}}{2} = v_{l\,j} + L_{arm}\frac{di_{lj}}{dt} + R_{arm}\,i_{l\,j} + L_{transfo}\frac{di_j}{dt} + R_{transfo}\,i_j - v_{grid\,j} \quad (3.12)$$

The following variable is defined

$$v_{conv\,j} = \frac{v_{l\,j} - v_{u\,j}}{2} \quad (3.13)$$

Using (3.13) and subtracting (3.11) and (3.12):

$$v_{grid\,j} - v_{conv\,j} = \left(\frac{L_{arm}}{2} + L_{transfo}\right)\frac{di_j}{dt} + \left(\frac{R_{arm}}{2} + R_{transfo}\right) i_j \quad (3.14)$$

By applying Park transformation, (3.14) becomes:

$$v_{conv_d} = -(i_{ref_d} - i_d)\left(k_p + \frac{k_i}{S}\right) + v_d + \left(\frac{L_{arm}}{2} + L_{transfo}\right)\omega\, i_q \quad (3.15)$$

$$v_{conv\,q} = -(i_{ref\,q} - i_q)\left(k_p + \frac{k_i}{S}\right) + v_q + \left(\frac{L_{arm}}{2} + L_{transfo}\right)\omega\, i_d \quad (3.16)$$

The inner controller permits controlling the reference voltages (Vd_{ref} and Vq_{ref}) that will be used for the Lower Level Control. In order to decouple the d- and q-axis, a feed-forward technique is used to compensate cross-coupling terms.

3.3.2 ACTIVE POWER CONTROL (P CONTROL)

As grid voltage vector is aligned with the d axis, the q component of the grid voltage is equal to zero and d component is equal to the voltage magnitude. Equation (3.8) becomes [90]:

$$P = v_d\, i_d$$

An integral control is sufficient to produce the desired d current reference (Id_{ref}). The control law of P control is defined respectively as:

$$i_{d\,ref} = \frac{1}{v_d}\left(K_p + \frac{K_i}{S}\right)(P_{ref} - P) \quad (3.17)$$

3.3.3 REACTIVE POWER CONTROL (Q CONTROL)

As the grid voltage vector is aligned with the d axis, the q component of the grid voltage is equal to zero and d component equal to the voltage magnitude. The equation (3.9) becomes [90]:

$$Q = -v_d i_q \quad (3.18)$$

An integral control is sufficient to produce the desired q current reference (iq_ref). The control law of Q control is defined as :

$$i_{q\,ref} = \frac{1}{v_d}\left(\frac{K_i}{S}\right)(P_{ref} - P) \quad (3.19)$$

Figure 3.4shows the active and reactive power controller block.

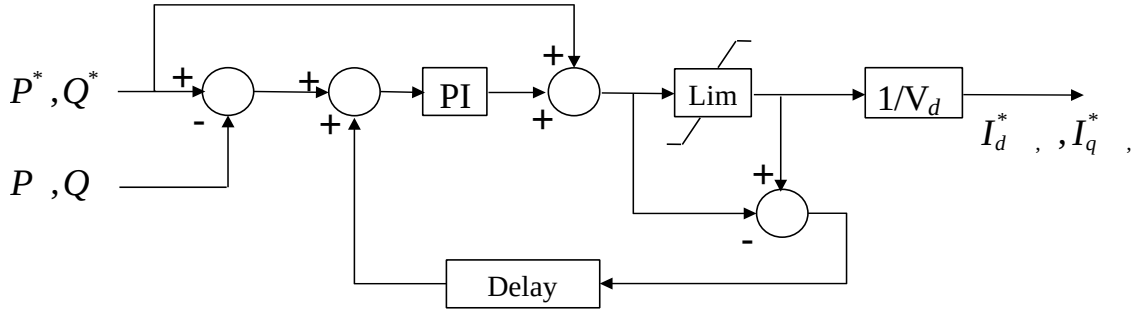

Figure 3.4 Active and reactive outer power controller [9]

3.3.4 DC VOLTAGE CONTROL (VDC CONTROL)

From the MMC model (described in chapter 2) it can be found that SM capacitors can be represented as an equivalent capacitor C_{dc}. Since the energy in the equivalent inductance L_{DC} is small, it can be neglected. The following equation can be deduced [88]:

$$C_{dc}\ \frac{dV_{dc}}{dt} = i_d\ - I_{dc} \tag{3.20}$$

After neglecting the feed-forward component I_{dc}, a PI-control can be applied to regulate the DC voltage, Figure 3.5 shows the DC voltage controller block.

$$i_{d\ ref} = (K_p\ + \frac{K_i}{S})(V_{dc\ ref} - V_{dc}) \tag{3.21}$$

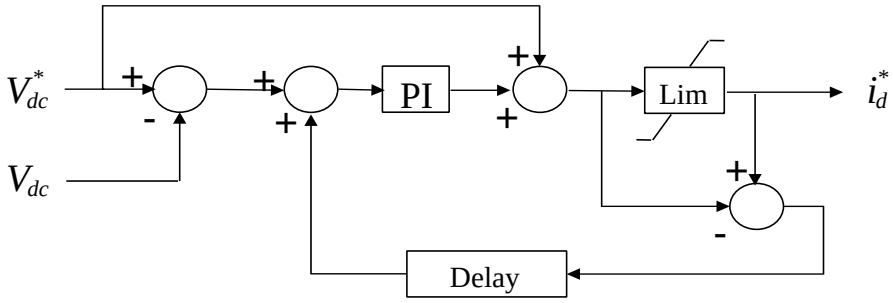

Figure 3.5 DC voltage controller [9]

3.3.5 P/VDC DROOP CONTROL

The Droop control functionality in the dc grid is similar to the Droop control in the ac grid. In the ac grid the relationship is between frequency and active power, in the dc grid the DC voltage is a function of active power and the DC voltage, the droop coefficient is given by:

$$K_{droop} = \frac{\Delta V_{dc}}{\Delta P} \tag{3.22}$$

The P/V_{dc} droop control block is shown in Figure 3.6

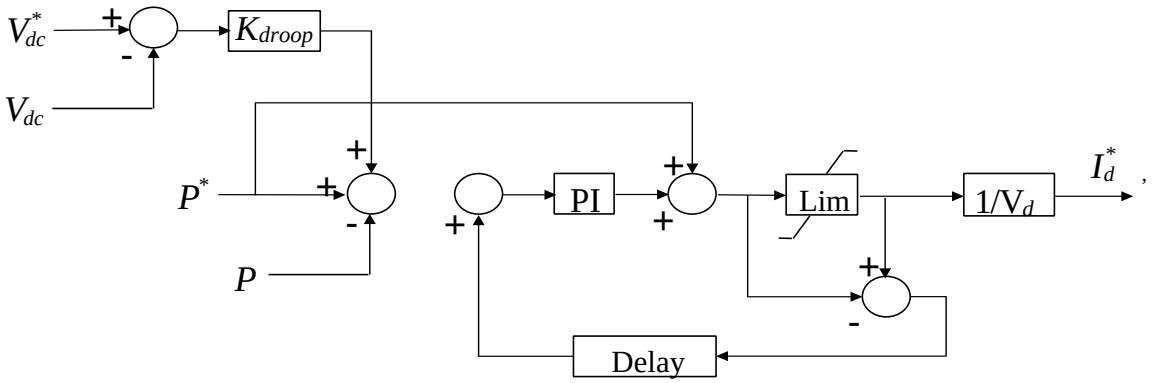

Figure 3.6 Active power controller with dc voltage droop control [9]

3.3.6 AC VOLTAGE CONTROL (VAC CONTROL)

From the reactive power equation (3.8), the voltage drop ΔV_{grid} over the reactance (X_{PCC}) of the ac grid at PCC can be approximated as:

$$\Delta v_{grid} = v_s - v_{grid} \approx \frac{X_{PCC}\,Q}{v_s} \tag{3.23}$$

Since the grid voltage vector is aligned with the d axis and using (3.18), (3.23) becomes:

$$\Delta v_{grid} \approx X_{PCC} i_d \tag{3.24}$$

An integral control is sufficient to produce the desired q current reference (Iq_ref):

$$i_{q\,ref} = -(\frac{K_i}{S})(V_{ref} - V_{grid}) \tag{3.25}$$

3.4 LOWER LEVEL CONTROL

Unlike previous VSC technology, the MMC topology requires additional controllers in order to stabilize internal variables. The top level view of the control structure is presented in Figure 3.2. Lower level control is composed of: Circulating Current Suppression Control (CCSC), modulation techniques and Capacitor Balancing Algorithm (BCA). In this section, only a brief description is given for each main component [8] [51] [9] [88] [52] [91].

3.4.1 CIRCULATING CURRENT SUPPRESSION CONTROL (CCSC)

Voltage unbalances between the arm phases of the MMC introduce circulating currents containing a second harmonic component which not only distorts the arm currents, but also increases the ripple of SM capacitor voltages. Circulating currents can be eliminated by adding a parallel capacitor (resonant filter) between the mid-points of the upper and lower arm inductances on each phase [92] or using an active control over the ac voltage reference v_{refabc} [93]. The latter is chosen in this control system.

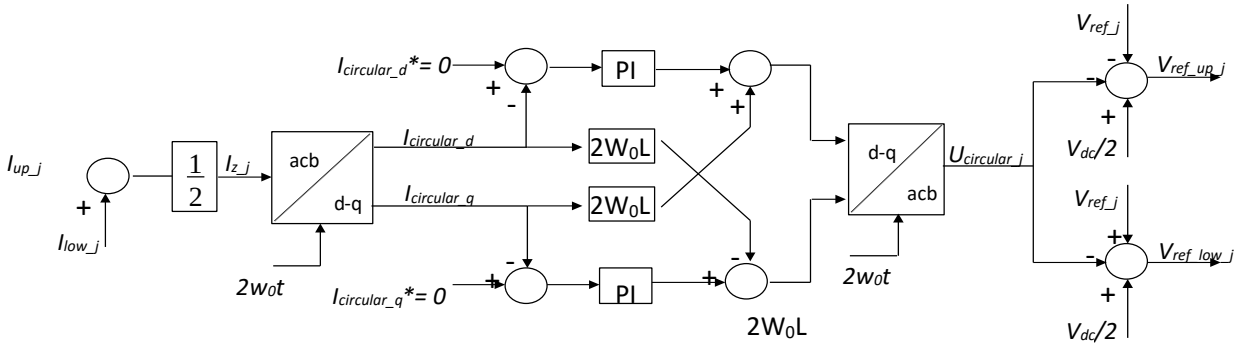

Figure 3.7 Circulating Current Suppression Control (CCSC) [9]

3.4.2 CAPACITOR BALANCING CONTROL

The capacitor voltage at all SMs must be balanced and kept the same during normal operation. To achieve this, the capacitor voltage (Figure 3.8) must be monitored and switched ON and OFF based on a Balancing Control Algorithm (BCA). The BCA measures the capacitor voltages at each SM at any instant and sorts them before selecting the upper and lower SM to switch ON. The number of SMs is determined based on the $N_{up}(t)$ and $N_{low}(t)$ switching functions, where $N_{up}(t)+N_{low}(t)$ corresponds to the total number of SMs per arm. To improve the efficiency of the algorithm, the model includes a trigger control that activates the BCA only when a new (ON/OFF) state in the $N_{up,low}(t)$ functions is reached. This will avoid switching the SMs at each time step [94] [95].

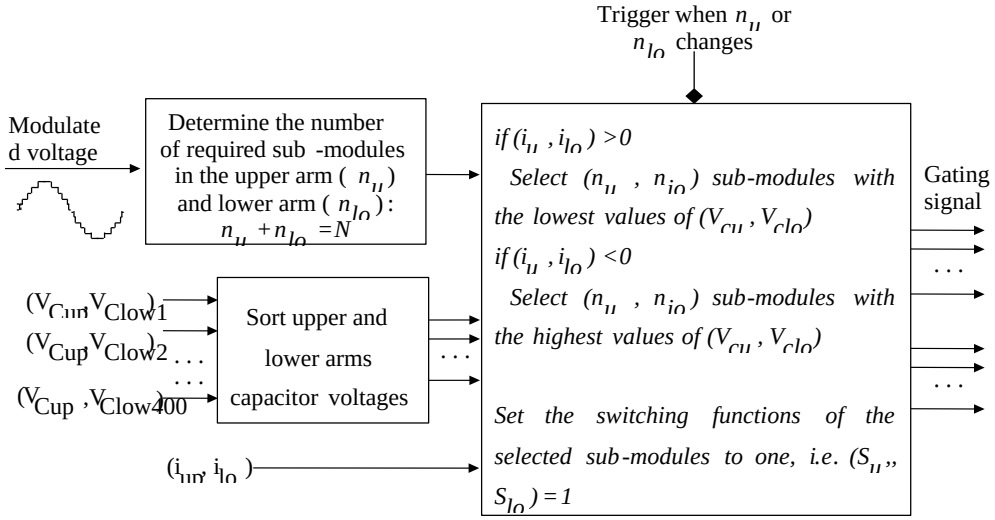

Figure 3.8 : Balancing control algorithm (BCA) [88]

It is noted that, all these controllers are included when the MMC Full detailed model and detailed equivalent model are adopted. However, if the Switching function model is adopted, the BCA device is excluded from the Lower Level Control and if the AVM model is adopted, the Lower Level Control is not represented.

3.4.3 NLC MODULATION

Traditional modulation techniques proposed to date for MMCs include Phase-Disposition Modulation (PD-PWM), Phase-Shift Modulation (PS-PWM), Space-Vector Modulation (SV-PWM), and the improved Selective Harmonic Elimination method (SHE). As the number of levels increases in MMCs, PWM and SHE techniques become cumbersome for EMT-type simulations. Therefore, more efficient staircase-type methods, such

as the Nearest Level Control (NLC) technique, can be used. The following section studies the differents modulation techniques [96].

3.4.4 MODULATION TECHNIQUES

Several different modulation methods have been proposed in the literature for multilevel converters; a popular categorization of these was presented in [97] and updated in [98]. The main parts of the categorization are shown in Figure 3.9. it can be also classified into two categories based on the switching frequencies and achieve higher output quality at the cost of increased switching losses. The fundamental frequency modulations techniques on the other hand have lower switching losses but decreased number of produced voltage levels. The criteria to select the proper modulation technique highly depend on the converter topology, design specification and application. The high switching frequency modulation techniques are mainly a part of carrier based pulse width modulation.Space-Vector strategy, which has been used in three-level inverters and selective harmonic elimination are among the well-known low switching frequency modulation techniques used in multilevel converters. The following sections provide a brief overview of these modulation techniques [91] [99] [9] [100] [101] [102] [103].

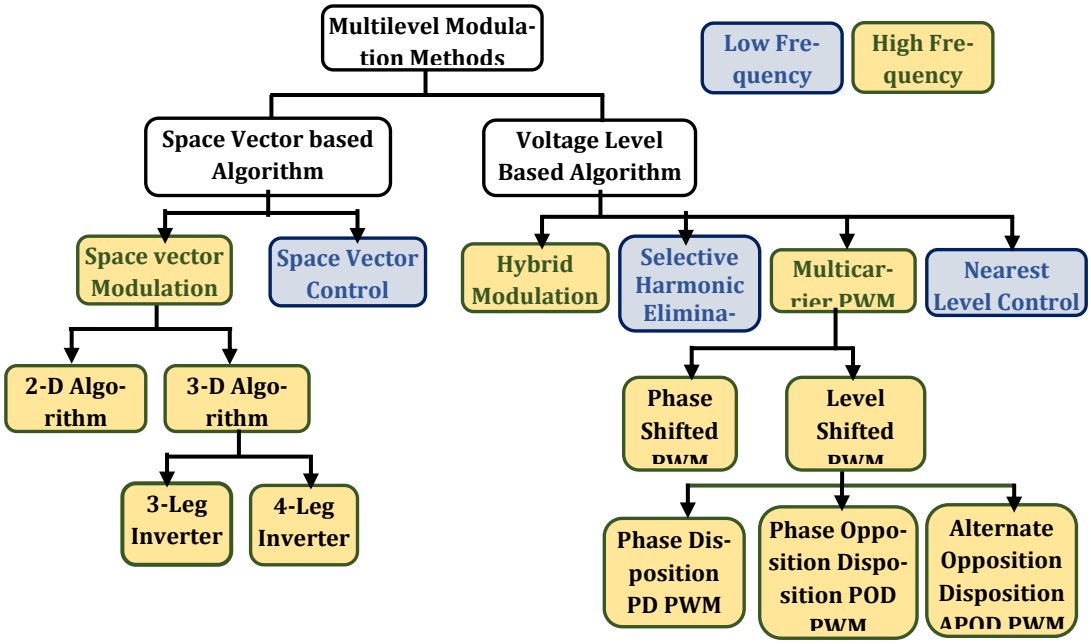

Figure 3.9 Modulation strategies for multilevel converters.

3.4.5 MULTICARRIER PWM TECHNIQUES

The pulse Width based Modulation (PWM) strategies used for a conventional inverter can be modified to use for multilevel inverters as well. Classic carrier-based sinusoidal PWM, which is a part of PMW family, is a very popular method in industrial applications for high switching frequency switching [104] [91] [51].

In carrier based modulation techniques, each generated level in a phase requires a carrier so each module has its own carrier waveform, which is compared to the reference waveform to generate the switching pulses.The carrier based modulation techniques are generally divided into two categories: the phase shifted pulse width modulation (PS-PWM) and the level shifted pulse width (LS-PWM). Both PS-PWM and LS-PWM have several categories, which differ by allocation of carriers with respect to each other.

A. Level shifted PWM

Several modulation techniques are developed based on the classical sinusoidal PWM (SPWM) with triangular carriers to reduce the distortion in multilevel inverters .Three of the most common techniques are the following [51] [105]:

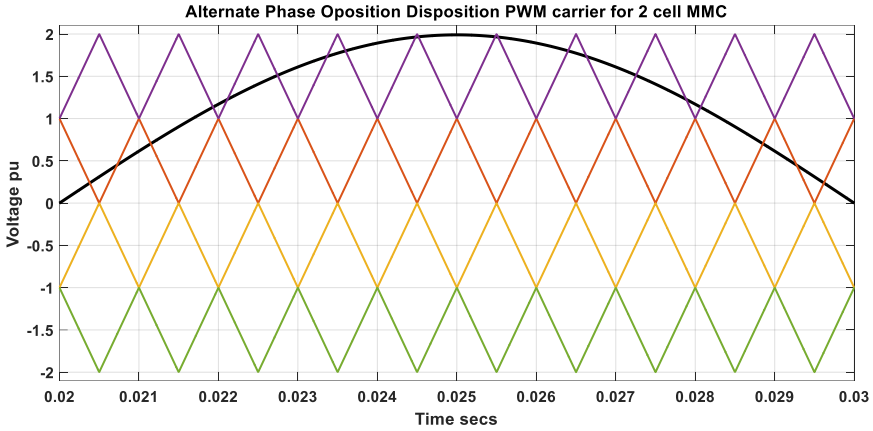

Figure 3.10 Alternate phase opposition disposition SPWM

The waveform of a carrier is phase shifted by 180° from the waveform of the next carrier (Alternate Phase Opposition Disposition, APOD), as shown in Figure 3.10

ALL positive carrier waveforms are in phase, but the positive carriers have the opposite phase from the negative ones.Positive and negative is defined by the reference signal values. (Phase Opposition Disposition, POD), as shown in Figure 3.11.

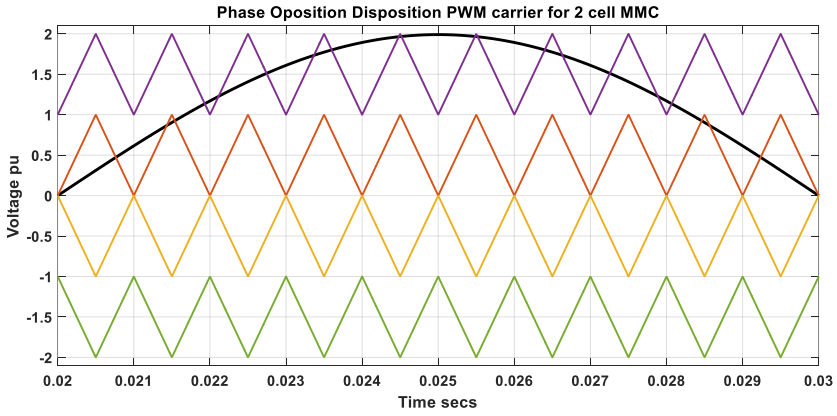

Figure 3.11 Phase opposition disposition SPWM

The phase disposition PWM uses carriers with the same frequency of $f_{SW} = 1/T_{SW}$ and the amplitude of the module DC link voltage U_{dc} for different modules .The reference voltage can change between -MU_{dc} and MU_{dc-} . The carriers of the first module changes from zero to U_{dc} and $2U_{dc}$ and the range inreases to (M-1) U_{dc} to MU_{dc} for last modules to cover the whole voltage range .The carriers are reordered for the negative side in the opposite order and there can be a phase shift between carriers as shown in Figure 3.12. The switching pulses are derived by comparing the reference voltage waveform with the modules carrier .The state of each module is U_{dc} when the reference is higher than the positive carrier and same comparison is made for the negative carrier and the module outputs zero if none of these conditions are satisfied.

$$U_{mod} = \begin{cases} U_{dc} & if\ u^{*}_{mod} > u^{pos}_{car} \\ -U_{dc} & if u^{*}_{mod} > u^{neg}_{car} \\ 0, & otherwise \end{cases} \tag{3.26}$$

In this method the switching frequency of the converter output is f_{SW} however the modules have a varying switching frequency depending on the carrier position [39].

The level shifted PWM leads into unequal loading of modules in some applications. Therefore the DC link capacitors of the modules are loaded differently that cause the capacitor voltage unbalance problem in topologies such as MMC because the first module will absorb most of the energy flowing back from the load.

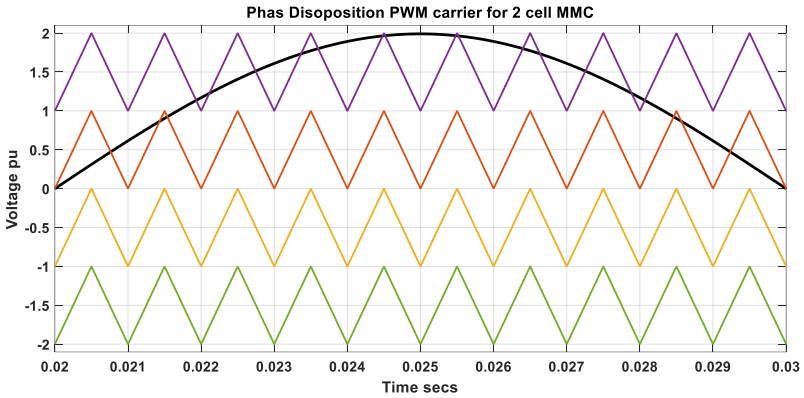

Figure 3.12 Phase disposition SPWM

B. Phase shifted PWM

The load-sharing problem of level shifted PWM is solved in phase shifted PWM technique.For multilevel inverters implemented using cascaded cells ,the phase shifted SPWM technique is proven to be producing a load voltage with the smallest distortion .In this modulation technique ,the carriers of N cascaded cells are phase-shifted by an angle of θ_C=360°/N as shown in Figure 3.13.The carriers are usually allocated using two approaches .The first approach uses two carriers for each module with the amplitude of MU_{dc}.The second method uses a 2MU_{dc} amplitude ranging from -MU_{dc} to +M$U_{dc}$and both methods use a carrier frequency of 1/MT_{SW} which is phase shifted by the defined angel.

$$U_{mod} = \begin{cases} U_{dc} & if -u^*_{mod} < U_{car} < u^*_{mod} \\ -U_{dc} & if \quad u^*_{mod} < U_{car} < u -^*_{mod} \\ 0, & otherwise \end{cases} \tag{3.27}$$

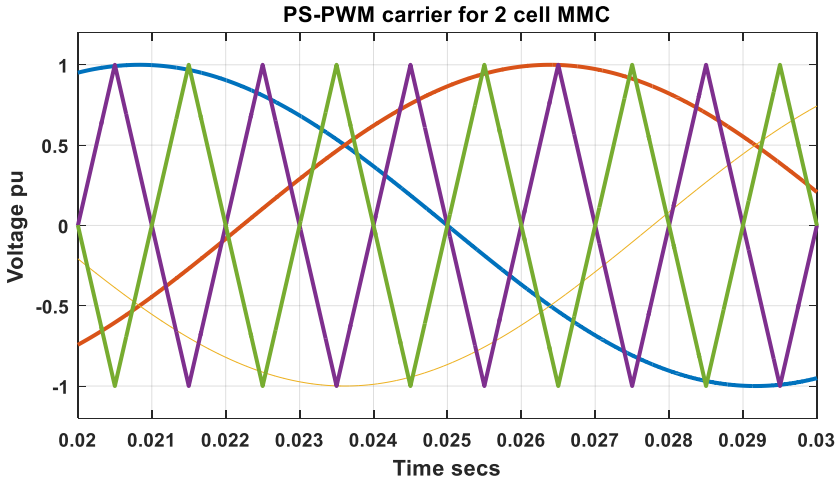

(a)

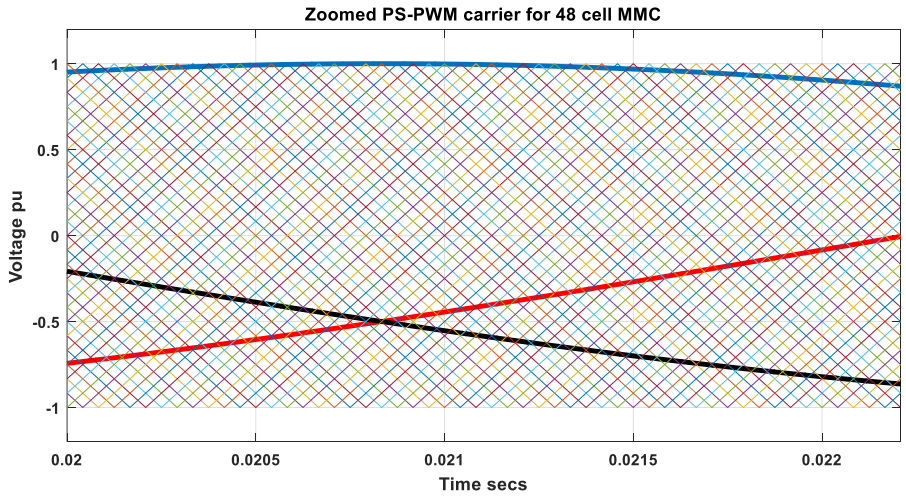

(b)

Figure 3.13 (a) Phase shifted SPWM for 2 cells MMC, (b) Phase shifted SPWM for 48 cell MMC

3.4.6 NEAREST LEVEL MODULATION (NLM)

Nearest level modulation is one of the most suitable modulation techniques for MMC with large number of sub-modules. The conventional NLM techniques works by dividing the reference voltage by individual sub-module voltage and generating the closest integer to the real number .Equations (3.28),(3.29),(3.30) and (3.31) show the total number of sub-modules in MMC arm,the AC reference voltage and number of calculated sub-modules by NLM upper and lower arm [43].

$$U_{SM} = \frac{U_{dc}}{N} \tag{3.28}$$

$$U_{ej}^{ref} = \frac{1}{2} m U_{dc} \cos(\omega t + \varphi j) \tag{3.29}$$

$$N_{ju} = round\left(\frac{0.5U_{dc} - U_{ej}^{ref}}{U_c^{ref}}\right) \tag{3.30}$$

$$N_{jl} = round\left(\frac{0.5U_{dc} + U_{ej}^{ref}}{U_c^{ref}}\right) \tag{3.31}$$

For a grid connected MMC the reference of AC emf is obtained by active and reactive power demands [44].The total number of sub-modules inserted in each phase is constant and defined by (3.32).

$$N_j = N_{jup} + N_{jlow} \tag{3.32}$$

N_j and U_{dc} are constant to ensure that sub-module capacitor voltages stay around U_{SM} however if no additional balancing technique is used the sub-module capacitor voltages might become unbalanced [51] [106].

3.5 PROTECTION SYSTEM

The main protection device employed by MMC systems is the ac breaker. It will operate to protect the system for during ac and dc disturbances. In the case of dc faults, the press-pack thyristor (K2 in Figure 3.14) is used to protect the converter semiconductors and cables from high fault currents. The switch K1 Figure 3.14is a high-speed bypass switch used to increase safety and reliability of the MMC in case of SM failure [22]. The anti-parallel free-wheeling diodes used in VSC have a low capacity for withstanding surge current

events without damage. This would be the case during a dc fault where the diodes would have to withstand a high fault current without damage until the circuit breaker opens which in most cases is at least three cycles [20] [88]. To avoid this, the fast thyristor switch (K2) is added to bypass the SM allowing the current to flow through the fast thyristor instead of the diodes. Once a dc fault is detected, the MMC is blocked (the IGBT valves are switched off) and the fast thyristor is switched on within a few microseconds (40 µs in our proposed model), allowing the fault current to flow from the ac to the dc side systems through the antiparallel free-wheeling diodes for only a short period of time. After a few cycles the main ac breaker is open and the fault cleared. This technology makes the HVDC transmission based on MMCs suitable for overhead transmission lines, an application previously reserved entirely for conventional LCC-HVDC systems [19].

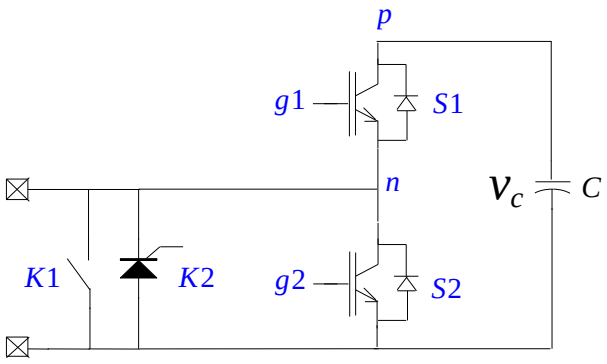

Figure 3.14 MMC sub-module protection

Chapter 4 MMC-HVDC LINK PERFORMANCE

This chapter assesses the steady-state and transient performance of the MMC-HVDC link models developed in Chapter 2 and the controller proposed in Chapter 3 for the HVDC link based on MMC converter, MMC-HVDC with 400 SMs (401 level) per arm performance is verified in this chapter in two cases, the interconnection of two asynchrounous AC networks (50/60 Hz) and the connection of a typical windfarm. The theory given in Chapter 3 is used to verify the simulation results.

4.1 BACK-TO-BACK HVDC SYSTEM

The VSC HVDC back-to-back arrangement is used when two asynchronous AC systems need to be interconnected for bulk power transmission or for AC system stabilization reasons. Besides controlling the through power flow, it can supply reactive power and provide independent dynamic control at its two terminals. As explained in chapter 3, active and reactive power can be controlled independently as long as they are not exceeding the operating limits fixed by the converter and the DC line rating. All these limits are reported in Figure 4.1 [107] [108]. The three main quantities, which limit the VSC range of operation, are:

- ✓ The maximal admissible AC current feeding in the converter.
- ✓ The maximal converter voltage on the AC side.
- ✓ The maximal DC current.

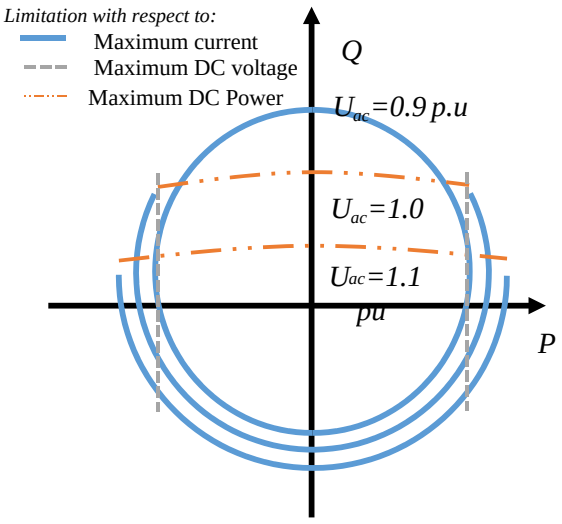

Figure 4.1 P-Q characteristics of a VSC-HVDC system

$$P^2+\left(Q-\frac{U_L^2}{X_L}\right)^2=\left(\frac{U_L\cdot U_{V(1)}}{X_L}\right)^2 \tag{4.1}$$

If the output voltage of the converter U_V (1) is reduced, e.i by using modulation techniques, supply of any active and reactive power within the circle is possible [108].

4.1.1 SYSTEM INVESTIGATED

Figure 4.2 shows a single-line diagram of the study system, the system comprises two back-to-back connected MMCs which are hereinafter referred to as MMC-1 and MMC-2. Each MMC consists of six arms where each arm includes series-connected, nominally identical, half-bridge submodules (SMs). Reactors L are to provide current control within the phase arms and limit fault currents. The ac terminal of each MMC is connected to a utility grid through a three-phase transformer.

The HVDC system of Figure 4.2, based on detailed model of chapter2 and the NLC strategy and control theory of chapter 3, is simulated in the EMTP-rv environment. Table II in appendix B provides parameters of the system of Figure 4.2 used for the simulation studies. The simulated test cases evaluate dynamic performance of the overall system of Figure 4.2, including power and control subsystems, under various conditions.

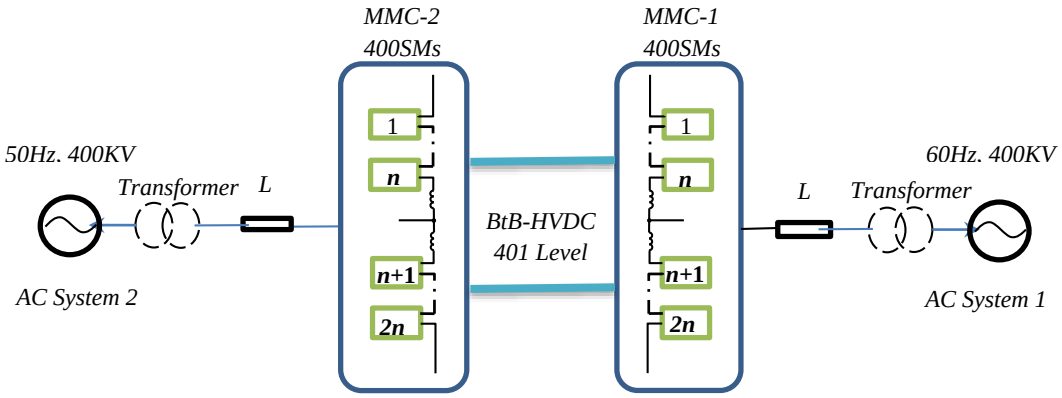

Figure 4.2 MMC-HVDC system configuration

4.1.2 MODEL PERFORMANCE ANALYSIS

The dynamic performance of the transmission system is verified by simulating the:

A. Normal operation of the BtB-HVDC system.
B. Active power flow reversal and dynamic response to step change applied to the reactive power regulator.
C. MMC1 and MMC2 response to external AC single phase to ground fault.

C. Case A

In Figure 4.3, the initial reference value of the power flow is at 1 p.u in the direction from MMC1 (rectifier mode) to MMC2 (inverter mode). The MMC 1 supply 1000 MW to the MMC 2 with dc voltage is set to 640 KV (voltage pole to pole), the active power follows the reference without any oscillation.

The MMC2 operates in the constant DC voltage and constant reactive power mode، and the DC voltage is set to 640 kV (±320KV). The MMC 1 operate in the constant active power and constant reactive power mode, the active power setting is 1000 MW in MMC1 (rectifier) and -1000MW in MMC 2 (inverter). Both MMC 1 and MMC 2 operate at unity power factor, the reactive power in both MMC 1 and MMC 2 is kept at 0 MVAr. The DC link voltage in HVDC-MMC system is maintained by the sum of submodule voltages inserted in the converter leg and there is no bulky DC link capacitor as in other VSC-HVDC systems. Figure 4.3 shows the capacitor voltages of the phase-a submodules of MMC 1 and MMC 2, respectively, which are kept balanced at their nominal values, only the average capacitors voltage of each arm is plotted for the sake of clarity.

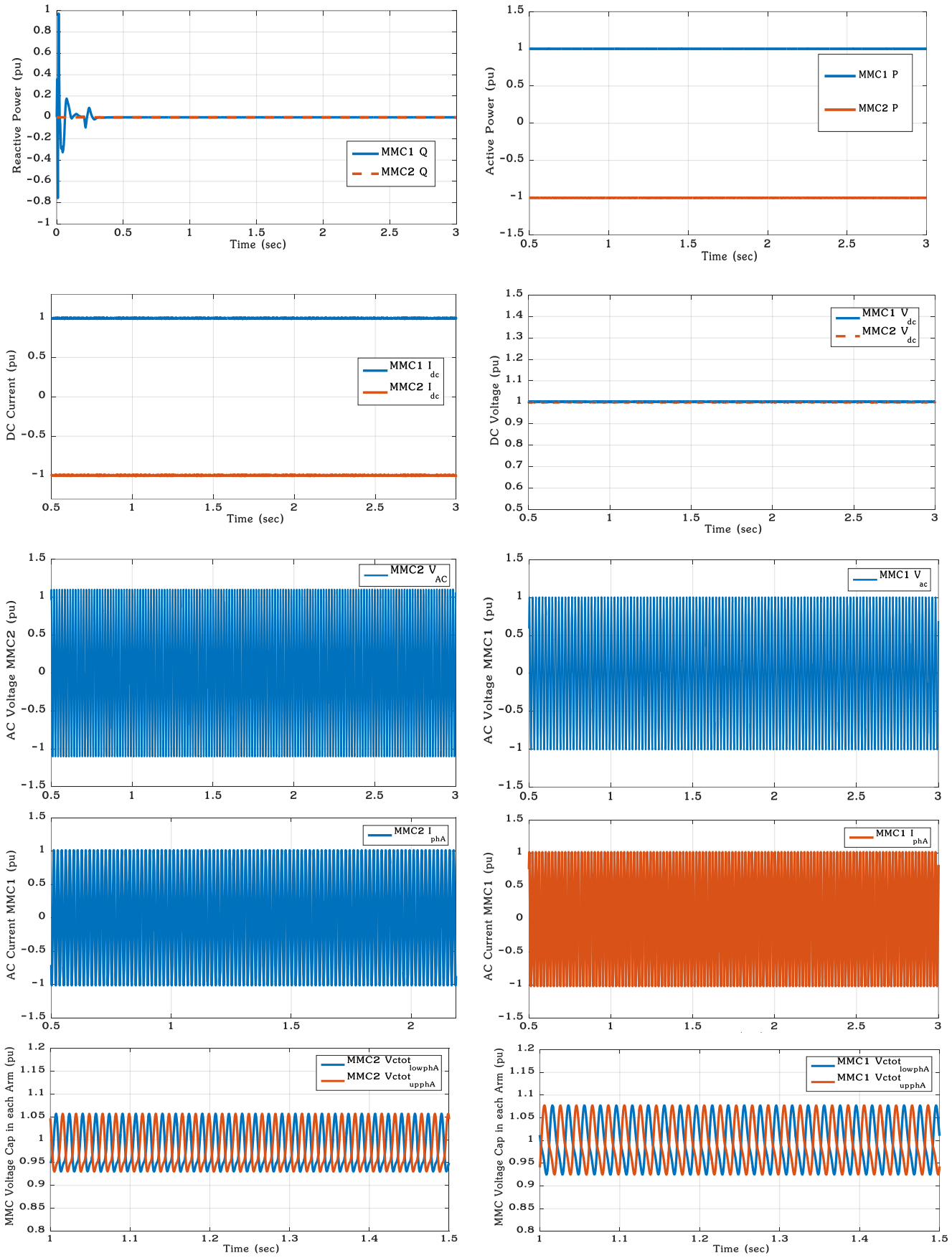

Figure 4.3 MMC 2 and MMC 1 in normal operation

D. Case B

In order to test the dynamic responses of the back to back MMC-HVDC regulators, two test cases have been studied. At t = 1s, the reactive power step change from 0 p.u to – 0.2 p.u of station 1 (MMC 1). At station 2 (MMC 2), the reactive power step change from -0.3 p.u to -0.1 p.u at t = 1.5 s (Figure 4.4, with the constant dc voltage of 1pu). These two steps change don't cause transients on the DC voltage, but, as expected, the step change of the active power causes a transient in the DC voltage. We can see that it has a good tracking accuracy. However, variables P1 and P2 are not affected at all. Obviously, the reactive power flow can be independently controlled at each AC network, and the reactive power and the active power control is independent. Notice that, considering the loss in the transmission cables, the sending active power equals the receiving active power plus the loss power in the cable. The active and reactive power responses are decoupled by the control design.

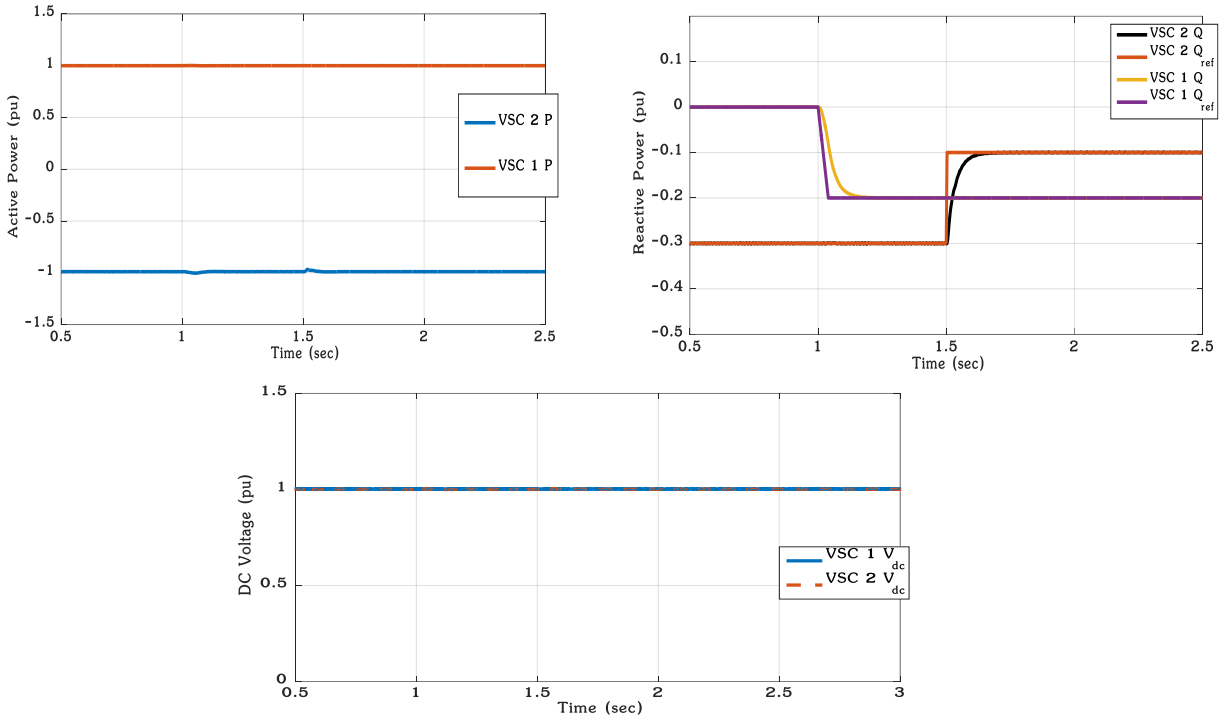

Figure 4.4 Steps on the reactive power regulators references in MMC1 and MMC2

In Figure 4.5, the initial reference value of the power flow is at 0.5 p.u in the direction from MMC 1 (rectifier mode) to MMC 2 (inverter mode). At t=1 s, the reference value is reversed from +0.5 p.u to -0.5 p.u (from 500 MW to -500 MW). It can be seen that the active power follows the reference rapidly without any oscillation and reaches the new reference of -0.5 pu within 0.2 s. Correspondingly, the measured active power P2 at MMC 2 changes around from -0.5 p.u. to 0.5 p.u (from -500 MW to +500 MW). At the same time, the active power flow reverses with the DC current direction change.

As can be seen, the active power can track the reference of the active power. The transferred active powers at both sides change the direction which causes transients on the DC voltage then returns to the reference value due to the DC voltage controller. The inverter is used to control the DC link voltage. As shown in Figure 4.5, there is a small transient on the DC link due to the step changes of powers, which is considered to be acceptable. The AC voltages (U_{AC1} and U_{AC2}), can be kept constant except for some transients that occur when both the step changes are applied. The control strategy for each MMC remains unchanged during the power flow reversal, but the ac voltage limiters in the outer controller are relaxed to allow the voltage to vary in a range of ±10%. As the reactive power reference remains unchanged (unity power factor), a voltage drop is observed at MMC-2 after power reversal. This voltage drop can be compensated by varying the reactive power set point in the outer controller.

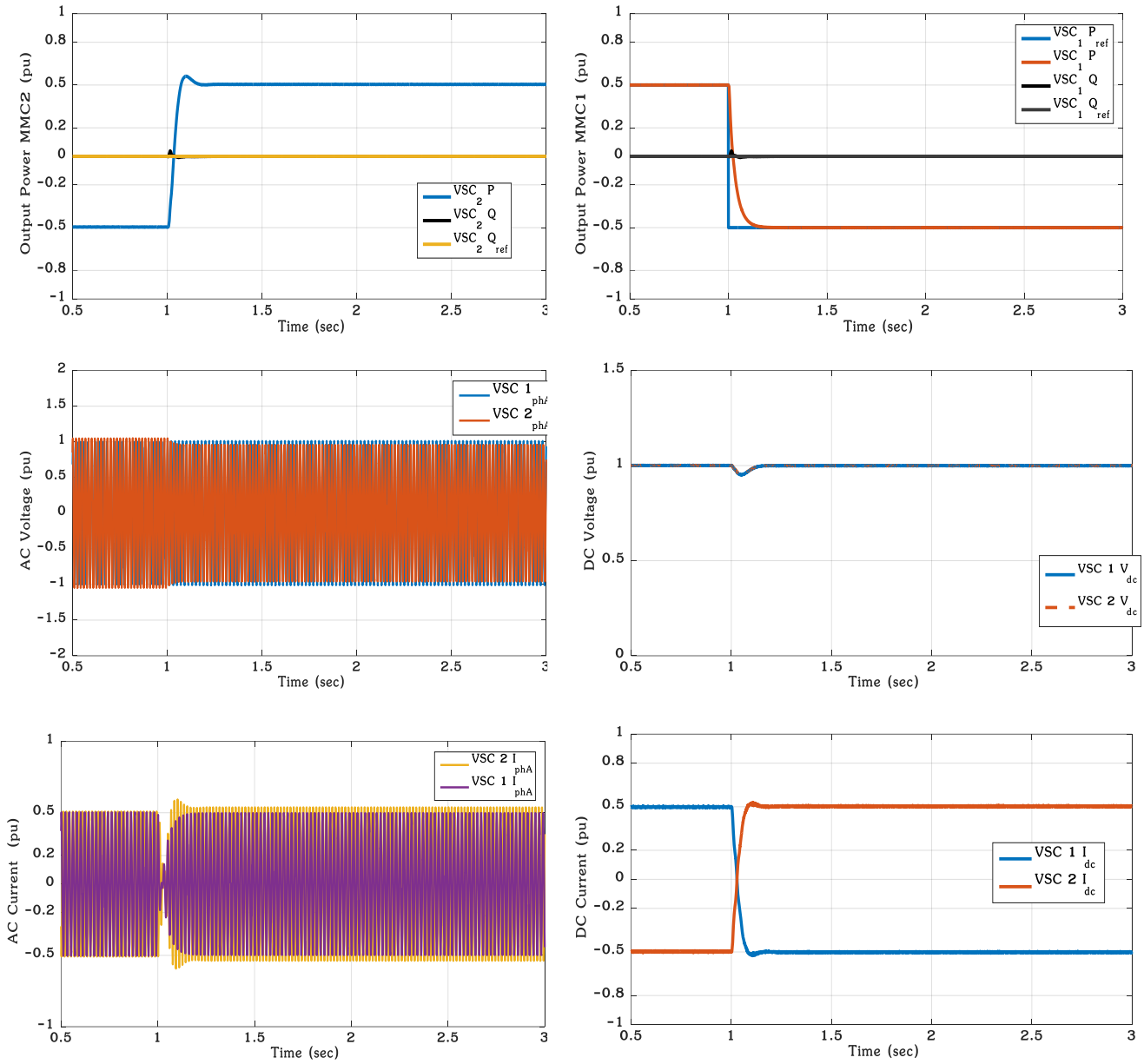

Figure 4.5 Real power flow reversal in MMC 1 and MMC 2.

E. Case C

A single phase to ground fault was first applied at t = 2 s during 0.12s (7 cycles) at station 1 AC bus (MMC 1) in order to investigate the behaviour of MMC-HVDC during unbalanced faults. A second perturbation follows. A single-phase to ground fault is applied at station 2 AC bus (MMC 2) at t = 4 s and is cleared at 6 cycles after the fault, i.e., at t = 4.12s. Figure 4.6 presents the simulations results of both converters MMC1 and MMC 2. From the simulation, it can be noted that before a single phase to ground fault at station 1, the active power flow is 1.0 pu, transmitted from MMC 1 to MMC 2, and is kept constant after fault clearance.

The DC voltage drops and it contains an oscillation during the fault. Consequently, the transferred DC power contains also the oscillation. At both converters after the faults occurs a protection system "block converters is activated to protect the submodules in each MMC from the short circuit current as shown in Figure 4.6, it is observed that the ac voltage on both MMC converters is only slightly impacted by the fault on the other side of the system, which confirms the assumption of independent voltage control on each MMC. It is

noticed that the reactive power is invariant during the faults and experiences a short transient right after fault clearing to slowly recover after approximately 200ms.

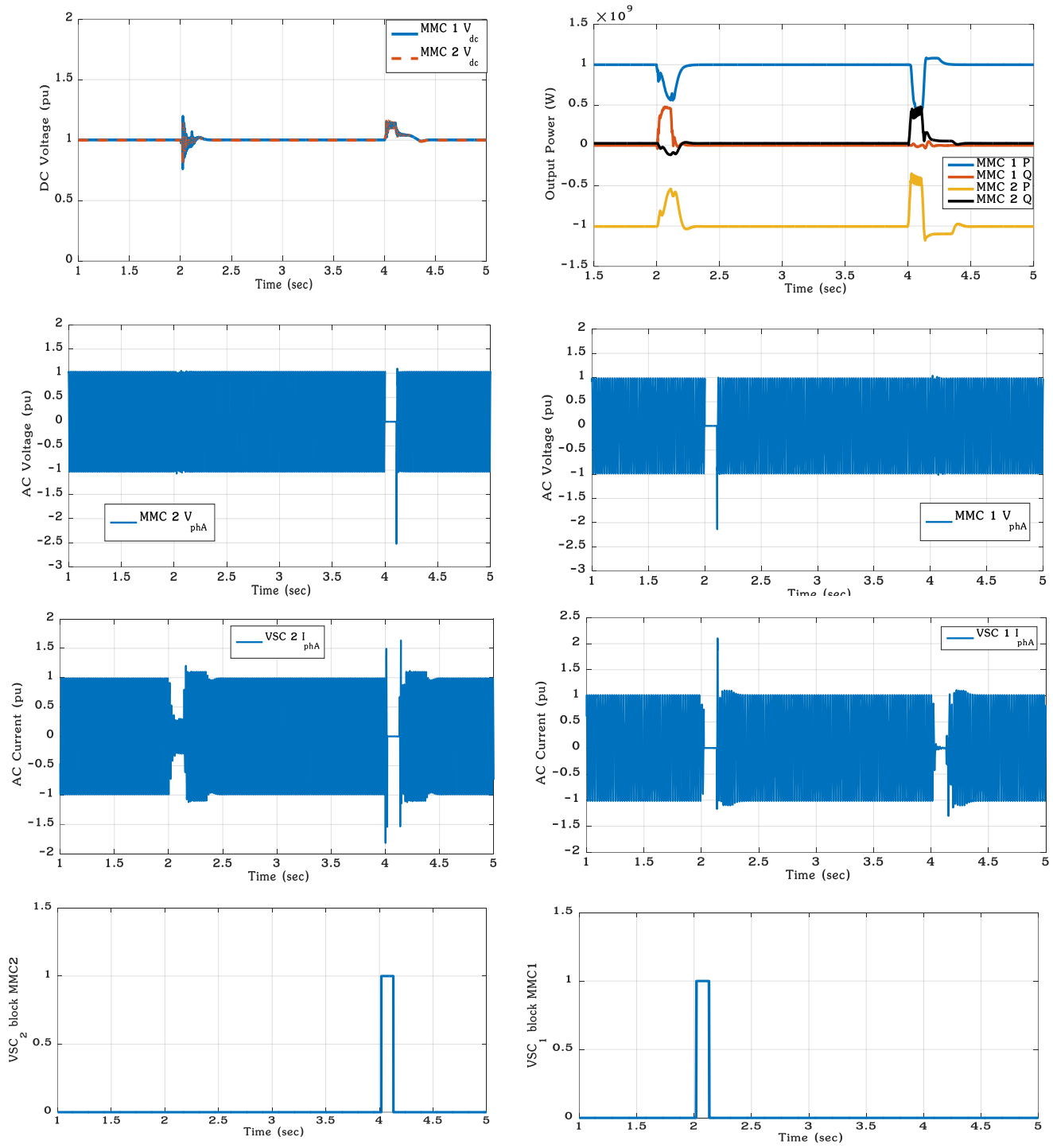

Figure 4.6 Dynamic response of the system after AC line to ground fault at MMC1 and MMC2.

4.2 OFFSHORE-WIND FARMS WITH HVDC CONNECTION SYSTEM

In this chapter, the presented approaches and assumptions are used to analyze the application of offshore wind farms with HVDC grid-connection system based on 401 level MMC converter. To that purpose, additionally, different scenarios in HVDC grid-connection system are presented. In state-of-the-art design, these systems contain one transformer and a MMC station on each side connected with reactors L which provide

current control within the phase arms and limit fault currents. As introduced before, the MMC converters additionally the opportunity to eliminate the filter in each side. Because of the location of the offshore station in the sea, the less filtering and the compact footprint MMC-HVDC station is very attractive and.

4.2.1 DFIG-BASED WIND TURBINES

Double Fed Induction Generators are the most commonly used generator type in modern wind turbines. Figure 4.7 shows a typical configuration of a DFIG system. The combination of the back-to-back frequency converter with the rotor blades pitch control enable variable speed operation, and leads to higher efficiency and energy yields compared to fixed speed wind turbines. Since the converter is located in the rotor circuit, its power rating should be a small portion of the total generator power (typically 20-30%, depending on the desired speed range).

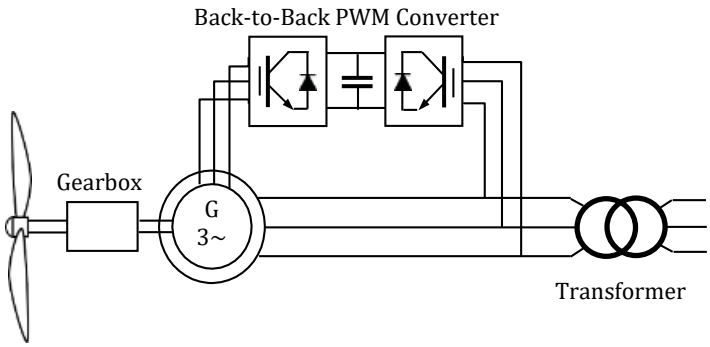

Figure 4.7 DFIG based wind turbine system

In a DFIG system, the functions of the grid side converter are maintaining the DC voltage and the support of the grid with reactive power during a fault. Especially when the machine rotor is short-circuited, the generator consumes reactive power. The grid side converter must compensate this reactive power.

The active and reactive power of the DFIG are controlled by the rotor side converter which follows a tracking characteristic in order to adjust the generator speed resulting in optimal power generation for a variable wind speed. A feed-forward decoupled current control is used for both of the converters controls [109] which is as the one used for the REC of the VSC-based HVDC. When the wind speed exceeds its nominal value, the pitch control pitches the rotor blades to reduce the mechanical torque and thereby recover the generator rated speed, see appendix C. A complete description of the DFIG control system can be found in [110].

4.2.2 FRT PROBLEM

During a fault at the ac grid, the onshore converter cannot transmit all the active power to the ac grid, however the offshore wind farm still inject active power to offshore converter, which results in power imbalance that will cause transient in DC voltage link (Figure 4.8). Without any actions taken, the dc voltage will increase quickly, that may damage the HVDC equipment.

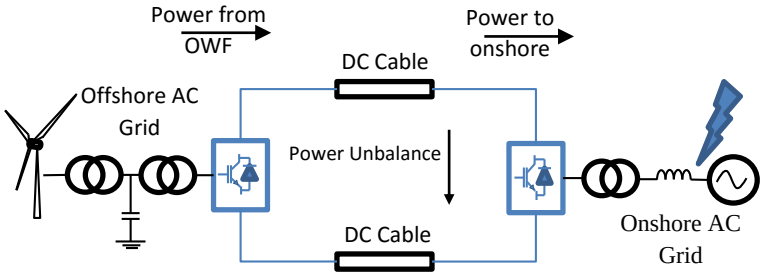

Figure 4.8 Circuit diagram of HVDC Connection of Offshore Wind Farms to the Transmission System

4.2.3 FAULT-RIDE-THROUGH (FRT) METHODS

The FRT problem can be avoided by using a DC chopper (or DC braking resistor), which represent a good solution at the consequence of higher investment costs. FRT methods based on fast reduction of power generation in OWFs have been discussed in recent literature [111], [112], [113]. These methods limit the overvoltage at the DC network and decrease the size of the DC chopper or maybe eliminate completely the need for chopper.

4.2.4 FREQUENCY CONTROL BASED FRT METHOD (F-FRT)

In this method (Figure 4.9(a)), the electrical frequency of the OWFs, i.e. the power outputs of the WTs in the OWFs are determined by the central DC voltage controllers located at the offshore MMCs. The WTs in the OWFs are equipped with a fast frequency control to respond to OWF frequency increase by reducing their output powers. The details of this method can be found in [111].

4.2.5 FAST OFFSHORE GRID VOLTAGE REDUCTION BASED FRT METHOD (V-FRT)

Fast voltage reduction in the offshore grid (Figure 4.9(b) can be done by MMC voltage control, ensuring a very quick decrease in OWF output power. The sudden voltage drop at generator terminals causes high DC currents, which can be avoided by an independent time-triggered voltage drop in all three phases in offshore MMC control [111].

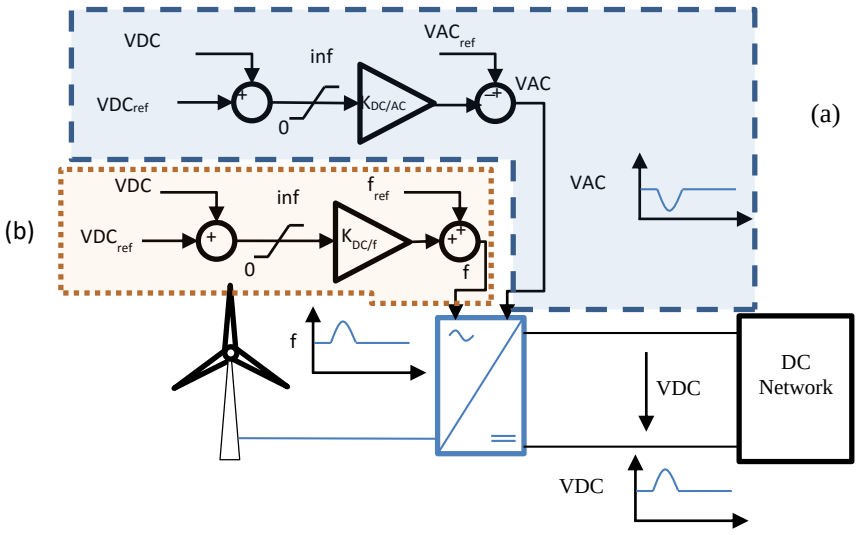

Figure 4.9 Control scheme for FRT provision based on dc voltage: (a) AC offshore grid voltage control. (b) AC offshore grid frequency control.

4.2.6 REACTIVE POWER SUPPORT AND ACTIVE POWER RESTORATION

Fast active and reactive power restoration to pre-fault values are included in the FRT requirements. Some grid codes additionally require during a fault the active and reactive power support.

Reactive power support means that wind farms should support the grid voltage with supplement reactive power production during a voltage drop (capacitive reactive current) or with reactive power overconsumption in the event of a voltage swell (inductive reactive current).

If the grid code requires both active and reactive current injection during a voltage drop, the network's short-circuit current is increased by the generating plant's active current. Feed-in of short-circuit current during a voltage drop is always agreed upon by the network operator. Active power restoration rates are also specified in various ways. This requirement is based on local grid characteristics for which active power restoration is more crucial for stabilizing the system in weak grids.

4.2.7 ONSHORE DC CHOPPER

During onshore AC disturbances, the onshore converter's ability to export active power is diminished. If the power generated by the windfarm is not curtailed to meet the demands of the onshore converter, the DC link voltage will rise. Several methods have been proposed for the curtailment of wind power during onshore AC faults. However, many of these methods require telecommunications, are not applicable for all wind turbine topologies, or require modifications to the offshore MMC and wind turbine controls. The use of a DC chopper in the HVDC link enables the DC link voltage to be controlled very effectively and does not impact on the windfarm. It is for these reasons that the use of a DC chopper is employed for these studies.

A DC chopper shown in Figure 4.10 composed of a dc resistor controlled through a power electronic switch and it is located at the HVDC–VSC onshore converter station. The detailed sizing of a dc chopper-based solution for FRT compliance in HVDC system depends on several factors, namely the DC grid power in-feeds (power infeeds from offshore WF or from other mainland ac grid areas) as well as on the mainland grid connection points and its electrical distance. In case of a fault, healthy converters (connected to non-faulted ac mainland grids) are not able to increase their power injection and power dissipation in chopper resistors is required in order to mitigate the dc voltage rise. Based on this assumption, each dc chopper must be sized to dissipate the nominal power of the HVDC–MMC to which it is connected.

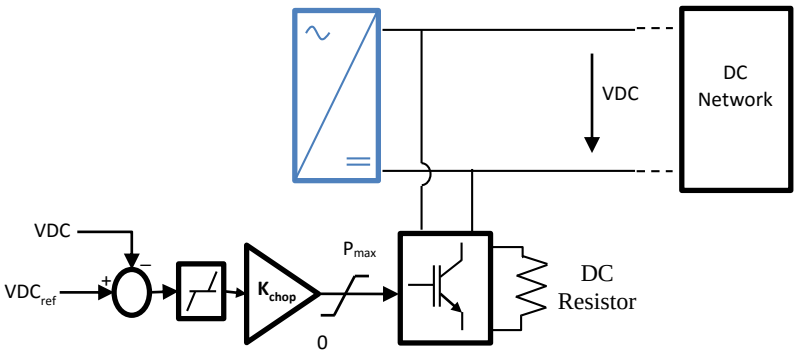

Figure 4.10 Scheme of onshore DC chopper resistor

Each control strategy of the DC chopper is enabled with regard to a dc voltage threshold that will activate power dissipation in the resistor. This dissipated power is locally adjusted based on a proportional control strategy with the overvoltage magnitude as input [5]. The dc chopper is disable if: (1) the magnitude of the dc voltage become less than the threshold activation level in our case study 1.025 pu of the dc voltage (eg: after fault clearance) or; (2) the temperature of the chopper resistor rises to its maximum value (thermal protection tripping), which means that the maximum energy dissipation capability of resistor has been exceeded. This

specific situation is often caused by a permanent fault and must be manipulated by supplemental control strategies to execute permanent active power reduction at offshore WF-level.

4.2.8 SYSTEM INVESTIGATED

The simplified single-line diagram of the offshore system is shown in Figure 4.11. The MMC-HVDC system is used to integrate up to 1000 MW of offshore wind generation through a single core 100 km submarine cable modeled with a frequency dependent (wideband) model. The dc voltage is ±320 kV and the onshore MMC is connected to a 400 kV, 50 Hz ac grid represented with Thevenin equivalent. Each set of 666 wind turbines (WTs), delivers 1.5 MW OWF (666 × 1.5 = 999 MW) and are collect in collector grid which are connected to the offshore MMC through 34.5 kV three-core submarine cables. The cables are modeled using a wideband model. The cluster is connected to 666 doubly-fed induction generators (DFIGs) of 1.5 MW, 600 V, 50 Hz via a transformer (600 V/34.5 KV).

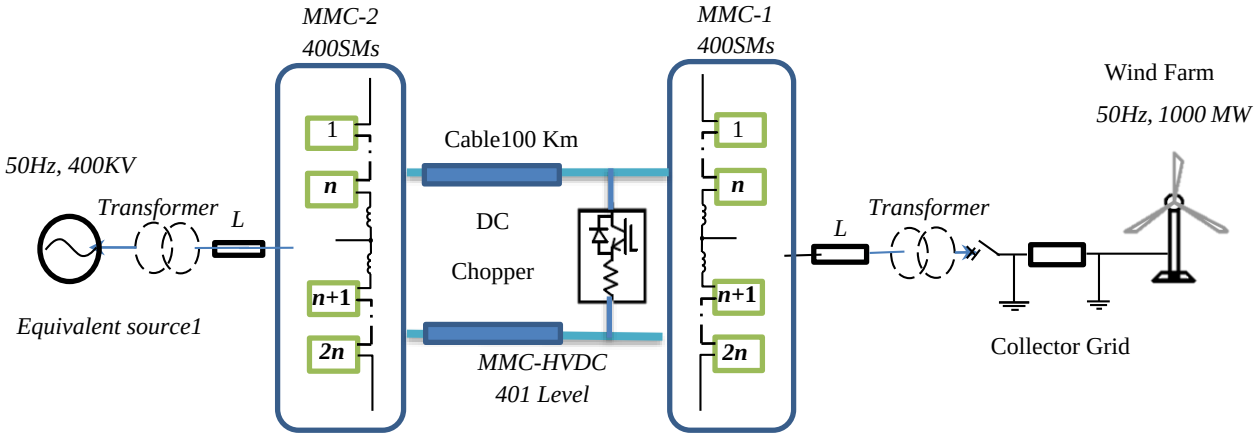

Figure 4.11 MMC-HVDC 401 level HVDC Connection of Offshore Wind Farms to the Transmission System

The HVDC system of Figure 4.11, based on switching function model of chapter 2 and the NLC strategy and control theory of chapter 3, is simulated in the EMTP-rv environment. Table III in appendix B provides parameters of the system of Figure 4.11 used for the simulation studies. The simulated test cases evaluate dynamic performance of the overall system of Figure 4.11, including power and control subsystems, under various conditions.

4.2.9 MODEL PERFORMANCE ANALYSIS

Several simulations were conducted to investigate the operation of the above MMC converter based wind power evacuation system.The dynamic performance of the transmission system is verified by simulating the:

A. Normal operation of the HVDC Connection of Offshore Wind Farms to the Transmission System.
B. Dynamic responses to steps change applied to the reactive power regulator and DC voltage regulator at MMC 2.
C. MMC 2 response to external AC single phase to ground fault (onshore fault).

A. Case A

Figure 4.12 present the active powers generated by the wind farms (666 × 1.5 MW) and exported from MMC1 (offshore station) to MMC2 (onshore station), respectively. The power reference at MMC1 is set to -1 p.u during the 3s simulation interval. The MMC2 operates in the constant active power and constant reactive power mode، and the DC voltage is set to 640 kV (±320KV), the MMC 2 operate at unity power factor. The MMC 1 operate in V_{AC}/F control and constant AC voltage mode, the active power setting is 1000 MW in MMC1 (rectifier) and - 1000 MW in MMC 2 (inverter). The reactive power in MMC 2 is kept at 0 MVAr. The offshore converter is initially set to absorb 150 MVAr while operating at maximum active power. Figure 4.12 shows that the MMC-HVDC link is capable of responding to the power demands of the windfarm and that the converter is able to meet the required reactive power demands set out in the grid code (leading and lagging power factor of 0.95). Figure 4.12 shows the capacitor voltages of the phase-a submodules of MMC 1 and MMC 2, respectively, which are kept balanced at their nominal values, only the average capacitors voltage of each arm is plotted for the sake of clarity.The phase voltages at the PCC for the onshore network ($V_{AC1}a$) and the offshore network ($V_{AC1}a$) are shown to be almost sinusoidal and as such have a small harmonic content. The DC voltages are smooth and stable.

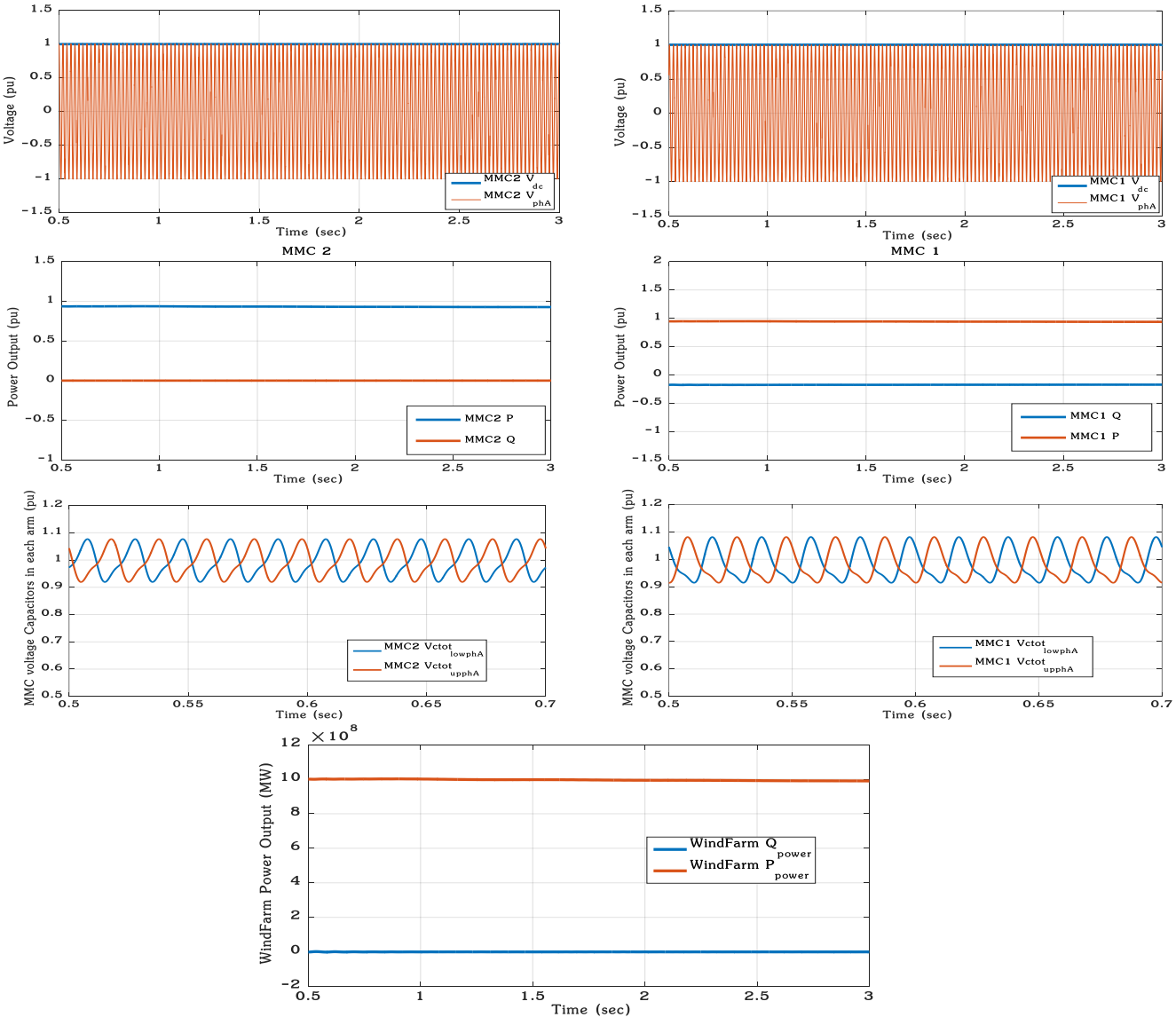

Figure 4.12 HVDC Connection of Offshore Wind Farms to the Transmission System in normal operation.

B. Case B

In order to test the dynamic responses of MMC converters regulators, two test cases have been studied. At t = 2 s, the reactive power order was increased from 0 p.u to 0.1 p.u of MMC station 2 (onshore station). We can see that it has a good tracking accuracy. It is achieved in 80 ms, without any effect on real power as shown in Figure 4.13, confirming the de-coupling of real and reactive power control loops. Obviously، the reactive power flow can be independently controlled at each AC network، and the reactive power and the active power control is independent. Figure 4.14 shows the response of onshore MMC to a sudden change in dc voltage order from 1 p.u to 0.9 p.u at t= 2 s. It is achieved in 50 ms، without any effect on reactive power. This step change cause transients on the active power.

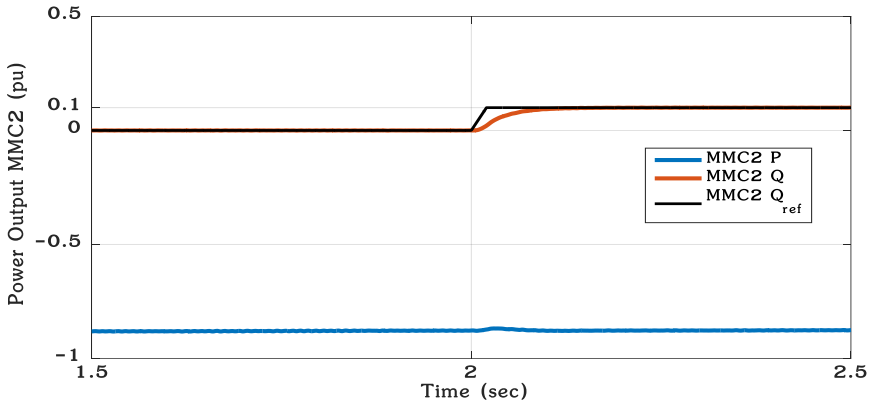

Figure 4.13 HVDC system responses for reactive power step changes at MMC2

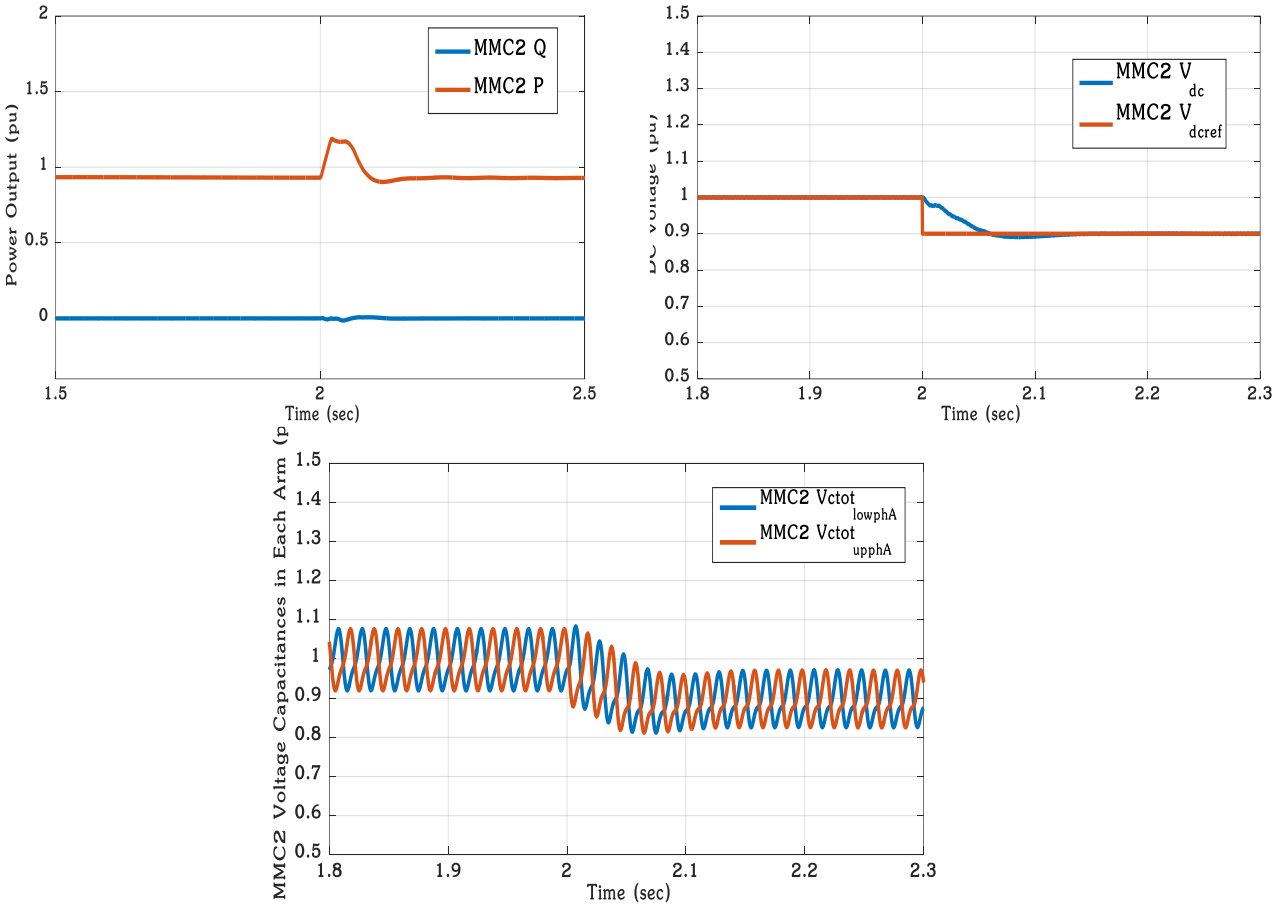

Figure 4.14 HVDC system responses for dc voltage step changes at MMC2.

C. Case C

A single phase to ground fault was first applied at t = 2 s during 0.12s (6 cycles) at station 2 AC bus (offshore MMC) in order to investigate the behaviour of MMC-HVDC during unbalanced faults. Figure 4.15 presents the simulations results of both converters MMC1 and MMC 2. From the simulation, it can be noted that before a single phase to ground fault at station 1, the active power flow is 1.0 p.u, transmitted from MMC 1 (offshore MMC) to MMC 2 (onshore MMC), and is kept constant after fault clearance.

The DC voltage fluctuates and it contains an oscillation during the fault. Consequently, the transferred DC power contains also the oscillation. At both converters after the faults occurs a protection system "block converters is activated to protect the submodules in each MMC from the short circuit current as shown in Figure 4.15 , it is observed that the ac voltage on both MMC converters is only slightly impacted by the fault on the other side of the system, which confirms the assumption of independent voltage control on each MMC.

The MMC1 (rectifier) is connected to a large wind farm, therefore its output power remains unchanged during the fault. During the fault on the onshore Point of Common Coupling (PCC), the inverter is effectively paralysed and is not able to delivery any active power to the grid. As a consequence, the power generated by the wind farm is injected into the DC link and causes the DC link voltage to rise continuously until the DC chopper is engaged, as demonstrated in Figure 4.15.

When the power injected into the DC link is greater than the power consumed, the DC link voltage will rise. To prevent the DC link voltage rising over the acceptable limit, a DC chopper is usually used to absorb the extra power. A DC brake resistor with an IGBT valve is implemented on the DC link to simulate the DC chopper. The configuration is shown in Figure 4.15. The value of the resistor is designed to prevent the DC link voltage from exceeding 1.075 p.u.

The DC link voltage continues to rise until it surpass 1.075 p.u. (688 kV), at which moment the DC chopper is activated to absorb the exceed power in the DC link. The firing signals can be seen in the DC Chopper curve in Figure 4.15.

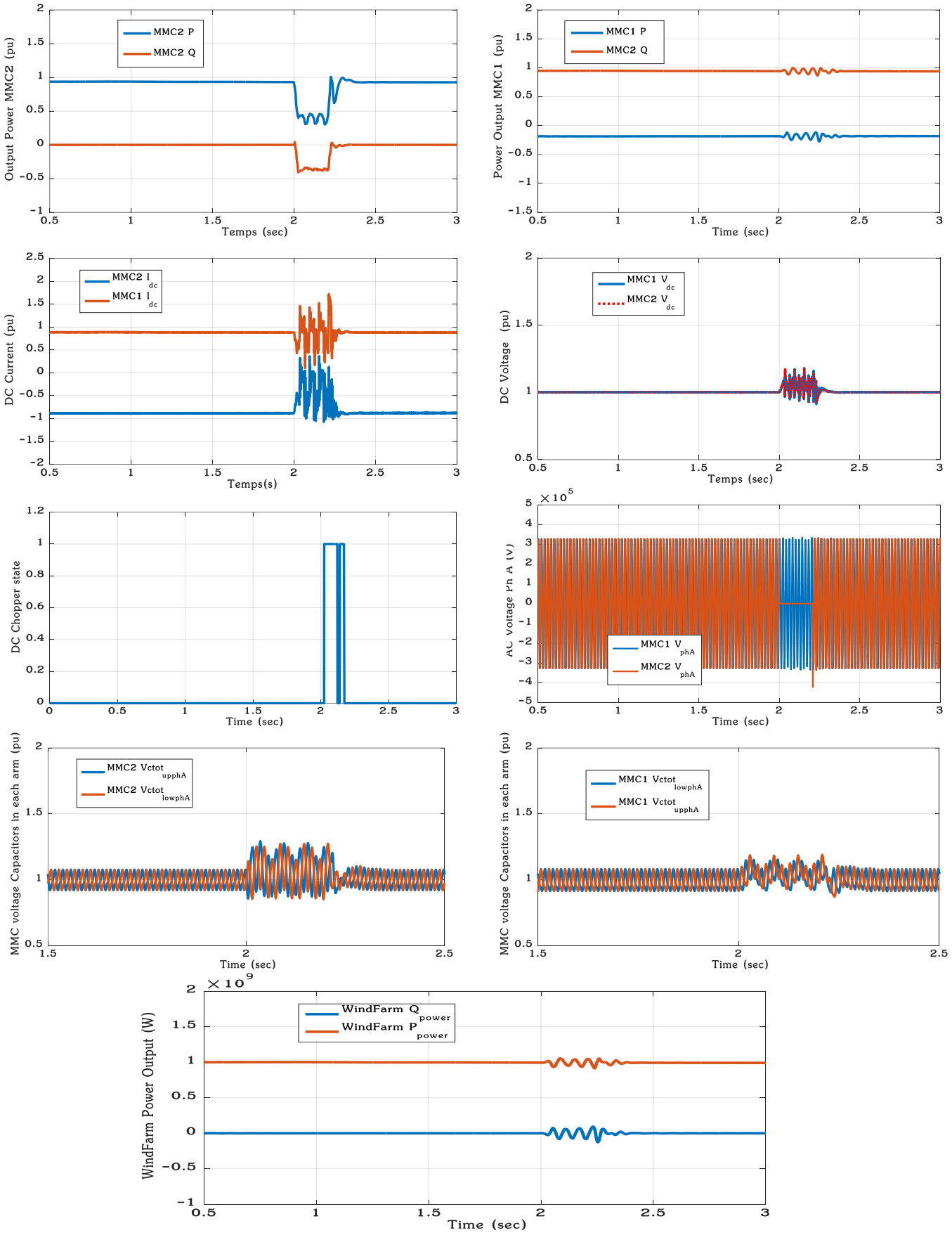

Figure 4.15 Dynamic response of the system after onshore single phase to ground fault.

4.3 CONCLUSION

This chapter has assessed the steady-state and transient performance of the MMC-HVDC link models developed in Chapter 2 through conducting a range of typical studies. The simulation results are shown to be in agreement with the control theory outlined in Chapter 3. The models developed in this thesis were used to investigate the links' ability to respond to reactive power demands and to ride-through disturbances in the AC grid. The results show that the models were able to meet the reactive power requirements and the AC fault ride through requirements set out in the grid code compliance.

This chapter studies in first a back-to-back MMC-HVDC transmission system based on a 401 level MMC converter (400 SMs). The chapter presents and evaluates the nearest level control and capacitor voltage balancing strategy for the HVDC system. This chapter also investigate the mathematical models for the modular multi level converter based HVDC system with the controller's design of the power flow controllers and dc bus voltage regulators, under balanced and unbalanced grid conditions. The studies are conducted in time-domain using the EMTP-rv simulation environment. The study results demonstrates that the modular multi-level converter, based on appropriately designed controllers, provides the desired dynamic response, under balanced and unbalanced grid conditions, for HVDC system applications. The studies also show that the proposed balancing capacity algorithm BCA strategy can effectively provide voltage balancing for the MMC capacitors under steady-state and dynamic operational conditions. Furthermore, the inherent scalability of the MMC renders it as a promising configuration, compared with the multi-level and multi-module VSC configurations, for HVDC system applications.

The differences between the control and protection of the interconnector, in comparison to the link employed for the connection of a windfarm, were also highlighted. The key difference is that the interconnector is able to maintain control of the DC link voltage in the event of a severe AC fault, with a DC chopper resistors, and controlling the active power at the both converters.

Chapter 5 VSC BASED MULTI-TERMINAL DC

As AC network and DC network are becoming more complex, VSC-HVDC, based on two-terminal HVDC, is developed to offer technology support for the accessing among multi supplier center, multi-loads center and distributed renewable power. Compared with the current source converter based high voltage direct current (CSC-HVDC) transmission system, VSC-HVDC is capable of controlling the active power and reactive power independently, and meeting the request of power supply to passive networks. Meanwhile, there is no commutation failure problem. When the power flows reverse, the DC voltage can also keep constant with the reversal of the DC current direction [114]. With the good controllability, the VSC-HVDC can easily be developed into multi-terminal HVDC (VSC-MTDC) system, namely the DC transmission network formed by three or more converter stations. Compared to the conventional two-terminal HVDC, MTDC can offer more than one power supplier, supply power to multi loads and its operation mode is more flexible. It can be widely applied in the following situations [114] [14] [115]: (1) The synchronous and non-synchronous interconnection with AC power network; (2) the accessing of wind power and other clean energy; (3) power supply to isolated passive loads (e.g.، island and offshore drilling platform).

The first part of this chapter is dedicated to considerations on the DC grid; first of all, actual discussions on the definition of DC grid topologies are presented and then differences and similarities between AC and DC systems are outlined. The second part is a literature review on methodology to control DC grids. The third part emphasizes the general dynamics of the master/slave and droop controlled DC grid through a simulations.

5.1 TOPOLOGIES OF VSC-MTDC

The first multi-terminal HVDC project that was put into operation officially is the Italy–Corsica–Sardinia three-terminal HVDC transmission project in 1987. However, it is a CSC-HVDC transmission system. The HVDC industry has already 3 decades of experience with multiterminal HVDC networks. However, since the 1990s no other project with more than 3 terminals has been built using the HVDC technology based on current-source converters.

When the number of converter stations, rectifiers and inverters, grows in a HVDC transmission system which uses the CSC technology, also the complexity of the master control increases [115] [27] . Since the master control is responsible for proper coordination between the terminals, also the need for fast telecommunication link increases. The telecommunication is needed for the synchronisation of the converters current orders, identifications and actions for clearing dc faults and start-up of the system after a power outage [116] [117] [118]. Moreover, when using HVDC Classic technology to form multiterminal networks, the reversal of power flow involves complex mechanical switchgear since the current flow through the thyristor valves cannot change direction [14] [119]. The increased complexity of the master control, the need for fast communications links, which may have not been available at the time; and the inability to change the direction of the current may have constituted the reasons why multi-terminal HVDC networks using CSC-HVDC were not further developed. Nevertheless, even without being able to build meshed networks, almost 200 GW of HVDC transmission capacity is installed, or under construction, in more than 140 projects throughout the world [114] [27]. In the meantime, the total installed capacity is continuously growing with countries such as China, India and Brazil building long dc transmission lines to integrate remotely located generation sources. China alone plans to build more than 30 HVDC links, which amount to circa 270 GW, up to 2030 [27].

Multi-terminal direct current networks are characterised when three or more converter stations become interconnected through the dc side of the transmission system. The MTDC configurations can be:

- ***CSC-MTDC:*** all the converter stations use the line commutated current-source converter HVDC technology;
- ***VSC-MTDC:*** all the converter stations use the forced commutated voltage-source converter HVDC technology;
- ***Hybrid-MTDC:*** when both HVDC technologies – CSC and VSC – are used together.

The topology of VCS-MTDC system is directly related to the reliability and practicability of the control strategy, which is always divided into three types: parallel structure, series structure and hybrid structure [14] [6]. For the parallel structure, the DC voltage level of each converter station is the same and the power allocation is achieved by changing the DC current of each converter. For the series structure, each converter station has equal DC current and the power allocation is achieved by changing the DC voltage of each converter. As for the hybrid structure, the control strategy can be designed flexibly according to the relationship between the DC current and DC voltage of converter station. When transmitting constant power, the system adopting the parallel structure spends less line cost, has a faster fault recovery speed, is more flexible for system expansion and is more economical compared with the series structure. Because of the importance of the topology structure of VSC-MTDC, the simple classification of topology structure cannot meet the request of a specific project.

- ***Series MTDC Network***

In a series connected MTDC network, all converter stations share the same dc current, whilst their voltages will vary according to the power to be extracted or delivered to its ac network. The MTDC is grounded in only one point, which can be arbitrarily chosen [27], but will affect the insulation needs of the different converter stations as shown in Figure 5.1(a).

- ***Parallel MTDC Network***

In a parallel connected multi-terminal dc network, all the converter terminals share the transmission system direct voltage. The MTDC transmission systems using parallel connections can yet be grouped into two categories: radial and meshed networks. Figure 5.1 shows the difference between a radial connected MTDC network and a meshed one as shown in Figure 5.1(b).

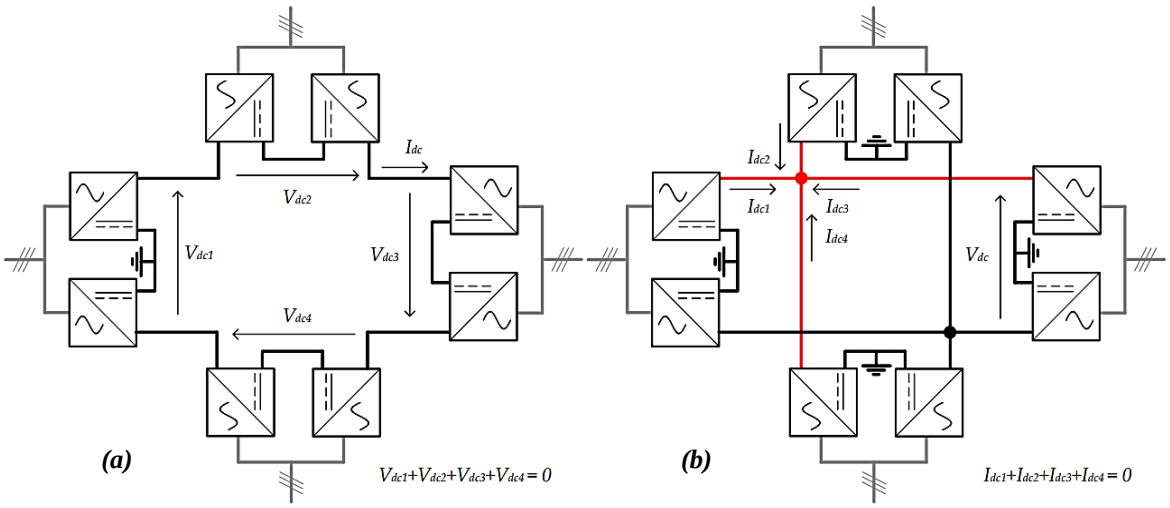

Figure 5.1 Multi-terminal dc network with bipolar HVDC stations connected in: (a) series; (b) parallel. [27]

Table 5.1 Comparison between series and parallel MTDC networks. [27]

Characteristic	Series MTDC	Parallel MTDC
Power Flow Reversal	In CSC-MTDC power flow reversal can easily be achieved by inverting the converter voltages. With VSC-MTDC it would not be easy to invert the converters voltage polarity, thus power flow reversal would involve mechanical switches.	In CSC-MTDC the current direction cannot be inverted, hence, there is need for mechanical switches. In VSC-MTDC the current direction can easily be inverted, hence power flow reversal can be achieved via control actions.
HVDC Terminal Power Rating	Depends on converter voltage rating (cheaper for smaller powers).	Depends on converter current rating.
Losses	Higher losses, which can be minimised by always operating with the minimum current possible.	Lower losses.
Insulation	Is difficult in series connection as the voltages in the MTDC network vary.	All converters need to be insulated to the rated voltage.
DC Faults	A permanent fault in a transmission line would make the whole MTDC network unavailable.	A permanent fault in a transmission line would only make the affected terminal unavailable (in meshed MTDC networks normal operation is still possible).
AC Faults	Leads to overvoltages in the remaining terminals.	Leads to overcurrents in the remaining terminals.
Protection	In series CSC-MTDC, dc faults can be handled via control actions. VSC-MTDC will need dc breakers.	For clearing dc faults parallel MTDC networks will need dc breakers.

Several types of MTDC connection concepts are possible to be established in practice, each presenting a number of advantages and drawbacks. The most important of these designs and probable to be actually implemented are summarized below [120] [121] [7] [122] [27] [20].

- ***Independent HVDC links***

This grid configuration, presented in Figure 5.2(a), follows the concept of having a grid with independent two-terminal HVDC links where a cluster of stations are located in the same geographical area, sharing the same ac busbar. In this case, all the connections are fully controllable without the need of a centralized control to coordinate the stations. It may consist of a mix of LCC- and VSC-HVDC links, operating at potentially different voltages. This setup is ideal to incorporate existing HVDC lines into an MTDC grid and has no need of dc-breakers.

- ***Radial grid***

Owing to the simplicity of the design and the possibility to offer a sufficient level of power-flow flexibility between multiple stations, the radial grid topology presented in Figure 5.2(b), will most likely be applied to the majority of the first MTDC grids. It is designed like a star without closed paths forming. The reliability of this configuration is lower than the other type of connections and in case of a station disconnection, portions of the dc grid could be ”islanded”.

- ***Ring grid***

The ring topology, shown in Figure 5.2(c), connects all converter stations in a closed serial circuit, with each converter featuring two dc-connections to other stations. The advantages of this connection type lie on the simplicity of the construction and operation. However, this type of connection suffers from low reliability and

high losses due to the long transmission lines (if the geographical location of the stations is big), which are necessary to close the grid loop. The impact of the latter is intensified in the presence of remote stations which need to be connected to the rest of the grid with two separate dc links.

- ***Meshed grid***

The meshed grid topology is presented in Figure 5.2(d). As it can be observed, this type of grid constitutes a"DC" replica of an"AC" transmission system, introducing redundant paths between dc nodes. An additional advantage of this connection scheme is that a station may be added on certain point of an HVDC link with a separate cable connection, without the need to interrupt the initial HVDC link and introduce the station at the interruption point. The meshed MTDC grid allows multiple power paths between dc nodes, increases the flexibility of power exchange between the respective ac nodes, increases the overall reliability and reduces the shortest connection distance between two nodes in the grid. However, a consequence of these features is the need for advanced power flow controllers and an increase in the cable cost since more (and potentially long) connections need to be established. Furthermore, the use of dc-breakers at every station is considered necessary to ensure the viability of the grid in case of dc-faults [18].

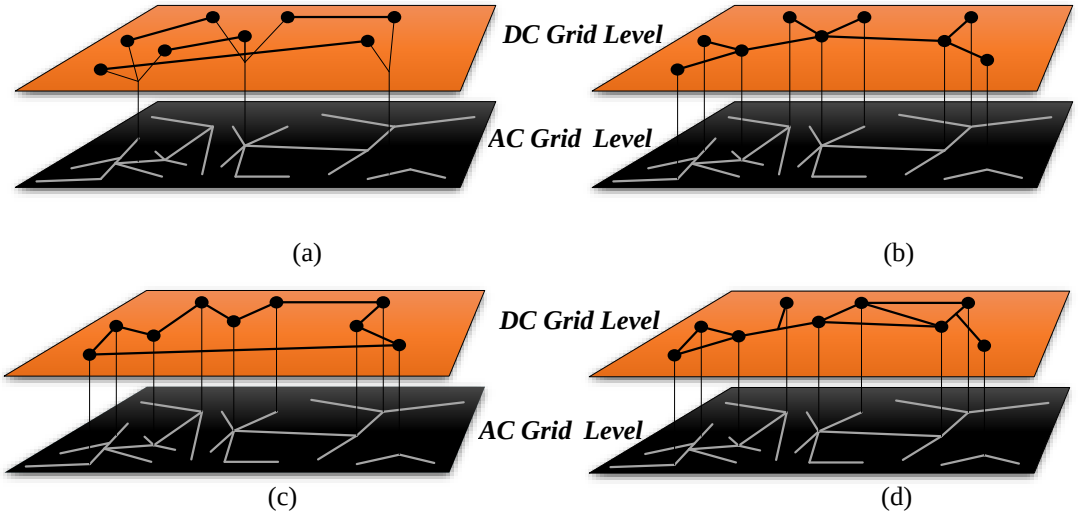

Figure 5.2 MTDC topologies: (a) independent HVDC links, (b) radial connection, (c) ring connection, (d) meshed connection

Table 5.2compares the four types of topologies considering cost, security and reliability. [14] investigate a classification of topology considering the request of communication, flexibility and redundancy. Anyw‹ for a specific project‹ a specific analysis of the topology combined with the local situation of power grid is needed.
.

Table 5.2 Comparison of VSC-MTDC topologies [114]

Topology	Advantage	Disadvantage
Radial	Low investment cost and the structure is simple	Low reliability and it is likely to lose a complete converter station in case of a DC-side fault.
Ring	The construction and operation is simple	Low reliability and high losses when applied to long distance transmission.

Meshed	High security and reliability, more flexible for power exchange and the shortest connection distance between two points in the grid is reduced	Total line length is increased. High cost

The first MTDC project based on VSC is the Shin-Shinano project in Japan in 2000. In China, there have been two VSC-MTDC projects completed by 2014, i.e. Nan'ao three-terminal transmission system and Zhoushan five-terminal transmission system. By far, the VSC-MTDC projects in operation or under construction all over the world are shown in Table 5.3.

Table 5.3 The VSC-MTDC projects in operation or under construction all over the world [114]

Project	Transmission capacity	DC voltage	Number of terminal	Year
Shin-Shinano VSC-MTDC project in Japan	153 MW	±0.6 kV	3	2000
Nan'ao VSC-MTDC project in China	200 MW	±160 kV	3	2013
Zhoushan VSC-MTDC project in China	1000 MW	±200 kV	5	2014
South-West Scheme VSC-MTDC project in Norway- Sweden	1440 MW	±300 kV	3	2015
Tres Amigas superconductor transmission project in North American	5 GW	±345 kV	3	2016

5.2 ANALOGIES BETWEEN AC AND DC SYSTEM

In this subsection, the similarities and differences between AC and DC systems are pointed out in order to see how already existing control methods used in AC systems could be adapted to the control of a DC system.

AC system dynamics is characterized by the kinetic energy stored in synchronous rotating machines connected to it. For DC systems, the energy is stored under an electrostatic form since it corresponds mainly to the energy stored in converter station capacitors (and in the core to screen capacitor of DC cables, to a certain extent):

$$E_c = \frac{1}{2} C_s U_{dc}^2 \tag{5.1}$$

Where:

U_{dc} is the DC voltage [V]

C_s is the converter station capacitor value [F]

E_c is the energy stored in a converter station capacitor [J]

The DC grid power mismatches lead to charging or discharging capacitors, which results in modification of the DC voltage level. The same phenomenon exists in AC systems, power imbalances lead to speed variation of electrical rotating machines and thus the frequency. This signal has been used by several generation units to adjust their power reference in order to reestablish the power balance between production and consumption. Similarly, the power balance of the DC grid could be achieved by controlling the DC voltage level.

In power systems, the inertia of a synchronous machine is commonly defined by an inertia constant (H) to normalize the kinetic inertia of each generator with respect to its nominal power [12], thus it can be possible

to compare units with different ratings. The same philosophy could be applied to DC systems; the electrostatic energy stored in the substation's capacitor can be weighted by the substation base power. This leads to an electrostatic constant which is homogeneous to a time:

$$H_c = \frac{\frac{1}{2}C_s U_{dc}^2}{P_{base}} \tag{5.2}$$

Where: P_{base} is the base power of the converter station [W]

H_c is the electrostatic constant [s]

Thanks to the electrostatic constant, the converter station energy can be compared to the kinetic inertia of conventional rotating units. The numerical application on leading HVDC converter stations [92]leads to an electrostatic constant close to 30-40 ms (i.e. 30-40 kJ/MVA) which is a very small value compared to conventional unit inertia constant (i.e. 3 s for hydropower plants, 2.5 s to 10 s for thermal power plants and several seconds for nuclear power plants).

Looking at the energy stored into the whole AC grids, it is the sum of all energy stored in rotating machines. The stored energy compared to the transmitted power drives the evolution speed when the system is subject to a disturbance. Therefore, in continental AC systems, AC grids are connected together to share the primary reserve and to make the overall system stronger. Thus, the sudden loss of one element has a small impact on the grid behavior. In islanded AC networks, there are considerably less generation units so the loss of one element leads to higher variations even if their size is relatively smaller than in the case of continental grids. In such networks, the frequency is more volatile than in huge AC systems such as the pan-European grid. In terms of number of connection points, a DC network could be assimilated to an islanded system. Since the energy stored in this system is very small, the voltage may be extremely volatile. To control the voltage level, it is necessary to have a very high speed closed system for the voltage control which is allowed by the fast dynamics of the power electronic converters [12].

The analogy between of AC and DC systems is summarized in Table 5.4. In this table quantities in the AC system are associated to their DC system counterpart.

Table 5.4 Analogy between AC and DC systems [12]

AC	DC
Frequency ω	DC voltage level U_{dc}
Impedance of connection X	Resistance of connection R
Active power transfer $\frac{V^2 \sin \delta}{X}$	Power transfer $U_{dc}\frac{\Delta U_{dc}}{R}$
Constant of mechanical inertia H	Electrostatic Constant H_C

5.3 OPERATION AND CONTROL HIERARCHY OF MTDC

The DC voltage in a DC grid is usually assigned a role that is similar to the frequency in an AC grid therefore any power imbalance is imaged in an increase or decrease of the DC system voltages. Yet, the comparison between AC grids and DC grids operation reveals two differences:

• Contrary to AC system, the DC system voltage is different for all nodes in the DC network resulting from the resistive voltage drops in the lines.

• The absence of a considerable amount of energy storage elements equivalent to the inertia in AC systems, makes DC voltage modifications quicker than AC frequency variations in AC grid.

These differences between AC and DC systems tend to make HVDC converter dynamics faster therefore a quasi-instantaneous inverter setpoint changes while considered from a traditional AC system stability perspective.converter setpoint changes constantly until it replies with AC grid stability perspective.The suitable control strategy for DC grid is similar to the AC grid, which includes primary, secondary and tertiary controllers [123] [124] [125]. Figure 5.3 shows hierarchical control of supergrid with typical time range of operation.

Primary Control: it's a local control that operates in a time range of a few seconds. It is responsible for maintaining the DC voltage if any disturbance within the DC system takes place and ensures the energy stability of HVDC grids. This is achieved by adapting a control mode at each converter in the HVDC grid system, there are some suitable candidates for primary control as shown in Figure 5.4(b) [126].

In constant voltage control VSC-HVDC voltage level (U_{dc}) remains constant regardless of the level of the power (P_{dc}). Hence the vertical characteristic line in Figure 5.4(b). Constant power control mode maintains the power flow at the VSC-HVDC terminal constant regardless of the level of the DC voltage (U_{dc}), The DC characteristic curve of a constant DC voltage controller is a horizontal line.

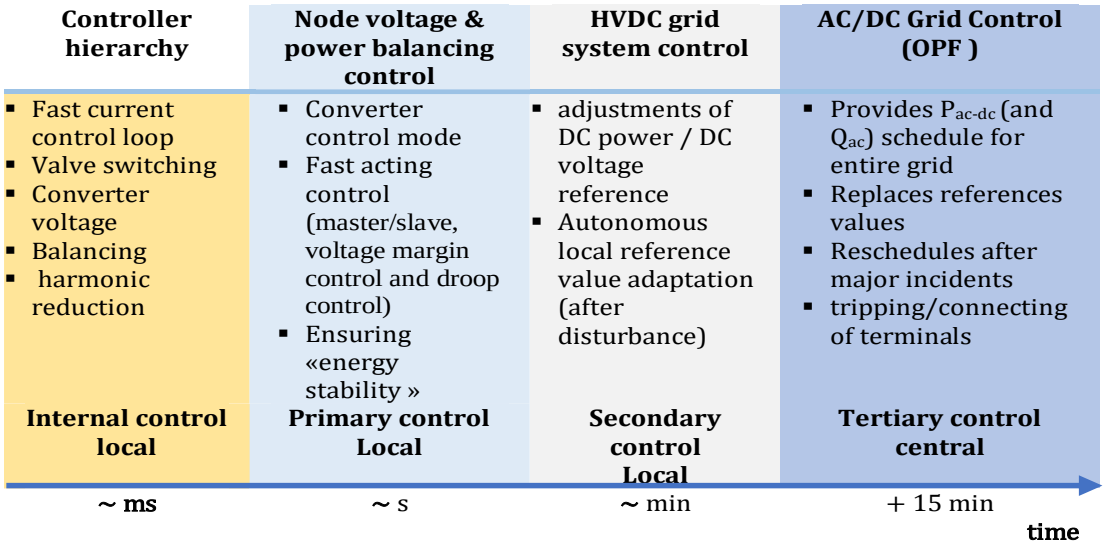

Figure 5.3 Hierarchical Control of Supergrid with typical time range of operation

Voltage margin control is a combination of constant power control and constant voltage control. A converter with voltage margin control normally operates in constant power control mode. If the voltage deviation reaches the limit of the voltage margin, the converter bascules to constant voltage control, clamping the voltage at the margin limit to prevent further voltage deviation. Voltage droop control in the HVDC grid is similar to the droop control in AC system, it employs a droop mechanism the regulate the DC voltage adapting the power reference at the VSC-HVDC terminal [120].

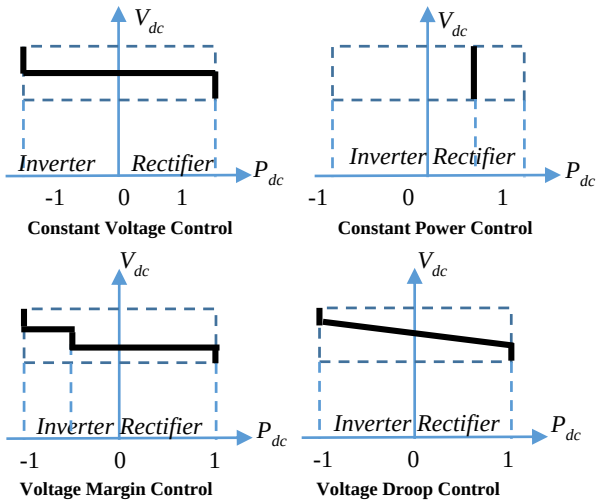

Figure 5.4 DC voltage versus power characteristics

Secondary Control: operates in time range of 5-10 min, implemented to reset converter's set point to re-establish pre-disturbance conditions after any disturbance, in order to ensure that DC voltages are within the required margins and that power flow is as close as possible to the desired values which allow to share the deviations between the AC system and the HVDC grid and the AC system. This control will typically involve some communication between the dispatcher centre and the terminals since data availability is key for the robust operation of this method [32] [7].

Tertiary control: may include human intervention and will happen within minutes and perhaps tens of minutes. Tertiary control is intended to determine converter power schedules based on global information and using an optimal power flow calculation (OPF) [127]algorithms considering AC and DC grids in order to find an optimal operating point for the overall system. It will be activated following a significant outage on the DC grid, like a large incident or line tipping. Tertiary control may include the following: significant changes in ref, tripping/connecting of terminal [128] [129].

5.4 DC VOLTAGE CONTROL OF MTDC

The DC voltage control is definitely one of the main tasks of the VSC in an HVDC transmission system. The DC voltage is required to be well controlled within rigid limits under all conditions in order to guarantee the power balance between all MTDC network transmission terminals.

In a point-to-point HVDC transmission system, one of the terminals controls the DC voltage of the transmission link while the other terminal controls the active power sent to the interconnection. This kind of control is called master/slave control strategy.

Nevertheless, when an MTDC network is considered, it may be complicated to operate the system with just one converter station controlling the DC voltage. This is mainly due to two reasons: limited power rating of the VSC station controlling the DC voltage and the possibility of faults in the AC network connected to this station which could trigger the protection equipment within only a few cycles of the AC network. Hence, distributing the DC voltage control responsibility to more than one VSC station seems to be an improved option to operate MTDC systems.

In this section, different DC voltage control strategies, which are proposed in the literature, will be analyzed and compared [13] [130] [131] [14] [18] [12] [132].

5.4.1 SLACK BUS CONTROL (MASTER/SLAVE CONTROL)

The Master-Slave method is a simple extension of the existing control method used to control point-to-point HVDC links (see chapter 03). Indeed, there is only one converter controlling the DC bus voltage to a constant value and the others are controlling their power they inject into (or absorb from) the DC grid. With this method the power balance is achieved by only one converter, therefore the AC grid connected to this substation has to be strong enough to accommodate with such power variations. Furthermore in case of this particular substation failure, the DC system collapses.

Within this strategy of control, all converters except one operate in a fixed power injection mode. The function of the remaining converter is to keep the voltage of the DC bus to its reference value. The convert-er controlling the DC voltage will act as a “battery” or “slack bus”, which means that, it will provide or absorb sufficient active power to achieve a power balance of the DC system [131]. Consequently, it adapts the output power to compensate all the losses in the DC system. This converter has to be connected to a strong node in the AC system and must have sufficient DC power rating; therefore, it needs to be oversized, reacting fast on DC grid transient such as a loss of converters or DC line [131]. In addition, an outage of this converter cannot be tolerated because it will entail the losing of the DC voltage control. The converter and its connected AC network must therefore be sufficiently rated to compensate for the total power variations of the other converters [14]. Furthermore ,in the event of a fault which diminishes the converter’ s power capability, the system may become unstable. It is for these reasons that a centralised DC slack bus is generally not considered suitable, especially for large MTDC systems [133].

A possible solution is to control the DC voltage at different nodes of the DC grid simultaneously. However, even though such multiplication could increase the overall reliability of the system, it also gives rise to suboptimal operating points (statically) and to voltage and power oscillations [131]. An additional inconvenience of the master/slave strategy is the problem of the geographic location of the slack bus converter. The system operator assuming this responsibility will be requested to cope with all the problems in the DC grid. Figure 5.5 shows a Pdc-Vdc characteristic (the DC voltage/DC power) of slack bus convert-er (constant DC voltage) and a P-controller (constant power injection).

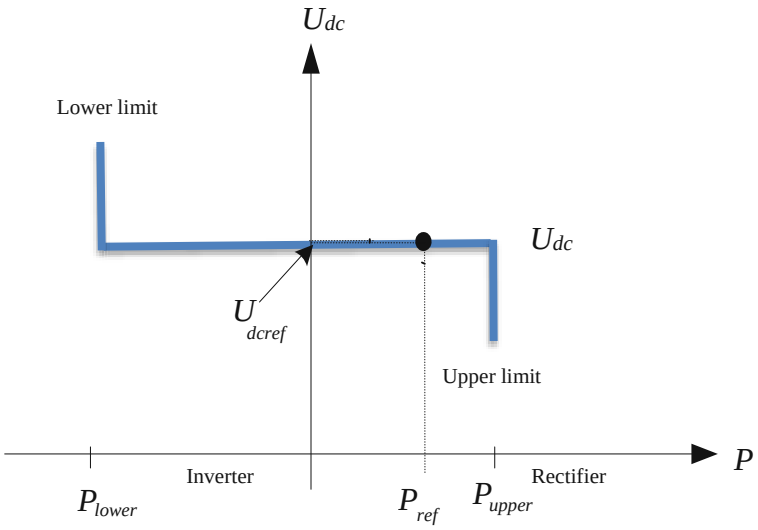

Figure 5.5 Udc−P characteristics of DC voltage slack bus controllers

In sum, there are several constraints of using only one converter to maintain the voltage of a MTDC system [134]:

- The slack bus station must have a sufficiently large power rating and the connected AC system has to be sufficiently strong to accommodate the total power variations of all the other terminals.
- Loss of this terminal may cause instability of the whole MTDC system if there is no backup DC slack bus and the communication is not sufficiently fast to schedule another terminal for voltage regulation.
- The feasibility of this control approach will be significantly reduced as the size of the DC network increases.

5.4.2 VOLTAGE MARGIN CONTROL

The voltage margin method can be considered as an extension of the master-slave method: the master role may be successively devoted to different substations depending on the level of power in each station. This method was first introduced in [135] and then by [136] for LCC based MTDC. Then this method has been tested in a three terminal back-to-back prototype based on GTO converters [137]. Finally, this method is introduced for the control of a VSC MTDC grid in [138]. Fake power limits are introduced in PV curves to define the power sharing [12].

This control method may be used as backup system, i.e. the slack role is changed when the substation, which controls the DC voltage, reaches its power limits. This method might not be suitable for large DC grids because، at any given time, only one converter is controlling the DC voltage, whilst the other operates in what is referred to as voltage margin control. The voltage-current characteristics for the two converters are shown in Figure 5.6. The converter operating in voltage margin control effectively operates in constant power control providing that its local DC link voltage is within pre-set limits (Vdc-low<Vdc<Vdc-high). If the DC link voltage exceeds the pre-set limits then the converter operates in DC link voltage control mode. This means that if the converter operating as the DC slack bus is unable to control the DC link voltage, the other onshore converter will take control. Voltage margin control therefore improves the reliability of the system in comparison to a centralised DC slack bus.

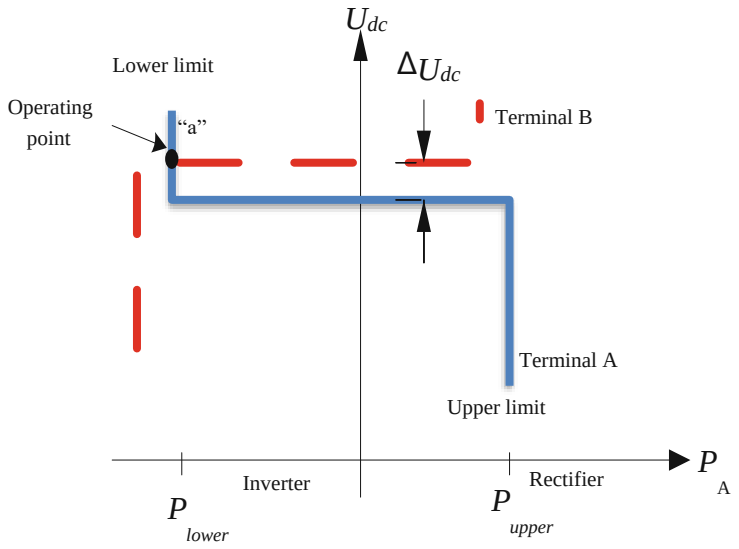

Figure 5.6 Udc−P characteristics of DC voltage margin controllers [90]

However, voltage margin control may not be considered as a satisfactory approach for coordination control of a large DC grid due to the following reasons [134]:

- Unless voltage droop control or other transient voltage control is incorporated by certain terminals, there is only one converter at a time regulating the DC voltage and this may lead to unsatisfactory transient performance, particularly for large DC grids
- The voltage margin must be carefully selected to avoid undesirable interaction between the converters whilst minimising losses and maximising the systems VA rating.
- Transitions from one voltage level to another may occur abruptly leading to additional system stress.
- The voltage margin needs to be sufficiently large to reduce the possibility of interactions between voltage controls of different terminals. However, large margins may result in unsatisfactory steady-state voltage levels.

As the size of a MTDC system grows, it becomes increasingly difficult to configure the voltage margins between converters to satisfy both steady-state and dynamic requirements [139] [140].

5.4.3 VOLTAGE DROOP CONTROL

An alternative control strategy is called droop control, where the DC voltage control is distributed over a number of converters, which simultaneously adapt their active power injections to deal with disturbed grid situations.

There are many similarities between the voltage droop control and the frequency droop used in AC systems, where the load-dependent frequency variation is used as an input signal for the control system to adjust the generated power to meet the demand in all times. However, the difference is that the frequency remains constant in the AC system and the DC voltage differs from one bus to another as a result of the power flows. The voltage deviations at different nodes do not entail the existence of transient conditions.

From the control point of view, there is an outstanding particularity in this control strategy, where the concept of reference values of active power and DC voltage given by the operator of the system is changed by the idea of set points. The difference lies on the new steady state condition after a disturbance. In the droop control, although the set points are equally given by the operator as a result of an optimal power flow in a nominal condition, it is not expected that the power, neither the voltage, return to their initial values after a disturbance [131].

In other words, in a non-disturbed condition, identical to the one established by the operator as the nominal one, the converters will follow the set points as their reference values and the desired power flow will be achieved. However, when the active power balance is disturbed, the DC voltages deviate and the converters under droop control (as those operating in DC voltage control mode, if any) will change their active power injection permanently to regain the power balance. In this new condition, the DC voltages of droop and power controller converters have also moved away from the set points as shown in Figure 5.7 [90]. Droop control can be employed to minimise some of the aforementioned limitations of voltage margin control. In droop control more than one converter is able to participate in regulating the DC voltage and therefore the burden of continuously balancing the system's power flow is not placed upon a single converter.

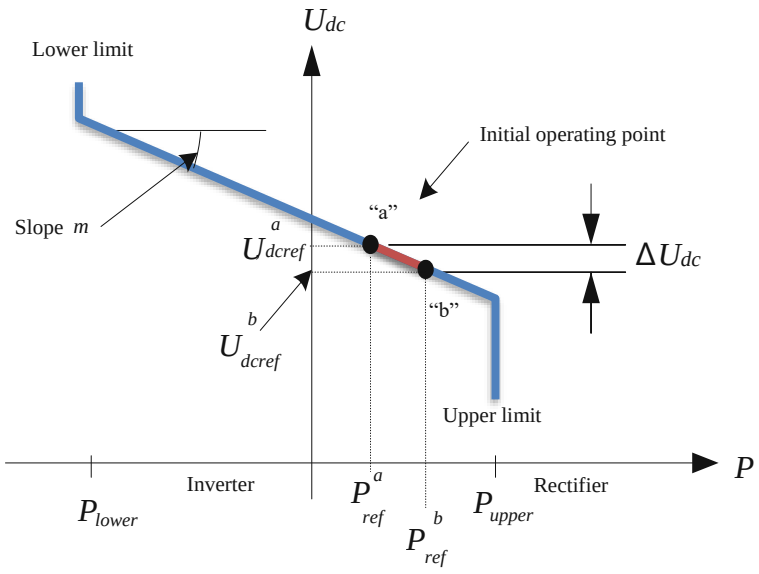

Figure 5.7 Udc−P characteristics of DC voltage droop controllers.

A majority of literature with respect to MTDC control schemes favours DC voltage droop control [141] [134] [142] [14] [12] to allow multiple converters to regulate the system voltage simultaneously and achieve a distributed sharing of power imbalance. The key advantages of this control strategy are:

- Stability and reliability of a MTDC system can be enhanced by incorporating more converter terminals with DC voltage droop control.
- Droop control is a general control scheme and could be configured without modifying the control schemes of other converters. This is preferable as a future DC grid is likely to be formed gradually by adding more multi-vendor converters in the system.
- The power surplus or deficit caused by a severe contingency will be shared by all the droop-controlled converters and thus the stresses on AC systems are reduced.
- In a large DC grid with long transmission distances, dynamic features of DC voltages between remote nodes could be significantly different, and a widespread droop control is advantageous in achieving satisfactory transient performance of the overall system.

The standard droop characteristic can be modified, so that the converter acts as a DC slack bus within preset voltage limits and then as a droop controller outside those voltage limits. This type of droop controller is effectively a hybrid between a voltage margin controller and a standard droop controller .This type of characteristic is sometimes referred to as a voltage droop with dead band .

5.5 THREE-TERMINAL VSC-HVDC TEST SYSTEM

5.5.1 SYSTEM INVESTIGATED

A 3-terminal VSC-MTDC connected three active AC networks, simulation model is established in PSCAD/EMTDC simulation tool and the system structure is shown in Figure 5.8. The base voltage of system and the transformer ratio are the same in system 1 and 2: 420 kV and 420/230 kV, the ones of system 3 are 500 kV and 500/230kV, the frequency is the same for system 2 and 3: 50Hz and 60 Hz for the system1. The VSC 1 operates in the constant DC voltage and constant AC voltage mode, and the DC voltage is set to 400

kV. The VSC 2 and VSC 3 operate in the constant active power and constant AC voltage mode, the active power setting is 100 MW in VSC2 (rectifier) and -200MW in VSC3 (inverter). Table IV in appendix B provides parameters of the system of Figure 5.8 used for the simulation studies [143].

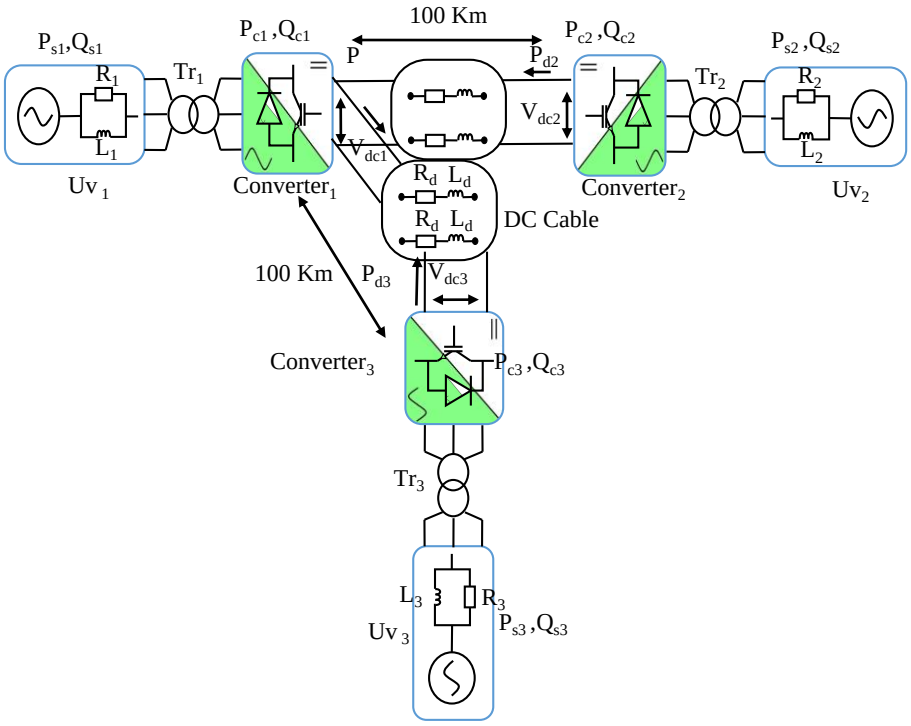

Figure 5.8 Three-terminal VSC-HVDC grid

5.5.2 Model Performance Analysis

The dynamic performance of the transmission system is verified using simulation of:

A. Active power flow reversal,

B. VSC_HVDC response to external AC single phase to ground fault.

C. VSC_HVDC response to external AC three phase to ground fault.

A. Case A

In Figure Figure 5.9, Figure 5.10, Figure 5.11, the initial reference value of the power flow is 100 MW at VSC1 and VSC2, and -200MW at VSC3. At t=2s, the reference value in VSC3 is reversed from -200 MW to +200 MW. It can be seen that the active power follows the reference rapidly with a slight oscillation and reaches the new reference of -300 MW within 0.05 s. correspondingly, the active power at VSC 1 changes around from 100 MW to -300 MW while the active power at VSC2 remains at the same value of 100 MW. At the same time, the reactive power flow changes with the active power reversal at VSC1 and VSC3 and remains the same at VSC2.

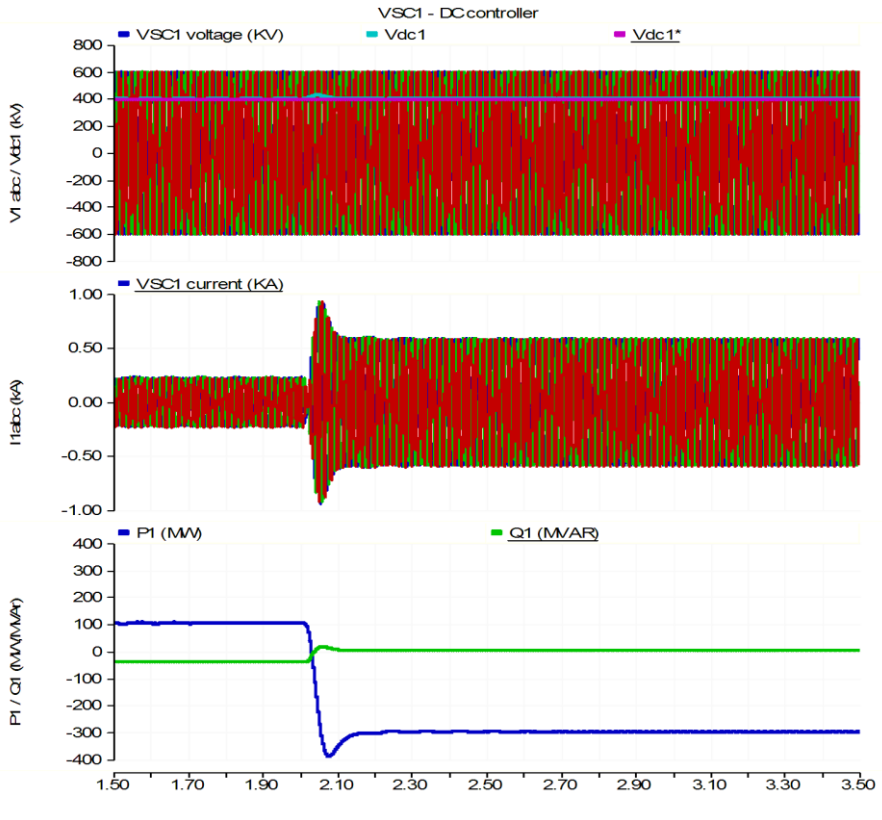

Figure 5.9 Steps on the regulators references (VSC1)

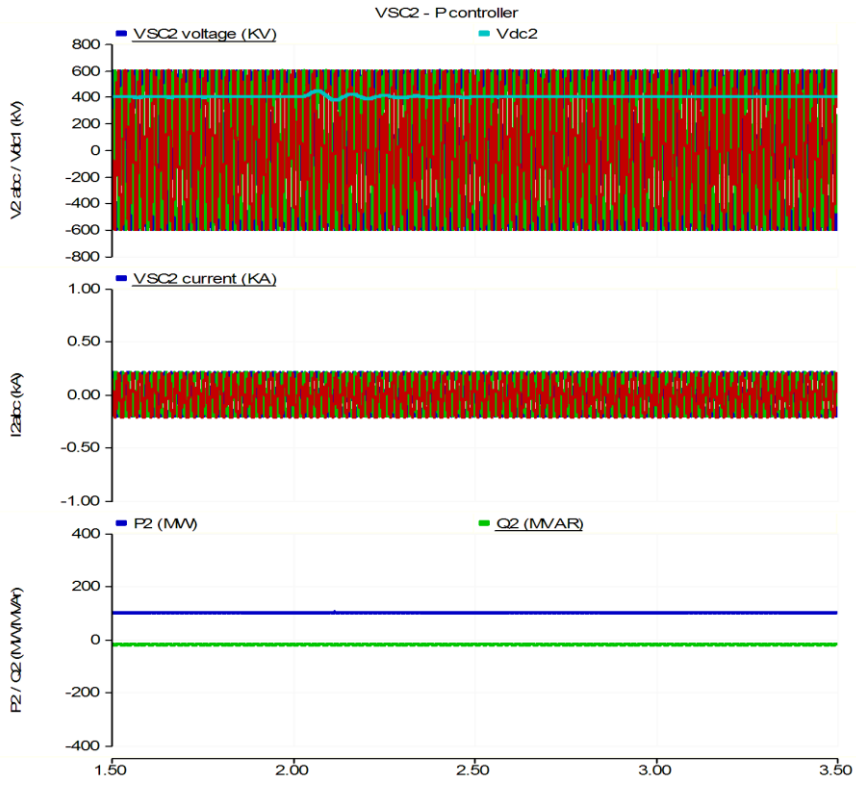

Figure 5.10 Steps on the regulators references (VSC2)

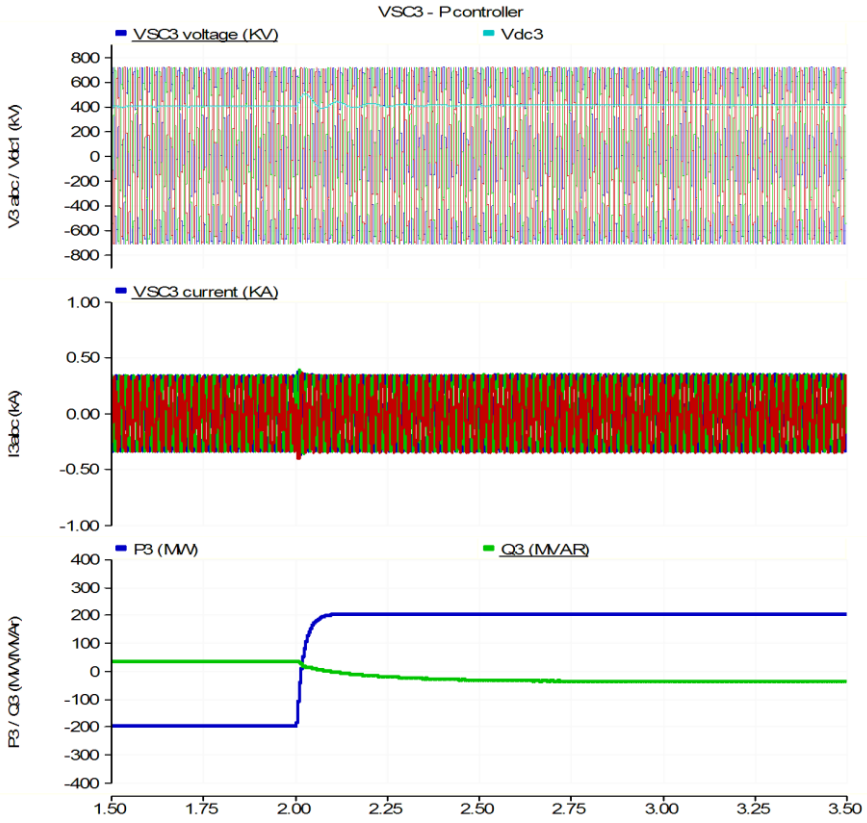

Figure 5.11 Steps on the regulators references (VSC3)

As can be seen, the active power can track the reference of the active power. The transferred active powers at VSC1 and VSC3 change the direction which causes slight transients on the DC voltage of the three converters then returns to the reference value due to the DC voltage controller. The AC current at VSC1 change from 0.25 kA to 0.75 kA caused by the active power reversal with an oscillation and stabilized after 0.05s while the AC currents at VSC2 and VSC3 remains the same. The AC voltages at the three converters can be kept constant without noticeable transients when the step changes are applied.

B. Case B

A single phase to ground fault was applied at t = 2 s during 0.1 s (6 cycles) at AC side of VSC3 in order to investigate the behavior of VSC-MTDC during unbalanced faults; Figure 5.12, Figure 5.13 and Figure 5.14 presents the simulations results.

From the simulation, Figure 1. 12shows that before a single phase to ground fault at VSC1, the active power flow is 100 MW, and shock seriously during the fault and restore stability after 0.2 s running when the fault is removed, while a slight oscillation is noticed on the reactive power flow. The fault causes also the AC current oscillation at VSC1, and stabilized after 0.2 s when the fault is removed. It can be seen from Figure 1. 13the VSC2 remains intact during the fault, and from Figure 1.14 the active and reactive power flow in VSC 3shock seriously during the fault and restore stability after 0.1s running when the fault is removed, the fault also causes transient on the AC current and voltage. The DC voltage of the three converters contains a slight oscillation during the fault. And the AC voltage of VSC1 and VSC2 can be kept constant.

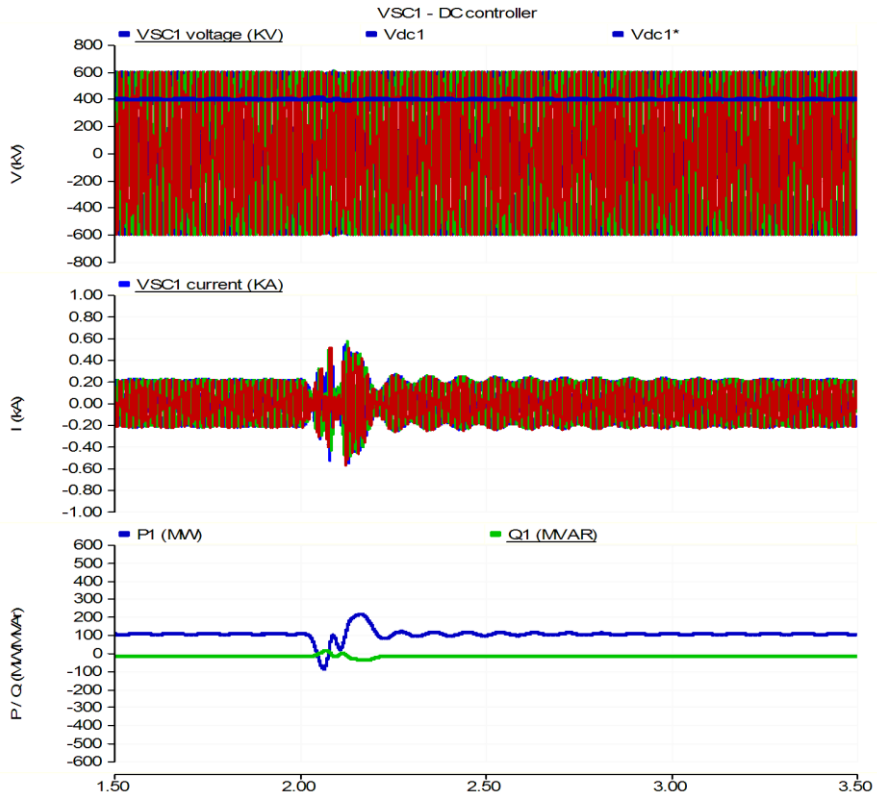

Figure 5.12 AC side perturbations (VSC1)

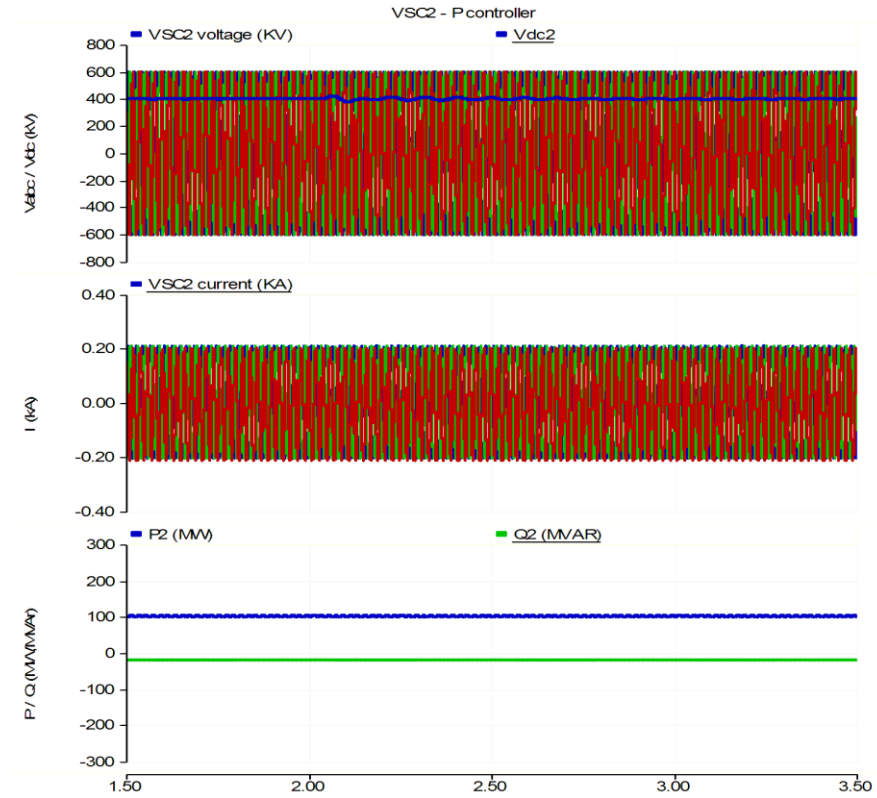

Figure 5.13 AC side perturbations (VSC2)

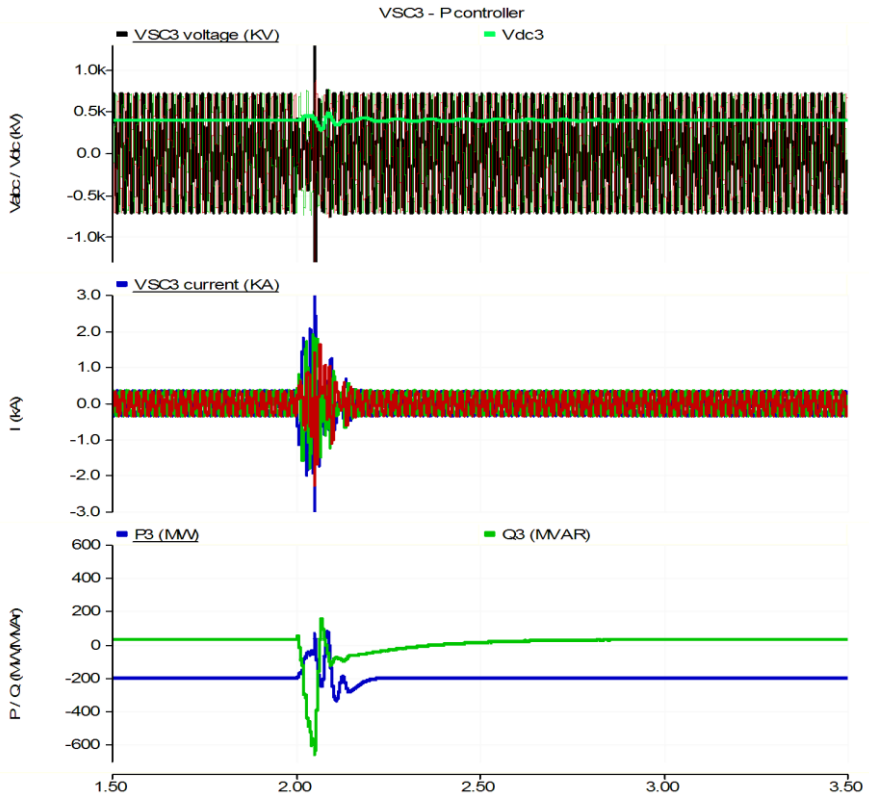

Figure 5.14 AC side perturbations (VSC3)

C. Case C

A three-phase to ground fault is applied at AC side of VSC3 at t = 2 s, in order to investigate the behavior of VSC-MTDC during symmetrical faults, and is cleared at 6 cycles after the fault, i.e., at t = 2.1s. Figure 5.15, Figure 5.16, Figure 5.17 presents the simulations results.

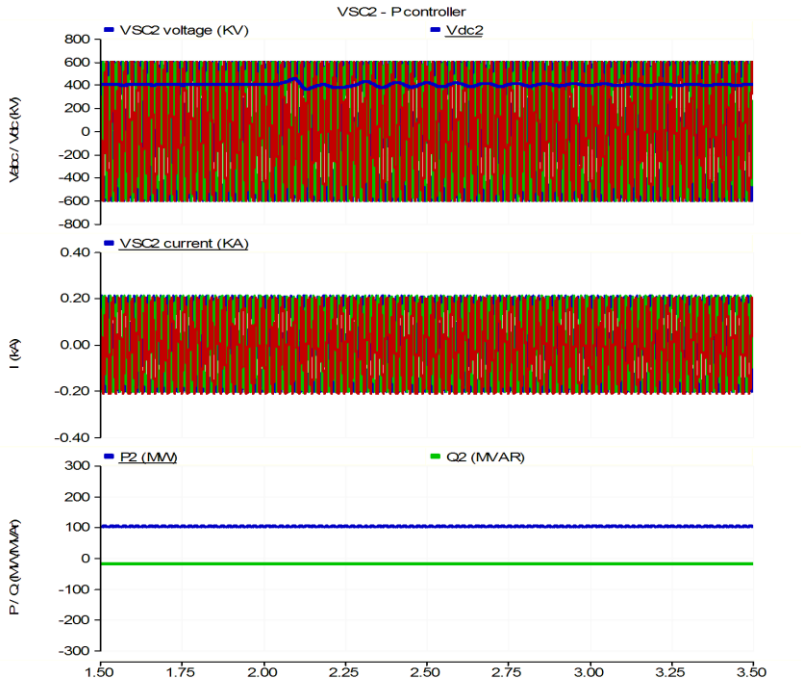

Figure 5.15 AC side perturbations (VSC2).

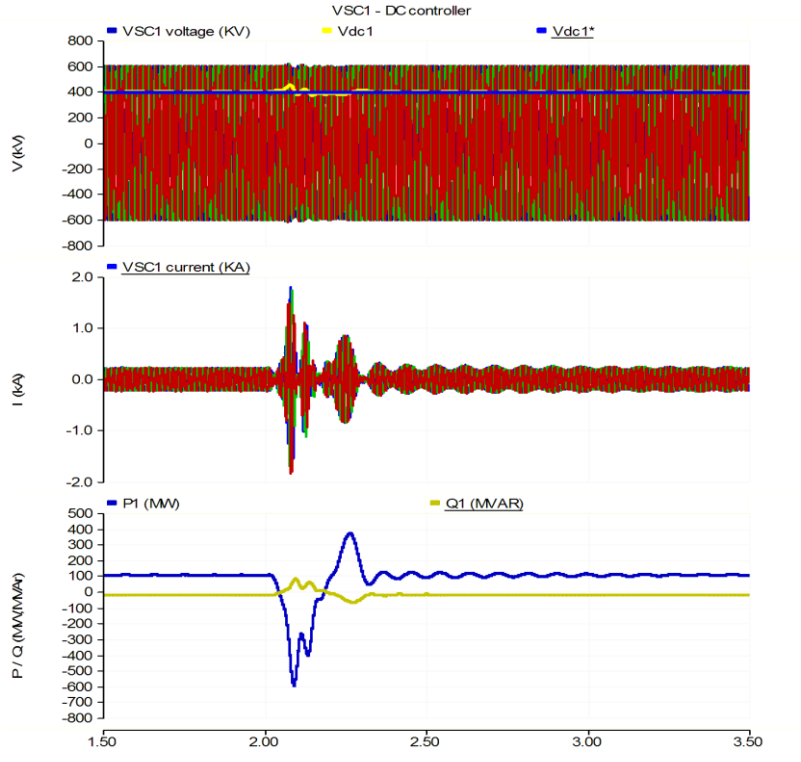

Figure 5.16 AC side perturbations (VSC1).

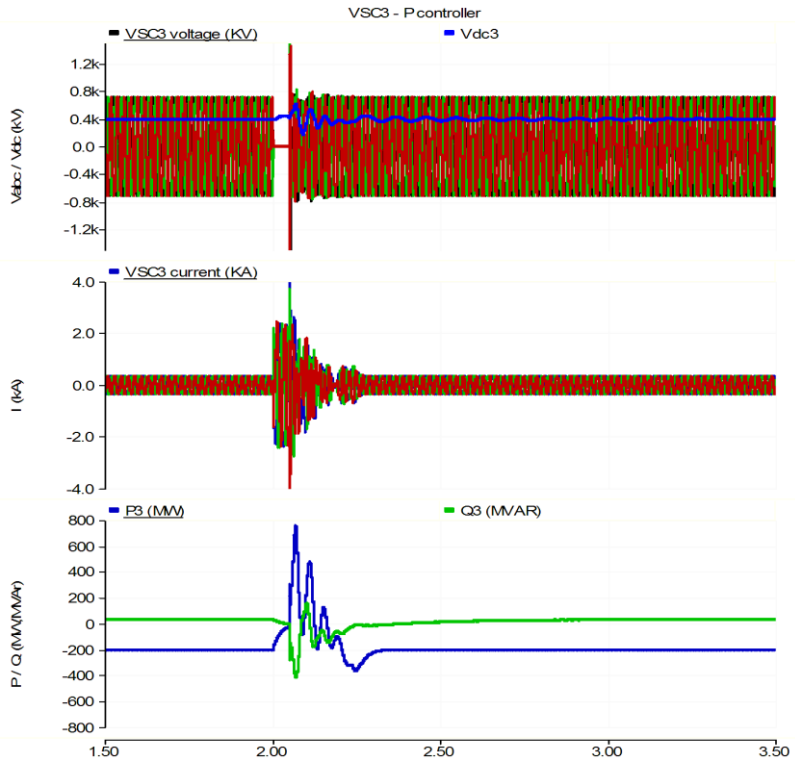

Figure 5.17 AC side perturbations (VSC3).

During the three-phase fault, the active and reactive power of the VSC1 and VSC3 still tracing the reference value with a noticeable oscillation, and reach stability after 0.8s when the fault is cleared, the AC current of the VSC1 and VSC3 also present a transient and restore stability after 0.3s, the AC voltage of the VSC1 remains intact while the AC voltage of the VSC3 drops to 0 and recovers after 0.2s running when the fault is removed. The DC voltage of the three converters contains a slight oscillation and the VSC2 remains intact during the fault.

5.6 FOUR-TERMINAL VSC-HVDC TEST SYSTEM

5.6.1 SYSTEM INVESTIGATED

The system under study is a four-terminal symmetric monopole (±200 KV) MT-HVDC system, as illustrated in Figure 5.18. It connects the offshore wind power plant at F1 and an offshore oil platform at E 1to the onshore nodes B 3and B2, this last one located further inland (labelling of converters is derived from [2]). This benchmark system consists of long overhead lines and cables in series, and HVDC-MMC power converters, in order to study interactions among these elements. Each MMC consists of six arms where each arm includes series-connected, nominally identical, half-bridge submodules (SMs). Reactors L are to provide current control within the phase arms and limit fault currents. The ac terminal of each MMC is connected to a utility grid through a three-phase trans-former.

The HVDC system of Figure 5.18, based on switching function model of chapter 2 and the NLC strategy and control theory of chapter 3, is simulated in the EMTP-rv environment. Table V in appendix B provides parameters of the system of Figure 5.18 used for the simulation studies.

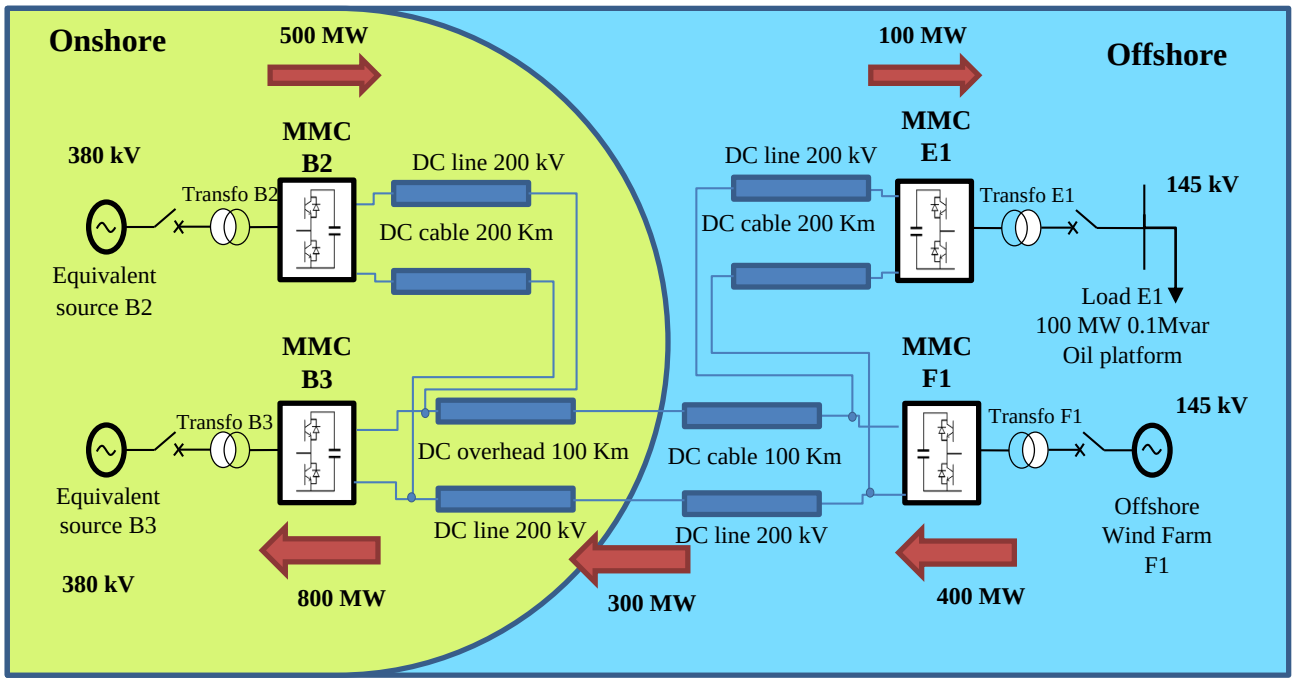

Figure 5.18 Four-terminal VSC-HVDC grid

The power converters forming the benchmark system have different control objectives. On the one hand, onshore converters, MMC B2 and MMC B3, are converters regulating AC power with three differents DC voltage control method, the first one is Active power control and the second one is droop control and the last one is constant DC voltage control. The droop control modifies the external power set-point of the converter in order to maintain the DC voltage within the operational range (1 ± 0.15 p.u). On the other hand, the offshore converters have different control objectives. Converter MMC F1 accepts the power drawn from the wind farm, and implements a three methods of the DC voltage control.The first implemented method is constant DC voltage control and the second method is active power control and the third is voltage droop control. This is to manage extreme cases; e.g. a fault on the AC side blocking the operation of the droop converters. Finally, the converter MMC E1 supplies the power demand of the oil platform. This converter does not actively contribute to the DC voltage regulation.

5.6.2 Model Performance Analysis

Several simulations were conducted to investigate the operation of the above MMC converter based multi terminal HVDC system.The dynamic performance of the transmission system is verified by simulating the:

A. Normal operation of the four terminal VSC-HVDC transmission system.
B. Dynamic responses of the four terminal VSC-HVDC transmission system after F1 converter outage under Master/Slave control (B3 as slack bus).
C. Dynamic responses of the four terminal VSC-HVDC transmission system after F1 converter outage under Master/Slave control (F1 as slack bus).
D. Dynamic responses of the four terminal VSC-HVDC transmission system after F1 converter outage under P/Vdc droop control.
E. Dynamic responses of the four terminal VSC-HVDC transmission system after E1 converter outage under P/Vdc droop control.
F. Dynamic responses of the four terminal VSC-HVDC transmission system after three-phase line-to-ground fault at B3 under P/Vdc droop control.

G. Case A

In this operation mode, no power-step-change is considered. As shown in Figure 5.19, the first two nodes MMC B2 and MMC B3 are considered as constant active power controllers, while the third node F1 has the slack function with constant DC voltage controller. The fourth node E1 (oil platform) is considered as V/F controller.

Using a master/slave control strategy, the results of the power flow calculation are shown in Table 5.5.

Table 5.5. DC power injections and DC voltage values at different nodes

Node	P_{dc}	V_{dc} [p.u.]
B2	Export 390 MW	1.001
B3	Import 780 MW	0.995
F1	Export 497 MW	1.001
E1	Import 100 MW	0.999

Figure 1.19 present the active powers generated by the AC system B_2 and the offshore wind farm F_1 and exported to AC system B_3 and the offshore oil platform E_1 ,respectively .The power reference at MMC B_2 is set to 500 MW during the 2s simulation interval. The MMC F1 operates in the constant DC voltage and constant reactive power mode، and the DC voltage is set to 400 kV (±200KV), the MMC F1 operate at unity power factor. The MMC E_1 operate in VAC/F control and constant AC voltage mode, the active power setting is 100 MW in MMC E_1 (import). The reactive power in both MMC B_2 and MMC B_3 is kept at 0 MVAr. The offshore converter of E1 is initially set to absorb 0.1 MVAr while operating at maximum active power. Figure 1.19 shows that the MMC-HVDC link is capable of responding to the power demands of the windfarm F1 and the oil platform E_1. The DC voltages are smooth and stable.

The phase current at the PCC for the onshore network I_{acB2}, I_{acB3} and the offshore network I_{acE1} and I_{acF1} are shown to be almost sinusoidal and as such have a small harmonic content as shown in Figure 1.20.

The phase voltages at the PCC for the onshore network V_{acB2}, V_{acB3} and the offshore network V_{acE1} and V_{acF1} are shown to be almost sinusoidal and as such have a small harmonic content as shown in Figure 5.21.

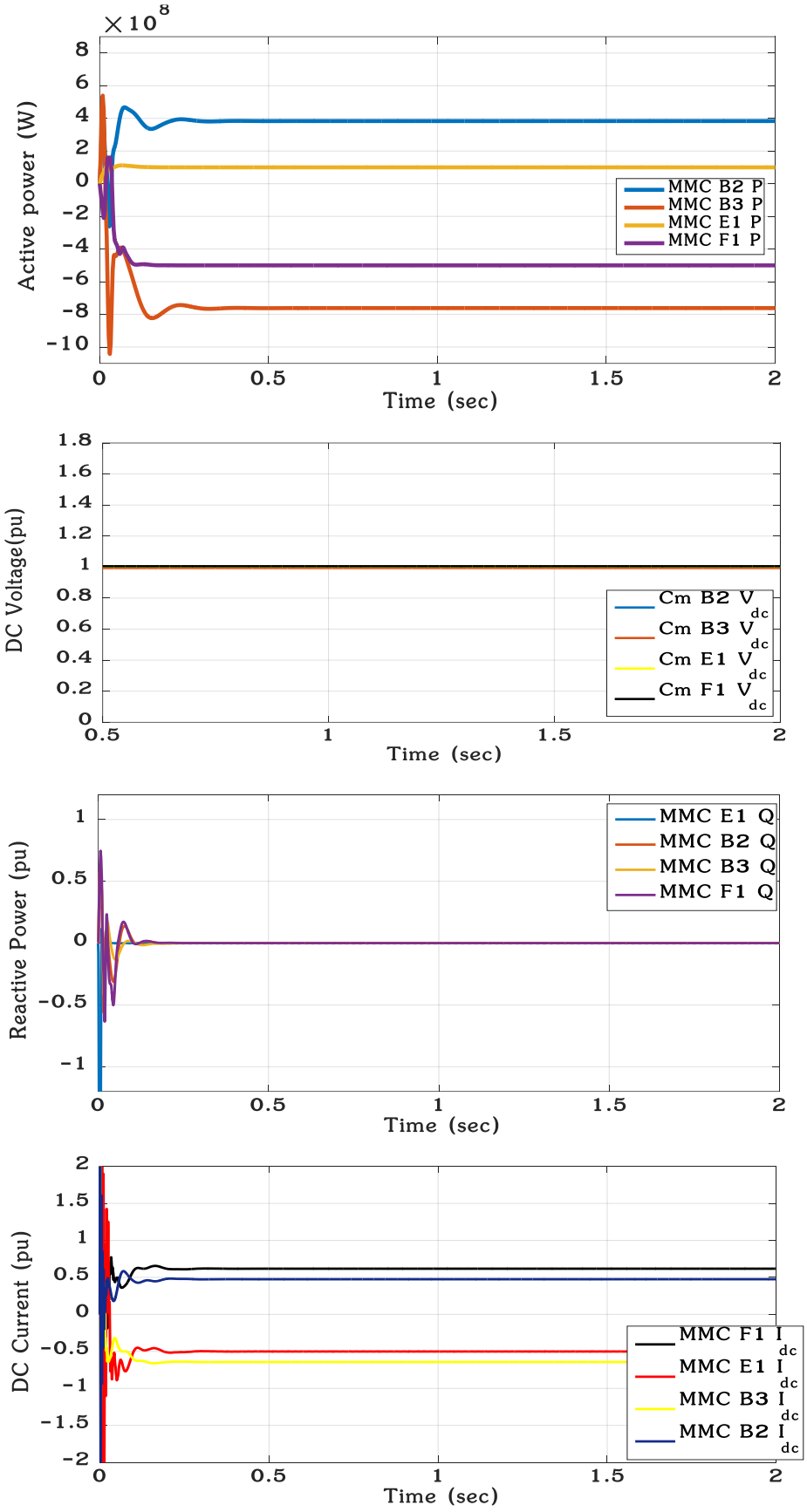

Figure 5.19 Simulation results MMC based MTDC under normal operation with master/slave control: active power, DC voltage, reactive power and DC current.

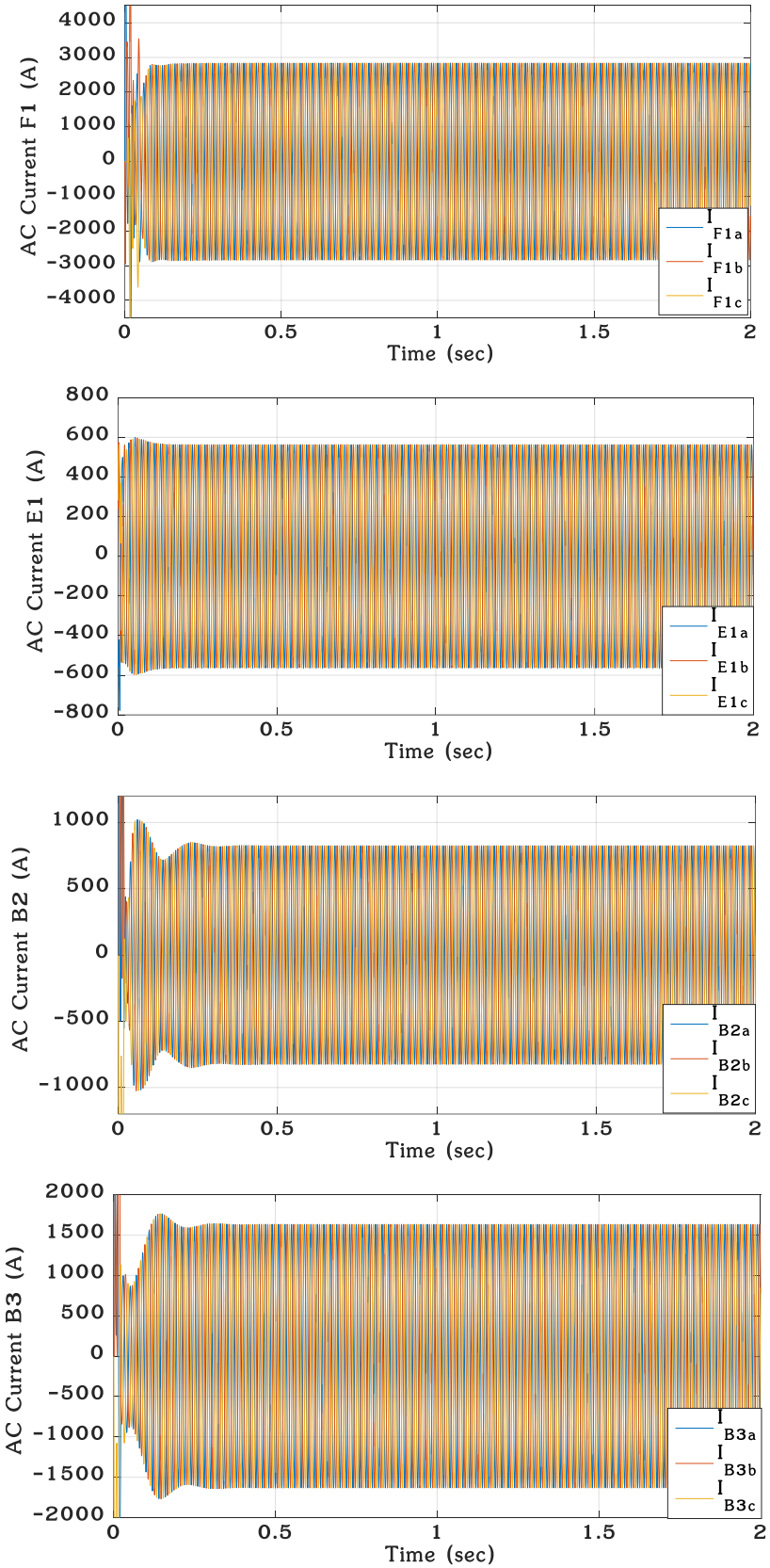

Figure 5.20 Simulation results MMC based MTDC under normal operation with master/slave control: AC current at buses F1, E1, B2 and B3

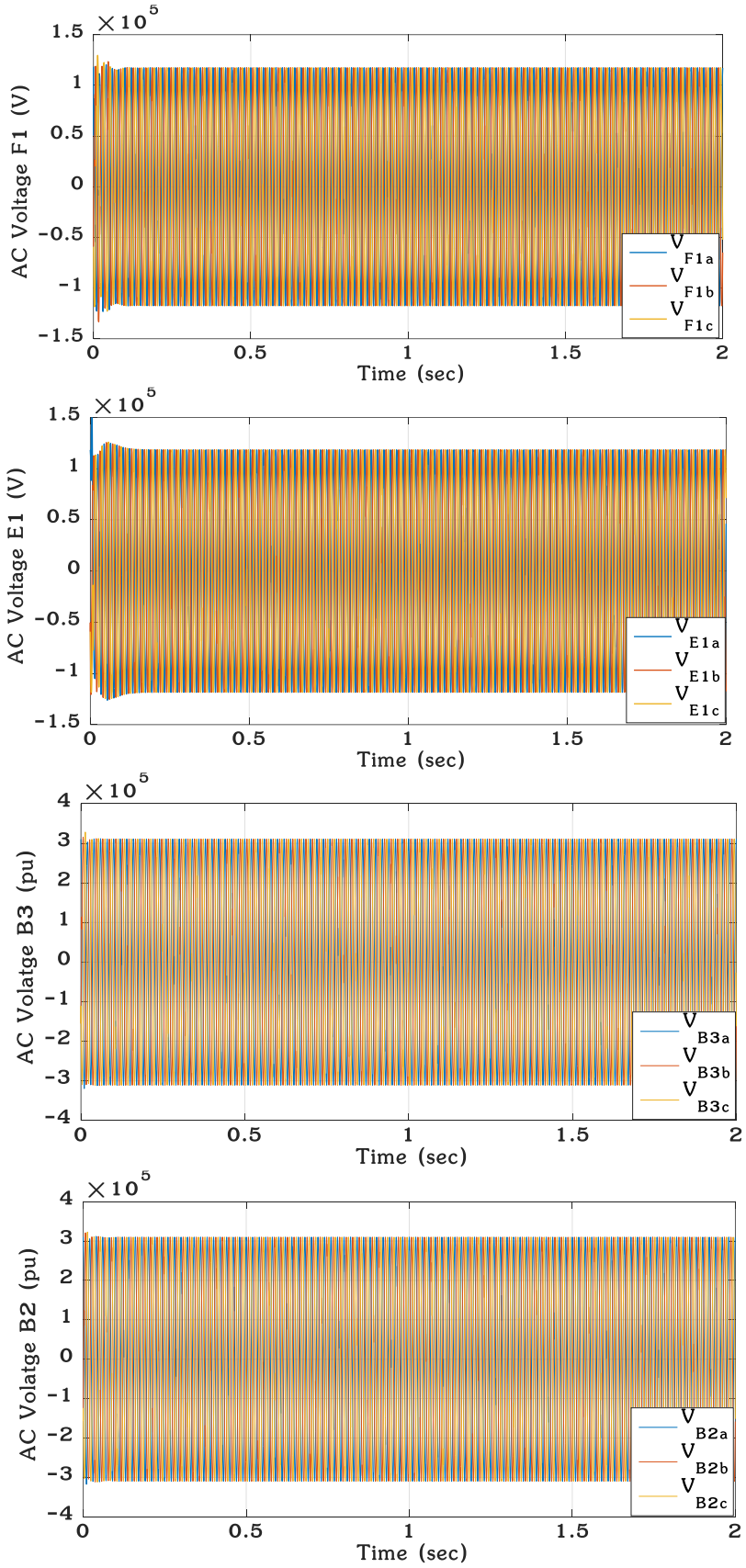

Figure 5.21 Simulation results MMC based MTDC under normal operation with master/slave control: AC voltage at buses F1, E1, B3 and B2

H. Case B

In this case, the performance of the proposed system under contingency is verified for a sud-den disconnection of MMC F_1 .The performance of the master/slave scheme is tested by means of control-ling the DC voltage in the station B3 at the reference voltage of 400kV (±200 KV) with a PI-dc voltage controller (explained in Chapter 3). Unequal loading conditions are considered to demonstrate the performance. If a DC fault of con-verter appears, the converter protection will be actuated. When a certain current level is reached, IGBTs would be blocked. As DC breakers have not been used, it is necessary to block converter stations and to use AC circuit breakers to clear the fault. In the beginning, MMC B3 and MMC E 1imports 780 MW and 100MW, respectively. MMC B2 and MMC F_1 export around 390 MW and 497into the DC grid. The outage of MMC F1 is considered at t=1s.

Loss of a rectifier as the offshore converter MMC F1 which export 479 MW to the DC grid will cause the drop of DC voltage. The power simulation is employed here to evaluate the impact of con-verter outages. It is assumed that the loss of the MMC F1 is caused by the disconnection of the con-verter AC side. The resulting DC voltage and power profiles of the four MTDC system is presented in Table 5.6.

Table 5.6 DC power injections and DC voltage values at different nodes

Node	**P_{dc}**	**V_{dc} [p.u.]**
B2	Export 390 MW	1.001
B3	Import 283 MW	1.001
F1	Disconnected	1.00
E1	Import 100 MW	0.995

The dynamic response of four-terminal HVDC system following F1 converter outage is shown in Figure Figure 5.22 Simulation results MMC based MTDC under contingency operation at MMC F1 with master/slave control: active power, DC voltage, reactive power and DC current.Figure 5.22 shows that in absence of MMC F1, slack converter MMC B3 operating in constant DC voltage control mode decrease its power from 780 MW to 283 MW to compensate the power imbalance of the DC grid. It can be seen that the active power follows the reference rapidly with a slight oscillation and reaches the new reference of 283 MW within 0.15 s. correspond-ingly, while the active power at MMC E1 end MMC B2 remains at the same value of 100 MW and 390 MW, respectively. At the same time, the reactive powers remains the same at all nodes. The change of active power value at MMC B3 causes slight transients on the DC voltage of the four converters then returns to the reference value due to the DC voltage controller.

I. Case C

The dynamic response of four-terminal HVDC system following F1 converter outage which considered as slack bus is shown in Figure 5.23. The results shows that in absence a master converter which take the control of the DC voltage cause the instability of the MTDC system, the MMC B3 operating in active power control mode decrease its power from 780 MW to 283 MW to compensate the power imbalance of the DC grid but the system still unstable. From the simulations it is clearly observed the instability produced of the MTDC network without voltage-controllers. MMC B2 and B3 are completely unstable and in a real case it should lead to a disconnection. The overall system controlled by the centralized method can not operate after the outage of the slack bus. In case the network or a part of it losses the slack, i.e. the voltage regulation, the system is directly collapsed. For this reason, the system can not assure the N-1 security criteria.

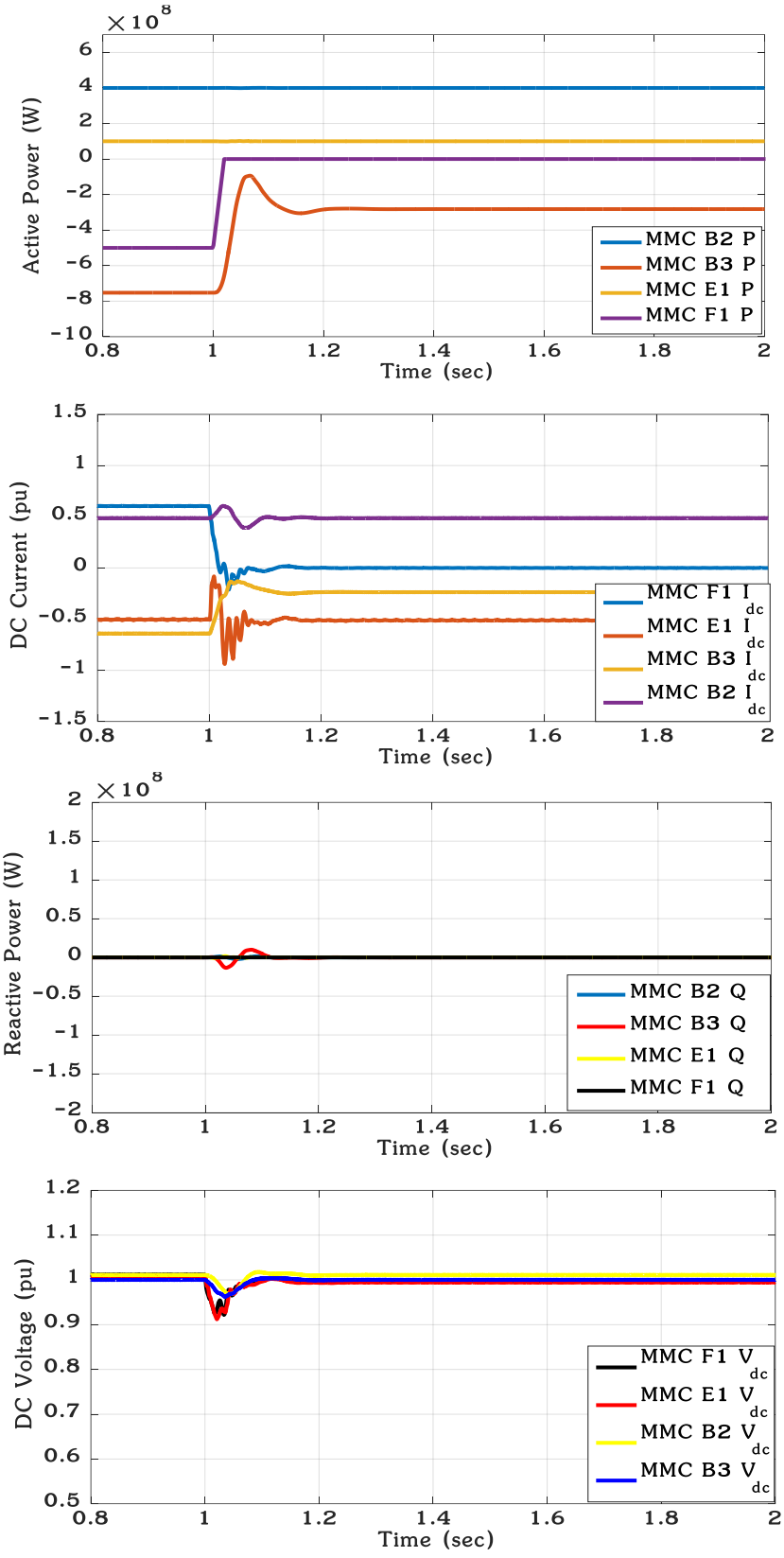

Figure 5.22 Simulation results MMC based MTDC under contingency operation at MMC F1 with master/slave control: active power, DC voltage, reactive power and DC current.

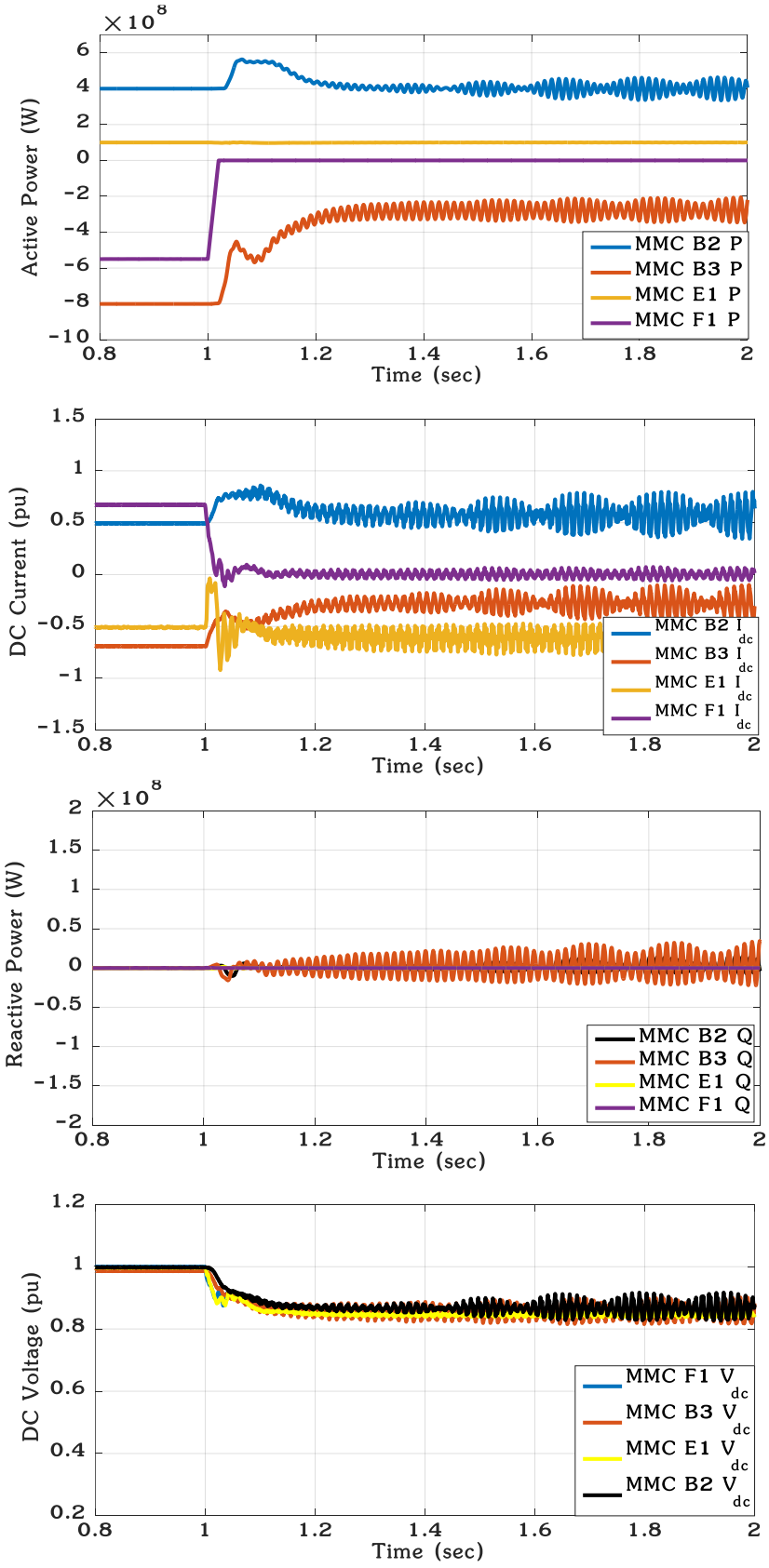

Figure 5.23 Simulation results MMC based MTDC under contingency operation at MMC F1 with master/slave control: active power, DC voltage, reactive power and DC current.

J. Case D

In this case, the performance of the proposed system under contingency is verified for a sud-den disconnection of MMC F1 .The performance of the droop voltage scheme is tested by means of controlling the DC voltage droop control in the MMC B3 ,MMC B 2and MMC F 1P/Vdc droop controller (explained in Chapter 3). Unequal loading conditions are considered to demonstrate the performance. If a DC fault of converter appears, the converter protection will be actuated. When a certain current level is reached, IGBTs would be blocked. As DC breakers have not been used, it is necessary to block converter stations and to use AC circuit breakers to clear the fault. In the beginning, MMC B3 and MMC E1 imports 780 MW and 100 MW ,respectively. MMC B2 and MMC F1 export around 390 MW and 497into the DC grid. The outage of MMC F1 is considered at t=1s .The power simulation is employed here to evaluate the impact of converter outages. The resulting DC voltage and power profiles of the four MTDC system is presented in Table 5.7 DC power injections and DC voltage values at different nodes.

Table 5.7 DC power injections and DC voltage values at different nodes

Node	P_{dc}	V_{dc} [p.u.]
B2	Export 560 MW	0.94
B3	Import 450 MW	0.94
F1	Disconnected	0.94
E1	Import 100 MW	0.94

The dynamic response of four-terminal HVDC system following F1 converter outage is shown in Figure 5.24 Generally, for an MTDC system based on droop control, loss of a rectifier will result in the drop of DC voltage and the increase of rectifying power (or reduction of inverting power) for the remaining terminals in droop control. The simulations obtained in the system controlled by the droop method shows the collaborative scheme of all droop-controlled converters in the function of balancing power in order to obtain a new steady state operation. After the wind farm disconnection, the system recovers immediately a new steady state operation. In this case, the current injection at each converter is logically adapted to a new value different to the nominal because of the current power flows and, consequently, it is generated a steady state error between current voltages and the values at normal operation as shown in Figure 5.25. In this way, accurate power control and effective voltage stabilization can be accomplished at the same time.

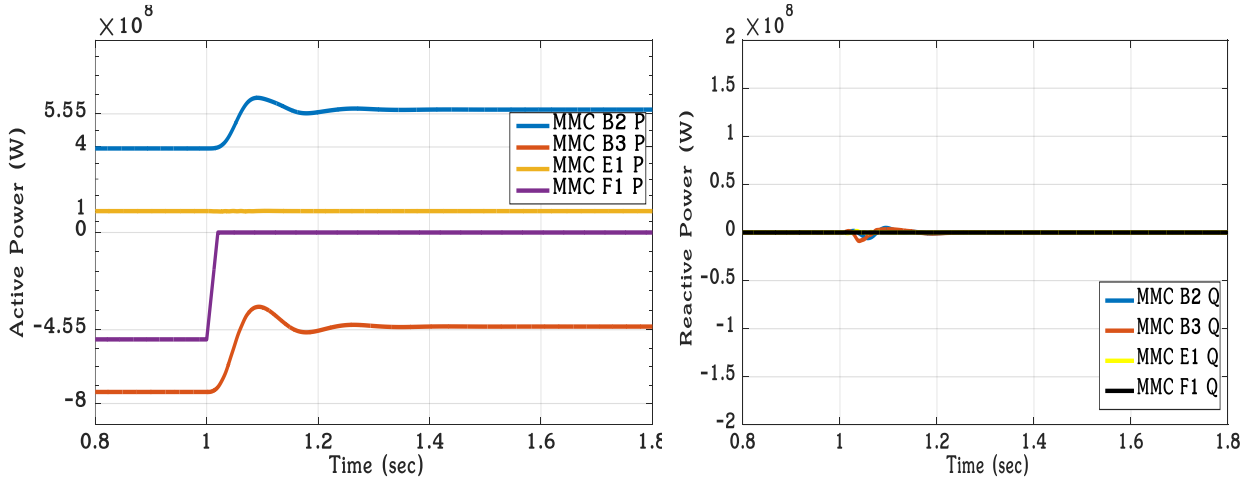

Figure 5.24. Simulation results MMC based MTDC under contingency operation at MMC F1 with droop voltage control: active power and reactive power

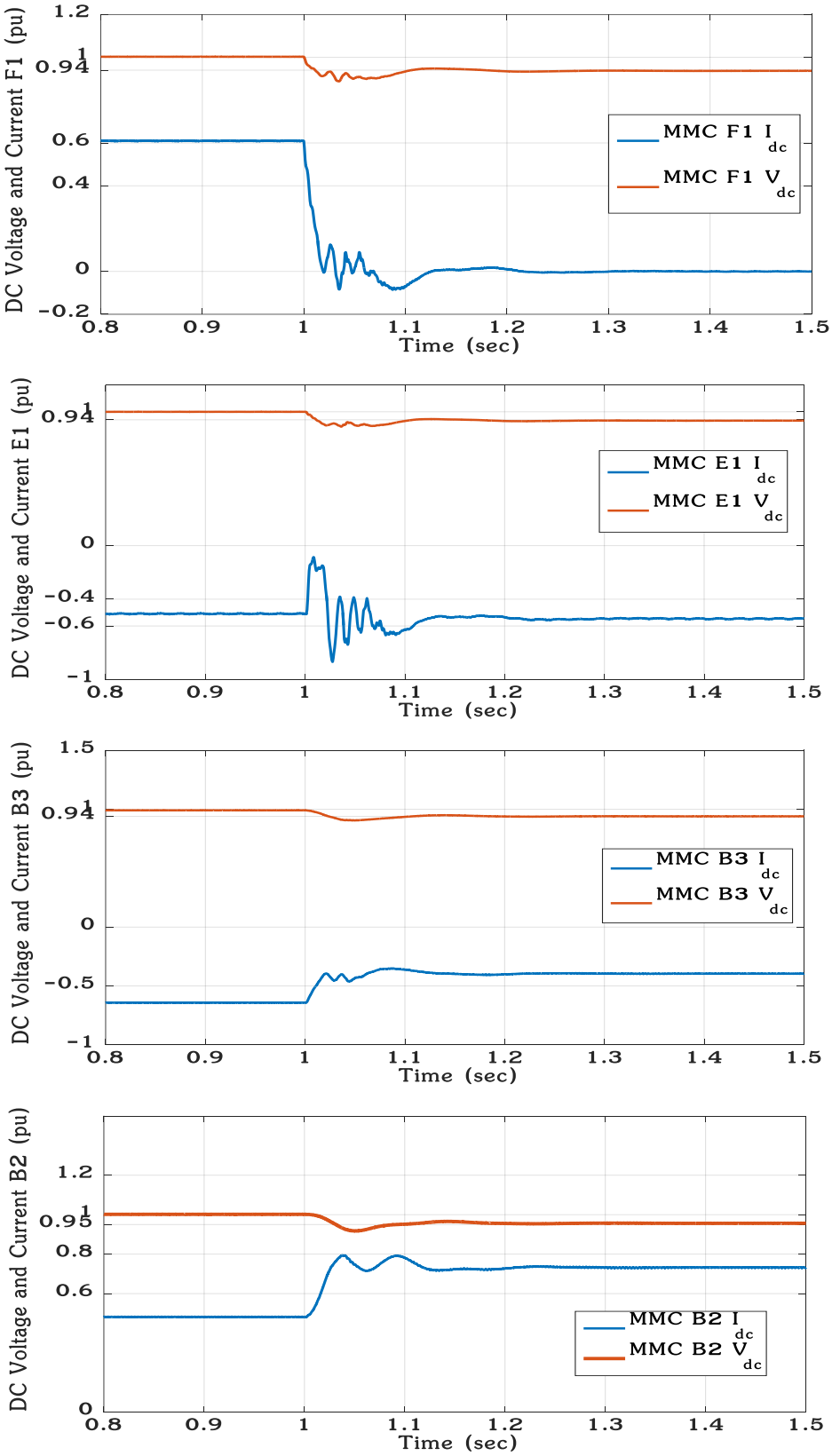

Figure 5.25 Simulation results MMC based MTDC under contingency operation at MMC F1 with droop voltage control: DC voltage and DC current.

K. Case E

In this case, the performance of the proposed system under contingency is verified for a sud-den disconnection of MMC F1 .The performance of the droop voltage scheme is tested by means of controlling the DC voltage droop control in the MMC B3 ,MMC B 2and MMC F 1P/Vdc droop controller (explained in Chapter 3). Unequal loading conditions are considered to demonstrate the performance. If a DC fault of converter appears, the converter protection will be actuated. When a certain current level is reached, IGBTs would be blocked. As DC breakers have not been used, it is necessary to block converter stations and to use AC circuit breakers to clear the fault. In the beginning, MMC B3 and MMC E1 imports 780 MW and 100 MW ,respectively. MMC B2 and MMC F1 export around 390 MW and 497 into the DC grid. The outage of MMC E1 is considered at t=1s.

The dynamic response of four-terminal HVDC system following E1 converter outage is shown in Figure Figure 5.25. Generally, for a MTDC system based on droop control, loss of an inverter will result in the rise of DC voltage and the increase of inverting power as MMC B3 and reduction of rectify-ing power as MMC B2, which are remaining in droop control. The simulations obtained in the system controlled by the droop method shows the collaborative scheme of all droop-controlled converters in the function of balancing power in order to obtain a new steady state operation. After the oil platform disconnection, the system recovers immediately a new steady state operation. In this case, the current injection at each converter is logically adapted to a new value different to the nominal because of the current power flows. In this way, accurate power control and effective voltage stabilization can be accomplished at the same time.

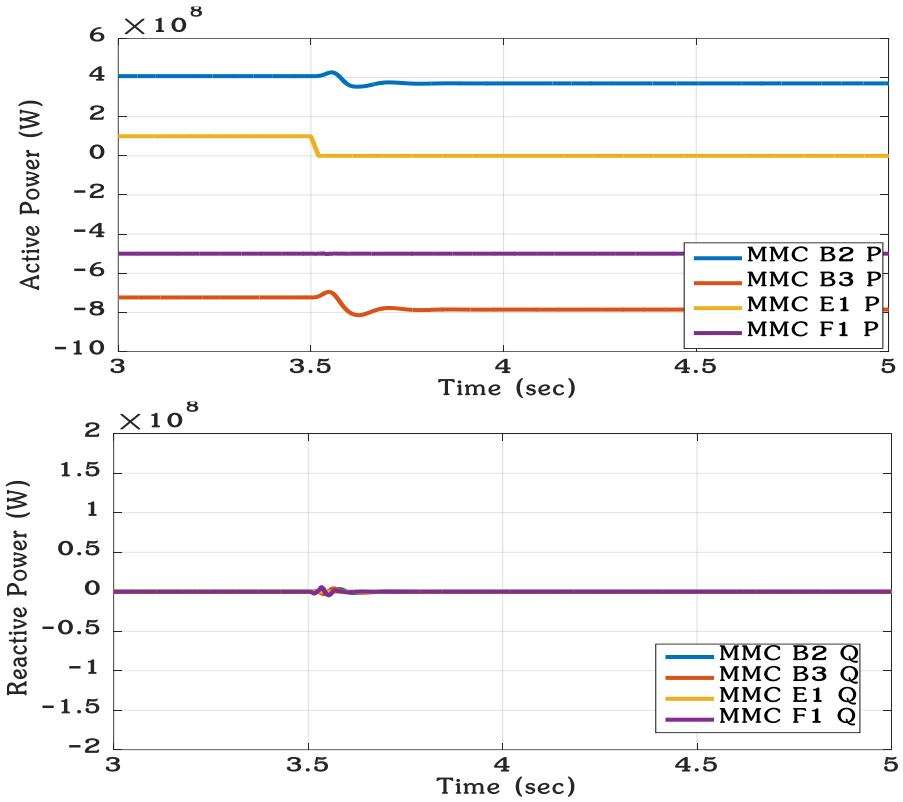

Figure 5.26 Simulation results MMC based MTDC under contingency operation at MMC E1 with droop voltage control: active power and reactive power

L. Case F

In this case, the performance of the proposed system under contingency is verified for a sudden three phase's line to ground fault at PCC of MMC B3.

MMC B3 and MMC E1 are ordered to absorb 800MW and 100 MW respectively. A three phase symmetrical fault is applied at PCC of MMC B3 starting at 2s in order to investigate the behavior of VSC-MTDC during symmetrical faults, and is cleared at 300 ms after the fault, i.e., at t = 2.3s. Figure 5.27 presents the simulations results. MMC B3 is therefore unable to import any significant quantity of active power during the fault.

During the fault for the system employing the DC voltage droop, there is a surplus of approximately 800 MW which must be dissipated to prevent uncontrollable DC voltage rise. When employing voltage droop control, both MMC B2 and MMC F1 decreases its exported power in response to the increase in DC link voltage. The DC voltage rise and it contains an oscillation during the fault. Consequently the transferred DC power contains also the oscillation. At all converters after the faults occurs a protection system "block converters is activated to protect the submodules in each MMC from the short circuit current when the current overtakes the limits.

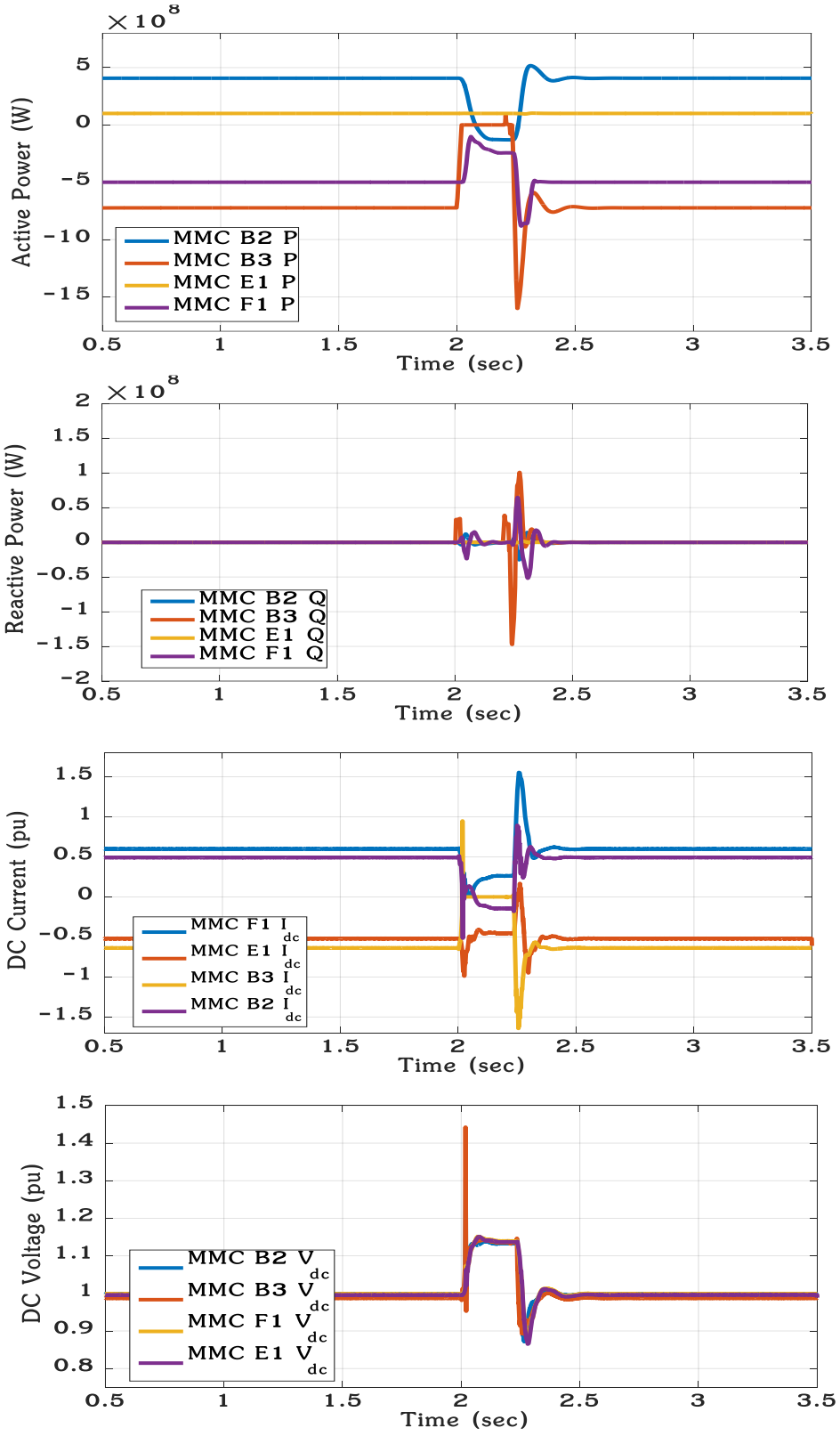

Figure 5.27 Simulation results MMC based MTDC under three phase line to ground fault at B3 with voltage droop control: active power, DC voltage, reactive power and DC current.

5.7 CONCLUSION

Compared with the conventional two-terminal VSC-HVDC, VSC-MTDC can offer more than one power suppliers and supply power to multi-loads, the operation mode of VSC-MTDC is more flexible, can offer technology support for the access of multi supplier center, multi-loads center and distributed renewable power like wind power, etc. The topology structure of VCS-MTDC system is directly related to the reliability and practicability of the control strategy and can be divided into three types: the parallel structure, series structure and hybrid structure. More specifically, there are 4 types, which are: Radial; Ring structure and meshed structure.

The performance of three MTDC control methods, namely, master/slave control (DC slack bus) and droop control, were investigated using an averaged MTDC system model. The controllers' response to onshore AC faults and the disconnection of an offshore wind farm and an offshore oil platform con-verter were simulated.

The control scheme is composed by a primary, a secondary and a tertiary control similar to the traditional AC grid controls. The primary control is in charge of the DC voltage stability. The secondary control permits to achieve a given power set points, also after a contingency. The operational points of the proposed method, under normal and fault operation have been described. Some simulation scenarios, including a power converter disconnection, have been simulated in order to test the proposed system. The system stability under normal and fault conditions has been demonstrated using simulations with 2 differents models.

Chapter 6 HVDC SUPERGRID

Over recent years, serious debates on supergrid infrastructure began as a consequence of some significant changes that occurred in the European energy sector recently, such as the increasing importance of the interconnections between countries, and the high price of electricity, the markets took off in the years before, based on the European Energy Market liberalization (2009); and showed high electricity price differences between the member states and market regions. This Price difference was a result of different power production portfolios and fuel mixes, calling for cross-border connections [144]. From 2009, transmission system operators (TSOs) and regulators started cooperating intensely inside their newly established associations, ENTSO-E, and regulators, on tasks defined by European politics, such as typical European grid planning and standard European network codes [145], which provide an overview of the future energy policy of Europe. The novelty of this task is the integration of energy and environment objectives of the EU by the use of market-based environmental, such as renewable energies (wind and solar energy) [146]. The idea of building a supergrid became quickly a matter of interest, because it facilitates the balancing of variations and sharing of reserves [147] [7]. Moreover, interconnections to large hydropower capacity in Scandinavia had been identified as a beneficial complement [147] ; wich enhances the flexibility of the power system and also reinforce the supply security. This chapter aims to review the current research status of different key technologies in supergrid. In this regard, this chapter will start with different key drivers for building such installation. Different components of supergrid are analysed. Finally a selection of several challenges not only technical but also political and economical standing up in the way to establish a supergrid and a keeping out its realisation is described.

6.1 KEY DRIVERS FOR BUILDING SUPERGRID

The Supergrid can be defined as “an electricity transmission system, mainly based on direct current, designed to facilitate large-scale sustainable power generation in remote areas for transmission to centres of consumption, one of whose fundamental attributes will be the enhancement of the market in electricity [148] [46],” Figure 6.1 shows an example of a HVDC supergrid with its main components. Therefore, we can count enough reasons why supergrid should be built; this section describes some of those reasons:

Figure 6.1 Example of a supergrid with its main components.

.

6.1.1 CO2 REDUCTION

one of the prerequisites to reach a carbon neutral Europe held in the construction of supergrid which allows meeting EU and national plans to decarbonise Europe's power sector: 20% by 2020 and 90% by 2050 [144].Knowing that currently, 50% of the world's carbon emissions is being emitted by the electricity sector from fossil fuels. The Supergrid will facilitate the integration of renewable energy sources and would, therefore, clean the environment significantly [11].

6.1.2 SECURITY AND SUSTAINABILITY OF SUPPLY

The Ukraine crisis showed several weaknesses of the energy systems in Europe. In fact, the security of supply became a priority in the agenda of the EU, especially due to parts of Europe's heavy dependence on Russian gas. Supergrid will reduce dependency on gas and oil from unstable regions, adding that, such infrastructure allows to transmit the electricity from the source to the consumers with sufficient redundancy at any moment and improves, moreover, the connections between big load centres and bypasses onshore energy transmission bottlenecks [7] [146].

6.1.3 INTEGRATION OF LARGE-SCALE RENEWABLE ENERGY SYSTEM

supergrid facilitates the increase in renewable energy system which is variable and geographically dispersed, and requires a high connection level like offshore wind power plants and other marine technologies, especially in the North and Baltic seas [149] [148], mixed with solar energy from the south of Europe and the north of Africa, and thereby reducing the variability and the resulting flexibility needs. Currently, we can't include cleaner energy from renewable sources in the European system only if we are connected which is not possible yet. Therefore, a back-up is needed for renewables [145] [150], which means that the wind and solar power are available at any moment somewhere. Supergrid with one big interconnected system ensures the security of supply if one source falls short, another carries on [121].

6.1.4 INTEGRATION OF PUMPED-STORAGE HYDROELECTRICITY

First of all, the connection to large hydropower capacity mostly located in Scandinavia(in Norway) and France (Alps, Pyrenees)will supply more flexibility and balancing in the power system and would decrease the curtailment of wind and solar energy, allowing a better exploitation of the available renewable energy systems [11].The second is,that it would be the only one capable of storing large scale of electricity in the type of battery so far developed for that goal: pumped hydro-storage by using the energy to pump water uphill when the electricity supply becomes higher than demand, and recapturing power as the water flows down again when the electricity supply becomes lower than demand, these dams can store electricity at more than 85% efficiency, providing a back-up and moreover, reducing costs and improving efficiency, while ensuring a higher security of supply [147].

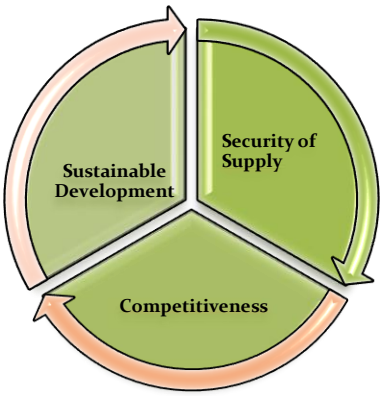

Figure 6.2 Policy drivers for the energy supply of the future

6.1.5 STEPS TO A SINGLE ELECTRICITY MARKET

price differences between the different synchronous coupled parts of the grid, plus network congestions indicate the existence of bottlenecks in the European power system, which are a significant weakness in cross-border electricity exchanges, that will persist or emerge in the coming decade; the transfer capability may not be sufficient to accommodate the likely power flows unless new interconnection projects are established [7]. Those price differences are variable in time due to fast changes in types of electricity generation, especially renewable ones [148]. The single electricity market will give more dispatch, efficiency, and flexibility; First of all, building super grid will extend the electricity market by connecting renewable energy generators to distant markets therefore improving cross-border trading capacity, so the bottlenecks and the congestion problems will be reduced. The second benefit is that the transportation and generation optimum will be greater thanks to the expanded network. Adding that, of course, the cost of energy will be reduced which leading to an overall cheaper electricity supply which benefits consumers.Furthermore it allows to give a clear incentive to the renewables industry to get more efficient, and most of all this market will improve the security of supply, boost competitiveness and decrease the price differences between price zones [123] [151] [152].

6.2 KEY TECHNOLOGIES IN SUPER GRIDS

6.2.1 HVDC CABLE TECHNOLOGY

HVDC cable systems are a mature technology. Insulating materials mass impregnated and DC XLPE are both applicable for VSC-converter systems depending on their application:

- For applications at voltages higher than 500 kV, the preferred insulation material is mass impregnated; relating to submarine connections due to the considerable experience obtained in long length manufacturing.
- For the other application, the preferred insulating material for VSC-HVDC transmission is XLPE; regarding land applications this is mainly due to the availability of premoulded accessories. Although XLPE cables have been in use for many years in the AC market, they are (relatively) new to the HVDC market [144]. As there is no experience in managing these cables to end of life, development in XLPE HVDC cables has been rapid, their construction is simpler, and they allow a lower bending radius, less expensive cost and have a number of other installation/transport advantages when compared with MI cables. Most XLPE DC cable installations are at voltages up to 320 kV, but currently XLPE cables are available at 525 kV [146].To achieve the ratings for supergrid cables, higher voltage levels are required over the next ten years. Their operating voltage would reach over 550 kV with a capacity increase up to 2 GW associated with a reduction of losses. Also, the maximum laying depth would be beyond 2500 m [153].

6.2.2 DC CIRCUIT BREAKERS

Actually HVDC systems are basically point to point connections, however suggesting the development of multi-terminal meshed HVDC grids may participate to enhance the power system reliability, flexibility in long distant bulk power transmission [154], redundancy and also lower the number of converter stations [155]. Yet some barriers keep out the achievement of similar grids such as the need for a protection system of HVDC – grid in order to reduce defects and conserve the remaining healthy parts of the grid [156] [157].Thereby HVDC breaker is required within its development, however multiple challenges are related to this development including [158] [144]:

• The circuit breaker must interrupt the current typically within 5 ms, since the rise of the fault current in DC (Direct Current) grids is higher than AC grids due to the low line impedance of DC lines. • The circuit breaker in DC grids must provide itself the zero current crossing, contrary to AC grids where the system provides the zero crossing in a natural way. • The DC circuit breaker must clear the magnetic energy maintained in the inductance line, counter to AC circuit breaker. • The DC circuit breaker has to tolerate remaining overvoltages after current interruption [30] [35] [159].

Four main types of design have been applied and demonstrated are shown inFigure 6.3:

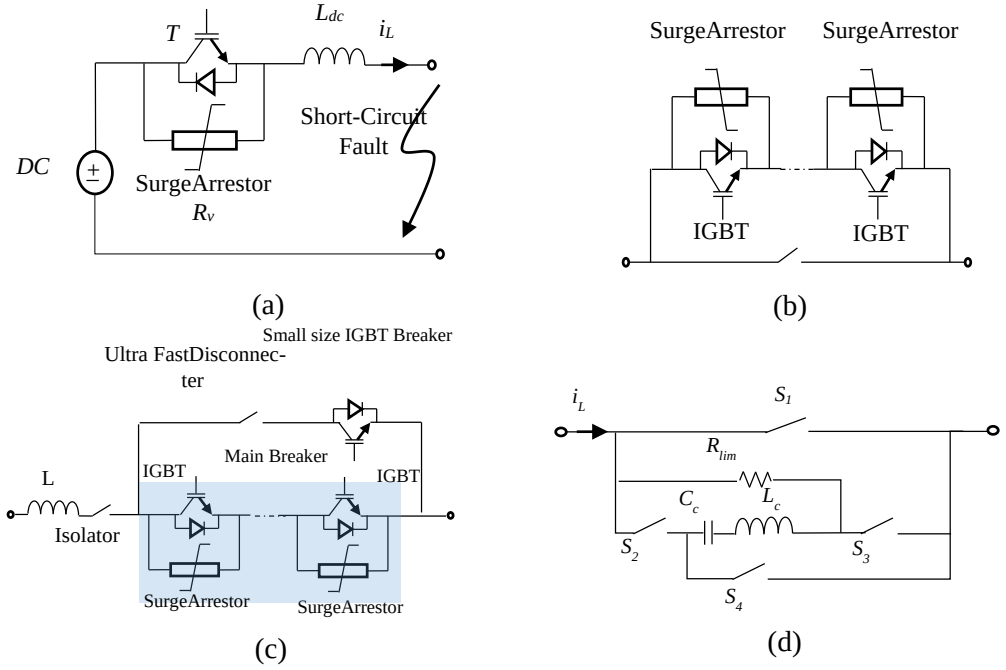

Figure 6.3 Review of the Proposed Topology of DCCB design: (a) solid-state CB, (b) hybrid I, (c) hybrid II, (d) Mechanical active resonance CB

1. Solid state CB: involves an IGBT in current path typically sited at the DC cable ends. Typically within a few ms, the on-state losses are high however the operating times are very fast (Figure 6.3(a)).

2. Hybrid CB: an integration of solid-state devices gathered with a mechanical breaker. Generally, in a hybrid CB, the commutation path is introduced by solid state switch which exclusively operates during the interruption process, where all the switches are controlled by electronic circuits. Using a hybrid electronic/mechanical devices may minimize remarkably the on-state losses (Figure 6.3b, c)).

3. Mechanical CB: A mechanical DC Circuit breaker uses advanced AC circuit breaker technology, replying to an additional resonant circuit required (Figure 6.3(d)), the cost of mechanical CBs is simultaneously low, as the opening times are generally quite slow (of the order of 30-50ms) [32] [160].

A summary of the most important parameters of the DC breakers technologies, which were presented above, is given in Table 6.1. For the implementation of the DC breakers in an HVDC network, they need to

fulfill certain requirements. The most important are: the low total current interruption time, the low losses during normal operation and the ability to break high currents when subjected to high voltage stress. Some DC/DC topologies are capable of reducing DC current without causing any overvoltage allowing a flawlessly operation thus the major inconvenient is that on-state losses seem to be very high [160].

Table 6.1 : DC breaker technologies comparison

	Solid State CB	**Hybrid I**	**Hybrid II**	**Passive Resonance**
Commutation [ms]	Switch:0.1	Switch: ≤0.2; Breaker: ≈0.25	Switch : ≈0.1; Breaker: ≤ 20; UFS:1-5	Breaker: ≤ 20; Resonance: ≈ 30-50
Energy Absorption [ms]	≈ 1	≈ 1	_	_
Interruption time (t_b) [ms]	≈ 1	≈ 2	≈ 30	≈ 60
Max.Voltage [kV]	≤ 800	Tested: 120; Expected 320	AC-CB: ≥ 500; UFS: ≤ 12	Available:≤ 550
Max. Current [kA]	≤ 5	Tested: 9; Expected: 16	Estimated 6-12	Tested: 4
Losses[% converter rating]	ICGT ≈ 30%, GTO ≈ 40%	≤ 1%	negligible	negligible

In November 2012 ABB declared a breakthrough in the technology to interrupt DC; ABB expanded the world's first Hybrid circuit breaker for HVDC. This hybrid circuit breaker consists of a combination between mechanical switch and power electronics, able to interrupt power equal to the output of a large power station within 5 milliseconds [7].

Alstom has also developed an Ultra-Fast Mechatronic Circuit Breaker (UFMCB) with its project partner RTE. This circuit breaker includes three branches, main branch which consists of ultra-fast mechanical disconnecting switch based on IGBT, auxiliary branch based on a series stack of thyristor and capacitor bank which force the current to commutate into the parallel connected surge arrester (energy absorption branch), therefore forcing the current to zero [7]. The demonstrator rated of 120 kV (nominal DC voltage) successfully interrupted a 5 kA at 163 kV with full current extinction in 5.3 milliseconds.

Another association has also created a new direction concerning that technology; Siemens that lately achieved DC commutation breaker for largest rated DC current of 5000A and succeeded to pass switching test at the Shuanglong converter station in China. In addition, Siemens supplied DC commutation breakers for the ultra-high-voltage DC (UHV DC) transmission project Xiluodu-Zhejiang. This new revolutionary technology of Siemens' permits the re-configuration of DC circuit and provides capabilities to commutate the inter-path DC currents besides it offers reliable transmission that is also ecologically friendly since it is clean & CO2 free power at highest loads [7] [161].

6.2.3 DC POWER FLOW CONTROL DEVICES (DCPFC)

To avoid overtaking the power rating of components in HVDC grid, the power flow across an HVDC line has to be monitored in the same way like AC grid. In radial HVDC Grid systems only one line combining two converter stations and the DC voltages of individual converter stations will control the flow across each line, in contrary in the meshed systems where more than one line combining two converter stations, the flow across parallel paths relies on the line impedances and the DC voltage inserted in series, these systems -in order to reach a required power flow– they may claim a supplementary DC Line Power Flow controllers, which are being developed at the present time.Figure 6.4 Review of the Proposed Topology of DC Power Flow Controller shows the proposed topology of DC Power Flow Controller in references [7] [32].

There are three main types of DCPFCs to realize the flexible power flow control:variable series resistors (VSR), and series voltage sources (SVS), DC transformers.Variable Series Resistors and Series Voltage Sources are series connected devices while DC transformers are shunt connected devices.

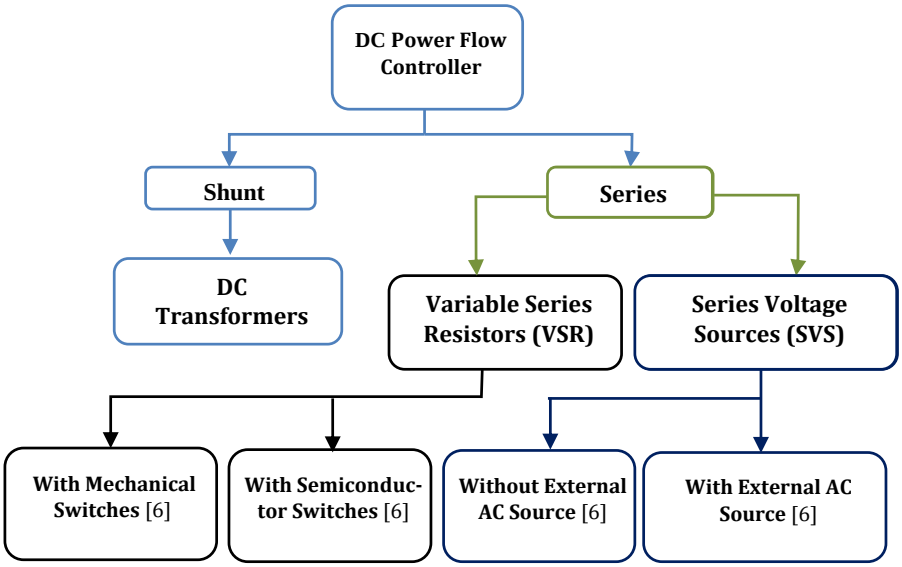

Figure 6.4 Review of the Proposed Topology of DC Power Flow Controller

A simple solution for DC power flow control is by using resistors that can be inserted in series with DC lines. A variable series resistors can be inserted in a DC grid to change the equivalent resistance of the DC line. The VSR regulates the active power through a DC line (not necessary the line where VSR is located) by adjusting the inserted resistance. Two main VSR topologies have been proposed in [6]: VSR with mechanical switches and VSR with semiconductor switches. Series voltage sources SVS have been used in AC systems [7], the same principle can be applied to DC grids but with DC voltage sources inserted into DC lines in series to change power flows. This series device acts as a controllable voltage source with a small voltage value. Normally it has a voltage magnitude on the order of 1–5% of the DC grid voltage. An SVS can be implemented by different devices and topologies.Two main VSR topologies have been proposed in [6]: SVS with external AC Source and SVS without external AC Source.

6.2.4 DC/DC Converters

The DC/DC converters were not used at transmission levels but with DC super grids, they will be important to connect HVDC grids with different voltages levels.DCDC converters will be highly controllable units; which allows its use to support other functions in DC grids. In ideal case DC/DC transformers can achieve:• DC voltage stepping, • DC voltage or DC power regulation, • DC fault isolation, • Interfacing different DC technologies like LCC with VSC or monopolar with bipolar DC systems [6] [162].

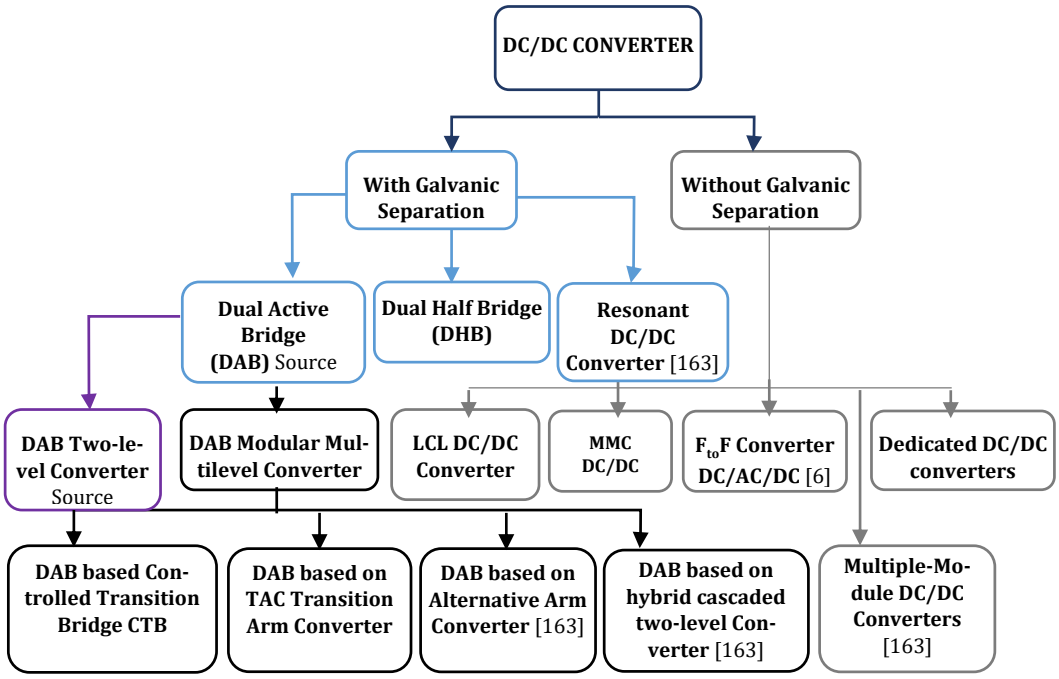

Figure 6.5 Review of the Proposed Topology of DC/DC converter

Selecting a DC/DC converter topology in an HVDC application involves multiple factors such as the required voltage ratio, the power rating, power flow directions as well as the system configurations and the grounding schemes of the systems to be interconnected whether galvanic separation is needed or not. In total, it is practical to order the relevant DC/DC converter topologies based on their capability to provide galvanic separation, the voltage ratio and the capability for controlling bidirectional power flow in HVDC grid system. Some appropriate sub-categories of DC/DC converter topologies for HVDC applications are represented in the review described in Figure 6.5 [163] [144] [164].

There are different sub-categories proposed in references from MMC converters which are shown in Figure 6.5.The introduction of DC/DC converters family based on MMC topology has created a new path for research and development of HVDC grid. Leading-edge modulation strategies which empower high voltage conversion ratio, high efficiency and reduced component stresses are claimed in order to take the extremely benefits of these converters for several applications [164] [165].

6.3 CHALLENGES AND OBSTACLES

The struggle to establish a European super grid results from the existence of many substantial challenges and barriers,in spite of all the advantages mentioned earlier. Figure 6.6 clarify technical,economic and political challenges that have to be overcome in order to develop supergrid [121] [154].

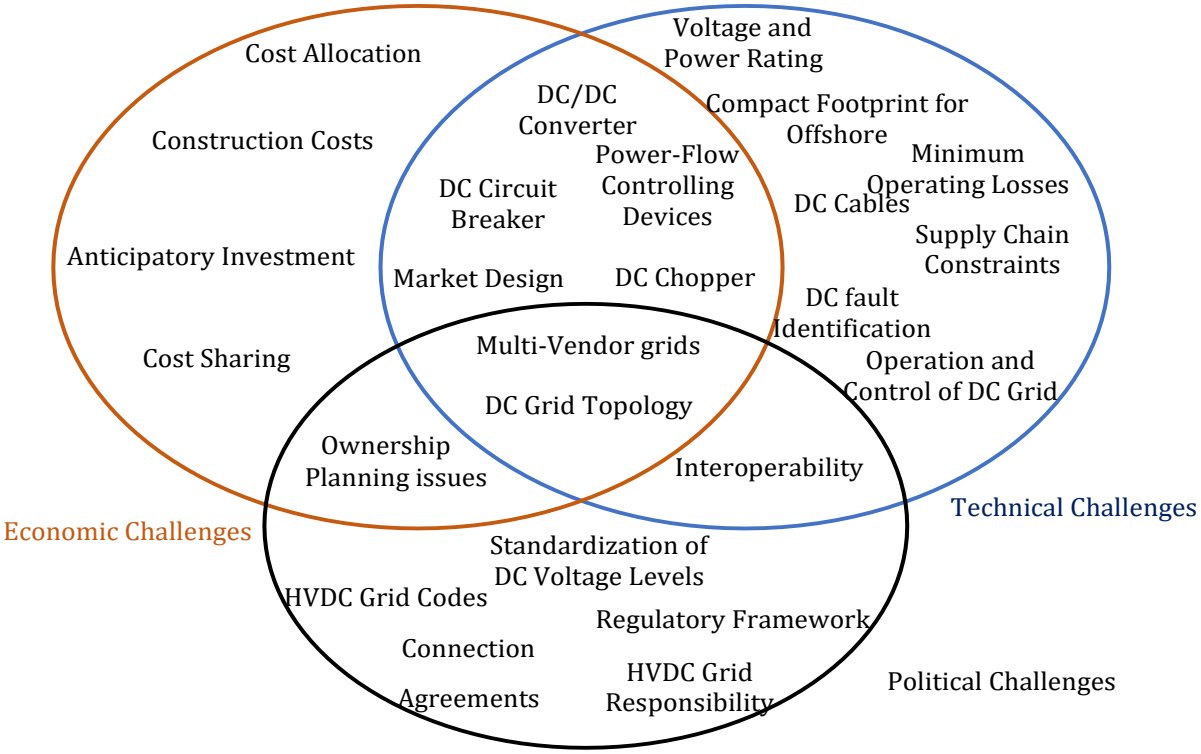

Figure 6.6 Challenges and difficulties laying to build supergrid

6.3.1 TECHNOLOGICAL BARRIERS

Converter technology suited for HVDC grids (VSC technology) have been commercially available since 1997. Bulk power and low loss converters have been available since the introduction of MMC technology. Despite the advantage and feasibility of MMC technology, MMC [166]and also VSC technologies, in general, are relatively new. Thereby, classical LCC is available for ultra-high voltages and power ratings; that's not the case with VSC technologies, the challenge with the VSC technology remains in the power rating and ultra-high voltage levels in order to fulfil transmission demands of the supergrid (>2GW and >500KV per converter) [167] [156] [134].

The extra challenges with HVDC grids are that it is not commercially available. Without the use of additional equipment in meshes such as DC/DC converters and DCPFC, DC power flows cannot be actively controlled on a specified line. Given that these devices are not typically needed in today's HVDC P2P and radial MTDC schemes, they are not commercially available, and there lacks a common strategy to operate them in a meshed HVDC topology [154].

6.3.2 OWNERSHIP AND RESPONSIBILITY OF THE SUPERGRID

We may define ownership as the sets that determine and clarify who owns and operates supergrid .in that concept; those are the incentives,responsibilities, and liabilities which manage the transmission of investment. The ownership of supergrid is not based only on the existing TSOs; multiple interested investors are needed to make it real.In the European case, ENTSOE seems to be the most likely owner of the supergrid [168].

The issue with investment relays on disagreement about the correct financial incentives of the investment projects; that means the more parties with different remuneration schemes are involved, the more difficulties appear in order to find a satisfying compromise for all concerned. We must mention that the procedure of investment may take years to be achieved, that makes delaying investments a very difficult task because of the

uncertainties of the future scenarios. Therefore, it would be necessary to optimise the timing transmission system investments [7] [121].

6.3.3 MULTI-VENDOR INTEROPERABILITY

We can define interoperability as a requirement for different technologies and equipment from multiple manufacturers to be compatible especially in the situation of multi-vendor multiple terminal DC grid [169]. Adding that the growth of super grid will be in an organic way if only super grid showed flexibility and modularity. Supergrid would be developed as an international power system. Therefore, Vendor lock-in will not be acceptable, besides the compatibility of equipment between the multiple manufacturers and DC technologies will allow competition between them and give more choice for alternatives [146].

Despite the differences between manufacturers concerning VSC-HVDC converter stations in particular based on Modular Multilevel Converters (HVDC Light, HVDC Plus, HVDC Maxsine), the technologies or the control algorithm used they will be all connected and working in the same system. When the ramping speeds on the different converters change remarkably, dynamic collateral effects may retard the performance of a system that's why control functions should be independent of each other [30] [35].

6.3.4 STANDARDS AND GRID CODE FOR HVDC GRID

Nowadays, standardization of HVDC systems is in its infancy, and no initiative on standardization of multiterminal DC systems exists. Nevertheless, standardization is a major problem, since the supergrid will include a large variety of facilities from multiple suppliers, some of them already existing, and has to struggle with rapid advances in HVDC technology. Despite the possibility to connect regional networks or converters of different operating voltages onto a common voltage, an agreed standard voltage level of HVDC VSC technology will be more practical since it would ease multi-terminal scheme and assure the interoperability of multi-vendor multiple terminal DC grid [170].

When HVDC grids with different voltages are interconnected or when the present point to point HVDC projects are linked to an HVDC grid and the voltages do not match DC/DC converters could be major.The working group will investigate the possibility of recommending standard voltages for DC Grids beginning from the standard voltage levels used for AC networks, argue the aspects of the converter station design that may require its standardization, therefore,permitting stations from different manufacturers to be connected to the DC super grid.In order to achieve the standardization of HVDC grids, important questions have to be answered, and some specific planning criteria have to be centred, including [170] [171] [172]:

- DC voltage levels Standardization
- Concepts for interconnecting local and inter-area DC grids, probably with different DC voltage levels
- DC grid topologies
- Control and protection principles: switching algorithms and voltage control.
- Fault behaviour: ramping effect, harmonics and over voltages.
- Typical block sizes for converter stations and cables.
- Communication protocols.

HVDC Grids will require rules in the same way that AC grids operate within AC Grid Codes. Since an HVDC grid will probably include many Transmission System Operators (TSOs) and converter stations from multiple suppliers, an earlier establishment of such a Grid Code will be needed to empower the achievement of HVDC grids. The study committee of Cigre B4 “HVDC and power electronics” have appointed two working groups; WG B4-52 “HVDC grid feasibility study” [32] [173];this feasibility study investigates the possibility of building large HVDC grids and whether it is economically attractive, and WG B4-56 Guidelines for Preparation of Connection Agreements or Grid Codes for HVDC whose mission is to supply information for HVDC grid designer whether it concerns information desired by anyone providing new equipment for an existing HVDC grid or it is in connection with the restrictions within which the network is supposed to be designed.

Those information offer a satisfying terminal integration in the existing system and perfect the performance of the whole system by making it completely free from negative impacts [121] [174].

6.4 ECONOMIC ASSESSMENT OF AN OFFSHORE HVDC GRID

Transmitting high capacities of energy from sea to shore presents a significant challenge due to the need for a very efficient, robust, and reliable technical solution that must be cost effective. High Voltage AC (HVAC) and High Voltage DC (HVDC), Voltage Source Converter (VSC) based, are possible transmission solutions to these challenges. Therefore, we present herein The economic comparison takes into account the investment costs, losses and annual maintenance of wind power transmission and present the necessary procedures to select the most cost-effective solution for a given application.

6.4.1 INITIAL INVESTMENT COSTS

The costs for the VSC-HVDC and HVAC transmission systems were broken down in different categories: substations (offshore and onshore), cables, cable installation, offshore platform, and in the case of HVAC reactive compensation equipment.

All cost figures represent a snap-shot from recent publications. However, since components and systems for bulk power transmission are not “off-the-shelf-products”, and costs are inherently strongly case sensitive, the provided cost figures are rough estimates, even though they have been taken from public sources such as newspaper articles and network extension studies. The accuracy of the station costs can be estimated to be around +/- 30%. Data regarding the costs of the components of the transmission systems was taken from different sources. [175] prepared a report for the north Seas Countries ' Offshore Grid (NSCOG) and TWENTY analyzing the relevant transmission technologies for the offshore wind farms and their costs, [176] analyzed the transmission system for a 300 MW offshore wind farm while working for ABB, [177] prepared a report for the costs for offshore wind energy in the WINDSPEED project , [178] made a survey with the HVAC technology industry in USA for offshore wind farms, and [2] prepared a report for a proposed HVDC link called Middletown-Norwalk in USA, and [179] and [180] prepared a thesis analyzing the interconnection of wind farm with HVAC and HVDC systems.

Generic values of costs of high voltage power transmission are of very limited use and may easily become misleading and thus, their use should be avoided. A more reliable method for comparing HVAC and HVDC costs on a case by case basis is achieved by sending out a call for quotation to different manufacturers. Even such values may be subject to an uncertainty of +/-15%. Therefore, it is strongly recommended that estimated for the costs of HVAC and HVDC for a specific project must be calculated and the weighed against the advantages and disadvantages of each option.

A. Substation Costs

The costs referred to as stations costs comprise all necessary equipment installation investments which have to be applied for a sustainable point-to-point connection excluding the high voltage transmission line.

For the HVDC substation, [175] reports prices of 98-105 M euro for 800MW ±320 kV and 121-150M euro for 1250 MW ±500 kV, including all electrical equipment (valves, reactors, filters, capacitors, etc). [176] report 45M euro for 375 MVA ±150kV. [177] report 139.65 M euro for a 600 MW substation which includes 120M euro for the converter ,4.05 M euro for the power and auxiliary transformers ,6.8 M euro for the HV and LV switchgears, 2.1 M euro for the standby generator,ancillary services,workshop accommodation and fire protection ,and finally 6.65 M euro for the installation of the electrical equipments (5% of the equipment cost). [2] reports 40.5 M euro [1] for a 370MW substation and 46.3M euro [2] for 530 MW (±150kV) including all previous studies ,installation and tests .As a compromise between these values a total costs for the 1GW substation offshore and onshore including all electrical equipment and installation is set to 120M euro each .the maximum voltage available as expressed by [175] for a VSC-HVDC converter is ± 320 kV ,which is the

voltage used in the proposed substations. Because of the modular setup of HVDC converter stations the investment costs for bulk power transmission may be assumed to increase linearly with the power rating as very rough estimate. There are several other factors which can have an influence on the costs. Due to the fact that there is little exact information on already commissioned projects the specific VSC-HVDC converter costs are taken from earlier studies. The specific costs of 0.102 M€/MVA are used for all power ratings and voltage levels.

Compared with VSC-HVDC, HVAC substations are simpler and include mainly power transformers and switchgears. [175] reports transformers of 180 MVA 132/33 kV at 1.12-2.07 M euro and 240 MVA 132/33 kV at 1.2-2.3 M euro ,also switchgears of 132 kV at 1.26-1.61 M euro and 275 kV at 3.34-3.68 M euro . [178] report transformers of 187 MVA 138/34 kV at 1.87 M euro [1] and 560 MVA 345/138 kV at 4M euro, and they also report a total cost for a 500 MW substation including offshore platform at 30.6 M euro. [177] report costs for the electrical equipment for a 600 MW substation at 18.8 M euro plus its installation of 0.9 M euro. [176] report costs for a 300 MW electrical equipment including transformers and switchgears at 10 M euro. [179] report the use of four 300 MVA 200/33 kV transformers and a 200 kV switchgear bay , the total costs including installation for each 1 GW substation would be 18 M euro.

Table 6.2 Station investment costs per station

Rating	HVAC	VSC-HVDC
500 MW	16 M€	51 M€
1000 MW	28 M€	100 M€
1500 MW	40 M€	150 M€

B. Transmission Line costs

The costs for a point-to-point connection depend strongly on the considered political and environmental framework and the cost for the rights-of-way. Especially the geographical conditions have impact on the costs. For example a double circuit transmission line in the Swiss Alps would be 4 times more expensive than a transmission line in Finland or Sweden. In addition to the construction cost, there are payments for environmental impact, labour costs and indemnifications for right of way usage. In this chapter the construction costs are the central point. Environmental impact and right of way are considered in later chapters.

[175] reports the HVDC cable cost as 0.345-0.518 euro/km/cable with 1200-1500 mm^2 cross-sectional area at ±320 kV . [177] reports 0.2 M euro/km/cable for 1600 mm^2 and [2] 0.274 M euro/km/cable-pair [3] for 700 mm^2 and 370MW ,and 0.456 M euro/km/cable-pair[4] for 1400 mm^2 and 530 MW including all the previous studies and tests . [176] suggest 0.6 M euro/km/cable-pair. The cable installation is very difficult to estimate due to many reasons [175].The values range between 0.575-1.035 M euro /Km for a twin cable in a single trench , 0.69-1.38 M euro/Km for two single cables in different trenches [175] 0.215 M euro/Km/cable-pair [176], 0.36 M euro/Km/cable -pair plus 5M euro for cable mobilization.

Table 6.3 Submarine Cable Cost per Km [181]

Project	Rating (MW)	Cable type	DC config	Cond.Size (mm^2)	DC Voltage (KV)	Length (Km)	Cost Estimate (€M/Km)
Transbay cable	400	Polymer	Symm. Monopole	1,100	± 200	85	1.29
SylWin	864	Polymer	Symm. Monopole	1,250	± 320	205	1.28

EWIC	550	Polymer	Symm. Monopole	1,650	± 200	186	1.23
SAPEI	1,000	MI	Bipolar (2×500MW)	1,000-1,150	± 500	425	1.15
Fennoskan2	800	MI	Sysmm. Monopole	2,000	500	200	0.87
Skagerrak4	700	MI	Sysmm. Mon-opole	__	500	140	0.67
Maritime Link	500	MI	Bipolar (2×250MW)	__	± 200	170	1.03

As it can be seen in Table 6.3, the prices differ from source to source, possibly because of the commodity price fluctuation e.g. copper and aluminium .An intermediate cost of 1.15 M euro/Km/cable for 1400 mm^2 is chosen.

For the cable selection, the commercial use points to three-core XLPE cables to avoid compensation along the cable. Such cables are more complicated to produce and can stand less current. Looking at the [1] catalogue for submarine cables , and without compromising the cable active power carrying capacity due to reactive power generation , a three -core XLPE cable of 1000 mm^2 cross sectional area , copper conductor ,operated at 200 kV is selected . The maximum current that such cable can stand is 825 A, and thus its maximum power is 286 MW. In that case four cables are needed in order to transfer 1 GW . [175] reports costs of 0.575-0.863 M euro/km/ three core cable of 300 MVA at 220 kV , [178] 0.543-0.619 M euro/km/single-core-cable of 630 mm^2, [177] 0.59 M euro/km/three- core -cable in the sea and 0.295 M euro/km/three-core-cable in the land , and [176] 0.75 M euro/km/three-core-cable of 500 mm^2.

As the cable becomes more complex, its installation process as well. [175] do not report any differentiation between HVDC and HVAC cable installation, hence the values are the same as in the last section . [176] report 0.17 M euro/km/cable. [178] report cable laying at 0.068-0.074 M euro/km/cable, cable transport from Europe at 0.042-0.061 M euro/Km/cable, [177] report 0.240 M euro /km/cable in the sea and 0.18 M euro/km/cable i the land plus a mobilization cost of 5 M euro . An intermediate value of 1.76M euro/km/three-core-cable for 1400 mm^2 is chosen.

Table 6.4 summarizes some of the cost figures and also shows the spread among the costs for different arrangements.

Table 6.4 Transmission line costs- Examples from various sources

	HVAC		**HVDC**	
Rating	Cable	OHTL	Cable	OHTL
500 MW	0.92 M€/km	0.35 M€/km	0.92 M€/km	0.24 M€/km
1000 MW	1.84 M€/km	0.39 M€/km	1.15M€/km	0.26 M€/km
1500 MW	2.15 M€/km	0.45 M€/km	1.7 M€/km	0.34 M€/km

C. Offshore Platform

An offshore platform is necessary to install the HVDC converter station offshore [182]. The cost of a top site structure offshore is unclear. The experience for offshore wind farms is limited and platform building

companies are reluctant to provide cost data because they vary strongly from situation to situation. The cost of an offshore installation platform is dependent on the depth of the water and the weight and volume of the installation. Compared to a HVAC offshore substation a HVDC offshore station is about 85% larger. [175] reports a study case of 800-1000MW at ±320-500 kV of 8000 ton,where the topside costs 69-92 M euro, the jacket 23-29 M euro and the installation 31-36 M euro, also it reports a self installing platform of 138-167 M euro. [176] report 24 M euro (1000 euro/m^3) for a 300 MW substation with dimensions of 30×40×20m. [177] report a 27.6 M euro offshore platform of 60×40×30 m of 600 MW and 4500 ton. In this case it is difficult to find an intermediate value due to the wide cost range, however the proposed offshore platform is more similar to the [175] characteristics that the ones reported by [177], therefore the cost is set at 100 M euro.

As the HVAC electrical equipment is less complex, the offshore platform is smaller and less expensive. [175] reports costs of a 500 MW 220/33 kV platform with dimensions 40x30x18 m, a weight of 2500 ton and 30-40 m water depth as: topside 27.5-32 M euro, jacket 9.2-11.5 M euro and installation 5.75-9.2 M euro, as well as a self installing platform at 42.5-46 M euro. [176] report a 300 MW platform of 35x25x15 m at 13.125 M euro (1000 euro/m^3). [176] report a 600 MW platform with equipment of 6.4 M euro and installation of 17.2 M euro. As it can be noticed there are no costs for a 1GW substation, hence taking into account the figures above the cost of the offshore platform is estimated as 50 M euro.

D. Reactive Power Compensation

One important cost in the HVAC system is the reactive compensation needed in order to lower cable losses and increase carrying capacity .Such cost is not present in HVDC as explained above. HVAC transmission lines and especially HVAC cables produce reactive power dependent on their load and line length. HVAC overhead transmission lines can be operated close to their natural load and would then require no compensation within normal operation. Nevertheless in very low or high load system operation overhead transmission lines need to be compensated to avoid severe impact on the voltage level in the grid. HVAC cables have a far higher demand for reactive compensation, as they cannot be operated close to their natural load restricted by thermal limitation.

To ensure safe and reliable system operation sufficient reactive power compensation is required at the line connection points of HVAC transmission lines. The superimposed reactive power current on the HVAC transmission line will also cause additional losses. Generally the overall reactive power demand is compensated one half each at the receiving and sending end of the line. The reactive power demand of HVAC transmission systems is shown in Table 6.5 for a single 380 kV overhead transmission line and a 380 kV cable solution. Both the cable solution and the overhead transmission line have to be compensated by mechanically switched reactors and capacitors, respectively. This requires an additional investment of 7 k€/MVar .

Table 6.5 Reactive power compensation

	380 kV HVAC cable	**380 kV HVAC OHTL**
Compensation Demand	8 .. 10 MVar/km	0 .. 3 MVar/km
Investment Cost	56 .. 80 k€/km	0 .. 21 k€/km

E. Investment Cost Comparison

The comparison of the investment costs for both technologies is shown in Figure 6.7. VSC-HVDC system has investment costs of 0.415 M euro /$MW_{installed}$ and HVAC 0.298 M euro/$MW_{installed}$. Other costs that include land use, subsea oil/gas pipeline crosses, insurance, development and consent activities, warranty, contingency and so on [183]; [184] might not be reflected in the figures above. In the case of HVAC, there is no point of

comparison since there is not an implemented system with the characteristics proposed here. For such transmission system the cable cost is more than 50% of the total investment costs .However, this is inevitable since the use of fewer cables would require higher voltages to transfer more power per cable, which increases the cable and compensation equipment prices. The costs of losses are also very important – in the evaluation of losses the energy cost and the time horizon for utilisation of the transmission have to be taken into account.

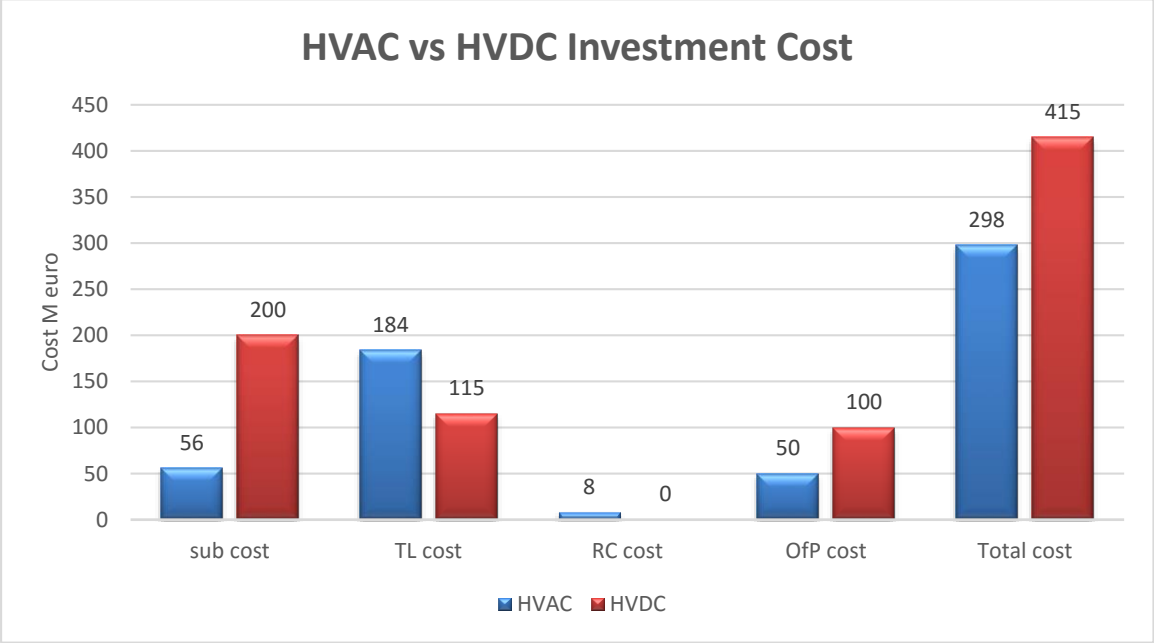

Figure 6.7 Investment cost for HVDC HVAC system at 100 Km

The previous figures highlight that the main costs are to be found in the cable systems (encompassing cable supply, cable installation, cable losses and reactive power compensation costs) for HVAC, which accounts for more than 80% of the total cost. The cost of the cable supply (i.e. the cost of the cables themselves) particularly stands out, representing 40-50% of the total cost. With higher voltages, a soft reduction of those costs is observed, thanks to the fact the lower cross-section can be used, which indeed translates in lower cable supply costs.

On the other hand, the converters account for more than 50% of the total cost in a HVDC transmission system. The expected cost reductions and loss reductions in the converters would definitively reduce the HVDC system costs. As the other costs are substantially lower than for HVAC, it is obvious that the further costs and losses reduction would make HVDC competitive at even shorter distances.

6.4.2 ANNUAL COSTS

A. Operation and Maintenance (O&M) Costs

Overhead transmission lines require maintenance like coating renewal, laser scanning etc. Cable transmission solution will demand less maintenance. The operation and maintenance costs should be outlined as a percentage of the capital costs per year. HVAC Operation and maintenance cost are rated by the capital transmission cost, whereas HVDC O&M costs comprise of both a converter station component and the estimated transmission solution expenses.

In order to determine O&M costs several assumptions are included :technicians ,onshore base and administration , offshore base ,service vessels and jack-up barges .Depending on the climate conditions the O&M costs might vary between 0.061-0.063 M euro/MW/year.However this analysis did not make any difference between VSC-HVDC and HVAC. [185] report 15% of the equipment costs (substations and reactive compensation equipment) for O&M costs during the lifetime of the wind farm connected through HVAC. [186] report

0.5% of the capital cost of the installation (substations only) for O&M costs per year for a VSC-HVDC connection in the Vancouver Island. It can be noticed that the cost of the cable for both systems was not included in the calculations since it is maintenance free.Operation ansd maintenance costs are presented in Table 6.6 O&M costs for VSC-HVDC and HVAC transmission systems.

Table 6.6 O&M costs for VSC-HVDC and HVAC transmission systems

Operation and maintenance	**(O&M) Costs**
VSC-HVDC	0.5% /year
HVAC	15% /lifetime

B. System Losses

- *VSC-HVDC System losses*

VSC HVDC losses are divided in two components: converter station losses and cable losses. The losses for a VSC HVDC converter depend on many parameters (switching frequency, IGBT losses, snubber circuits, etc.) and are complicated to calculate in a model. The first one depend on valve (IGBTs), transformer, reactor and filter losses. For the purpose of this thesis, it is chosen to use the losses measured in a real project. For the new generation of VSCs that use cascade two -level converters like the one used in the DolWin 2 system , [92]report total losses up to 1% of the power sent through the link per converter substation (see Figure 6.8).

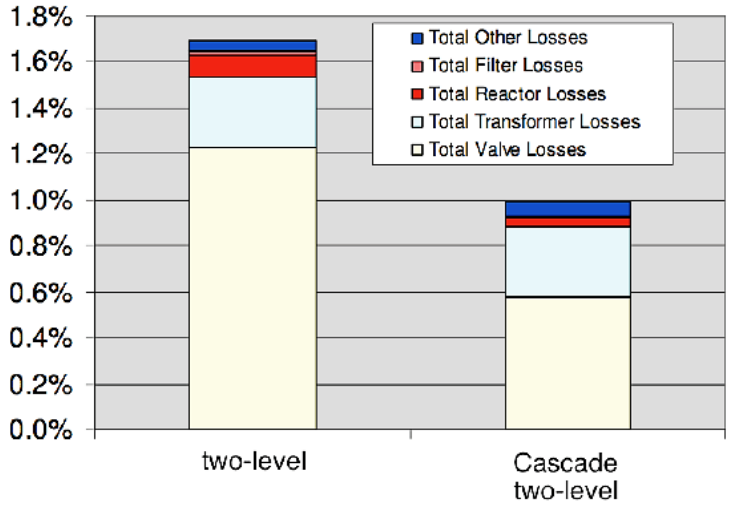

Figure 6.8 Total losses per converter station.

The cable losses in a VSC-HVDC transmission system are basically ohmic losses (I^2R) that are present due to the resistance of the conductor and vary with the distance and the power sent through the cable. [1] reports the resistance of a XLPE cable with 1400 mm^2 cross sectional areas as 0.0126 ohm/km/cable (at 20 °C). Therefore, with a system comprising two cables, the total losses adjusted for a distance of 100 km are shown in Figure 6.9.

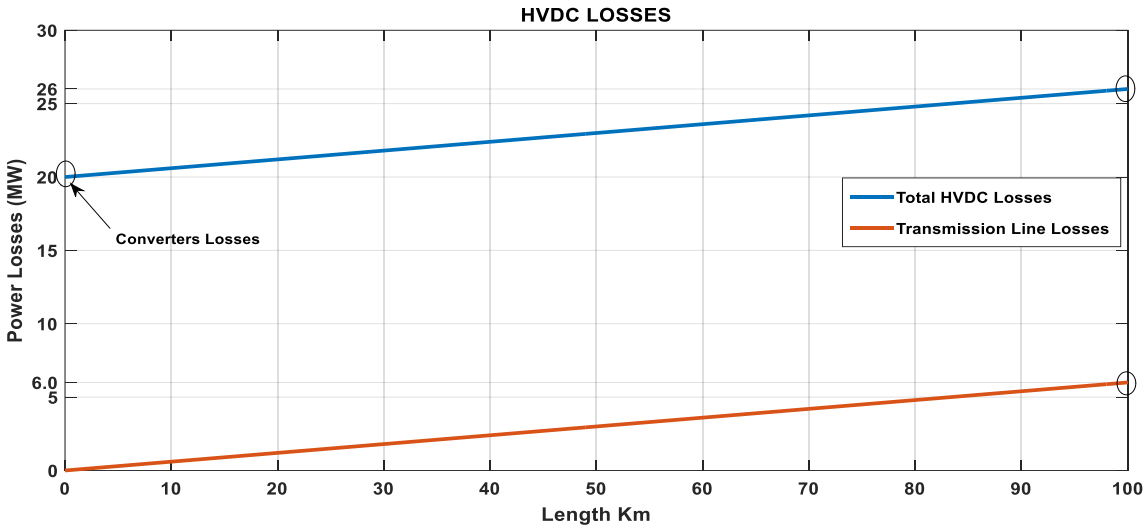

Figure 6.9 Total losses for HVDC system at 100 Km

Converter losses compromise the performance of the HVDC system, accounting for almost the half of the losses. Nevertheless, with a higher cross-section and lower electric resistance, the cable ohmic losses are lower in DC system. Additionally, accounting that it has no dielectric losses and no compensation is needed (thus no losses in the reactive compensation systems), HVDC presents lower losses than the HVAC systems. For higher distances, this is even more exaggerated, as ohmic losses continue to grow over the distance, whereas the converter losses remain the same.

- *HVAC system losses*

Losses in the HVAC system mainly comprise cable, transformer and compensation equipment losses. Cable losses come from current-dependent phenomena in the conductor ,sheaths and armoring , and also from current -independent effects in the cable insulation .The maximum cable insulation temperature determines the maximum current allowed through the cable , which in the case of XLPE cables is 90° C.

The most important losses in the cable system are ohmic losses (I^2R). In the case of HVAC the current varies considerable along the cable, and it is especially high in both ends of the cable where the reactive compensation equipment is located .In order to calculate the cable losses the current distribution should be taken into account and its consequent temperature fluctuations. [10] presents the equations to calculate the losses per unit of length as follows (per three-core XLPE cable):

$$P_{joule} = 3 \int_0^l R_{cable} . I_{cable}^2 . dx \quad (6.1)$$

The current in a HVAC cable varies throughout the entire length of the cable. The total current consists of an active and a reactive component.

$$I_{cable} = \sqrt{I_{active}^2 + I_{reactive}^2} \quad (6.2)$$

The active current per cable (n in parallel) depends on the power output.

$$I_{active} = \frac{P}{n\sqrt{3}U_{cable}} \quad (6.3)$$

And $I_{reactive}$ as follows:

$$I_{reactive} = 2.\pi.f.C.\frac{U_{cable}}{\sqrt{3}} \quad (6.4)$$

Cables under AC operation also have induced losses which occur due to induced currents in other metallic parts of the cable then the conductor. The currents are induced due to the alternating electromagnetic field. For

a cable under DC operation there will be no alternating electromagnetic field and accordingly there will also be no induced losses.

The induced losses are also ohmic and are mainly caused by induced currents in the metallic sheath and armor which depend on the type of material used and the type of bonding of the sheath and armor of the cable. Because of the ohmic character of these losses they are modeled as an increase in the cable resistance and will be given by the manufacturer of the cable as loss factors for the sheath and armor:

$$R_{cable} = R_{DC}.(1+Y_s+Y_p).(1+LF_{sheath}+ LF_{armor}) \quad (6.5)$$

R_{DC}= 0.0176 ohm/km per phase (ABB, 2010d); Y_s=0.0242, Y_p= 0.0247 [187]; $LF_{sheaths}$=0.28, LF_{armor}=0.56).

When paper and solid dielectric insulations are subjected to alternating voltage, they act as large capacitors and charging currents flow in them. The work required to effect the realignment of electrons each time the voltage direction changes (50 or 60 times a second) produces heat and results in a loss of real power that is called dielectric loss, which should be distinguished from reactive loss. For a unit length of a cable, the magnitude of the required charging current is a function of the dielectric constant of the insulation, the dimensions of the cable, and the operating voltage. For some cable constructions, notably for high-voltage, paper-insulated cables, this loss can have a significant effect on the cable rating. The dielectric losses are computed from the following expression:

$$P_D = Q_C.L_F \quad (6.6)$$

Where 'C' is the electrical capacitance of the cable ($0.2*10^{-6}$ F/Km); 'LF' is the loss factor (0.005 for XLPE cables above 36 kV). Additionally, it must be taken in account that compensation systems also present their own losses.

In order to include transformer and compensation equipment losses, [10] assumed them at 1.2% of the total power flowing through the link. This value corresponds to a 500 MW transmission system at 245 kV and 100 Km from shore.Therefore in the proposed case the transformer and compensation equipment losses are assumed at 1.2% as well.

Figure 6.10 shows the losses for the proposed HVAC system with four three-core XLPE cables at 100 km and shows the total HVAC losses.

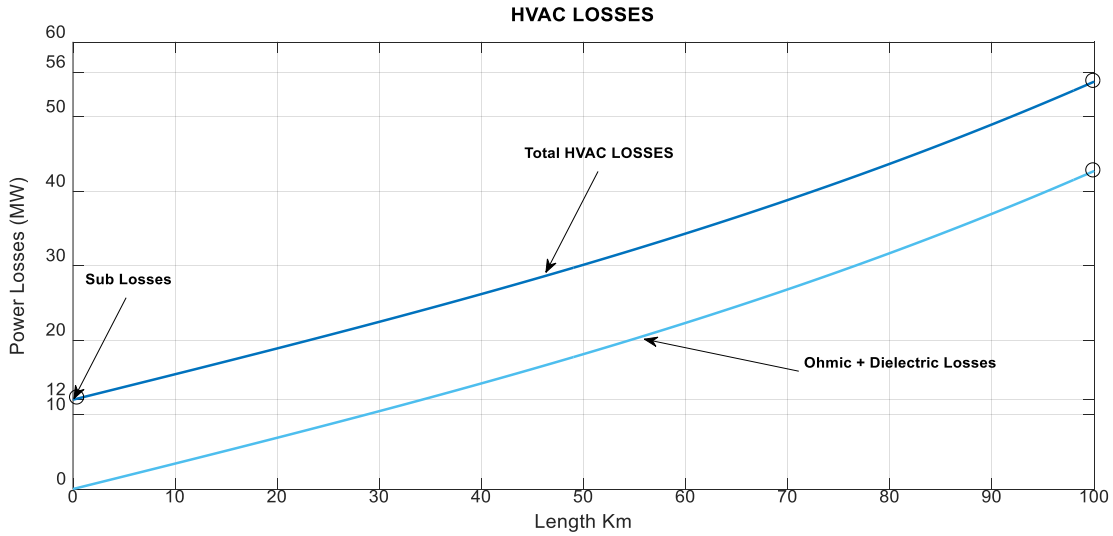

Figure 6.10 Total losses for HVAC system at 100 Km

Regarding HVAC systems, it is noticed that the higher losses are in the 150-kV system. A higher voltage level implies higher reactive power, thus more dielectric and compensation losses. One could expect to observe a substantial decrease in the ohmic losses as the voltage level goes up, but in fact, the ohmic losses are more or less the same for each voltage level. That is because a lower cross-section is employed for higher voltages, to reduce the cable costs. The reduction on the current is compensated by the reduction on the cross-section, which increases the electric resistance.

6.4.3 TOTAL COSTS DURING THE LIFETIME OF THE TRANSMISSION SYSTEM

To calculate the total costs during the lifetime of both transmission systems, the annual costs (O&M and losses) are added to the investment costs .In order to include the losses , which so far have been presented as a percentage of the system's power input , they need to be quantified i economic values . For that matter, the system's power input requires to be yearly quantified as well.

As the owner of the transmission system assumes the losses presented in table 3.6, their economic value is set to the electricity market prices (EMP).Eurostat [2] presented in its website the electricity market prices for the second half of 2015 for household and industrial consumers in different countries in Europe .Such prices are divided in three categories: energy and supply, network costs and taxes. The energy and supply prices are used here as estimates of the loss costs (LC), Table 6.7and Figure 6.11shows the comparison of the total costs during the lifetime of both technologies when the loss cost (LC) is 50 euro/MWh.

Table 6.7 comparison of total costs for HVAC and VSC-HVDC transmission systems

	HVAC		VSC-HVDC	
	Year 0	Year 1-25	Year 0	Year 1-25
Investment(M eur)	298	0	415	0
O&M (M eur)	0	36.96 [M eur/25 Years]	0	39.37[M eur/25 Years]
Losses (M eur)	0	599 [Meur/25 Years]	0	285 [Meur/25 Years]

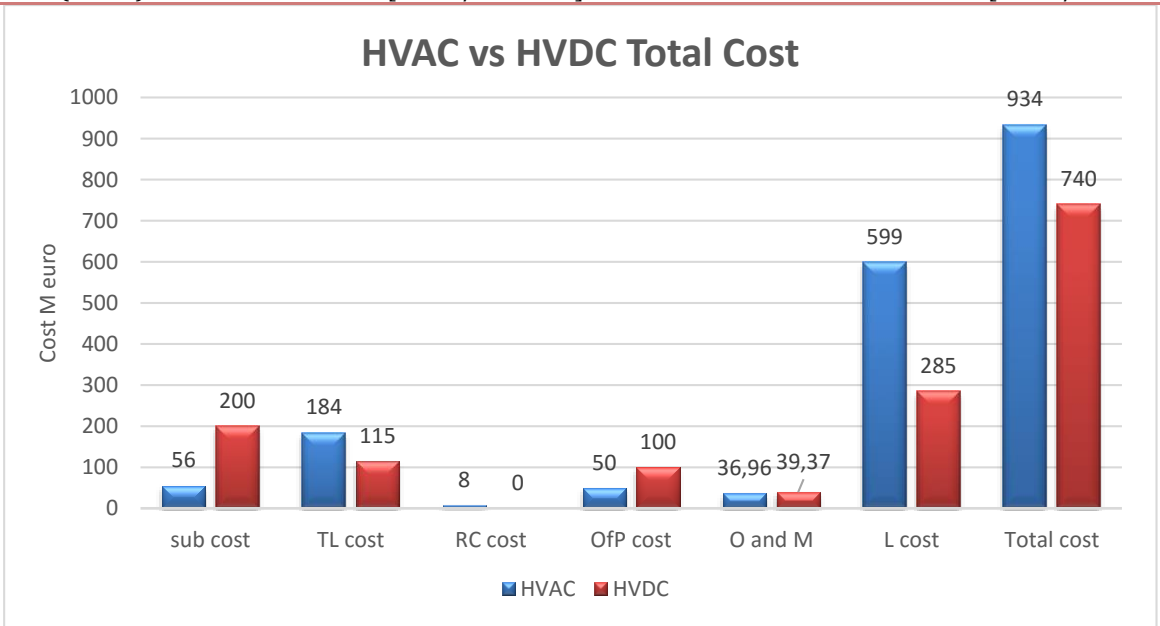

Figure 6.11 Total cost for HVDC vs HVAC system at 100 Km

Figure 6.11shows for the proposed transmission system (1 GW of installed capacity at 100 km from the PCC and with a lifetime of 25 years) that the total costs during its lifetime for HVAC are higher than for VSC-HVDC at any loss cost .At 50 euro/MWh the HVAC solution costs 912.2 M euro and the VSC-HVDC costs 709 M eur.

Figure 6.12shows the total costs and the investment costs of a 1 GW transmission system with HVAC or VSC-HVDC when the distance varies from 0 to 100 Km.

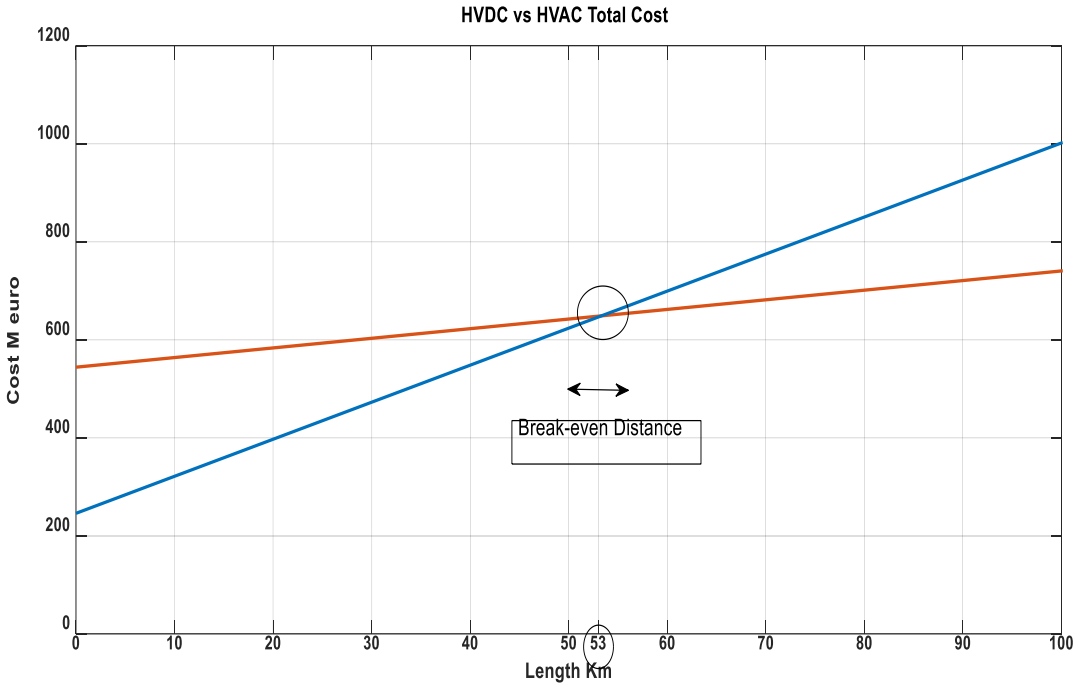

Figure 6.12 Break-even distance for HVAC and HVDC solutions for 1GW transmission system

For both solutions, either HVAC or VSC-HVDC, the variation of the distance has effect on the cable and cable installation costs, as well as in the system losses. Especially in the case of HVAC, the reactive power generated by the cable and the costs of the ancillary compensation equipment are substantially modified .The O&M costs were assumed as Figure 6.7, the loss cost as 50 eur/MWh and lifetime 25 years. It can be noticed that the slope of the investment costs and total costs for VSC-HVDC is very similar .As explained before, the cable losses in HVDC do not increase in considerable quantities. For distances shorter than 53 km the HVAC solution is less costly. A distinction is made between HVAC and HVDC connections based on the results of the electrical design of the grid configurations. In general, HVDC is chosen for large wind farms which are far offshore.

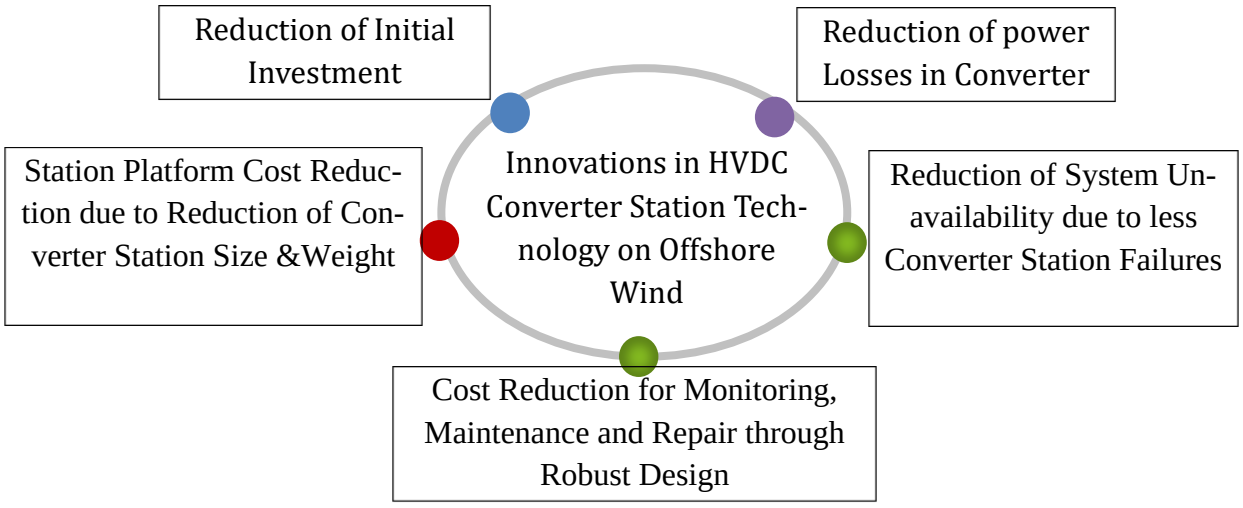

Figure 6.13 Innovations in HVDC Converter Station Technology on Offshore Wind

6.5 CONCLUSION

Over the recent years, several HVDC applications have been installed and they were mainly either point to point or Multi terminal only with radial topology, most of them were close to each other, especially in the North Sea. Which is the reason that there is a tendency to interconnect those systems for building a supergrid HVDC system. This paper summarizes recent developments in HVDC supergrid technologies and discusses the main obstacles and limitation. The introduction of modular multilevel converter made a significant contribution to the progress in HVDC system, moreover, it offers flexibility in particular power and voltage rating further substantial DC circuit breaker, DC power flow controlling devices and DC/DC converter research and development are anticipated. Technically, it is possible to establish an HVDC Supergrid, as described above, some aspects, however, need to be improved such as the control and operation of supergrid and HVDC Grid protection. In fact, several Political, financial, and legal barriers stand in the way of developing this sector.

The evolving grid needs to be increasingly flexible and interconnected, as well as more reliable and intelligent to address new challenges like large scale integration of renewables. The ability to transfer large quantities of electricity across vast distances with low losses and using minimal space combined with the feasibility of going underwater or underground make HVDC a sought after technology across the world.

CONCLUSION

ACHIEVED WORK

A future DC grid is anticipated due to the increasing power and clean energy demand [2],[3], [18]. As renewable energy sources are located far from urban load centres where power is needed, long distance HVDC transmission is required. HVDC technology has advanced over the years due to the development in semiconductor devices which has led to the development of LCC, VSC technology.

The comparison of both LCC and VSC technologies leads to choose VSC; since recent advances made in power electronics, VSCs are becoming more and more reliable, flexible and efficient. Conversely to LCC, they can be connected to passive or weak AC grids (e.g. wind farms), can control quickly, smoothly and independently active and reactive powers and can easily reverse their power flow. For all these reasons, VSC technologies are considered as the best candidate for HVDC grids. In the last part of Chapter 1, the commercialised project of VSC technology is presented.

The newly introduced multilevel converters has many features over the conventional LCC converter topology. Research into the contribution of multilevel converter in the future HVDC system is highly important and it is considered the most viable option for integration of remote energy sources to the grid [10]. This thesis investigates design and control of multilevel converter based on IGBTs for HVDC applications. MMC with half-bridge submodules has minimum number of devices among multilevel converters commercially used for HVDC applications but the control system is more complex than two or three level converters hence improving the design and control of MMC without making the system more complicated is very important.

MMC uses several sub-modules for high power applications such as HVDC and it is usually operated at very low switching frequencies as low as fundamental frequency compared to two or three level converter but losses of MMC-HVDC system is still a significant number in high power applications. The 3-phase half-bridge sub-module HFSMs based MMC configuration as well as its operating principle is briefly introduced in Chapter 2. Through KVL, equivalent circuits of MMC on both the ac side and the dc side are derived. A review of typical modelling methods for the simulation of power electronics based networks was also presented. Detailed representation of VSC-HVDC systems in EMT-type programs includes the modelling of thousands IGBT valves which requires the use of small integration time-steps to accurately represent fast and slow transients. Computational burden introduced by such detailed models significantly reduces the efficiency to study of dynamic and transient events. This limitation is accentuated when complexity and size of the power system is significantly increased as it would be the case of large transmission systems including VSC-based MTDC systems and renewable generation based on power electronic technology. This challenge generates the need to develop more efficient models that provide similar behaviour and dynamic response.

The main objective of Chapter 2 was to develop models to accurately replicate the steady-state, dynamic and transient behaviour of VSC-based HVDC systems in EMT-type programs. In particular, the purpose of this work was to overcome the existing computing limitations associated with the detailed modelling of VSC-based HVDC system integrated into large power grids. The methodology proposed involved the development of detailed models in EMTP-RV that accurately represent the actual behaviour of VSC-HVDC technologies. Detailed model offer several advantages due to its increased accuracy in the modelling of the IGBTs valves. They allow modelling the non-linear behaviour of switching events (through diodes) and representing both switching and conduction losses. Detailed model also allow simulating specific operation conditions and IGBT states such as blocked states (when both switches in the SMs are OFF) as well as converter's start-up sequence

and internal faults. These detailed model were used to validate the proposed equivalent detailed model, switching function model and averaged value model for different test cases and transient events. Developed efficient models for different VSC-HVDC technologies and applications that accurately represent the dynamic and transient behaviour of this technology when integrated into large grids.

In Chapter 3 the control system was implemented based on vector control which permitted independent control of both active and reactive power (and/or voltage) at each VSC terminal. Different modulation techniques and capacitor balancing algorithm applied for MMC are discussed concisely. In MMC there is no central DC link capacitor and DC link voltage is shared among converter's sub-modules therefore each phase can operate independently without causing ripple distortion across other phases. This is an advantage of MMC over other converters with central capacitor. The balancing capacitors control is an algorithm based on the charge-discharge characteristics of the individual cells. In the implementation of the scheme, the voltages of the cells were sampled at regular intervals and a sorting algorithm applied to the voltages. Sorting indices were assigned to the cell units based on the amplitude of its voltage and the quadrant of converter operation. Regulation of capacitor voltages also prevents unnecessary charge and discharge times of the capacitors which can slow the MMC converter response.

The modelling approach and the control theory were validated against their averaged representation for three test cases including a Back to Back VSC-HVDC interconnection, the connection of a typical windfarm with VSC-HVDC system and a multi-terminal VSC-based (MTDC) system used to integrate large amounts of offshore wind generation. A detailed description of different VSC-based technologies and control systems were also presented in Chapter 4 and 5.

In Chapter 5, the analogy between AC systems and DC systems reveals that the inertia constant of rotating machines can be compared to an electrostatic constant which represents the converter station capacitor. Since this electrostatic constant is much lower than the inertia constant, it results that the storage which stabilizes the system during disturbances is lower in DC grids. Numerous studies have been carried out to assess the performance of MTDC control strategies. The main candidate strategies for the DC voltage control of MTDC have been examined. Steady-State and dynamic modelling of various master/slave, voltage margin and voltage droop characteristics have been presented. Key advantages, weaknesses and dynamic features of these control strategies have been identified. With appropriate designs, both voltage margin and voltage droop control could provide a good degree of reliability and stability for MTDC system with a small number of converters. As the scale of the DC system grows, it becomes more difficult to maintain the DC voltage stability using one converter at a time. Hence, droop control is recommended for large DC grids due to its superior scalability, reliability and power sharing capability. These studies have however employed two MTDC system models, which can accurately represent the MMC dynamics and which may have an impact on the MTDC system's response to transient events, such as the loss of a converter. The performance of three and four MTDC control methods, namely, master/slave and droop control, were investigated using the developed detailed MTDC system model for a range of studies.

Over the recent years, several HVDC applications have been installed and they were mainly either point to point or Multi terminal only with radial topology, most of them were close to each other, especially in the North Sea. Which is the reason that there is a tendency to interconnect those systems for building a supergrid HVDC system. The Chapter 6 summarizes recent developments in HVDC supergrid technologies and discusses the main obstacles and limitation. The introduction of modular multilevel converter made a significant contribution to the progress in HVDC system, moreover, it offers flexibility in particular power and voltage rating further substantial DC circuit breaker, DC power flow controlling devices and DC/DC converter research and development are anticipated. Technically, it is possible to establish an HVDC Supergrid, as described above, some aspects, however, need to be improved such as the control and operation of supergrid and HVDC Grid protection. In fact, several Political, financial, and legal barriers stand in the way of developing this sector.

FUTURE DEVELOPMENT

Future works will focus on the following list:

- Lead an investigation on DC grid variant control methods: Dead band droop method and piecewise droop method.
- Calculation of power losses for MMC-based VSC HVDC with different topologies.
- Study of operating principles and control theory of full bridge submodule based MMC converter.
- Study of different emerging new topologies for MMC converter, namely, the alternating arm converter (AAC) and the symmetrical bridge converter (SBC).
- The use of MMC topology in application of renewable energy especially wind and solar energies.
- Investigation of FACTS capability using modular multi-level converter (MMC) topology.
- Economic assessment of HVDC project in Algeria.

APPENDIX A

EMTP-RV Model Design of DM Model Converter

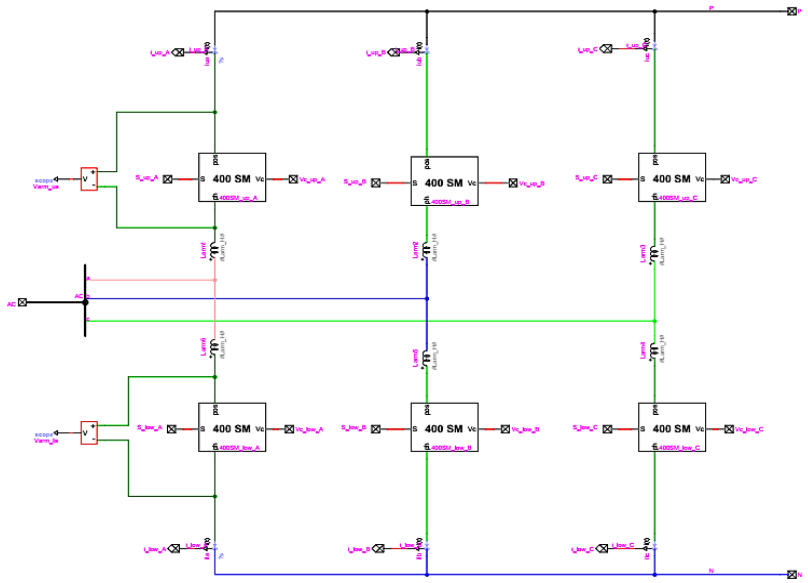

EMTP-RV Model Design of EM Model Converter

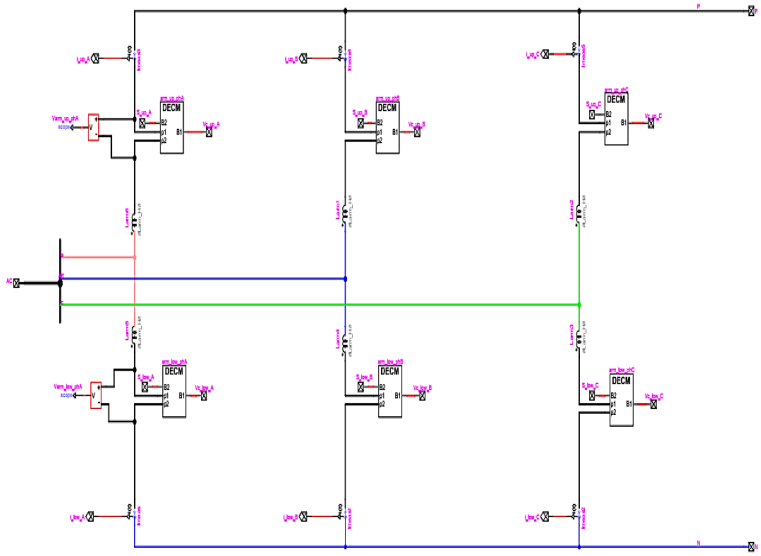

EMTP-RV Model Design of SF Model Converter

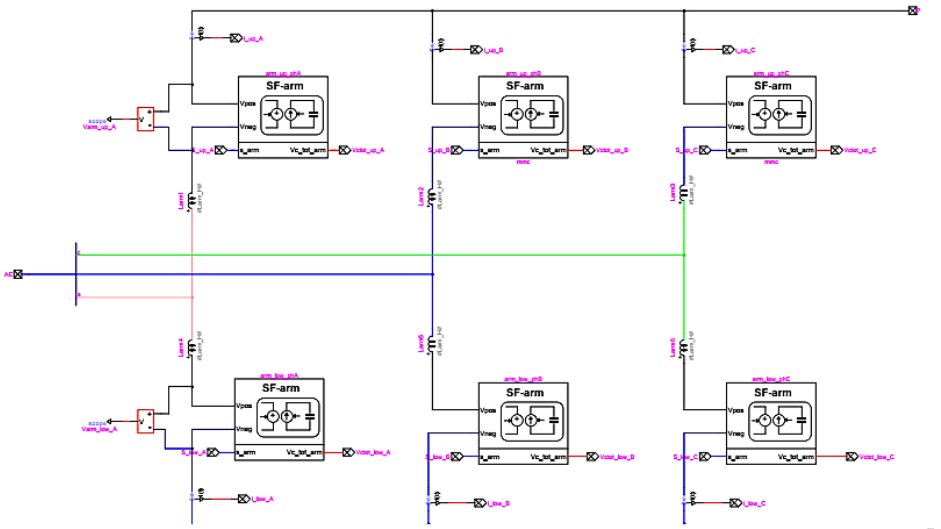

EMTP-RV Model Design of AVM Model Converter

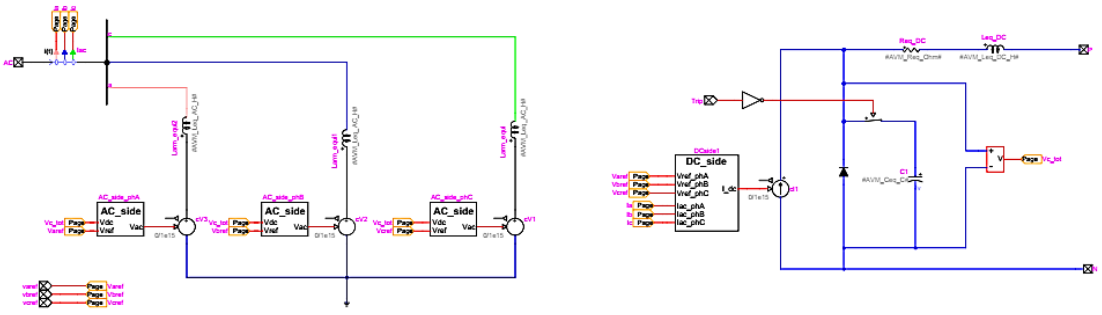

APPENDIX B

Table 01: System Data of Point -to-point MMC -HVDC transmission test system

parameter	Units	VSC 1	VSC 2
Rated power	MVA	1000	1000
AC primary voltage	kVRMSLL	400	400
AC secondary voltage	kVRMSLL	320	320
Frequency	Hz	50	50
DC pole-to-pole voltage	kV	640	640
Transformer reactance	Pu	0.18	0.18
Transformer resistance	Pu	0.001	0.001
MMC arm Inductance	Pu	0.15	0.15
Capacitor energy in each Submodule(SM)	Kj/MVA	40	40
Number of submodules per arm	-	100	100
Conduction losses of each IGBT/diode	Ω	0.001	0.001

Table 02: System Data of Back to Back MMC -HVDC transmission test system

parameter	Units	VSC 1	VSC 2
Rated power	MVA	1000	1000
AC primary voltage	kVRMSLL	400	400
AC secondary voltage	kVRMSLL	320	320
Frequency	Hz	60	50
DC pole-to-pole voltage	kV	640	640
Transformer reactance	Pu	0.18	0.18
Transformer resistance	Pu	0.001	0.001
MMC arm Inductance	Pu	0.15	0.15
Capacitor energy in each Submodule(SM)	Kj/MVA	40	40
Number of submodules per arm	-	400	400
Conduction losses of each IGBT/diode	Ω	0.001	0.001

Table 03: System Data of MMC -HVDC Connection of Offshore Wind Farms to the Transmission System

parameter	Units	VSC Offshore	VSC Onshore
Rated power	MVA	1060	1060
AC primary voltage	kVRMSLL	400	400
AC secondary voltage	kVRMSLL	320	320
Frequency	Hz	50	50
DC pole-to-pole voltage	kV	2*320	2*320
Transformer reactance	Pu	0.18	0.18
Transformer resistance	Pu	0.001	0.001
MMC arm Inductance	Pu	0.15*2	0.15
Capacitor energy in each Submodule(SM)	Kj/MVA	33	33
Number of submodules per arm	-	400	400
Conduction losses of each IGBT/diode	Ω	0.001	0.001

Table 04: System Data of Three-terminal VSC-HVDC grid

	VSC 1	**VSC 2**	**VSC 3**
***Uv*(kV)**	420	420	500
S(MVA)	1500	1500	1500
SCR	2.5	2.5	2.5
Z(Ω)∠(degree)	26.45 ∠80°	26.45 ∠80°	26.45 ∠80°
f(Hz)	60	50	50
Transformer	Yg/Δ,420kV/230kV	Yg/Δ,420kV/230kV	Yg/Δ,500kV/230kV
Main DC capacitor	2x300 μF		
DC Cable	100 Km×2 (R_d=0.0139 Ω /km, L_d = 0.159 mH/km)		
Switching frequency	1980 Hz		

Table 05: System Data of Four-terminal VSC-HVDC grid

Parameter	**Units**	**MMC E1**	**MMC F1**	**MMC B2**	**MMC B3**
Rated power	MVA	200	800	800	1200
AC primary voltage	kVRMSLL	145	145	380	380
AC secondary voltage	kVRMSLL	220	220	220	220
Frequency	Hz	50	50	50	50
DC pole-to-pole voltage	kV	400	400	400	400
Transformer reactance	Pu	0.18	0.18	0.18	0.18
Transformer resistance	Pu	0.001	0.001	0.001	0.001
MMC arm Inductance	Pu	0.15	0.15	0.15	0.15
Capacitor energy in each Submodule(SM)	Kj/MVA	30	30	30	30
Number of submodules per arm	-	200	200	200	200
Conduction losses of each IGBT/diode	Ω	0.06	0.015	0.015	0.01

REFERENCES

[1] ABB, “Grid connection of offshore wind farms-BorWin 1(POW -0050 rev-12),” ABB AB Grid systems HVDC, Ludvica,Sweden, 2010.

[2] ABB power Technologies, “Middletown-Norwalk Transmission Project.Technical description of VSC HVDC converter and cable technology,” ABB, Ludvika ,Sweden., 2004.

[3] J. Arrillaga, Y. H. Liu and N. Watson, Flexible Power Transmission: The HVDC Options, John Wiley & Sons, 2007.

[4] M. P. Bahrman, DIRECT CURRENT POWER TRANSMISSION, ed., ser. Standard Handbook for Electrical Engineers, Mcgraw-hill, 2006.

[5] Alstom, “Hvdc maxsine,” August 2013.

[6] D. Jovcic and K. Ahmed, High Voltage Direct Current Transmission: Converters, Systems and DC Grids, John Wiley & Sons, 2015.

[7] D. Van Hertem, O. Gomis-Bellmunt and J. Liang, HVDC Grids: For Offshore and Supergrid of the Future, Wiley-IEEE Press, 2016.

[8] H. A. SAAD, MODÉLISATION ET SIMULATION D’UNE LIAISON HVDC DE TYPE VSC-MMC, Montreal, Canada: ÉCOLE POLYTECHNIQUE DE MONTRÉAL , 2015.

[9] J. Peralta, DYNAMIC AVERAGED MODELS OF VSC-BASED HVDC SYSTEMS FOR ELECTROMAGNETIC TRANSIENT PROGRAMS, Montreal, Canada: ÉCOLE POLYTECHNIQUE DE MONTRÉAL, 2013.

[10] H. Brakelmann, "Efficiency of HVDC power transmission from offshore-windmills to the grid," in *the IEEE Bologna Power Tech Conference*, Bologna , Italy, 2003.

[11] M. Blarkea and B. M. Jenkinsb, “SuperGrid or SmartGrid: Competing strategies for large-scale integration of intermittent renewables?,” *Energy Policy*, vol. 58, 2013.

[12] P. RAULT, Dynamic Modeling and Control of Multi-Terminal HVDC Grids, university Lille Nord-de-France, March 20, 2014.

[13] F. Gonzalez-Longatt and J. Roldan, “Effects of DC Voltage control strategy on voltage response on multi-terminal HVDC following loss of a converter station,” in *Power and Energy Society General Meeting (PES), 2013 IEEE*, 21-25 July 2013 .

[14] J. Beerten, Modeling and Control of DC Grids, Heverlee: ARENBERG DOCTORAL SCHOOL, May 2013.

[15] G. Asplund, L. Carlsson and O. Tollerz, “50 Years HVDC part II -The semiconductor 'take over',” *The corporate technical journal of the ABB group 4/2003,* 2003.

[16] G. Stamatiou, Converter interactions in VSC-based HVDC systems, Göteborg, Suède: Chalmers University of Technology, June 2015.

[17] N. Flourentzou, V. G. Agelidis and G. D. Demetriades, “VSC based HVDC power transmission systems: an overview,” *IEEE Transactions on Power Systems,* vol. 24, no. 3, p. 592–602., 2009.

[18] G. STAMATIOU, Converter interactions in VSC-based HVDC systems, Gothenburg, Sweden: Department of Energy and Environment CHALMERS UNIVERSITY OF TECHNOLOGY , 2015.

[19] A. J. Beddard, Factors Affecting the Reliability of VSC-HVDC for the Connection of Offshore Windfarms, Manchester: Faculty of Engineering and Physical Sciences, The University of Manchester, 2014.

[20] W. Wang, Operation, Control and Stability Analysis of Multi-Terminal VSC-HVDC Systems, Manchester, UK: The University of Manchester, 2015.

[21] F. Wang, L. Bertling, T. Le and A. B. Anders Mannikof, “An Overview Introduction of VSC-HVDC: State-of-art and Potential Applications in Electric Power Systems,” in *Cigré*, Bologna, 2011.

[22] D. V. Hertema and M. Ghandharia, “Multi-terminal VSC HVDC for the European supergrid: Obstacles,” *Renewable and Sustainable Energy Reviews,* vol. 14, no. 9, p. 3156–3163, 2010.

[23] Z. Melhem, Electricity Transmission, Distribution and Storage Systems, 1st Edition, UK: Woodhead Publishing, 2013.

[24] B. R. Andersen, “VSC Transmission Workgroup B4: HVDC and Power Electronics, Technical report 269,” Cigré, 2005.

[25] W. G. o. H. a. F. B. a. Records, “HVDC PROJECTS LISTING,” Prepared for the DC and Flexible AC Transmission Subcommittee of the IEEE Transmission and Distribution Committee, Canada, 2006.

[26] R. S. Thallam, High-Voltage Direct-Current Transmission, ser. The Electrical Engineering Handbook, CRC Press, 2000.

[27] R. Teixeira Pinto, Multi-Terminal DC Networks System Integration, Dynamics and Control, Delft, Nederland: Delft University of Technology, March 2014.

[28] K. Eriksson, “Operational experience of HVDC Light,” in *Seventh International Conference on AC-DC Power Transmission, (Conf. Publ. No. 485)*, 2001.

[29] U. Axelsson, A. Holm, C. Liljegren, M. Aberg, K. Eriksson and O. Tollerz, “The Gotland HVDC Light project-experiences from trial and commercial operation,” in *16th International Conference and*

Exhibition on Electricity Distribution, Part 1: Contributions. CIRED. (IEE Conf. Publ No. 482) , Amesterdam, 2001.

[30] N. Ahmed, A. Haider, D. Van Hertem, Z. Lidong and H. Nee, "Prospects and challenges of future hvdc supergrids with modular multilevelconverters," *Proceedings of the 2011-14th Power Electronics and Applications (EPE 2011),* 2011.

[31] H. P. Nee and A. Ängquist, "Perspectives on Power Electronics and Grid Solutions," Elforsk rapport, November 2010.

[32] S. Henry, O. Despouys, R. Adapa, L. Barthold and all, "Working Group B4-52-HVDC Grid Feasibility Study," *Electra,* vol. 267, pp. 79-86, 2013.

[33] A. Lesnicar and R. Marquardt, "An innovative modular multilevel converter topology suitable for a wide power range," *Power Tech Conference Proceedings,* vol. vol. 3, p. pp 6, june 2003.

[34] A. Lesnicar and R. Marquardt, ""A new modular voltage source inverter topology,"," *Conf. Rec. EPE,* may 2003.

[35] N. Ahmed, S. Norrga, H. Nee, A. Haider, D. Van Hertem and L. Zhang, "HVDC SuperGrids with modular multilevel converters—The power transmission backbone of the future," *2012 9th International Multi-Conference Systems, Signals and Devices (SSD),* 2012.

[36] R. Marquardt, "Modular multilevel converter topologies with DC-short circuit current limitation," *IEEE 8th International Power Electronics and ECCE Asia* , 2011.

[37] H. Akagi, "Classification, terminology, and application of the modular multilevel cascade converter (mmcc)," *IEEE Transactions on Power Electronics,* vol. vol. 26, p. pp. 3119–3130, 2011.

[38] S. Debnath, J. Qin, B. Bahrani, M. Saeedifard and P. Barbosa, "Operation, Control, and Applications of the Modular Multilevel Converter: A Review," vol. 30, Jan. 2015.

[39] S. Rohner, S. Bernet, M. Hiller and R. Sommer, "Modulation, Losses, and Semiconductor Requirements of Modular Multilevel Converters," *IEEE Transactions on Industrial Electronics,* vol. 57, 2010.

[40] R. Marquardt, "Modular multilevel converter: An universal concept for hvdc-networks and extended dc-bus-applications," *International Power Electronics Conference (IPEC),* p. 502 –507, june 2010.

[41] S. Norrga, X. Li and L. Ängquist, "Converter topologies for HVDC grids," *IEEE International Energy Conference (ENERGYCON),* pp. 1554 - 1561, 2014.

[42] G. P. Adam, S. J. Finney, K. Bell and B. W. Williams, "Transient capability assessments of HVDC voltage source converters," in *IEEE Power and Energy Conference at Illinois (PECI)*, Champaign, IL, 2012.

[43] B. Badrzadeh, "Power conversion systems for modern ac–dc power systems," *European Transactions on Electrical Power,* vol. 22, no. 7, pp. 879-906, 2012.

[44] J. Peralta, H. Saad, S. Dennetiere, J. Mahseredjian and S. Nguefeu, "Detailed and Averaged Models for a 401-Level MMC–HVDC System," *IEEE Transactions on Power Delivery,* vol. 27, no. 3, pp. 1501-1508, 2012.

[45] S. P. Teeuwsen, "Simplified dynamic model of a voltage-sourced converter with modular multilevel converter design," in *IEEE/PES Power Systems Conference and Exposition, PSCE '09.*, Seattle, WA, USA, 2009.

[46] Siemens, "HVDC -High Voltage Direct Current Transmission : unrivaled practical experience," Erlangen ,Germany, 2012 .

[47] J. Dorn, H. Gambach, J. Strauss, T. Westerweller and J. Alligan, "Trans bay cable - a breakthrough of vsc multilevel converters in hvdc transmission," 2012.

[48] M. Davies, M. Dommaschk, J. Dorn, J. Lang, D. Retzmann and D. Soerangr, "HVDC PLUS – Basics and Principle of Operation," Siemens PTD,, Germany, 2008.

[49] Glasdam and J. Bærholm, Harmonics in Offshore Wind Power Plants -Application of Power Electronic Devices in Transmission Systems-, Springer International Publishing, 2016.

[50] Y. Jiang, J. Hu, H. Song, M. Zhang, X. Wang, Z. Rao, G. Wang and G. Zhu, "Study on start-up control strategies for HVDC-Flexible system based on MMC," in *Chinese Automation Congress (CAC)*, China, 2013.

[51] G. Falahi, Design, Modeling and Control of Modular Multilevel Converter based HVDC Systems, Raleigh, North Carolina: North Carolina State University , December 2014.

[52] C. Wang, Modular Multilevel Converter HVDC Based on Harmonic Function Analysis, Montreal, Canada : McGill University, August 2014 .

[53] F. ERTÜRK, INVESTIGATION OF MODULAR MULTILEVEL CONVERTER CONTROL METHODS, MIDDLE EAST TECHNICAL UNIVERSITY, MAY 2015.

[54] T. S. Gum, L. Hee-Jin, S. N. Tae, C. Yong-Ho, L. Uk-Hwa, B. Seung-Taek, H. Kyeon and P. Jung-Wook, "Design and Control of a Modular Multilevel HVDC Converter With Redundant Power Modules for Noninterruptible Energy Transfer," *IEEE Transactions on Power Delivery,* p. 1611–1619, 2012.

[55] G. P. Adam and K. F. S. a. W. B. . Ahmed, "AC fault ride-through capability of VSC-HVDC transmission systems," in *IEEE Energy Conversion Congress and Exposition (ECCE) Conference*, 2010.

[56] J. Glasdam, L. Zeni, C. L. Bak, J. Hjerrild, P. E. Sørensen, A. D. Hansen and P. C. Kjær, "An assessment of converter modelling needs for offshore wind power plants connected via VSC-HVDC networks," in *Proceedings of the 12th International Workshop on Large-Scale Integration of Wind Power into Power Systems as well as on Transmission Networks for Offshore Wind Power Plants*, London, 2013.

[57] U. Gnanarathna, S. K. Chaudhary, A. Gole and R. Teodorescu, "Modular multi-level converter based HVDC system for grid connection of offshore wind power plant," in *9th IET International Conference on AC and DC Power Transmission*, 2010.

[58] U. N. Gnanarathna, A. M. Gole and R. P. Jayasinghe, "Efficient modeling of modular multilevel HVDC converters (MMC) on electromagnetic transient simulation programs," *IEEE Trans Power Deliv*, vol. 26, no. 1, pp. 316-324, 2011.

[59] P. T. Krein, J. Bentsman, R. M. Bass and B. L. . Lesieutre, "On the use of averaging for the analysis of power electronic systems," *IEEE Transactions on Power Electronics,* vol. 5, no. 2, pp. 182-190, 1990.

[60] R. D. Middlebrook and S. A. Cuk, "general unified approach to modelling switching power converter stages," in *IEEE PESC*, Cleveland, OH, USA, June 8–10, 1976.

[61] H. Jin, "Behavior-mode simulation of power electronic circuits," *IEEE Transactions on Power Electronics,* vol. 12, no. 3, p. 443–452, 1997.

[62] S. A. L. I. K. e. a. Norrga, "Frequency-domain modeling of modular multilevel converters," in *IECON 2012–38thAnnual Conference on IEEE Industrial Electronics Society*, 25–28 Oct. 2012.

[63] J. T. Hsu and K. D. T. Ngo, "Behavioural modeling of the IGBT using the Hammerstein configuration," *IEEE Trans. Power Electronics*, p. 746–754, 1996.

[64] B. J. Baliga, "Analysis of insulated gate transistor turn-off characteristics," *IEEE Electron Device Lett*, pp. 74-77, 1985.

[65] A. R. Hefner, "Analytical modeling of device-circuit interactions for the power insulated gate bipolar transistor (IGBT)," in *IEEE Ind. Appl. Soc. Conf. Rec*, 1988.

[66] A. R. Hefner, "Dynamic electro-thermal model for the IGBT," *IEEE Trans. Ind. Appl,* vol. 30, p. 364–405, 1994.

[67] A. R. Hefner and D. M. Diebolt, "Experimentally verified IGBT model implemented in the Saber circuit simulator," *IEEE Transaction on Power Electronics,* vol. 9, p. 532–542, 1994.

[68] C. H. Kao, T. C. C and Y. C. Liang, "Equivalent circuit model for an insulated gate bipolar transistor," in *IEE Proceedings on electrical power application*, 2005.

[69] K. Sheng, B. W. Williams and S. J. Finney, "A review of IGBT models," *IEEE Trans. Power Electron,* vol. 15, no. 6, p. 1250–1266, 2000.

[70] T. Y. Huang, J. Gong and S. H. Chen, "Modeling the turn-off characteristics of insulated-gate bipolar transistor," *Jpn. J. Appl. Phys,* vol. 41, p. 1288–1292, 2002.

[71] Y. Yue and J. J. Liou, "An analytical insulated gate bipolar transistor (IGBT) model for steady-state and transient applications under all free-carrier injection conditions," *Solid-State Electron,* vol. 39, no. 9, p. 1277–1282, 1996.

[72] D. S. Kuo, C. Hu and S. P. Sapp, “An analytical model for the power bipolar-MOS transistor,” *Solid-State Electron,* vol. 29, no. 12, p. 1229–1237, 1986.

[73] H. Saad, J. Peralta, S. Dennetiere, J. Mahseredjian, J. Jatskevich, J. A. Martinez, . Davoudi, M. Saeedifard, V. Sood, X. Wang, J. Cano and A. Mehrizi-Sani, “Dynamic averaged and simplified models for MMC-based HVDC transmission systems,” *IEEE Trans. Power Deliv,* vol. 28, no. 3, p. 1723, 2013.

[74] H. W. Dommel, EMTP Theory Book, Portland: Bonneville Power Administration, 1996.

[75] A. Gole and al, “Guidelines for modeling power electronics in electric power engineering applications,” *IEEE Trans. Power Deliv,* vol. 12, no. 1, p. 505–514 , 1997.

[76] J. Xu, C. Zhao, W. Liu and C. Guo, "Accelerated model of modular multilevel converters in PSCAD/EMTDC," *IEEE Trans. Power Del,* vol. 28, no. 1, p. 129–136, Jan. 2013.

[77] M. G. H. Aghdam and G. B. Gharehpetian, "Modeling of Switching and Conduction Losses in Three-Phase SPWM VSC Using Switching Function Concept," in *IEEE Power Tech Conference, PTC’05*, St. Petersburg, Jun. 2005.

[78] S. Chiniforoosh, J. Jatskevich, A. Yazdani, V. Sood, V. Dinavahi, J. A. Martinez and A. Ramirez, "Definitions and Applications of Dynamic Average Models for Analysis of Power Systems," *IEEE Trans. on Power Delivery,* vol. 25, no. 4, p. 2655–2669, 2010.

[79] S. R. Sanders, J. M. Noworolski, X. Z. Liu and G. C. Verghese , "Generalized Averaging for Power Conversion Circuits," *IEEE Trans. on Power Electronics,* vol. 6, no. 1, pp. 251-259, Apr. 1991.

[80] J. ,. S. H. ,. D. S. Peralta and J. Mahseredjian, "Dynamic performance of averaged-value models for multi-terminal VSC-HVDCsystems," *IEEE Power Energy Soc. Gen.*, pp. 1-8, 2012.

[81] S. Qiang, L. Wenhua, L. Xiaoqian, R. Hong, X. Shukai and L. Licheng, "A Steady-State Analysis Method for a Modular Multilevel Converter," *IEEE Transactions on Power Electronics,* vol. 28, pp. 3702-3713, 2013.

[82] P. Munch, D. Gorges, M. Izak and S. Liu, "Integrated current control energy control and energy balancing of modularmultilevel converters," in *Proc. 36th Annu. Conf. IEEE Ind. Electron. Soc.*, Nov. 7–10, 2010.

[83] A. Antonopoulos, L. Angquist and P. Nee, "On dynamics and voltage control of the modular multilevel converter," in *the 13th Eur. Conf. Power Electron. Appl.*, Barcelona, Spain, Oct. 2009.

[84] B. R. ,. X. L. ,. W. K. T. G. Andersen, "Topologies for VSC transmission," in *Proc. 7th Int. Conf. AC-DC Power Transm.*, London, U.K, Nov. 2001.

[85] H. Ouquelle, L. A. Dessaint and S. Casoria, "An average value model-based design of a deadbeat controller for VSC-HVDC transmission link," in *IEEE Power Energy Soc. Gen. Meeting*, Calgary, AB, Canada, July 2009.

[86] S. Ruihua, C. Zheng, R. Li and X. Zhou, "VSCs based HVDC and its control strategy," in *Proc. IEEE Transm. Distrib. Conf. Exhibit.*, Asia Pacific, Dalian, China, 2005.

[87] H. Saad, C. Dufour, J. Mahseredjian, S. Dennetière and S. Nguefeu, "Real Time simulation of MMCs using the StateSpace Nodal Approach," in *IPST International Conference on Power Systems Transients*, Vancouver, BC, Canada , July 18-20, 2013.

[88] H. Saad, J. Mahseredjian and S. Dennetière, "MODULAR MULTILEVEL CONVERTER in EMTP-RV," École Polytechnique de Montréal, Montréal, Canada, January 20, 2014.

[89] V. Naumanen, MULTILEVEL CONVERTER MODULATION: IMPLEMENTATION AND ANALYSIS, Lappeenranta, Finland: Acta Universitatis Lappeenrantaensis , 7th of June, 2010.

[90] F. M. Gonzalez-Longatt, J. L. R. Rueda, B. S. Rajpurohit, C. A. Charalambous and J. M. Roldan, Implementation of Simplified Models of Local Controller for Multi-terminal HVDC Systems in DIgSILENT PowerFactory, UK: PowerFactory Applications for Power System Analysis, 2014.

[91] S. R. Baljit, Design and Control of Modular Multilevel Converters, Auckland: The University of Auckland, 2015.

[92] B. Jacobson, P. Karlsson, G. Asplund, L. Harnefors and T. Jonsson, "VSC-HVDC transmission with cascade tow-level converters," in *CIGRE session* ,, Paris ,France, 2010.

[93] G. Falahi and A. Huang, "Control of modular multilevel converter based HVDC systems during asymmetrical grid faults," in *IECON 2014 - 40th Annual Conference of the IEEE Industrial Electronics Society*, 2014.

[94] Y. Chen and X. Zhang, "Voltage Balancing Method on Expert System for 51-Level MMC in High Voltage Direct Current Transmission," 2016.

[95] W. Li, L.-A. Grégoire and J. Bélanger, "A Modular Multilevel Converter Pulse Generation and Capacitor Voltage Balance Method Optimized for FPGA Implementation," *IEEE Transactions on Industrial Electronics*, vol. 62, no. 5, pp. 2859 - 2867, May 2015.

[96] M. M. Prafullachandra and B. B. Vijay, "A Simplified Nearest Level Control (NLC) Voltage Balancing Method for Modular Multilevel Converter (MMC)," *IEEE Transactions on Power Electronics*, vol. 30, no. 1, pp. 450 - 462, Jan. 2015.

[97] J. Rodriguez, J.-S. Lai and F. Z. Peng, "Multilevel inverters: a survey of topologies, controls, and applications," *IEEE Transactions on Industrial Electronics*, vol. 49, no. 4, pp. 724 - 738, 2002.

[98] L. G. Franquelo, J. Rodriguez, J. I. Leon, S. Kouro, R. Portillo and M. A. M. Prats, "The age of multilevel converters arrives," *IEEE Industrial Electronics Magazine*, vol. 2, no. 2, pp. 28 - 39, 2008.

[99] G. Falahi and A. Huang, "Low voltage ride through control of modular multilevel converter based HVDC systems," in *IECON 2014 - 40th Annual Conference of the IEEE Industrial Electronics Society*, 2014.

[100] P. Hu and D. Jiang, “A Level-Increased Nearest Level Modulation Method for Modular Multilevel Converters,” vol. 30, April 2015.

[101] G. Konstantinou, J. Pou, S. Ceballos and V. G. Agelidis, “Switching Frequency Analysis of Staircase Modulated Modular Multilevel Converters and Equivalent PWM Techniques,” *IEEE Transactions on Power Delivery,* vol. 31, no. 1, pp. 28 - 36, MAY 2015.

[102] J. Wang, R. Burgos and D. Boroyevich, “A survey on the modular multilevel converters — Modeling, modulation and controls,” in *Energy Conversion Congress and Exposition (ECCE), 2013 IEEE,* 15-19 Sept. 2013.

[103] X. Yao, L. Herrera and J. Wang, “Modulation and control of MMC based multiterminal HVDC,” in *Energy Conversion Congress and Exposition (ECCE),* 14-18 Sept. 2014.

[104] M. Rejas, L. Mathe, P. D. Burlacu, H. Pereira, A. Sangwongwanich and al, “Performance comparison of phase shifted PWM and sorting method for modular multilevel converters,” in *Power Electronics and Applications (EPE'15 ECCE-Europe), 2015 17th European Conference on,* 8-10 Sept. 2015.

[105] G. Adam, O. Anaya-Lara, G. Burt, D. Telford, B. Williams and J. Mcdonald, “Modular multilevel inverter: Pulse width modulation and capacitor balancing technique,” in *Institution of Engineering and Technology,* 26 August 2010.

[106] H. Pengfei and J. Daozhuo, “A Level-Increased Nearest Level Modulation Method for Modular Multilevel Converters,” *IEEE Transactions on Power Electronics,* vol. 30, no. 4, pp. 1836 - 1842, April 2015.

[107] M. Saeedifard and R. Iravani, “Dynamic performance of a modular multilevel back-to-back HVDC system,” in *2011 IEEE Power and Energy Society General Meeting,* 2011.

[108] M. Djehaf, S.-A. Zidi, S. Hadjeri, Y. D. Kobibi and S. Sliman, “Steady-state and dynamic performance of asynchronous back-to-back VSC HVDC link,” in *Electric Power and Energy Conversion Systems (EPECS), 2013 3rd International Conference on,* Istanbul, Turkey, 2013.

[109] R. Pena, J. C. Clare and G. M. Asher, “Doubly fed induction generator using back-to-back PWM converters and its application to variable-speed wind-energy generation,” *IEE Proceedings - Electric Power Applications,* vol. 143, no. 3, pp. 231 - 241, 1996.

[110] I. Erlich, J. Kretschmann, J. Fortmann and S. Mueller-Engelhardt, “Modeling of Wind Turbines Based on Doubly-Fed Induction Generators for Power System Stability Studies,” *IEEE Transactions on Power Systems,* vol. 22, no. 3, pp. 909 - 919, 2007.

[111] J. M. H. S. S. J. L. C. U. Karaagac, “Examination of Fault-Ride-Through Methods for Off-Shore Wind Farms with VSC-Based Multiterminal HVDC,” in *International Conference on Power Systems,* Vancouver, Canada, 2013.

[112] C. Feltes, H. Wrede, F. W. Koch and I. Erlich, “Enhanced Fault Ride-Through Method for Wind Farms Connected to the Grid Through VSC-Based HVDC Transmission,” *IEEE Transactions on Power Systems ,* vol. 24, no. 3, pp. 1537 - 1546, 2009.

[113] L. Harnefors, Y. Jiang-Häfner and M. Hyttinen, “Ride-through methods for wind farms connected to the grid via a VSC HVDC transmission,” in *Nordic Wind Power Conference*, Roskilde, Denmark, 2007.

[114] J. Binkai and W. Zhixin, “The key technologies of VSC-MTDC and its application in China,” vol. 62, September 2016.

[115] E. Kontos, R. T. Pinto, S. Rodrigues and P. Bauer, “Impact of HVDC transmission system topology on multiterminal DC network faults,” *IEEE Transactions on Power Delivery,* vol. 30, no. 2, pp. 844-852, 2014.

[116] G. Siyu, Grid Synchronisation of VSC-HVDC System, the Faculty of Engineering and Physical Sciences, 2014.

[117] F. M. Gonzalez-Longatt, J. M. Roldan and J. L. Rueda, “Impact of DC control strategies on dynamic behaviour of multi-terminal voltage-source converter-based HVDC after sudden disconnection of a converter station,” in *PowerTech (POWERTECH), 2013 IEEE Grenoble,* 16-20 June 2013 .

[118] T. Pinto, S. Rodrigues, P. Bauer and J. Pierik, “Control of MTdc Networks,” vol. 22, no. 04, 2013.

[119] J. Beerten, S. Cole and R. Belmans, “Modeling of Multi-Terminal VSC HVDC Systems With Distributed DC Voltage Control,” vol. 29, Jan. 2014.

[120] D. Westermann, D. van Hertem, A. Küster, R. Atmuri, B. Klöckl and T. Rauhala, “Voltage source converter (VSC) HVDC for bulk power transmission -technology and planning method,” in *9th IET International Conference on AC and DC Power Transmission*, London,UK, 2010.

[121] D. Van Hertem and M. Ghandhari, “Multi-terminal VSC HVDC for the European supergrid: Obstacles,” *Renewable and sustainable energy reviews,* 2010.

[122] T. K. Vrana, System DesignandBalancing Controlof theNorth Sea Super Grid, Trondheim: Norwegian University of Science and Technology Faculty of Information Technology, Mathematics and Electrical Engineering , October 2013.

[123] S. A. M. Bohn, A. K. Marten and D. Westermann, “A pan-European-MENA HVDC overlay grid for bulk energy exchange,” *IEEE PES Transmission and Distribu-tion Conference and Exposition,* 2014.

[124] A. Egea-Alvarez, J. Beerten, D. Van Hertem and O. Gomis-Bellmunt, “Hierarchical power control of multiterminal HVDC grids,” *Electric Power Systems Research* , vol. 121, pp. 207-215, 2015.

[125] A. Egea-Alvarez, J. Beerten, D. Van Hertem and O. Gomis-Bellmunt, “Primary and secondary power control of multiterminal HVDC grids,” in *AC and DC Power Transmission (ACDC 2012), 10th IET International Conference on,* 4-5 Dec. 2012.

[126] J. Beerten, O. Gomis-Bellmunt, X. Guillaud, J. Rimez and A. van der Meer, “Modeling and control of HVDC grids: a key challenge for the future power system,” *Power Systems Computation Conference (PSCC),* 2014.

[127] M. Aragues-Penalba, J. Beerten, J. Rimez and D. Van Hertem, "Optimal power flow tool for hybrid AC/DC systems," *11th IET International Conference on AC and DC Power Transmission*, 2015.

[128] T. K. Vrana and O. B. Fosso, "Technical Aspects of the North Sea Super Grid.," *ELECTRA*, 2011.

[129] F. Gonzalez-Longatt, "Optimal power flow in VSC-HVDC networks for DC-ISO: Constant current operation," in *Smart Grid Technologies - Asia (ISGT ASIA), 2015 IEEE Innovative*, 3-6 Nov. 2015.

[130] F. Gonzalez-Longatt and J. M. Roldan, "Effects of dc voltage control strategies of voltage response on multi-terminal HVDC following a disturbance," in *Universities Power Engineering Conference (UPEC), 2012 47th International*, 4-7 Sept. 2012.

[131] A. Benchaib, "Time Scale Tools: A Control Solution for MTDC Complex Systems with Plug-and-Play Requirements," in *Advanced Control of AC/DC Power Networks*, John Wiley & Sons, Inc., 29 AUG 2015, pp. 17-56.

[132] T. K. Vrana, J. Beerten, R. Belmans and O. B. Fosso, "A classification of DC node voltage control methods for HVDC grids," *A classification of DC node voltage control methods for HVDC grids*, vol. 103, p. 137–144, October 2013.

[133] C. Barker, R. Whitehouse, S. Wang and J. Lang, "Risk of Multiple Cross-Over of Control Characteristics in Multiterminal HVDC," in *AC and DC Power Transmission, 11th IET International Conference on*, 10-12 Feb. 2015.

[134] G. Asplund, K. Lindén, C. Barker, A. Marzin and a. Baur, "HVDC Grid Feasibility Study," *Electra*, pp. 50-59, 2013.

[135] T. Sakurai, K. Goto, S. Irokawa, K. Imai and T. Sakai, "A New Control Method for Multiterminal HVDC Transmission Without Fast Communications Systems," *IEEE Transactions on Power Apparatus and Systems*, no. 5, pp. 1140-1150, 1983.

[136] T. Nakajima and S. Irokawa, "A control system for HVDC transmission by voltage sourced converters," in *Proc. IEEE Power Engineering Society Summer Meeting*, 1999.

[137] N. Seki, "Field testing of 53 MVA three-terminal DC link between power systems using GTO converters," in *Proc. IEEE Power Engineering Society Winter Meeting*, 2000.

[138] T. Haileselassie, Control of Multi-terminal VSC-HVDC Systems, Trondheim, Norway: Norwegian University of Science and Technology, Department of Electrical Power Engineering, 2008.

[139] F. Gonzalez-Longatt and A. C. Charalambos, "Power Flow Solution on Multi-Terminal HVDC Systems: Supergrid Case," in *International Conference on Renewable Energies and Power Quality (ICREPQ'12)*, March 2012.

[140] F. Gonzalez-Longatt, J. M. Roldan and C. A. Charalambous, "Solution of ac/dc power flow on a multiterminal HVDC system: Illustrative case supergrid phase I," in *Universities Power Engineering Conference (UPEC), 2012 47th International*, 4-7 Sept. 2012.

[141] Z. Xiongguang, S. Qiang, R. Hong, L. Xiaoqian, L. Xiaolin and L. Wenhua, “Control of Multi-Terminal VSC-HVDC System to Integrate Large Offshore Wind Farms,” *International Journal of Computer and Electrical Engineering,* vol. 05, no. 2, p. 201, April 2013.

[142] T. Ackermann, A. Orths and K. Rudion, "Transmission systems for offshore wind power plants and operation planning strategies for offshore power systems "-In wind power in power systems," Wiley Publication, Croydon ,UK, 2012.

[143] M. A. Djehaf, S. A. Zidi and Y. Djilani Kobibi, “Modeling of a Multi-level Converter Based MTDC System for the Study of Power System Steady-State and Transient Characteristics,” *Journal of Electrical Engineering,* vol. 16, no. 1, pp. 116-124, 2016.

[144] M. Callavik, F. Schettler, M. S. Debry and al, “Roadmap to the Supergrid Technologies,” Friends of the Supergrid, 2013.

[145] EU, “Renewable energy :prgressing towards the 2020 target,” Brussels, 2011.

[146] N. MacLeod, M. Callavik, M. Boden, M. Dhesi, R. Huuva, N. Kuljaca and F. Schettler, “A Technological Roadmap for the Development of the European Supergrid,” *CIGRE, the Council on Large Electric Systems,* 2015.

[147] S. Rehmana, L. M. Al-Hadhramia and M. Mahbub Alam, “Pumped hydro energy storage system: A technological review,” *Renewable and Sustainable Energy Reviews,* 2015.

[148] Friends of the Supergrid, “THE FIRST PHASE FOR A EUROPEAN SUPERGRID -A common vision for the grid of the future-,” 2011.

[149] S. Cole, T. K. Vrana, J.-B. Curis, C.-C. Liu, K. Karoui, O. B. Fosso and A.-M. Denis, “A European Supergrid,” *17th Power Systems Computations Conference PSCC 2011,* 2011.

[150] A. Purvinsa, H. Wilkeninga, G. Fullia, E. Tzimasa and al, “A European supergrid for renewable energy: local impacts and far-reaching challenges,” *Journal of Cleaner Production,* vol. 19, 2011.

[151] A. Orths, J. Bialek, M. Callavik, J. De Decker and al, “Connecting the Dots,” *ieee power & energy magazine* , pp. 83-95, 18 October 2013.

[152] A. Orths, A. Hiorns, R. v. Houtert, L. Fisher and C. Fourment, “The European North Seas Countries' Offshore Grid initiative — The way forward,” in *Power and Energy Society General Meeting, 2012 IEEE*, 22-26 July 2012.

[153] A. Gustafsson, M. Saltzer, A. Farkas, H. Ghorbani, T. Quist and M. Jeroense, “The new 525 kV extruded HVDC cable system -World´s most powerful extruded cable system-,” ABB Grid Systems, Aug 2014.

[154] D. Van Hertem, M. Ghandhari and M. Delimar, “Technical limitations towards a SuperGrid—A European prospective,” *International Energy Conference and Exhibition (EnergyCon)* , pp. 302-309, 2010.

[155] F. Sass, A. K. Marten and D. Westermann, “Save HVDC overlay grid operation using redundant and cascaded system operation methods,” in *Proc. CRIS 2015,* St. Petersburg, Russia, 06/2015..

[156] D. Jovcic, D. Van Hertem, K. Linden, J. Taisne and B. Grieshaber, “Feasibility of DC Transmission Networks,” *Proceedings of the IEEE PES Innovative Smart Grid Technologies Europe 2011,* 2011.

[157] E. Kontos, R. T. Pinto and P. Bauer, “Fast DC fault recovery technique for H-bridge MMC-based HVDC networks,” in *2015 IEEE Energy Conversion Congress and Exposition (ECCE),* 20-24 Sept. 2015.

[158] M. Callavik, “Hvdc grid for integration of renewable power sources,” 2010.

[159] W. L. D. V. H. B Geebelen, “Analysis of DC breaker requirements for different HVDC grid protection schemes,” *11th IET International Conference on AC and DC Power Transmission,* 2015.

[160] Y. Xang and R. Marquardt, “Future HVDC-grids employing modular multilevel converters and hybrid DC-breakers,” *15th European Conference on Power Electronics and Applications (EPE),* 2013.

[161] W. Wang, M. Barnes, Marjanovic and O. Cwikowski, “Impact of DC Breaker Systems on Multiterminal VSC-HVDC Stability,” *IEEE Transactions on Power Delivery,* vol. 31, no. 2, pp. 769 - 779, April 2016.

[162] D. Jovcic, “Bidirectional, high-power dc transformer,” *IEEE Transactions on Power Delivery* , vol. 24, pp. pp.2276 -2283, 2009.

[163] G. P. Adam, I. A. Gowaid, S. J. Finney, D. Holliday and B. W. Willams, “Review of dc–dc converters for multi-terminal HVDC transmission networks,” *IET Power Electronics* , vol. 9, pp. 281-296, 2016.

[164] A. Far, M. Hajian, D. Jovcic and Y. Audichya, “High-power modular multilevel converter optimal design for DC/DC converter applications,” *IET Power Electronics,* 2016.

[165] C. Sheridan, M. Merlin and T. Green, “Assessment of DC/DC converters for use in DC nodes for offshore grids,” Birmingham, UK, 4-6 December 2013.

[166] S. Zhaohui, H. Yaowei, C. Dongdong and C. Guozhu, “ High power Modular Multilevel DC-DC Converter based on dual-loop CPS modulation,” in *Power Electronics and Motion Control Conference (IPEMC-ECCE Asia), 2016 IEEE 8th International,* 22-26 May 2016 .

[167] S. Azad, W. Leterme and D. Van Hertem, “Fast breaker failure backup protection for HVDC grids,” *Electric Power Systems Research,* 2016.

[168] ENTSOE, "10-year Network development plan 2012," European Network of Transmission System Operators for Electricity, Brussels, Belgium, 2012.

[169] G. P. Adam, S. J. Finney and B. Williams, “Interoperability of voltage source converters in dc grids,” *IET Generation, Transmission & Distribution,* 2013.

[170] H. K. Müller, S. G. M. Shariat Torbaghan and M. Roggenkamp, “The need for a common standard for voltage levels of HVDC VSC,” *Energy Policy,* 2013.

[171] F. Schettler, D. Dragon, G. Imgrund, A. K. Marten, D. Westermann, R. Whitehouse and W. Winter, “Standardization and common Grid Codes forming the technical framework for European wide HVDC Grids,” *European Energy Journal,* vol. 5, 2015.

[172] F. Gonzalez-Longatt, C. Carmona-Delgado, J. Riquelme, M. Burgos and J. L. Rueda, “Risk-based DC security assessment for future DC-independent system operator,” in *Energy Economics and Environment (ICEEE), 2015 International Conference on*, 27-28 March 2015.

[173] J. B. F. Dragon, M. Callavik, D. Eichhoff, J. Hanson and A. -K. M. A. Marten, “Development of Functional Specifications for HVDC Grid Systems,” in *the AC and DC Power Transmission conference in London, UK*, Birmingham, February 10-12,2015.

[174] S. Cole, D. Van Hertem, I. Pardon and R. Belmans, “ Randstad HVDC”.

[175] ENTSOE, "Offshore transmission technology," European Network of Transmission System Operators for Electricity, Brussels, Belgium, 2012.

[176] B. Van Eeckhout, D. Van Hertem, M. Reza, K. Srivastava and R. Belmans, "Economic comparison of VSC-HVDC and HVAC as transmission system for a 300 MW offshore wind farm," *European Transactions on Electrical Power,* pp. 661-671, 2010.

[177] J. Jacquemin, D. Butterworth, C. Garret, N. Baldock and A. Henderson, "Inventory of location specific wind energy cost," Garrad Hassan & Partners Ltd, 2011.

[178] J. Green, A. Bowen, L. Fingersh and Y. Wan, "Electrical collection and transmission systems for offshore wind power," in *the 2007 Offshore Technology Conference*, Houston (TX),USA, 2007.

[179] C. Lancheros, "Transmission systems for offshore wind farms: A technical environmental and economic assessment," Hamburg University of Technology, Hamburg, 2013.

[180] J. Rebled Lluch, "Power transmission systems for offshore wind farms: Technical economic analysis," BarcelonaTech UPC, Barcelona, 2015.

[181] L. Brand, R. De Silva, E. Bebbington and K. Chilukuri, “Grid west project: HVDC Technology Review,” PSC, 2014.

[182] Z. Guo, R. Wu, Y. Yang, S. Zhao and al, “Application of HVDC light system in offshore oil platform,” in *Electrical Machines and Systems (ICEMS), 2011 International Conference on*, 20-23 Aug. 2011.

[183] RAB, “Value breakdown for the offshore wind sector,” the Renewables Advisory Board, 2010.

[184] D. Lane, "Round 3 offshore wind farm connection study -Version 1.0," Senergy Econnect and National Grid for the Crown Estate, 2008.

[185] P. Djapic and G. Strbac, "Grid integration options for offshore wind farms," Imperial College London, London, 2006.

[186] M. Rashwan, "Evaluation of HVDC light as an alternative for the Vancouver Island Transmission Reinforcement (VITR) Project -Appendix Q," Winnipeg (Manitoba).Canada, 2005.

[187] T. Short, Electric power distribution handbook, Boca Raton, USA: CRC press, 2004.

[188] Y.-H. Park, D.-H. Kim, J.-H. Kim and B.-M. Han, “A New Scheme for Nearest Level Control with Average Switching Frequency Reduction for Modular Multilevel Converters,” vol. 16, no. 02, March 2016.

[189] L. Weixing and T. O. Boon, “Simultaneous inter-area decoupling and local area damping by voltage source HVDC,” in *Power Engineering Society Winter Meeting, 2001. IEEE*, 28 Jan.-1 Feb. 2001.

RESUME

Le développement atteint dans le domaine de l'électronique de puissance, précisément la progression de la technologie des semi-conducteurs commandés à l'ouverture et à la fermeture (les thyristors GTO et les transistors IGBT), a permis de réaliser des liaisons HVDC équipées de convertisseurs source de tension VSC qui peuvent aussi interrompe le courant, et non seulement le commuter, comme dans le cas des convertisseurs à commutation de phase (à base des thyristors). La nouvelle technologie VSC-HVDC offre des nouvelles possibilités de transport tel que la connexion avec les réseaux faibles et morts et bien d'autres avantages, on peut citer en autre la rentabilité, la compacité, et le respect de l'environnement, et la facilité d'application. Il est prévu que cette technologie deviendra rapidement la solution privilégiée pour le transport de l'énergie, dans le cas de nombreuses applications où le transport en CA et les liaisons HVDC conventionnelles présentent des limitations. Dans ce contexte, l'intérêt d'utiliser des convertisseurs à niveaux multiples réside dans leur capacité à générer des formes d'ondes de très bonne qualité, et de définition temporelle augmentée. Ces propriétés sont liées à de nombreux avantages, à commencer par la réduction des harmoniques de courant produits dans le circuit interfacé, en plus on peut attendre des niveaux de tension très élevés.

MOTS CLES

HVDC; VSC-HVDC; Convertisseurs Multiniveaux; PWM.

ABSTRACT

The development achieved in power electronics field, precisely, the progress of semiconductor opening/closing controlled devices (GTO thyristors and IGBT transistors) allow the installation of HVDC transmission systems equipped with voltage source converters which can not only switch the current, as in the case of the Line-Commutated Converters (thyristors based), but also, interrupt it.The new VSC-HVDC technology offers new transportation options such as the connection with the weak and dead networks and many other advantages including the profitability, compactness, environmental sustainability and ease of application. It is envisaged that this technology will quickly become the preferred solution for energy transport for many applications where public AC and conventional HVDC links have many limitations. In this context, the advantage of using multilevel converters lies in their ability to generate high quality waves. These properties are related to many advantages, starting with the reduction of current harmonics in the circuit interfaced, and more can be expected voltage levels

KEYWORDS

HVDC; VSC-HVDC; Multilevel Converter; PWM.

ملخص

أدى التطور الحاصل في مجال الإلكترونيات الصناعية والمحرز تحديدا في تكنولوجيا أنصاف النواقل، ترنزستر ثنائي القطبية ذو بوابة معزولة والثايرستور ذو بوابة الإطفاء الى تطوير نظام تيار الجهد العالي المستمر مزود بمحولات منبع التوترقادرة على قطع التيار الكهربائي وليس فقط تحويله كما هو الحال بالنسبة لمحولات منبع التيار القائمة على الثايرستورات. هذا وتفتح التكنولوجيا الجديدة-تيارمستمر.محول منبع الثوثر سبلا جديدة للنقل على غرار الاتصال مع الشبكات الضعيفة والميتة والعديد من المزايا الأخرى المتعلقة بالربحية و العائدات اضافة الى احترام البيئة و سهولة التطبيق ومن المتوقع أن تصبح سريعا هذه التكنولوجيا الخيار الامثل لنقل الطاقة، في حالة العديد من التطبيقات التي يتعرض فيها النقل بواسطة التيارالمتناوب و التيارالمستمر بالطرق التقليدية الى العيد من العوائق في هذا السياق، تكمن اهمية استخدام المحولات متعددة المستويات في قدرتها على توليد موجات عالية الجودة تترتب عنها العديد من المزايا بدءا بالحد من التوافقيات الواقعة في في الشبكات المغلقة ، وصولا الى تحقيق مستويات عالية جدا من الجهد.

الكلمات المفتاحية

نظام تيار الجهد العالي المستمر (HVDC)، محول منبع الثوثر(VSC-HVDC)، PWM.